THÈSE

En vue de l'obtention du

DOCTORAT DE L'UNIVERSITE DE TOULOUSE

Délivré par l'Université Toulouse Capitole

École doctorale : **Sciences Economiques-Toulouse School of Economics**

Présentée et soutenue par

NYAWA WOMO Serge Luther

le 25 juillet 2018

THREE ESSAYS ON FINANCIAL RISKS USING HIGH FREQUENCY DATA

Discipline : **Sciences Economiques**

Unité de recherche : **TSE-R (UMR CNRS 5314 – INRA 1415)**

Directeur de thèse : Mr Nour MEDDAHI, Professeur d'université, Université de Toulouse I

JURY

Rapporteurs Mr Christian Gouriéroux, Professeur d'université, University of Toronto
Mr Dacheng XIU, Professeur d'université, Booth School of Business, University of Chicago

Suffragants Mr Eric GAUTIER, Professeur d'université, Université de Toulouse I
Mr Tim BOLLERSLEV, Professeur d'université, Duke University
Mr Jihyun KIM, Professeur d'université, Université de Toulouse I

THREE ESSAYS ON FINANCIAL RISKS USING HIGH FREQUENCY DATA

PhD Thesis

Serge NYAWA [1]
Toulouse School of Economics

[1] Contact: Toulouse School of Economics, 21 Allée de Brienne, 31000 Toulouse, France. Email: serge.nyawa@tse-fr.eu

Abstract

This thesis is about financial risks and high frequency data, with a particular focus on financial systemic risk, the risk of high dimensional portfolios and market microstructure noise. It is organized on three chapters.

The first chapter provides a continuous time reduced-form model for the propagation of negative idiosyncratic shocks within a financial system. Using common factors and mutually exciting jumps both in price and volatility, we distinguish between sources of systemic failure such as macro risk drivers, connectedness and contagion. The estimation procedure relies on the GMM approach and takes advantage of high frequency data. We use models' parameters to define weighted, directed networks for shock transmission, and we provide new measures for the financial system fragility. We construct paths for the propagation of shocks, firstly within a number of key US banks and insurance companies, and secondly within the nine largest S&P sectors during the period 2000-2014. We find that beyond common factors, systemic dependency has two related but distinct channels: price and volatility jumps.

In the second chapter, we develop a new factor-based estimator of the realized covolatility matrix, applicable in situations when the number of assets is large and the high-frequency data are contaminated with microstructure noises. Our estimator relies on the assumption of a factor structure for the noise component, separate from the latent systematic risk factors that characterize the cross-sectional variation in the frictionless returns. The new estimator provides theoretically more efficient and finite-sample more accurate estimates of large-scale integrated covolatility, correlation, and inverse covolatility matrices than other recently developed realized estimation procedures. These theoretical and simulation-based findings are further corroborated by an empirical application related to portfolio allocation and risk minimization involving several hundred individual stocks.

The last chapter presents a factor-based methodology to estimate microstructure noise characteristics and frictionless prices under a high dimensional setup. We rely on factor assumptions both in latent returns and microstructure noise. The methodology is able to estimate rotations of common factors, loading coefficients and volatilities in microstructure noise for a huge number of stocks. Using stocks included in the S&P500 during the period spanning January 2007 to December 2011, we estimate microstructure noise common factors and compare them to some market-wide liquidity measures computed from real financial variables. We obtain that: the first factor is correlated to the average spread and the average number of shares outstanding; the second and third factors are related to the spread; the fourth and fifth factors are significantly linked to the closing log-price. In addition, volatilities of microstructure noise factors are widely explained by the average spread, the average volume, the average number of trades and the average trade size.

Résumé

Le sujet général de cette thèse est le risque financier dans un contexte de disponibilité des données à hautes fréquences, avec un accent particulier sur le risque systémique, le risque des portefeuilles de grande dimension et le bruit de microstructure. Elle s'articule en trois principaux chapitres.

Le premier chapitre propose un modèle de forme réduite, à temps continu, afin de caractériser la propagation des chocs idiosyncratiques négatifs à l'intérieur d'un ensemble de plusieurs entités financières. En utilisant un modèle à facteurs avec des sauts mutuellement excités, à la fois sur les prix et la volatilité, nous distinguons différentes sources de transmission de chocs financiers telles que la correlation, la connectivité et la contagion. La stratégie d'estimation repose sur la méthode des moments généralisés et tire profit de la disponibilité des données à très haute fréquence. Nous utilisons certains paramètres spécifiques du modèle pour définir des réseaux pondérés pour la transmission des chocs. Aussi, nous fournissons de nouvelles mesures de fragilité du système financier. Nous construisons des cartes de propagation des chocs, d'abord pour certaines banques et compagnies d'assurance clés aux USA, et ensuite pour les neuf plus grands secteurs de l'économie américaine. Il en sort qu'au-delà des facteurs communs, les chocs financiés se propagent via deux canaux distincts et complémentaires: les prix et la volatilité.

Dans le deuxième chapitre, nous développons un nouvel estimateur de la matrice de covolatilité réalisée, applicable dans les situations où le nombre d'actifs est grand et les données à haute fréquence sont contaminées par des bruits de microstructure. Notre estimateur repose sur l'hypothèse d'une structure factorielle de la composante du bruit, distincte des facteurs de risque systématiques latents qui caractérisent la variation transversale des rendements. Le nouvel estimateur fournit des estimations théoriquement plus efficientes et plus précises en échantillon fini, relativement aux autres méthodes d'estimation récentes. Les résultats théoriques et basés sur des simulations sont corroborés par une application empirique liée

à l'allocation de portefeuille et à la minimisation du risque impliquant plusieurs centaines d'actions individuelles.

Le dernier chapitre présente une méthodologie permettant d'estimer les caractéristiques du bruit de microstructure et les rendements latents dans une configuration à grande dimension. Nous nous appuyons sur des hypothèses factorielles tant sur les rendements latents que sur le bruit de microstructure. La procédure est capable d'estimer les rotations des facteurs communs, les coefficients de charge et les volatilités du bruit de microstructure pour un grand nombre d'actifs. En utilisant les actions incluses dans le S & P500 au cours de la période allant de janvier 2007 à décembre 2011, nous estimons les facteurs communs du bruit de microstructure et les comparons à certaines mesures de liquidité à l'échelle du marché, calculées à partir de variables financières réelles. Il en résulte que: le premier facteur est corrélé au spread moyen et au nombre moyen d'actions en circulation; les deuxième et troisième facteurs sont uniquement liés au spread; les quatrième et cinquième facteurs varient significativement avec le prix moyen des actions à la fermeture. De plus, les volatilités des facteurs du bruit de microstructure s'expliquent largement par le spread moyen, le volume moyen, le nombre moyen de transactions et la taille moyenne desdites transactions.

Contents

List of Figures

List of Tables

Acknowledgements

I am grateful to my advisor Nour Meddahi for his invaluable guidance and help during my PhD as well as for his support in my orientation decisions. His ongoing and highly relevant advices contributed into making me a researcher. I would like to thank also Tim Bollerslev, for his unvaluable collaboration as co-author, his helpful comments and advices that significantly improved my thesis.

I am also very indebted to the TSE econometrics group, and in particular to Jihyun Kim, Jean-Pièrre Florens, Eric Gautier, Thierry Magnac, Christian Bontemps, Pièrre Dubois, who taught me a lot and made econometrics interesting and challenging. Finally, I would like to thank the TSE finance group who convinced me that financial economics is worth a life's career.

I greatly benefited from my visit at the Duke University. The support and advice I received from Tim Bollerslev, Georges Tauchen, Jia Li, and Andrew Patton was a decisive step in the progress of my research.

I am also thankful to my fellow PhD students from Toulouse School of Economics whose support and kindness have made my PhD an unforgivable experience.

I am more than grateful to my family, and to my parents in particular, for their continuing support. Their enthusiasm and interest helped me get through those five years and never forget the purpose of my choice in entering a PhD. Finally, I want to thank my wife, Rose Valérie, and my kids. They were always confident and optimistic when I had doubts, and this thesis would not be in your hands without their loving support.

General Introduction

During the last decades, there has been a huge increase in the amount of observations on financial variables. Data are now recorded at an intraday time scale, and are often irregularly spaced over time. Advances in computer technology and storage have facilitated the availability of such high frequency financial data to researchers. They most often contain information about transactions and quotes for stocks, bonds, currencies, options, and other financial instruments. Taking advantage of the availability of such huge amount of data has lead to important developments in the financial econometrics literature. A non-exhaustive list of hot topics during last decades includes: modeling price dynamics through stochastics volatility models, volatiliy/covolatility estimation, realized regressions, volatility forecasting, jump detection, modeling shock transmission or financial contagion, measuring liquidity through the size of the market microstructure noise, etc.

The probabilistic theory that supports these studies was initiated by Jacod (1994), Jacod and Protter (1998), and Aït-Sahalia and Jacod (2014) and the econometrics theory pioneered by Andersen, Diebold, and Labys (2001) and Barndorff-Nielsen and Shephard (2002). Applications are in the field of risk management, hedging, execution of transactions, portfolio allocation, algorithm trading and forecasting.

Using high frequency data, this thesis contributes to the debates on three important topics in financial econometrics: i) modeling shock transmission within financial institutions; ii) volatiliy/covolatility estimation; iii) understanding the market microstructure noise.

Since the global financial crisis of 2007-2009, financial shock propagation is of a huge importance in financial economics. Regulators want to contain it, and investors want to be hedged again such type of global market risk when they carry out their optimal portfolio allocations. To achieve their goals, regulators need information about which firms are shock providers, which ones are shock receivers, or what is the origin of shocks (common factor or idiosyncratic). From the answer of this last question the type of regulation policy to carry out is going to depend. If the shock originates from a common factor, stabilization macro policies need to be carried out, but if shocks are idiosyncratic, then interbank exposure need to be reduced. In the investor side, the portfolio allocation is going to be optimal if they have information about different types of dependency between constituents of their portfolio, and information about patterns through which shocks propagate. The first chapter of this thesis provides such useful information.

Information on the propagation of shocks within a financial system is present both in balance sheets as well as transaction prices of related assets. However, balance sheets' information is complex and difficult to access. Prices are the best alternative source of information to model shock transmission patterns. This is the approach we use in this thesis.

As it is common in the financial econometrics literature, we assume throughout this thesis that the vector of log-prices X_t is a multidimensional semimartingale process during calm periods; it is defined on a complete probability space $(\Omega,\ \Im,\ \mathbb{P})$; the information filtration is an increasing family of σ-fields, $(\Im_t)_{t\geq 0}$, and satisfies $\mathbb{P}$-completeness and right continuity. Log-prices are $\Im_t$ measurable such that

$$dX_t = \mu dt + \sqrt{V_t} dB_t \tag{1}$$

where V_t (sometime called σ_t^2) is the spot volatility, B_t is a Wiener processes.

When we are interested in shocks transmission, it is well established that during periods of crisis, the previous representation can't explain large drops in asset markets, nor transmission patterns of idiosyncratic shocks over time and across assets, with volatility variables calibrated to realistic values. Eraker (2004) documented that a better fit of the observed data is obtained when the model contains stochastics volatility and jumps both in price as well as in volatility. Thus, our model for shock transmission will be a reduced-form model such that:

$$\begin{aligned} dX_t &= \mu dt + \sqrt{V_t} dB_t + \boldsymbol{Z_t dN_t} \\ dV_t &= \kappa\left(\theta - V_t\right) dt + \eta\rho\sqrt{V_t} dB_t + \boldsymbol{Z_t^v dN_t^v} \end{aligned} \tag{2}$$

where Z_t is the jump size and N_t a poisson point process with rate λ_t. The same notation holds for the volatility equation using Z_t^v, N_t^v and λ_t^v.

Most often, financial shocks tend to cluster serially and cross-sectionnally: a large shock to a given asset at a given time t predicts future large shocks to this asset, and increases the probability of large shocks to other assets. Allowing a time varying jump intensity λ_t is a natural technic to model this propagation phenomenon. To be more precise, for a stock i, jump intensity of price and volatility, respectively λ_{it} and λ^v_{it}, will be defined by:

$$d\lambda_{it} = \alpha_i \left(\lambda_{i\infty} - \lambda_{it}\right) dt + \sum_{j=1}^{m} \beta_{ij} dN_{jt} \tag{3}$$

$$d\lambda^v_{it} = \alpha^v_i \left(\lambda^v_{i\infty} - \lambda^v_{it}\right) dt + \sum_{j=1}^{m} \beta^v_{ij} dN^v_{jt} \tag{4}$$

From the previous equations, it comes out that a jump in the stock j at time t increases the probability of further jump in the stock i between time t and t+1. The use of this type of jumps is justified by some empirical evidences: during periods of distress, jumps are clustered serially and cross-sectionnally. This property is observed both in price and volatility. The usual poisson point processes are not able to reproduce these types of clustering. A point proces with jump intensity defined as previously is called a Hawkes point process.

Our model decomposes the semimartingale representation of the price equation into a common component and an idiosyncratic component. It permits to account for different mechanisms of systemic failure such as: correlation effect (through common factors) and connectedness/contagion effects (through mutually exciting jumps both in price and volatility).

Our model is more general than existing models of financial contagion (e.g. Aït-Sahalia, Cacho-Diaz, and Leaven (2015) and Maneesoonthorn, Forbes, and Martin (2016)): we control for the systematic risk (through common factors); our model is multidimensional with no restriction on the number of stocks; we have less restriction on the model (more specifically on excitation matrices β and β^v). Aït-Sahalia, Cacho-Diaz, and Leaven (2015) proposed a model for two assets, constant volatity and restriction on the excitation matrix (some sparsity assumptions). It cannot address the question of connection within a set of more than 2 assets. Maneesoonthorn, Forbes, and Martin (2016)) has stochastic volatility, jump in price and volatility, but their model is uni-dimensional. None of their approaches controls the co-movement due to common factors.

Our entire model is estimated using a multi-step GMM approach: In the **step 1**, we remove all the jumps present into the data, and estimate the resulting diffusion model; in **step 2**, coefficients of the first step are kept fixed while we estimate parameters of the discontinuous part of the model; in the **step 3**, coefficients obtained in steps 1 and 2 are used as starting values for the estimation of the global model. The identification of parameters is facilitated by a combination of moments of returns and moments of volatility measures constructed using high frequency data. Once centered, moment of order 3 and 4 of returns isolate parameters of the jump component up-to the factor loading vector b, while moment of order 2 places the contributions from the diffusive and jump components of the model on the same order. Moments of volatility measures facilitate the identification of parameters of the volatility (both factor and idiosyncratic volatility parameters).

Within the set of estimated parameters, there are excitation parameters (β and β^v) which contain information about the strength of links between stocks. We use these excitation parameters to construct new measures of the financial system fragility, and network maps for the propagation of different types of shocks. Excitation matrices of prices and volatility are used as adjacency matrices for network constructions. An edge is drawn between an asset i and an asset j if and only if the corresponding excitation parameter is significantly different from zero. Our measures permit to know which stocks are shock providers, which one are shock receivers, and what is the level of the financial system fragility. Our measures have similar intuitions as the Marginal Expected Shortfall by Acharya, Pedersen, Philippe, and Richardson (2017), or the Co-VaR by Adrian and Brunnermeier (2016). The popular measure of the financial system connectedness of Diebold and Yilmaz (2015a) is not able to identify the type of connection we emphasize here. Applied to our setup, it produces a lot of self-excitation.

We use our methodology to track associations within a number of key US banks and insurance companies as well as within nine S&P500 largest economic sectors. We find that shoch transmission has three related but distinct channels: common factors, price and volatility jumps. Also, the risk of volatility shocks to propagate throughout this financial system is bigger than the one of price shocks. Concerning financial institutions, we found that BAC, WFC, ACE and MET are main contributors to systemic risk. For S&P500 sectors, Distress in energy, financial, health care, and consumer staples sectors have the highest negative impacts on the economic system fragility. Our network maps and fragility measures provide important information to market participants to reduce the adverse selection risk, and to regulators to design a stable financial system.

Relying on high frequency data, the aim of the second chapter of this thesis is to estimate the covolatility matrix of a huge number of assets, when data are contaminated by market microstructure noise. Considered as one measure of the financial risk, volatility is of a particular interest in financial econometrics. Estimating the integrated volatility/covolatility matrix has been an active topic. Over a trading time of length $T = 1$, the integrated covolatility of a p-dimensional process of latent frictionless log-price $X_t^* = (X_{1t}^*, ..., X_{pt}^*)$ satisfying the equation 1.1, is the $p \times p$ matrix defined by,

$$ICV \;=\; \int_0^1 \sigma_s \sigma_s^{'} ds. \tag{5}$$

where $\sigma_s = \sqrt{V_s}$. ICV is a daily measure of the co-movement between assets. It is of a huge importance in the areas of risk management, portfolio allocation, hedging and asset pricing. When $p = 1$, this object is called the integrated volatility.

By the theory of quadratic variation, ICV may be consistently estimated by the realized variance,

$$RCV \;=\; \sum_{t_i} (X_{t_{i+1}}^* - X_{t_i}^*)(X_{t_{i+1}}^* - X_{t_i}^*)', \tag{6}$$

where X_t^* is the latent frictionless log-price, $0 \leq t_i \leq 1$ refer to the within day sampling times, $t_i - t_{i-1} \to 0$.

The realized variance is a consistent estimator of ICV under the assumption of frictionless markets. However, this assumption is not realist, because in practice, high frequency data on returns contain market microstructure noise coming from: bid-ask bounds, transaction prices, non-trading periods or price discreteness, trades occurring on different markets or networks, rounding errors, etc. Thus, the recorded log-price vector X_t is noisy such that:

$$X_t = X_t^* + \varepsilon_t \tag{7}$$

It is now accepted in the literature that this noise plays an essential role when studying financial data. The presence of such noise renders inconsistent the realized variance. To provide some solutions to this inconsistency under microstructure noise, for $p = 1$, some estimators have been proposed. The subsampling and averaging approach of Zhang, Mykland, and Ait-Sahalia (2005) provides the Averaging and Two Scales estimators. The intuition of the averaging estimator is the following: The initial full grid containing all observation points is partitioned into K nonoverlapping subgrids, and K sub-realized variances are computed over each subgrid. The estimator is obtained by taking the average of the K sub-realized variances. The Two Scales estimator is a consistent and unbiased adjustment of the averaging estimator. Another approaches are the realized kernel of Barndorff-Nielsen, Hansen, and Shephard (2008a) and the pre-averaging estimator of Jacod, Li, Mykland, Podolskijc, and Vetter (2009a). The realized kernel is a weighting average of realized autocoviance. The idea of the pre-averaging approach is to choose a window of length k_n, a weigthing function g, and to construct from the initial return series a new one by averaging returns over consecutive and overlapping blocs of length k_n. It is with this latter series that the pre-averaging realized variance is construted. The two second approaches (Kernel and Pre-averaging) provide good finite sample and convergence properties. The subsampling and averaging approach has many others advantages : a) this device is model-free ; b) it takes advantage of the rich sources in tick-by-tick data while preserving the continuous time assumption on the underlying returns ; c) to a great extent it corrects for the adverse effects of microstructure noise on volatility estimation (Zhang, Mykland, and Ait-Sahalia (2005)).

These estimators have been extended to the multivariate case, when observations of all the different assets were synchronous, it means recorded exactly at the same time, and when the number of assets was small relatively to the sample size. However, very often, high frequency data of different assets are rarely simultaneous. Thus, estimating the covolatility matrix in this asynchronous framework with market microstructure noise is challenging. In this case, there are at least three types of problems to deal with: the non-synchronicity of observations, the epps-effect, and market microstructure noise. When these problems exist, the usual estimators of the covolatility matrix are seriously biased. The asynchronicity often leads to some undesirable features as the Epps-effect (see, e.g., Epps (1979)), meaning that correlation estimates tend to become lower when the sampling frequency increases.

To provide a solution to the non-synchronicity problem when estimating the covolatility matrix, Hayashi and Yoshida (2005) propose an estimator of the covariation of two diffusion processes when they are observed only in discrete time. Their estimator is based on overlap intervals and is free of any synchronization process of the original data. However, the estimator of Hayashi and Yoshida (2005) doesn't deal with the microstructure noise. Thanks to the multivariate realized kernel estimator of Barndorff-Nielsen, Hansen, and Shephard (2008a). These authors construct the first estimator which guarantees simultaneously: consistency, positive semi-definiteness, robust to microstructure errors, and handles non-synchronous trading. The non-synchronicity issue is resolved using the refresh time approach. Also, Christensen, Kinnebrock, and Podolskij (2010a) propose another estimator of the covolatility matrix of continuous Itô semimartingales, observed with noise. His Modulated Realized Covariance estimator is a multivariate extension of the pre-averaging estimator of Jacod, Li, Mykland, Podolskijc, and Vetter (2009a).

These estimators perform well when the number of assets is small relatively to the sample size. However, in realistic situations, the number of assets can be huge. In this case, the previous estimators perform poorly because of the lack of accuracy in estimating high-dimensional matrices. One solution popular in the literature is to impose a structure in that matrix. Two main approaches have been proposed in the high dimensional framework: sparsity or decay assumptions and the use of factor structures.

Estimators that rely on sparsity and decay assumptions include Wang (2010) and Zheng and Li (2011). They postulate that the covolatility matrix is comprised of only a small number of non-zero block diagonal matrices, or that the absolute magnitude of the elements in the matrix somehow decay away from the diagonal. The blocking and regularization approach of Hautsch and Podolskij (2013), in which assets with similar observation frequency are grouped together in order to reduce the data loss stemming from the use of refresh-time sampling, also implicitly builds on similar ideas. As does the composite realized kernel estimator of Lunde, Shephard, and Sheppard (2016), in which bivariate realized kernel estimators for all pairs of assets is combined and regularized in the construction of an estimator for the full high-dimensional covolatility matrix for all assets.

When the problem concerns the stock returns, a factor representation seems natural (see, e.g., Ross (1976), Chen, Roll, and Ross (1986), Sharpe (1994), and Ledoit and Wolf (2003)). The idea is to deal with the curse of dimensionality and to force the estimator to be well-conditioned, meaning that estimation error is not amplified by inverting. The use of a factor structure to estimate the covolatility is not recent. Fan, Fan, and Lv (2008) examine how the dimensionality impact the estimation of the covariance matrices. They use a multi-factor model for the vector of excessive returns of p assets to resolve the problem due to the dimensionality and to estimate the covariance matrix. Their factors are assumed to be observable. Tao, Wang, and Chen (2011) propose an approach which combines low-frequency and high-frequency data in order to estimate the integrated covolatility matrix in the high dimension framework. Bannouh, Martens, Oomen, and van Dijk (2012) introduce a Mixed-Frequency Factor Model to estimate the vast covolatility matrix of asset returns. They consider as factors highly liquid assets such as exchange traded funds (ETFs) and use these very high-frequency data to estimate the covolatility matrices of the observed factors and regressions to estimate loadings and the idiosyncratic risk covolatility matrix. Fan, Liao, and Mincheva (2011) through their approximate factor models, assume observable factors and allow the presence of the cross-sectional correlation in a sparse error covariance matrix. Ait-Sahalia and Xiu (2016) propose an approach based on the principal component analysis for the estimation of a high dimensional factor models. Fan, Liao, and Mincheva (2013) introduce the Principal Orthogonal Complement Thresholding Estimator (Henceforth, POET). They assume a sparse error covariance matrix in an approximate factor model, and allow for the presence of some cross-sectional correlation, after taking out common but unobservable factors. Dai, Lu, and Xiu (2017) rely on the pre-averaging method with refresh time to solve the microstructure problems, while using three different specifications of factor models, and their corresponding estimators, respectively, to battle against the curse of dimensionality.

This thesis contributes to this exciting literature on high-dimensional covolatility matrix estimation. We provide a new factor-based estimator of the covolatility matrix, applicable in situations when the number of assets is large and the high-frequency data are contaminated by market microstructure noise (noise coming from the way the market is organized: bid-ask spread, rounding errors, transaction prices, etc.). Our estimation strategy takes advantage of a factor structure for the noise component with different features than the factor structure in the latent returns. We showed that the new estimator is theoretically more efficient and more accurate in finite-sample than other recently developed realized estimation procedures. These findings are corroborated by an empirical application related to portfolio allocation and risk minimization involving several hundred individual stocks.

As it is usually the case in the literature, our estimation methodology consists on reducing the impact of market microstructure noise prevalent at high frequency, while accurately estimating volatility of the latent log-price. In general, understanding microstructure noise is not the main purpose when estimating volatility. In the empirical literature on microstructure noise, existing procedures are most often limited to estimate only the noise volatility. Nevertheless, useful information can be extracted from this noise component for a better understanding of its behavior.

The objective of the last chapter of this thesis is to contribute to the growing literature which consists on studying the information contain of microstructure noise. Considering a huge number of stocks, our aim is firstly to estimate microstructure noise components through a factorial decomposition. Secondly, we want to study the information contain of the factor component of this noise by relating it to some liquidity measures. Thirdly, we are interested on approximating frictionless prices.

Our contribution on this topic is closely related to the ones by Aït-Sahalia and Yu (2009), Li, Xie, and Zheng (2016), Jacod, Li, and Zheng (2017) and Chaker (2017). Aït-Sahalia and Yu (2009) study the nature of the information contained in high frequency statistical measurements of microstructure noise volatility and relate them to observable financial characteristics of the underlying assets and, in particular, to different financial measures of their liquidity. Li, Xie, and Zheng (2016) consider a setting where market microstructure noise is a parametric function of trading information, possibly with a remaining noise component, and show that higher efficiency can be obtained by modeling and removing the noise component caused by trading and then applying existing estimators to the estimated log-prices. Jacod, Li, and Zheng (2017) study the non-parametric estimation of autocovariances and autocorrelations of microstructure noise based on high frequency data. Chaker (2017) explicitly models microstructure noise and removes it from observed prices to obtain an estimate of the frictionless price.

Nevertheless, our approach presents important differences with the existing literature. Firstly, our methodology relies on factor assumptions both in latent returns and microstructure noise. Thus, variables that explain microstructure noise are unobservable latent common factors. They will be estimated through the process. Contrary to the existing literature, when specifying noise equations, our approach will not suffer for the misspecification or missing explanatory variables issues. Secondly, our approach is high dimensional in term of number of stocks: microstructure noise characteristics and frictionless prices are estimated jointly for a huge number of stocks. As it is common in this literature, we compare the extracted common factors of microstructure noises to some liquidity measures. Here, liquidity measures are not stock specific, but are averages or principal components of individual stock liquidity measures.

Our methodology is able to estimate rotations of common factors, loading coefficients and volatilities of microstructure noise for a huge number of stocks. Using stocks included in the S&P500 during the period spanning January 2007 to December 2011, we estimate microstructure noise common factors and compare them to some market-wide liquidity measures computed from real financial variables. We obtain that: the first factor is correlated to the average spread and the average number of shares outstanding; the second and third factors are related to the spread; the fourth and fifth factors are significantly linked to the closing log price. In addition, volatilities of those microstructure noise factors are widely explained by the average spread, the average volume, the average number of trades and the average trade size.

Chapter 1

A Factor Model for Systemic Risk Using Mutually Exciting Jump Processes

Serge Nyawa[1]

Abstract

We provide a reduced-form model for the propagation of negative idiosyncratic shocks from any specific economic unit to the entire financial system. This phenomenon is referred as systemic risk. Our continuous time model generalizes popular existing econometric models for financial contagion. Using common factors and mutually exciting jumps both in price and volatility, we distinguish between sources of systemic failure such as macro risk drivers, connectedness and contagion. The estimation procedure relies on the GMM approach and takes advantage of high frequency data. We use models' parameters to define weighted, directed networks for shock transmission, and we provide new measures for the financial system fragility. We construct paths for the propagation of shocks, firstly within a number of key US banks and insurance companies, and secondly within the nine largest S&P sectors

[1]We are very grateful to Nour Meddahi and Tim Bollerslev for helpful comments that significantly improved the paper. We have also benefited comments by Jihyun Kim, Yacine Aït-Sahalia, Bruno Biais, Kamil Yilmaz, Rene Garcia, Jean-Pièrre Florens, Eric Gautier, Jia Li, Thierry Magnac, Christian Bontemps, Pièrre Dubois, Wilfried Sand-Zantman, Sophie Moinas, as well as workshop participants at Toulouse School of Economics and IAE Toulouse. We acknowledge financial support of the grant ERC POEMH. We are grateful to Dacheng Xiu for providing us a part of the dataset.

during the period 2000-2014. We find that beyond common factors, systemic dependency has two related but distinct channels: price and volatility jumps.

1.1 Introduction

1.1.1 Motivation

In the aftermath of the global financial crisis of 2007-2009, designing a stable financial system has become one of the biggest challenges for regulators and policy makers. The primary goal is to reduce the possible propagation of negative idiosyncratic shocks to the entire financial system, a phenomenon referred as systemic risk. The losses tend to spread across financial institutions, thus threatening the whole financial system as well as potentially adverse consequences for the supply of credit to the real economy. Market participants pay much attention to systemic risk and choose their strategies to reduce its impact on their future investments. The systemic risk is ascribed to one of the following three mechanisms (See, e.g., Rauch and Litan (1998) and Scott (2010) and Jenkins (2011)):

(i) *Correlation effect*, wherein a severe downturn in the economy results in insolvency of financial institutions mainly due to the devaluation of assets widely held, price correlations or exposures to common factors. Hellwig (2009) refers to this as *Domino effect through asset prices*. The bubble in housing prices that preceded the financial crisis of 2007-09 was a source of correlation risk that caused the collapse of several major banks, which were exposed to the U.S. real estate sector.

(ii) *Connectedness effect*, wherein a chain of domino-like failures of institutions occur because of their connections through financial claims to insolvent institutions. This systemic risk channel is also called *Domino effect through contractual relations*. Interconnectedness can arise through a variety of discrete channels, e.g., interbank deposits, derivative contracts, etc.

(iii) *Contagion effect*, wherein a response to the failure or disruption of a financial institution, risk averse investors with limited information, decide to liquidate their positions from this institution as well as from other similar firms[2]. This phenomenon has been observed in september 2008, after the failure of Lehman Brothers: the liquidation of the

[2]Firms with investments in the same asset classes.

Reserve Primary Fund, a Lehman Brothers debt securities' holder, generated investor fears and decrease the market value of others money market funds.

It follows that information on the propagation of shocks within a financial system is present both in balance sheet as well as prices of related assets. However, due to proliferation of derivatives and securitization, balance sheets' information is complex and difficult to access. Prices are the best alternative source of information to model shock transmission patterns. The primary focus of this paper is to provide a reduced-form model for shock transmission within financial institutions, during periods of distress. The model will highlight various sources of systemic risk, as well as different and complementary channels for shock transmission. It relies on price and volatility dynamics. We model price dynamic by a *jump diffusion factor model* with time varying jump intensity both in prices and volatilities.

In the absence of arbitrage, jump diffusion models with jumps both in price and volatility are increasingly used to capture price dynamic during period of turmoil. Stock price crisis data exhibit much higher volatility as well as sudden jumps which the standard model is unable to capture.

Figure 1.1. Periods of distress: sudden jumps as well as higher volatility.

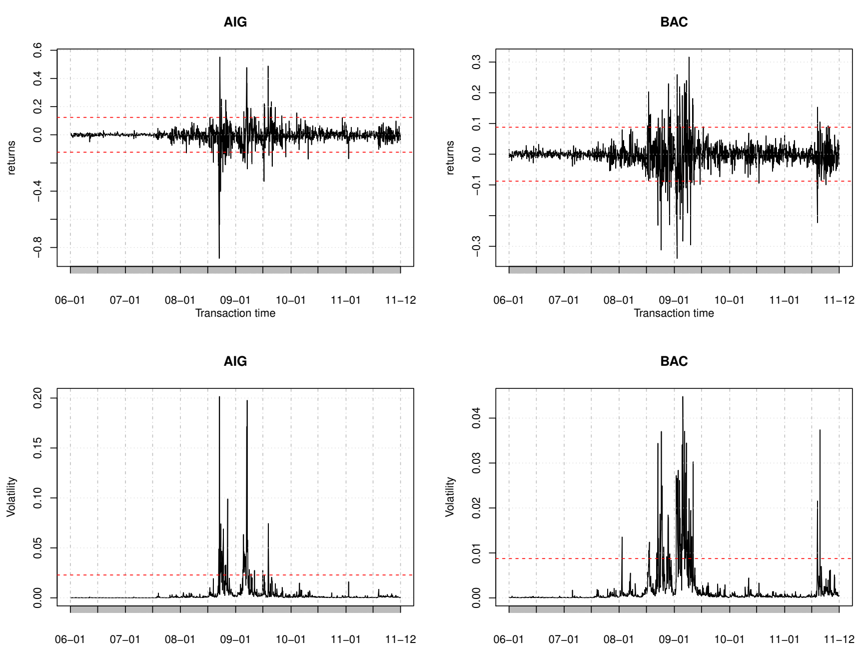

Notes: Jumps are identified when the observed absolute value is bigger than 2× the corresponding standard deviation. Observations out of the two horizontal red dashed lines correspond to jumps.

Figure 1.1 provides such evidence for two stocks namely the American International Group (AIG) and the Bank of America Corporation (BAC). As it is a common pratice, we consider as jumps, observed absolute returns greater than $2 \times standard\ \ deviation$. During the 2006-2008 financial crisis, these stocks experienced respectively 68 and 76 sudden price jumps. Their volatility jumped at least 50 and 75 times respectively.

Standard Diffusion models with stochastic volatility assume that asset log-returns follow a semimartingale dynamics and instantaneous variance follows a Heston (1993) model

$$\begin{aligned} dX_t &= \mu dt + \sqrt{V_t} dB_t \\ dV_t &= \kappa\left(\theta - V_t\right) dt + \eta\rho\sqrt{V_t} dW_t \end{aligned} \tag{1.1}$$

where X_t is the log-price, V_t spot the volatility, B_t and W_t are Wiener processes. This model can't explain large drops in asset markets with volatility variables calibrated to realistic values. Even more unlikely would be to generate crashes that happen in not just one, but multiple markets around nearly the same time and its propagation in time like aftershock effects.

In order to match the crisis data, the first approach proposed in literature was to add a jump component to the diffusion model. However, Eraker (2004) documented that a Poisson jump-diffusion model with stochastic volatility explains neither the large increases observed in the implied volatility following a crisis, nor the systematic variation observed in prices. They concluded that a significantly better fit of the observed data is obtained when the model contains jumps both in price as well as volatility. In an extension of model (1.1), we allow jump component both in price and volatility.

$$\begin{aligned} dX_t &= \mu dt + \sqrt{V_t} dB_t + \boldsymbol{Z_t dN_t} \\ dV_t &= \kappa\left(\theta - V_t\right) dt + \eta\rho\sqrt{V_t} dB_t + \boldsymbol{Z_t^v dN_t^v} \end{aligned} \tag{1.2}$$

where Z_t is the jump size and N_t a poisson point process with rate λ. However, fitting individual crisis data is not the only interesting property a good jump diffusion model must have. It should also be able to model transmission patterns of idiosyncratic shock over time and across assets. We want to emphasize this latter property throughout this paper.

At a portfolio level, shocks tend to cluster serially and cross-sectionnally. A large shock to a given asset at a given time t predicts future large shocks to this asset (known as time series clustering in Polson and Scott (2012), or self-excitation in Aït-Sahalia, Cacho-Diaz, and Leaven (2015)). In addition, an initial large idiosyncratic shock increases the probability of large shocks to other assets (referred as "mutual excitation" in Aït-Sahalia, Cacho-Diaz, and Leaven (2015)). The figure 1.2 exhibits a mutual excitation originated from Lehman Brothers, and oriented to AIG and Morgan Stanley.

Figure 1.2. Price dynamics of Lehman Brothers, AIG and Morgan Stanley during the year 2008.

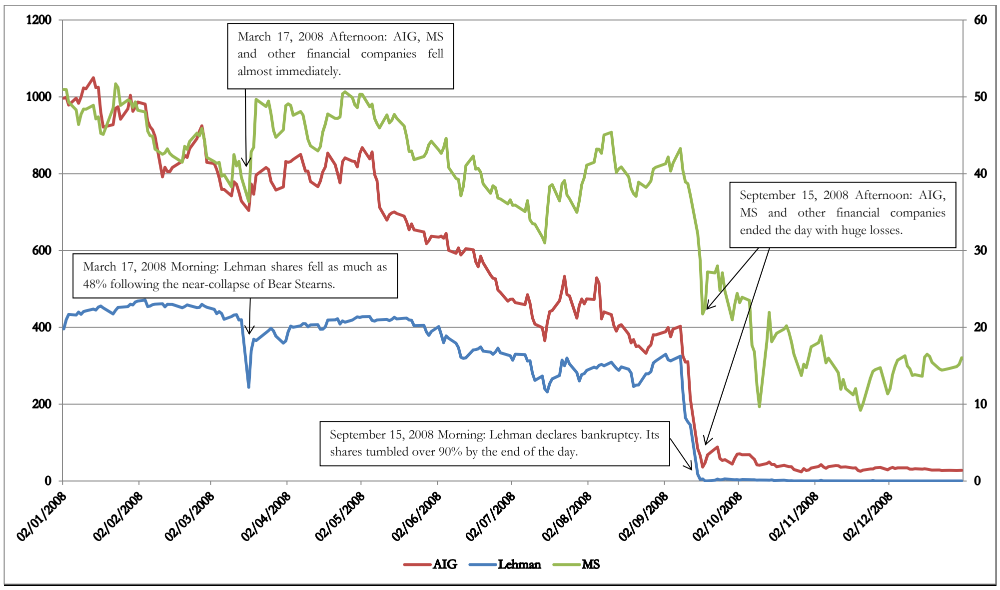

Notes: Mutual excitation originated from Lehman Brothers and was transmitted to AIG, MS and others financial institutions.

Using poisson point processes with constant rates, a jump diffusion model with jumps both in price and volatility can't replicate serial and mutual excitations. However, mutually exciting jump processes with time varying rates, known as Hawkes processes, are natural candidates for modeling this "contagion" phenomenon. To more formally, let $X_t = (X_{1t}, ..., X_{mt})$ be a m-dimensional vector of log-price processes as in equation (1.2). The jump intensity λ_{it} of the point process N_{it} is now defined by:

$$d\lambda_{it} = \alpha_i \left(\lambda_{i\infty} - \lambda_{it}\right) dt + \sum_{j=1}^{m} \beta_{ij} dN_{jt} \tag{1.3}$$

In order for the asset return process to be stationary, we assume that the degree of excitation of various jumps, or jump intensities, mean revert until the next jump with speed α_i. $\lambda_{i\infty}$ is the long term jump intensity. N_{it} is called a Hawkes point process (for more details see Hawkes (1971a), Hawkes (1971b) or Hawkes and David (1974)). Here, the jump intensity of the asset i is affected by its own idiosyncratic jump as well as jump in another asset j.

Since parameters $(\beta_{ij})_{1\leq i,j\leq N}$ are assumed to be positive, any jump in the asset j at time t increases the jump intensity λ_{it} of the asset i by β_{ij}. Thus, after a jump in the asset j at time t, the likelihood of further jumps in the asset i within the time interval $[t; t+\Delta]$ increases by $\beta_{ij}\Delta$, where Δ is the sampling frequency. This specification mostly encompasses the intuition for connectedness and contagion effects, while the common factors are used to model the risk of a failure of the entire system arising from a severe downturn of the economy i.e. correlation effect. Hence, a jump diffusion factor model with Hawkes point processes, provides an ideal framework to model the systemic risk. For future reference, we call $\beta_{ij}, 1 \leq i, j \leq N$, *excitation parameters.*

When a negative jump is observed in a stock price, there are three potential sources: a discontinuous and sudden fall of the price, a sudden explosion of the volatility, or a huge drop in a common factor. The existing literature is unclear whether systemic dependency, during the periods of financial distress, is an evidence of idiosyncratic jump dependencies in price, in volatility, in common factors, or both. For policy decisions, it is important to distinguish between these different sources of systemic risk, as emphasized in De Vries (2005). If the source of systemic risk is the idiosyncratic jump dependency, then interbank exposures must be reduced, but if the causes come from common factors, stabilization macro policies must be carried out. Aït-Sahalia, Cacho-Diaz, and Leaven (2015) showed that a part of the jump transmission dynamic on large stock index returns around the five world regions was explained by Hawkes dynamic in jump price intensity. They didn't allow jumps in volatility. However, volatility is also subject to sudden and explosive movements during the crisis. Maneesoonthorn, Forbes, and Martin (2016) argued that volatility jump intensity is much more informative than the jump price intensity when we are interested in impending financial crisis. In addition, Polson and Scott (2012) pointed that mutually exciting volatility shocks explain an important part of the correlation increase during a crisis. Thus, jump dynamic in volatility channel reveal important feature and must be incorporated into the model.

After controlling for common effects, the incorporation of price and volatility channels for shock transmission permits us to disentangle two different and complementary channels. Through price jump dynamics, we primarily focus on the transmission of market expectation shocks or the propagation of negative market perception (see Diebold and Yilmaz (2015b)): a big decrease in the price of one asset is perceived by investors as having pessimistic information about its future profitability as well as values of similar or correlated assets. As a consequence, it generates a decline in prices of all similar assets. The price jump is transmitted through a common anticipation or through a rational expectation (by investors) of the future price movements. Secondly, the price jump transmission scheme also shed some light on the transmission path of liquidity micro-crises induced by order flow fluctuations (see Joulin, Lefevre, Grunberg, and Bouchaud (2008)) and liquidity shocks: after a sudden loss faced by a given asset, investors use fire sales in other assets to raise cash in order to rebalance their portfolios. The drop in price moves from this asset to others.

On the volatility side, modeling the jump transmission helps to understand how a sudden and large increase in fear, or uncertainty about future profitably, or a huge deterioration of the market expectation of future risks of investors is transmitted. Clements and Todorova (2016) described the volatility jumps as the transmission of behavioral shocks or information flow. Clark (1973) showed from the mixture of distribution hypothesis that return volatility is related to the flow of information into the market. Polson and Scott (2012) describes volatility jumps as a proxy for investor behavior and for changes in the informational efficiency of equity markets. Hence, modeling the volatility jump transmission allows us to study how new information flow propagates through related assets, a point of view also shared by Fernandez-Rodriguez and Sosvilla-Rivero (2016)).

The importance of studying the systemic risk through common factors and jumps both in price and volatility is twofold. Firstly, it provides information to contain the global market risk, defined as the risk associated with the change in the market value of a portfolio. The global market risk inherently depends on the interdependence between constituents of this portfolio. In order to minimize the global portfolio risk, the effective diversification must incorporate different type of linkages between underlying assets, including the tail dependency through jump intensities. The aim of this paper is to provide such useful information in order to optimize market activities such as portfolio allocation, risk management or asset pricing. Secondly, modelling systemic risk is important for the real time monitoring (see Diebold and Yilmaz (2015b)) because it provides strategic information on how news, investor fear, or common expectational behaviour spread and cluster across assets and time. It allows us to also know net receivers or transmitters of different shocks. When formulating economic policy, all this information is essential.

1.1.2 Main Contribution

The existing literature of shock transmission among connected objects are usually modeled through either returns or volatilities (see Diebold and Yilmaz (2015b)). In this paper, we allow connections through their returns as well as their volatilities. This paper is closely related to Aït-Sahalia, Cacho-Diaz, and Leaven (2015) and Maneesoonthorn, Forbes, and Martin (2016), but with several distinctions. We extend their perspectives to the multidimensional setup, without any restriction on the number of assets, fewer structure on jump intensity dynamics, mutually exciting jumps both in price and volatility, and controlling for the systematic risk.

We adopt a factor-modelling approach used in Polson and Scott (2012). By introducing a factor component in the log-price equation, we control co-movements related to fundamentals or the correlation-based risk. It permits us to focus on the two other forms of systemic risk, namely connectedness and financial contagion. Polson and Scott (2012) argued that an increase of the co-movement among asset returns does not necessarily provide evidence of contagion or connectedness, common factors need to be firstly controlled for. Our main contributions are described as follow:

- We provide a reduced-form model for financial systemic risk ;
- We construct a model which distinguishes among different sources of systemic failure such as macro risk drivers or correlation effect (using common factors), connectedness and contagion effects (through mutually exciting jumps both in price and volatility);
- We generalize existing econometric models for financial contagion:
  - Our model has similarities with Maneesoonthorn, Forbes, and Martin (2016), but we are multidimensional with the additional feature of controlling for the systematic risk through common factors;
  - We don't restrict the structure of the excitation matrix and also allow jumps in volatility which is more general than specification considered in Aït-Sahalia, Cacho-Diaz, and Leaven (2015) and it also resolves misspecification and missing variable issues due to imposed restrictions. We also allow additional channels of the shock transmission: volatility jumps and common factors.
- We propose an estimation methodology based on high frequency data for our *"doubly*[3] *Hawkes" jump-diffusion model with factors*.
- We contribute to the growing literature which uses partial information to reconstruct networks: we use excitation parameters to define weighted, directed networks for the

[3]Jumps both in price and volatility based on hawkes point processes

shock transmission. Our methodology is applied to a number of key US banks, insurance companies, and the nine largest S&P sectors during the period 2000-2014. We find that systemic risk has three related but distinct channels: common factors, price and volatility jumps.

1.2 The Continuous Time Model

We model the shock transmission using a doubly-Hawkes jump-diffusion model with common factors, which is a generalization of the models considered in Maneesoonthorn, Forbes, and Martin (2016) and Aït-Sahalia, Cacho-Diaz, and Leaven (2015) as we don't restrict the number of assets in the model and also allow "Hawkes-jump" both in prices and volatility. Now, we will introduce each component of our model.

• ***Prices dynamics:*** Let $X_t = (X_{1t}, ..., X_{mt})$ be the log-price vector at time $t > 0$. We assume that X_t follows a Itô semimartingale with jumps and factors. It is defined on a complete probability space $(\Omega, \Im, \mathbb{P})$. The information filtration is an increasing family of σ-fields, $(\Im_t)_{t\geq 0}$, and satisfies $\mathbb{P}$-completeness and right continuity. Prices are $\Im_t$ measurable and follows the dynamics: $\forall i = 1, ..., m$,

$$dX_{it} = b_i dF_t + dE_{it} = \sum_{k=1}^{K} b_{ik} dF_{kt} + dE_{it} \tag{1.4}$$

$$dF_{kt} = \mu_{_{Fk}} dt + \sqrt{V_{Fkt}} dB_{Fkt} + Z_{Fkt} dN_{Fkt} \tag{1.5}$$

$$dE_{it} = \mu_{_{Ii}} dt + \sqrt{V_{Iit}} dB_{Iit} + Z_{Iit} dN_{Iit} \tag{1.6}$$

where K is the number of factors. The role of common factors dF_t is to control for the *correlation risk*, the failure of the entire system arising from a severe downturn of the economy or drops in fundamentals. Since *systemic risk* is more about the increase of the co-movement above and beyond levels purely justified by fundamentals. After controlling for the correlation risk, our main focus will be on the idiosyncratic part of the model dE_{it}. The log-price dynamic of the asset i can be summarized as

$$\begin{aligned} dX_{it} = &\left(\sum_{k=1}^{K} b_{ik}\mu_{_{Fk}} + \mu_{_{Ii}}\right) dt + \sum_{k=1}^{K} b_{ik}\sqrt{V_{Fkt}} dB_{Fkt} \\ &+ \sqrt{V_{Iit}} dB_{Iit} + \sum_{k=1}^{K} b_{ik} Z_{Fkt} dN_{Fkt} + Z_{Iit} dN_{Iit} \end{aligned} \tag{1.7}$$

The randomness in the price dynamic has two different sources: the diffusion component $\sum_{k=1}^{K} b_{ik}\sqrt{V_{Fkt}}dB_{Fkt} + \sqrt{V_{Iit}}dB_{Iit}$ and the jump component $\sum_{k=1}^{K} b_{ik}Z_{Fkt}dN_{Fkt} + Z_{Iit}dN_{Iit}$. The former is responsible of small movements observed in the price dynamic, while large drops come from the jump component. In the model (1.7), a jump at time t ($dN_{Fkt} = 1$ or $dN_{Iit} = 1$) is felt at time t. But depending on the nature of point processes (N_{Ft} and N_{It}), clustered high or low values of returns can be observed.

• ***Volatility:*** We allow jumps in stochastic volatility processes. The presence of jumps in volatility improves the fit of crisis data relatively to a simple stochastic volatility model (See, e.g., Eraker (2004)). Let V_{Fkt} and V_{Iit} be respectively the volatilities of the factor F_{kt} and the idiosyncratic component E_{it}. By the Feller (1951) representation, we assume that

$$\begin{aligned} dV_{Fkt} &= \kappa_{_{Fk}}\left(\theta_{_{Fk}} - V_{Fkt}\right)dt + \eta_{_{Fk}}\rho_{_{Fk}}\sqrt{V_{Fkt}}dB_{Fkt} \\ &\quad + \eta_{_{Fk}}\sqrt{(1-\rho_{_{Fk}}^2)V_{Fkt}}dW_{Fkt} + Z_{Fkt}^v dN_{Fkt}^v \qquad (1.8) \\ dV_{Iit} &= \kappa_{_{Ii}}\left(\theta_{_{Ii}} - V_{Iit}\right)dt + \eta_{_{Ii}}\rho_{_{Ii}}\sqrt{V_{Iit}}dB_{Iit} \\ &\quad + \eta_{_{Ii}}\sqrt{(1-\rho_{_{Ii}}^2)V_{Iit}}dW_{Iit} + Z_{Iit}^v dN_{Iit}^v \qquad (1.9) \end{aligned}$$

where B_{Fkt}, W_{Fkt}, B_{Iit}, W_{Ikt} are standard Wiener processes, such that $B_{Fkt}\perp W_{Fkt}$, $B_{Iit}\perp W_{Iit}$; Z_{Fkt}, Z_{Iit}, Z_{Fkt}^v, Z_{Iit}^v are respectively random jump sizes of: the price factor component, the price idiosyncratic component, the volatility of the factor component and the volatility of the idiosyncratic component.

A positive jump affecting the volatility at time t mean-reverts with a rate κ. Thus, the volatility remains high in subsequent periods that leads to large variation in prices. Depending on the nature of point processes (N_{Ft}^v or N_{It}^v), we can generate clusters (time series and cross-sectional clusterings) of high volatility values. Our model also allows for the *leverage effect*: a large drop coming from the diffusion part of the model is associated to a large increase of the volatility. Leverage effects are present both in factor and idiosyncratic components, through parameters $\rho_{_{Fk}}$ and $\rho_{_{Ii}}$.

• ***Jump sizes***. The theoretical model doesn't need to impose any restriction on the distribution of jump sizes of prices and volatility: the estimation approach can be a function of these jump size moments. Nevertheless, to move to the data, we need additional information about these jump sizes. As in Maneesoonthorn, Forbes, and Martin (2016), we assume that only positive jumps are observed in the volatility, such that

$$Z^v_{Fkt} \sim \text{Exp}\left(\mu^v_{_{Fk}}\right)$$
$$Z^v_{Iit} \sim \text{Exp}\left(\mu^v_{_{Ii}}\right)$$

The choice of the exponential distribution to model the volatility jump size is common in the literature (see Eraker (2004) or Todorov and Tauchen (2011)). The probality distribution functions of the price jump sizes Z_{Fkt} and Z_{Iit} satisfy the following equations, as in Aït-Sahalia, Cacho-Diaz, and Leaven (2015) and Kou and G. (2002):

$$F_{Z_{Fk}}(x) = \begin{cases} p_{_{Fk}} e^{-\gamma_{_{Fk1}}(-x)}, -\infty < x \leq 0 \\ p_{_{Fk}} + (1-p_{Fk})(1-e^{-\gamma_{_{Fk2}}(-x)}), 0 < x \leq \infty \end{cases}, \quad \forall k = 1, ..., K \tag{1.10}$$

$$F_{Z_{Ii}}(x) = \begin{cases} p_{_{Ii}} e^{-\gamma_{_{Ii1}}(-x)}, -\infty < x \leq 0 \\ p_{_{Ii}} + (1-p_{_{Ii}})(1-e^{-\gamma_{_{Ii2}}(-x)}),\ 0 < x \leq \infty \end{cases}, \quad \forall i = 1, ..., m \tag{1.11}$$

where $p_{_{Ii}}$ and $(1-p_{_{Ii}})$ represent the probabilities of downward and upward jumps (The same explanation holds for $p_{_{Fk}}$ and $(1-p_{_{Fk}})$). $\gamma_{_{Ii1}}$ and $\gamma_{_{Ii2}}$ can be interpreted as follow: for the jump size Z_{Ii},

$$Z_{Ii} =^d \begin{cases} -\xi_1, \quad \text{with} \quad \text{probability} \quad p_{Ii} \\ \xi_2, \quad \text{with} \quad \text{probability} \quad (1-p_{Ii}) \end{cases}$$

such that ξ_1, and ξ_2 are exponential random variables with means $1/\gamma_{_{Ii1}}$ and $1/\gamma_{_{Ii2}}$, respectively. In others words, the size of downward jumps follows the opposite of an exponential distribution with rate $\gamma_{_{Ii1}}$ and the probability distribution of the size of upward jumps follows an exponential distribution with ate $\gamma_{_{Ii2}}$. The same interpretation holds, of course, for $\gamma_{_{Fk1}}$ and $\gamma_{_{Fk2}}$. As a result, the moments of these jump sizes satisfy

$$E[Z^l_{Fk}] = (-1)^l \frac{l! p_{Fk}}{\gamma^l_{Fk1}} + \frac{l!(1-p_{Fk})}{\gamma^l_{Fk2}}, \quad l = 1, 2, ... \tag{1.12}$$

$$E[Z^l_{Ii}] = (-1)^l \frac{l! p_{Ii}}{\gamma^l_{Ii1}} + \frac{l!(1-p_{Ii})}{\gamma^l_{Ii2}}, \quad l = 1, 2, ... \tag{1.13}$$

• ***Homogeneous poisson point processes***. In the factor component, we assume that jumps in price and volatility are compounded poisson processes. This is a simplifying assumption as we are more focused on the contagion and connectedness effects. Thus, we assume that N_{Fkt} and N^v_{Fkt} are homogeneous poisson point processes, with rates λ_{Fk} and λ^v_{Fk}, such that:

$$dN_{Fkt} \sim \text{Poisson}\left(\lambda_{Fk} dt\right) \tag{1.14}$$

$$dN^v_{Fkt} \sim \text{Poisson}\left(\lambda^v_{Fk} dt\right) \tag{1.15}$$

• ***Hawkes processes***. The model must replicate types of clusterings observed in the real data: time series clustering (or self-excitation) and cross-sectional clustering (or mutual excitation). To achieve this important feature, we emphasize on the dynamic of jump intensity which is just a measure of the probability of observing a jump per unit of time interval. The systemic risk is summarized as follow: a jump in a firm j increases the probability of observing a jump in any other firm i in the nearest future, i.e increases the jump intensity of any other firm i. Thus, idiosyncratic point processes N_{Iit} and N^v_{Iit}, must have time varying jump intensities λ_{it} and λ^v_{it} defining by

$$\mathbb{P}\left[N_{it+\Delta} - N_{it} = 0 | \Im_t\right] = 1 - \lambda_{Iit}\Delta + o(\Delta) \tag{1.16}$$

$$\mathbb{P}\left[N_{it+\Delta} - N_{it} = 1 | \Im_t\right] = \lambda_{Iit}\Delta + o(\Delta) \tag{1.17}$$

$$\mathbb{P}\left[N_{it+\Delta} - N_{it} > 1 | \Im_t\right] = o(\Delta) \tag{1.18}$$

$$\mathbb{P}\left[N^v_{it+\Delta} - N^v_{it} = 0 | \Im_t\right] = 1 - \lambda^v_{Iit}\Delta + o(\Delta) \tag{1.19}$$

$$\mathbb{P}\left[N^v_{it+\Delta} - N^v_{it} = 1 | \Im_t\right] = \lambda^v_{Iit}\Delta + o(\Delta) \tag{1.20}$$

$$\mathbb{P}\left[N^v_{it+\Delta} - N^v_{it} > 1 | \Im_t\right] = o(\Delta) \tag{1.21}$$

where Δ is the sampling frequency or the time between two observations. Jump intensities λ_{it} and λ^v_{it} can also be interpreted as the average number of jumps per unit of time interval. We assume that they are time-varying and path-dependent respectively on the point processes N_{it} and N^v_{it}, with the following mean-reverting dynamics

$$d\lambda_{Iit} = \alpha_i \left(\lambda_{Ii\infty} - \lambda_{Iit}\right) dt + \sum_{j=1}^{m} \beta_{ij} dN_{Ijt} \tag{1.22}$$

$$d\lambda^v_{Iit} = \alpha^v_{Ii} \left(\lambda^v_{Ii\infty} - \lambda^v_{Iit}\right) dt + \sum_{j=1}^{m} \beta^v_{ij} dN^v_{jt} \tag{1.23}$$

Under the mean-reverting assumption of jump intensities λ_{it} and λ^v_{it}, asset returns process will be stationary. The jump intensity λ_{Iit} (respectively λ^v_{Iit}) of the asset i also increases with his own jumps as well as jump in other related asset j. More specifically, any price (repectively volatility) jump affecting j at time t, i.e, $dN_{jt} = 1$ (respectively $dN^v_{jt} = 1$), increases the probability of furthers jumps in i by $\beta_{ij}\Delta$ (respectively $\beta^v_{ij}\Delta$) within the time interval $[t; t+\Delta]$.

The parameters $(\beta_{ij})_{1\leqslant i,j\leqslant m}$ (respectively $\left(\beta^v_{ij}\right)_{1\leqslant i,j\leqslant m}$) are called "*excitation parameters*" and will be of a particular interest for the construction of network maps for shock transmission. For instance, if we consider two assets i and j, β_{ij} (respectively β^v_{ij}) summarizes information about the tail dependence between i and j. When $\beta_{ij} \neq 0$ (respectively $\beta^v_{ij} \neq 0$) a shock to j significantly affects i. Thus, there exists an edge between i and j summarizing the shock transmission pattern. The type of dependency summarizes by β_{ij} (respectively β^v_{ij}) is far beyond and above *the correlation* at least for three reasons. Firstly, it is a tail dependency, since the link between i and j is captured only for extreme events. Secondly, returns are allowed to have fat tails, and the direct consequence is the failure of the normality assumption of asset returns and the useless of the correlation as a measure of the dependency between assets. Thirdly, correlation measures the dependency between only two assets, but the excitation parameters $(\beta_{ij})_{1\leqslant i,j\leqslant m}$ and $(\beta^v_{ij})_{1\leqslant i,j\leqslant m}$ will provide information on the dependence structure between m assets (m is unrestricted). This matrix doesn't need to be symmetric, since the impact of the asset i on j is not necessary the same than the one of j on i. As an example, Aït-Sahalia, Cacho-Diaz, and Leaven (2015) found that: "When the US stock market jumps, there is a strong increase in the probability of a consecutive jump in other regions of the world...There is no evidence for the reverse transmission".

• ***Assumptions on factors***. Conditional on the information set $\Im_t$ available at time t, factors are assumed to be uncorrelated with each other, and uncorrelated to the idiosyncratic component. More precisely, we assume that

$$\operatorname{Corr}\left(dB_{Fkt}, dB_{Fk't} | \Im_t\right) = 0, \quad \forall k \neq k'; \tag{1.24}$$

$$\operatorname{Corr}\left(dB_{Fkt}, dB_{Iit} | \Im_t\right) = 0, \quad \forall k, \forall i; \tag{1.25}$$

$$\operatorname{Corr}\left(dB_{Iit}, dB_{Ijt} | \Im_t\right) = 0, \quad \forall i \neq j; \tag{1.26}$$

same assumptions hold for dW_{Fkt} and dW_{Iit}.

• ***Additional assumptions***. We further assume that for factors and idiosyncratic components, B, N and Z are mutually independent:

$$B \perp N \perp Z \tag{1.27}$$

Our model is a multidimensional model which combine into the same framework a factor structure and a multivariate Hawkes jump-diffusion model with jumps both in price and volatility. Throughout the paper, we will refer to our model as *"doubly Hawkes" jump-diffusion model with factors*. With this machinary, we are able to take into account different channels for systemic risk. All the information about the network maps of the systemic risk is contained into the excitation parameters $(\beta_{ij})_{1\leqslant i,j\leqslant m}$ and $(\beta^v_{ij})_{1\leqslant i,j\leqslant m}$. These excitation paramters will be used to construct network maps for shock transmission. The main challenges now is to estimate the entire model and in particular get consistent estimates of excitation parameters.

Notation: Let $u = (u_1, ..., u_p)$ be a vector. Throughout the paper, we call $\overline{D}_g(u)$ the diagonal matrix with u as the diagonal:

$$\overline{D}_g(u) = \begin{pmatrix} u_1 & ... & 0 \\ & \ddots & \\ 0 & ... & u_p \end{pmatrix} \tag{1.28}$$

If b is a $m \times K$ matrix, we call b_i the row number i of b, and b'_i the transpose of b_i.

1.3 Estimation of the Model

1.3.1 Parameters

The model is high-dimensional in term of parameters to estimate. Without any restriction, there are $2m^2 + mK + 13m + 11K$ parameters, where m is the number of assets and K the number of factors. Parameters of the model are summarized into the following table

Table 1.1. Parameters

b_{ik}	μ_{Fk}	η_{Fk}	μ_{Ii}	κ_{Fk}	θ_{Fk}	γ_{Ii2}	ρ_{Fk}	κ_{Ii}	θ_{Ii}	μ^v_{Ii}	ρ_{Ii}	λ_{Fk}	λ^v_{Fk}
α_{Ii}	$\lambda_{Ii\infty}$	β_{ij}	α^v_{Ii}	$\lambda^v_{Ii\infty}$	β^v_{ij}	γ_{Ii1}	γ_{Fk2}	p_{Ii}	γ_{Fk1}	μ^v_{Fk}	p_{Fk}	η_{Ii}	

The model is estimated via GMM as in Aït-Sahalia, Cacho-Diaz, and Leaven (2015): we compute a set of moment equations incorporating all the parameters, including parameters of the latent equations (volatility and jump intensity parameters). The moment equations are derived in closed forms. Thus, it is easy to find good estimators for the moments and optimization routine is fast. The choice of the GMM estimation approach is justified by the stationary assumption of the model, and the infeasibility of other procedures as the MLE.

Since the model is highly parametric (large number of parameters), we need large number of moment conditions for the estimation. To achieve this goal, our estimation equations incorporate both moments of returns, moments of integrated volatity and quadratic variation (Henceforth, IV and QV), and their autocorrelation functions. Since the integrated volatity and quadratic variation are unobserved variables, we rely on high frequency data for consistent estimations. They are approximated using realized power variation measures. The underlying assumption is that, the sample of high frequency data available is sufficiently large in order to approximate the integrated volatity and the quadratic variation by their respective realized power variation estimators.

1.3.2 Moment Conditions

The estimation strategy is based on moments relevant in financial studies: the variance, the skewness, the kurtosis, autocovariance of returns, autocovariance of squared returns, mean of integrated volatilities, mean of quadratic variations, mean of the squared integrated volatilities, mean of the squared quadratic variation, autocovariance of integrated volatilities and autocovariance of quadratic variations. Due to large number of parameters, there is a need of a lot of relevant moment conditions in order to render the estimation procedure feasible. Integrated moments provide those additional relevant moments and the availability of high frequency data gives us the possibility to accurately estimate intergrated moments.

In general, the first moment provides information about drift parameters. Centered moment of order 3 and 4 isolate parameters of the jump component up-to the factor loading vector b, while moment of order 2 places contributions from the diffusive and jump components of the model on the same order. Diffusive parameters are identified by the moment of the integrated volatility $\mathbb{E}\left[\mathrm{IV}_i\right]$, while jump parameters are isolated by considering differences: $\mathbb{E}\left[\mathrm{QV}_i\right] - \mathbb{E}\left[\mathrm{IV}_i\right]$, $\mathbb{E}\big[\mathrm{QV}_{it}\mathrm{QV}_{it+\tau}\big] - \mathbb{E}\big[\mathrm{IV}_{it}\mathrm{IV}_{it+\tau}\big]$, $\forall i = 1, ..., m$ and $\forall \tau > 0$. Here is quick summary of moments used:

- $\mathbb{E}\left[\Delta X_{it}\right], \forall i = 1, ..., m;$

- $\mathbb{E}\big[\,(\Delta X_{i,t} - \mathbb{E}[\Delta X_{i,t}])^r\,\big], \forall i = 1, ..., m; r = 2, 3, 4;$

- $\mathbb{E}\big[\,(\Delta X_{i,t} - \mathbb{E}[\Delta X_{i,t}])^r\,(\Delta X_{j,t} - \mathbb{E}[\Delta X_{j,t}])^s\,\big], \forall i \neq j; r + s \leq 4;$

- $\mathbb{E}\big[(\Delta X_{it}^r - \mathbb{E}[\Delta X_{it}^r])(\Delta X_{jt+\tau}^r - \mathbb{E}[\Delta X_{jt+\tau}^r])\big]$, $\forall i, j = 1, ..., m; r = 1, 2;$

- $\mathbb{E}\left[\mathrm{IV}_i\right], \mathbb{E}\left[\mathrm{QV}_i\right] - \mathbb{E}\left[\mathrm{IV}_i\right], \forall i = 1, ..., m;$

- $\mathbb{E}\big[\mathrm{QCov}_{ij}\big], \mathbb{E}\big[\mathrm{ICov}_{ij}\big], \forall i \neq j;$

- $\mathbb{E}\big[\mathrm{IV}_i^2\big], \mathbb{E}\left[\mathrm{QV}_i^2\right], \forall i = 1, ..., m;$

- $\mathbb{E}\big[\mathrm{QV}_{it}\mathrm{QV}_{jt+\tau}\big] - \mathbb{E}\big[\mathrm{IV}_{it}\mathrm{IV}_{jt+\tau}\big], \forall i \neq j, \tau = 1, ..., 6.$

1.3.3 Estimation Methodology

Let's denote, θ_0 the set of model parameters, Δ_0 the sampling frequency, $X_{n_0\Delta_0}$ the stock price vector at time $n_0\Delta_0 \in [0, T]$, s.t., $n_0 = 1, ..., N_0$, $N_0\Delta_0 = T$. Each price vector $X_{n_0\Delta_0}$ is observed N_0 times at a high frequency Δ_0. As $\{X_{n_0\Delta_0}, n_0 = 1, ..., N_0\}$ is also used to compute estimators of the integrated volatility (IV) and the quadratic variation (QV), Δ_0 should be to be sufficiently small such that errors coming from approximations of integrated quantities by realized measures are neglected. It appears that $X_{n_0\Delta_0}$ and IV (or QV) may have different frequencies. We take as final frequency Δ, the smallest one. Let N be the number of observations for each variable at the frequency Δ; $U_{n\Delta}$, $n = 1, ..., N$, the value at time $n\Delta \in [0, T]$ of the vector of variables available for the estimation , s.t. $N\Delta = T$ ($U_{n\Delta}$ contains stock prices, and realized measures). Then, we can summarazie our moment condition as

$$\mathbb{E}\big[f(U_{n\Delta}, \theta_0)\big] = 0 \qquad (1.29)$$

where function f is just the vector with all moment conditions mentioned in previous subsection. Let's define

$$f_N(\theta_0) = \frac{1}{N}\sum_{n=1}^{N} f(U_{n\Delta}, \theta_0) \tag{1.30}$$

The GMM estimator $\hat{\theta}$ of θ_0 is given by

$$\hat{\theta} = \arg\min_{\theta\in\Theta} f_N(\theta)\hat{W} f_N(\theta) \tag{1.31}$$

where $\hat{W}$ is a positive definite weight matrix such that $\hat{W} \xrightarrow{p} W$, and W is a positive definite matrix. The choice of $\hat{W}$ is irrelevant when the number of moment equations is exactly equal to the number of parameters to estimate. In other cases, $\hat{W}$ need to be chosen optimally. Since moment conditions are persistent in the presence of stochastic volatility, some care is needed for $\hat{W}$. Following Aït-Sahalia, Cacho-Diaz, and Leaven (2015), $\hat{W}$ is chosen using the following steps:

(i) Set $\hat{W} = I$, with I the identity matrix.

(ii) Consider $\tilde{\theta}$ the solution of (1.31) corresponding to $\hat{W} = I$.

(iii) Define $\hat{S}_N = \hat{\Gamma}_{0,N} + \sum_{\nu=1}^{q}\left(1 - \frac{\nu}{q+1}\right)\left(\hat{\Gamma}_{\nu,N} + \hat{\Gamma}'_{\nu,N}\right)$, the *Newey-West* covariance estimator with $\hat{\Gamma}'_{\nu,N} = \frac{1}{N}\sum_{n=\nu+1}^{N} f(U_{n\Delta}, \tilde{\theta}) f(U_{n\Delta}, \tilde{\theta})'$.

(iv) $\hat{S}_N^{-1}$ is an optimal estimator of $\hat{W}$.

The equation (1.31) doesn't admit an analytical solution. We need to rely on numerical optimization to resolve this problem. Also, the objective function $f_N(\theta)\hat{W} f_N(\theta)$ is highly non-linear and not necessary a convex function: local minimums are possible. Thus, there is a dependency to the initial value when minimizing this objective function. To overcome this issue, a minimization procedure with a multiplicity and clever choices of starting points should be carried out. In order to estimate the diffusion and the jump part of the model, we will use a three-steps procedure as in Aït-Sahalia, Cacho-Diaz, and Leaven (2015):

Setp 1 Remove all the jumps present into the data, and estimate the resulting diffusion model;

Setp 2 Coefficients of the first step are kept fixed while estimating the parameters of the discontinuous part of the model;

Setp 3 Coefficients obtained in steps 1 and 2 are used as starting values for the estimation of the global model.

Aït-Sahalia, Cacho-Diaz, and Leaven (2015) provided evidence that this three-steps estimation procedure delivers parameter estimates with sufficient degree of precision in a realistic context.

1.3.4 Moment Equations

In this sub-section, we provide closed form expressions of our moment equations. As a preliminary step, we need to derive explicit expressions for the first and second unconditional moment of volatilities: $\mathbb{E}[V_{Fk}]$, $\mathbb{E}[V_{Ii}]$, and $\mathbb{E}[V_{Fk}^2]$ as most of our moment equations are function of these quantities.

Lemma 1.3.1 *Under assumptions (1.4) - (1.27) of the model, the following equations hold:*

$$\mathbb{E}[V_{Fk}] = \theta_{Fk} + \frac{\mathbb{E}[Z_{Fk}^v]\lambda_{Fk}^v}{\kappa_{Fk}} \tag{1.32}$$

$$\mathbb{E}[V_{Ii}] = \theta_{Ii} + \frac{\mathbb{E}[Z_{Ii}^v]\mathbb{E}[\lambda_{Ii}^v]}{\kappa_{Ii}} \tag{1.33}$$

$$\mathbb{E}\big[V_{Fk}^2\big] = \theta_{Fk}\mathbb{E}[V_{Fk}] + \frac{\eta_{Fk}^2\mathbb{E}[V_{Fk}]}{2\kappa_{Fk}} + \frac{\mathbb{E}[V_{Fk}]\mathbb{E}[Z_{Fk}^v]\lambda_{Fk}^v}{\kappa_{Fk}} + \frac{\mathbb{E}\big[(Z_{Fk}^v)^2\big]\lambda_{Fk}^v}{2\kappa_{Fk}} \tag{1.34}$$

where $\mathbb{E}[\lambda_{Ii}^v]$ is the solution of the following equation

$$\begin{pmatrix} \mathbb{E}\left[\lambda_{I1}^v\right] \\ \vdots \\ \mathbb{E}\left[\lambda_{\mathrm{Im}}^v\right] \end{pmatrix} = \left[\overline{D}_g\left(\alpha_I^v\right) - \beta^v\right]^{-1} \begin{pmatrix} \alpha_{I1}^v\lambda_{I1\infty}^v \\ \vdots \\ \alpha_{IN}^v\lambda_{IN\infty}^v \end{pmatrix} \tag{1.35}$$

Since $Z_{Fkt}^v \sim \mathrm{Exp}\left(\mu_{Fk}^v\right)$ and $Z_{Iit}^v \sim \mathrm{Exp}\left(\mu_{Ii}^v\right)$, we have $\mathbb{E}\big[(Z_{Fkt}^v)^l\big] = \frac{l!}{(\mu_{Fk}^v)^l}$ and $\mathbb{E}\big[(Z_{Iit}^v)^l\big] = \frac{l!}{(\mu_{Ii}^v)^l}$.

Due to the presence of a jump component in the volatility (both for factor and idiosyncratic volatilities), its unconditional first and second moments contain two components: a continuous part, and a jump term. The later is a function of the volatility jump size, the average jump intensity and the volatility mean-reversing parameter. When we focus on the unconditional moments of the idiosyncratic volatility V_{Ii}, we observe that excitation parameters β^v_{ij} appear through the first moment of its jump intensity, $\mathbb{E}[\lambda^v_{Ii}]$.

Another unavoidable quantity in the computation of moment equations in closed forms is *the covariance density matrix* of a stationary $m-variate$ point process.

Definition 1.3.1 *Let's consider a stationary m-variate point process N_{It}, where N_{Iit} represents the cumulative number of jumps in the i^{th} asset price idiosyncratic component up to time t. Its* ***covariance density matrix*** *is defined by*

$$R_I(\tau) = \mathbb{E}\left[\frac{dN_{It+\tau}}{dt}\frac{dN_{It}^T}{dt}\right] - \mathbb{E}[\lambda_{It}]\mathbb{E}[\lambda_{It}]^T, \quad \forall\tau > 0 \tag{1.36}$$

where M^T is the transpose of M and $R_I(-\tau) = R_I(\tau)^T$. Since there is an atom at 0, R_I is not defined on the whole $\mathbb{R}$. Hawkes(1971) extended this function to $\mathbb{R}$ by defining ***the complete covariance density***

$$R_I(\tau)^{(c)} = D\delta(\tau) + R(\tau) \tag{1.37}$$

With $D = \overline{D}_g\left(\mathbb{E}[\lambda_{I1}], ..., \mathbb{E}[\lambda_{Im}]\right)$, $\delta(\tau)$ the Dirac delta function (it takes the value 1 at 0 and 0 elsewhere). $R_I(0)$ is such that $R_I()^{(c)}$ is continuous everywhere.

When jump point processes are homogeneous poisson point processes, the covariance density matrix is null, since poisson point processes have independent increment by definition. But, with Hawkes point processes, this matrix is non null. Due to its omnipresence in our moment equations, it need to be computed in closed form. The following theorem provides such results.

Theorem 1.3.1 *Let N_{It} be a stationary m-variate point process. We assume that jumps cannot occur multiply such that $\mathbb{E}[dN_{it}^2] = \mathbb{E}[dN_{it}]$, $\forall i = 1, ..., m$. Under the assumptions (1.4) - (1.27) of the model, the covariance density matrix R_I is given by*

$$R_I(\tau) = e^{(\beta-\alpha)\tau}\left(\bar{\Lambda}_\infty + \beta D\right), \quad \forall\tau > 0 \tag{1.38}$$

and $R_I(-\tau) = R_I(\tau)^T, \quad \forall\tau > 0$, where $\bar{\Lambda}_\infty$ is the solution of the Lyapounov matricial equation given by

$$(\beta-\alpha)\bar{\Lambda}_\infty + \bar{\Lambda}_\infty(\beta-\alpha)^T + \beta D\beta = 0 \tag{1.39}$$

With $\beta = (\beta_{Iij})_{1\leqslant i,j\leqslant m}$ the matrix of excitation parameters, $\alpha = \overline{D}_g\left(\alpha_{I1},...,\alpha_{Im}\right)$ and $D = \overline{D}_g\left(\mathbb{E}[\lambda_{I1}],...,\mathbb{E}[\lambda_{Im}]\right)$.
Similar results hold for the stationary m-variate point process N^v_{It}, where N^v_{Iit} represents the cumulative number of jumps in the i^{th} asset price idiosyncratic volatility component up to time t.

Closed form expression of the covariance density matrix provided in the Theorem 1.3.1 is derived using results from Fonseca and Zaatour (2015). They provided a methodology for computing moments and autocorrelation functions of the number of jumps over a time period. Their approach relies on the infinitesimal generator of the process and Dynkin's formula. They extend results in Hawkes (1971b) by relaxing restrictions on the excitation matrix β. Expressions of moment conditions contain the previous covariance density matrix through some double integrals. We need to compute them in closed-forms. The following corollary provides these useful formulae.

Corollary 1.3.1 *Under assumptions (1.4) - (1.27) of the model, following equalities hold*

$$\int_0^{\Delta}\int_0^{s} R_I(t-s)dtds = \left[\bar{\Lambda}_\infty + \beta D\right]^T \frac{\Delta^2}{2} \tag{1.40}$$

$$\int_0^{\Delta}\int_{\tau}^{\Delta+\tau} R_I(s-t)dtds = \left[e^{(\beta-\alpha)\tau}\left(\bar{\Lambda}_\infty + \beta D\right)\right]^T \Delta^2 \tag{1.41}$$

$$\begin{aligned}\int_t^{t+1}\int_{t+\tau}^{t+\tau+1} R_I(u-s)dsdu = \Big[&\left(I - e^{-(\beta-\alpha)}\right)(\beta-\alpha)^{-2} \\ &\left(e^{(\beta-\alpha)(\tau+1)} - e^{(\beta-\alpha)\tau}\right)\left(\bar{\Lambda}_\infty + \beta D\right)\Big]^T\end{aligned} \tag{1.42}$$

From the corollary 1.3.1, the first, second and third integrals are used to compute respectively moments of returns, autocovariance functions of returns and autocovariance functions of integrated measures. They have a central contribution in the identification and estimation of the jump intensity parameters, namely: the matrix β of excitation parameters, the vector of mean-reversing parameters α, and the vector of long term jump intensities λ_∞.

Moment equations based on returns we use in this paper are derived using the Itô's Lemma for jump-diffusion processes. We recall this lemma.

Definition 1.3.2 *Let U_t, $t \geq t_0$ be a jump-diffusion process with the following dynamic*

$$U_t = U_{t_0} + \int_{t_0}^{t} b(s, U_{s^-})ds + \int_{t_0}^{t} \sigma(s, U_{s^-})dW_s + \sum_{n=1}^{N(t)} \Delta U_n \tag{1.43}$$

where $b(t, U_{t-})$ and $\sigma(t, U_{t-})$ are two non-anticipating processes (adapted to a filtration) with $\mathbb{E}_{t_0}\left[\int_{t_0}^{t} \sigma(s, U_{s^-})^2 ds\right] < \infty$, $\Delta U_n = U_{T_n} - U_{T_{n-}}$ and T_n, $n = 1, ..., N(t)$ are the jump times, $U_t = \lim\limits_{s \downarrow t} U_s$ and $U_{t-} = \lim\limits_{s \uparrow t} U_s$. Then, for any $C^{1,2}$ function $f : [0, \infty) \times \mathbb{R} \longrightarrow \mathbb{R}$

$$\begin{aligned} f(t, U_t) = f(t_0, U_{t_0}) &+ \int_{t_0}^{t} \left[\frac{\partial f}{\partial s}(s, U_{s^-}) + \frac{\partial f}{\partial U}(s, U_{s^-})b(s, U_{s^-})\right] ds \\ &+ \int_{t_0}^{t} \frac{\partial f}{\partial X}(s, U_{s^-})\sigma(s, U_{s^-})dW_s + \int_{t_0}^{t} \frac{1}{2}\frac{\partial^2 f}{\partial X^2}(s, U_{s^-})\sigma^2(s, U_{s^-})ds \\ &+ \sum_{n=1, T_n \leq t}^{N(t)} \left[f\left(T_n, U_{T_{n^-}} + \Delta U_n\right) - f\left(T_n, U_{T_{n^-}}\right)\right] \end{aligned} \tag{1.44}$$

For more material about the Itô lemma for jump-diffusion process, the reader can rely on Crosby (2012). The Itô lemma is applied on the return process defined for the asset i within $[0, \Delta]$ by

$$\begin{aligned} r_{i,\Delta} = \left(\sum_{k=1}^{K} b_{ik}\mu_{Fk} + \mu_{Ii}\right)\Delta &+ \sum_{k=1}^{K} b_{ik} \int_0^{\Delta} \sqrt{V_{Fkt}} dB_{Fkt} \\ &+ \int_0^{\Delta} \sqrt{V_{Iit}} dB_{Iit} + \sum_{k=1}^{K} b_{ik} \int_0^{\Delta} Z_{Fkt} dN_{Fkt} + \int_0^{\Delta} Z_{Iit} dN_{Iit} \end{aligned} \tag{1.45}$$

Moment equations are provided in closed forms up to the order Δ^2 (Δ is the sampling frequency or the time between two observations) for moments of log-returns, and in complete close form for integrated moments.

Theorem 1.3.2 *Under assumptions (1.4) - (1.27), our model implies the following moment* *equations of log-returns up to the order* Δ^2*:*

$$\mathbb{E}\left[\Delta X_{i,t}\right] = \Big\{ b_i\mu_F + \mu_{Ii} + b_i\mathbb{E}\big[\overline{D}_g(Z_F)\big]\lambda_F + \mathbb{E}[Z_{Ii}]\mathbb{E}[\lambda_{Ii}] \Big\}\,\Delta + o(\Delta^2) \tag{1.46}$$

$$\begin{aligned}\mathbb{E}\big[\,(\Delta X_{i,t} - \mathbb{E}\left[\Delta X_{i,t}\right])^2\,\big] &= \Big\{ b_i\mathbb{E}\big[\overline{D}_g(V_F)\big]b_i^{'} + \mathbb{E}[V_{Ii}] + b_i\mathbb{E}\big[\overline{D}_g(Z_F)^2\big]\overline{D}_g(\lambda_F)b_i^{'} \Big\}\,\Delta \\ &\quad + \mathbb{E}\big[Z_{Ii}^2\big]\mathbb{E}[\lambda_{Ii}]\Delta + 2\mathbb{E}[Z_{Ii}]^2 \int_{s=0}^{\Delta}\int_{t=0}^{s} R_{Iii}(t-s)dtds + o(\Delta^2)\end{aligned} \tag{1.47}$$

$$\begin{aligned}\mathbb{E}\big[\,(\Delta X_{i,t} - \mathbb{E}\left[\Delta X_{i,t}\right])^3\,\big] &= \Big\{ b_i\overline{D}_g(b_i)\mathbb{E}\big[\overline{D}_g(Z_F)^3\big]\overline{D}_g(\lambda_F)b_i^{'} + \mathbb{E}\big[Z_{Ii}^3\big]\mathbb{E}[\lambda_{Ii}] \Big\}\,\Delta \\ &\quad + \frac{3}{2}b_i\overline{D}_g(b_i)\overline{D}_g(\eta_F)\overline{D}_g(\rho_F)\overline{D}_g(\mathbb{E}[V_F])b_i^{'}\Delta^2 + \frac{3}{2}\eta_{Ii}\rho_{Ii}\mathbb{E}[V_{Ii}]\Delta^2 \\ &\quad + 6\mathbb{E}\big[Z_{Ii}^2\big]\mathbb{E}[Z_{Ii}] \int_{s=0}^{\Delta}\int_{t=0}^{s} R_{Iii}(t-s)dtds + o(\Delta^2)\end{aligned} \tag{1.48}$$

$$\begin{aligned}\mathbb{E}\big[\,(\Delta X_{i,t} - \mathbb{E}\left[\Delta X_{i,t}\right])^4\,\big] &= \Big\{ b_i\overline{D}_g(b_i)^2\mathbb{E}\big[\overline{D}_g(Z_F)^4\big]\overline{D}_g(\lambda_F)b_i^{'} + \mathbb{E}\big[Z_{Ii}^4\big]\mathbb{E}[\lambda_{Ii}] \Big\}\,\Delta + 3\Big\{\mathbb{E}[V_{Ii}] \\ &\quad + b_i\mathbb{E}\big[\overline{D}_g(V_F)\big]b_i^{'} + b_i\mathbb{E}\big[\overline{D}_g(Z_F)^2\big]\overline{D}_g(\lambda_F)b_i^{'} + \mathbb{E}\big[Z_{Ii}^2\big]\mathbb{E}[\lambda_{Ii}]\Big\}^2\Delta^2 \\ &\quad + 3\Big\{ b_i\overline{D}_g(b_i)\mathrm{Var}\big[\overline{D}_g(V_F)\big]b_i^{'} + \mathbb{E}\big[V_{Ii}^2\big] - \mathbb{E}[V_{Ii}]^2 \Big\}\,\Delta^2 \\ &\quad + \Big\{ 6\mathbb{E}\big[Z_{Ii}^2\big]^2 + 4\mathbb{E}[Z_{Ii}]\mathbb{E}\big[Z_{Ii}^3\big] \Big\} \int_{s=0}^{\Delta}\int_{t=0}^{s} R_{Iii}(t-s)dtds + o(\Delta^2)\end{aligned} \tag{1.49}$$

where Var *of a matrix is component wise. Some moments of* V_I *and* V_F *are given by the lemma 1.3.1, explicit formula of* $\mathbb{E}[V_{Ii}^2]$ *is available in the appendix, equation 1.71;* $\int_{s=0}^{\Delta}\int_{t=0}^{s} R_{Iij}(t-s)dtds$ *is the element in row* i *and column* j *of the matrix* $\int_{s=0}^{\Delta}\int_{t=0}^{s} R_I(t-s)dtds$ *as defined in corollary 1.3.1.*

Rare and extreme movements dominate the higher-order moments of the unconditional return distribution. More specifically, once centred, moment of order 3 and 4 isolate parameters of the jump component up-to the factor loading vector b, while moment of order 2 places the contributions from the diffusive and jump components of the model on the same order. This feature will facilitate the identification of parameters of the model. Under our specification, each moment equation can be disentangle into two components: a factor component and an idiosyncratic one. Since excitation parameters β are contained only in the idiosyncratic component of moment equations, this separation facilitates their estimation which is primary parameters for network mapping.

In the next result, we provide closed-form formulae of covariance functions of log-returns which will help identification of factor compenents.

Theorem 1.3.3 *Up to the order* Δ^2*, and under assumptions (1.4) - (1.27), our model im-*

plies the following formalae for covariances of log-returns: $\forall i \neq j$

$$\begin{aligned}
&\mathbb{E}\left[(\Delta X_{i,t}-\mathbb{E}[\Delta X_{i,t}])\,(\Delta X_{j,t}-\mathbb{E}[\Delta X_{j,t}])\right] \\
&\qquad = \left\{b_i\mathbb{E}\big[\overline{D}_g(V_F)\big]b_j' + b_i\mathbb{E}\big[\overline{D}_g(Z_F)^2\overline{D}_g(\lambda_F)\big]b_j'\right\}\Delta \\
&\qquad\quad + 2\mathbb{E}[Z_{Ii}]\mathbb{E}[Z_{Ij}]\int_{s=0}^{\Delta}\int_{t=0}^{s} R_{Iji}(t-s)dtds + o(\Delta^2) \qquad (1.50)\\
&\mathbb{E}\left[(\Delta X_{i,t}-\mathbb{E}[\Delta X_{i,t}])\,(\Delta X_{j,t}-\mathbb{E}[\Delta X_{j,t}])^2\right] \\
&\qquad = \left\{b_i\mathbb{E}\big[\overline{D}_g(Z_F)^3\big]\overline{D}_g(\lambda_F)\overline{D}_g(b_j)b_j'\right\}\Delta + \frac{3}{2}b_i\overline{D}_g(\eta_F)\overline{D}_g(\rho_F)\mathbb{E}\big[\overline{D}_g(V_F)\big]\overline{D}_g(b_j)b_j'\Delta^2 \\
&\qquad\quad + 2\mathbb{E}[Z_{Ii}]\mathbb{E}\big[Z_{Ij}^2\big]\int_{s=0}^{\Delta}\int_{t=0}^{s} R_{Iij}(t-s)dtds + o(\Delta^2) \qquad (1.51)
\end{aligned}$$

Moments of V_F *are given by the lemma 1.3.1 and* $\int_{s=0}^{\Delta}\int_{t=0}^{s} R_{Iij}(t-s)dtds$ *is the element in row* i *and column* j *of the matrix* $\int_{s=0}^{\Delta}\int_{t=0}^{s} R_I(t-s)dtds$ *as defined in corollary 1.3.1. (expression for* $\mathbb{E}\big[\,(\Delta X_{i,t}-\mathbb{E}[\Delta X_{i,t}])\,(\Delta X_{j,t}-\mathbb{E}[\Delta X_{j,t}])^3\,\big]$ *and* $\mathbb{E}\big[\,(\Delta X_{i,t}-\mathbb{E}[\Delta X_{i,t}])^2\,(\Delta X_{j,t}-\mathbb{E}[\Delta X_{j,t}])^2\,\big]$ *are provided in the appendix equation (1.74) and (1.73)).*

From the previous theorem, it appears that leading terms of covariance functions come from the factor component of the model. Specifically, for covariance functions of order 3 and 4, leading terms are jump components of the factors. Once again, in the covariance functions of order 2, contributions of diffusion and jump parts of factors are of the same order. Covariance functions of log-returns facilitate the identification and estimation of parameters of the factor component.

Next, we compute the autocorrelation functions of log-returns. From the stochastic dynamic of volatility processes, additional quantities are needed in closed-forms, such as: $\int_0^{\Delta}\int_{\tau}^{\Delta+\tau}\mathbb{E}[V_{Fks}V_{Fkt}]dtds$ and $\int_0^{\Delta}\int_{\tau}^{\Delta+\tau}\mathbb{E}[V_{Iis}V_{Ijt}]dtds$. Their expressions are provided in the appendix by the lemma 1.8.1. Next result provide closed-forms for autocovariance functions of log-returns and squared log-returns.

Theorem 1.3.4 *Up to the order* Δ^2*, and under assumptions (1.4) - (1.27), our model im-*

plies the following autocovariance equations of log-returns and squared log-returns: $\forall \tau > 0$,

$$\begin{aligned}
&\mathbb{E}\left[\Delta X_{it}\Delta X_{jt+\tau}\right] - \mathbb{E}[\Delta X_{it}]\mathbb{E}[\Delta X_{jt}] \\
&\qquad = \mathbb{E}[Z_{Ii}]\mathbb{E}[Z_{Ij}]\int_0^{\Delta}\int_{\tau}^{\Delta+\tau} R_{Iij}(s-t)dtds + o(\Delta^2) \qquad (1.52)\\
&\mathbb{E}\left[\Delta X_{it}^2\Delta X_{jt+\tau}^2\right] - \mathbb{E}\left[\Delta X_{it}^2]\mathbb{E}[\Delta X_{jt+\tau}^2\right] \\
&\qquad = \sum_{k=1}^{K} b_{ik}^2 b_{jk}^2 \int_0^{\Delta}\int_{\tau}^{\Delta+\tau}\left(\mathbb{E}[V_{Fks}V_{Fkt}] - \mathbb{E}[V_{Fks}]^2\right)dtds + \int_0^{\Delta}\int_{\tau}^{\Delta+\tau}\mathrm{Cov}[V_{Iis}, V_{Ijt}]dtds \\
&\qquad\quad + \mathbb{E}[Z_{Ii}^2]\mathbb{E}[Z_{Ij}^2]\int_0^{\Delta}\int_{\tau}^{\Delta+\tau} R_{Iij}(s-t)dtds + o(\Delta^2) \qquad (1.53)
\end{aligned}$$

where R_{Iij} is the element in row i and column j of the covariance density matrix R_I, as defined in Definition 1.3.1; $\int_0^{\Delta}\int_{\tau}^{\Delta+\tau} R_{Iij}(s-t)dtds$ is given by the corollary 1.3.1. To save the space, closed-form expressions of $\int_0^{\Delta}\int_{\tau}^{\Delta+\tau}\mathbb{E}[V_{Fks}V_{Fkt}]dtds$, and $\int_0^{\Delta}\int_{\tau}^{\Delta+\tau}\mathbb{E}[V_{Iis}V_{Ijt}]dtds$ are given by the lemma 1.8.1.

Autocovariance of log-returns doesn't include parameters of the prices's diffusive component. Autocovariances of volatilities and jump components generate the autocorrelation of squared log-returns.

Our framework assume the availability of high frequency data. Those data are used to consistently estimate daily volatility measures. The next paragraph provides some definitions of these quantities.

Definition 1.3.3 *Under the model (1.7), let's take δ as the sampling frequency. We have following definitions:*

- ***The integrated volatility*** *of the asset i during a trading time $[t; t+1]$*

$$\mathrm{IV}_{it,t+1} = \sum_{k=1}^{K} b_{ik}^2 \int_t^{t+1} V_{Fks}ds + \int_t^{t+1} V_{Iis}ds \qquad (1.54)$$

It represents the share of the total variation of the asset i within a trading time $[t; t+1]$, which is due to the diffusive component of the model. Using high frequency data, $\mathrm{IV}_{it,t+1}$ is estimated using the realized bipower variation defined by

$$\widehat{\mathrm{IV}}_{it,t+1} = \mu_1^{-2}\sum_{l=2}^{\lfloor\frac{1}{\delta}\rfloor}|\Delta X_{it+l\delta}||\Delta X_{it+(l-1)\delta}| \qquad (1.55)$$

Where

$$\mu_1 = \mathbb{E}[|u|] = \sqrt{2}/\sqrt{\pi}; \text{ and } u \sim N(0;1) \tag{1.56}$$

The choice of this estimator is motivated by the presence of jumps in returns. Barndorff-Nielsen and Shephard (2003) provide the asymptotic theory of this estimator.

• ***The quadratic variation*** *of the asset i during a trading time $[t;t+1]$*

$$\mathrm{QV}_{it,t+1} = \lim_{\delta \to 0} \sum_{l=1}^{\lfloor \frac{1}{\delta} \rfloor} \Delta X_{it+l\delta}^2 \tag{1.57}$$

It provides a measure of the total variation of the asset i during the trading time $[t;t+1]$. Here, the variation is due both to continuous and jump parts. It is well established in the literature that $\mathrm{QV}_{it,t+1}$ is consistently estimated by the realized quadratic variation defined below

$$\widehat{\mathrm{QV}}_{it,t+1} = \sum_{l=1}^{\lfloor \frac{1}{\delta} \rfloor} \Delta X_{it+l\delta}^2 \tag{1.58}$$

• ***The integrated covariation*** *between assets i and j provides information on diffusive components comovement of two assets i and j during a trading time $[t;t+1]$. From our setup, it is defined by*

$$\mathrm{ICov}_{ijt,t+1} = \int_t^{t+1} \left(\sum_{k=1}^{K} b_{ik} b_{jk} V_{Fks} \right) ds \tag{1.59}$$

According to Barndorff-Nielsen and Shephard (2003), a consistent estimator is given by

$$\begin{aligned}\widehat{\mathrm{ICov}}_{ijt,t+1} = \frac{\mu_1^{-2}}{4} \sum_{l=2}^{\lfloor \frac{1}{\delta} \rfloor} \Big[&\left(\Delta X_{it+l\delta} + \Delta X_{jt+l\delta} \right) \left(\Delta X_{it+(l-1)\delta} + \Delta X_{jt+(l-1)\delta} \right) \\ &- \left(\Delta X_{it+l\delta} - \Delta X_{jt+l\delta} \right) \left(\Delta X_{it+(l-1)\delta} - \Delta X_{jt+(l-1)\delta} \right) \Big]\end{aligned} \tag{1.60}$$

• ***The quadratic covariation*** *between assets i and j during a trading time $[t;t+1]$*

$$\mathrm{QCov}_{ijt,t+1} = \lim_{\delta \to 0} \sum_{l=1}^{\lfloor \frac{1}{\delta} \rfloor} \Delta X_{it+l\Delta} \Delta X_{jt+l\Delta} \tag{1.61}$$

It measures the total comovement between assets i and j explained by diffusive and jump *components. It is consistently estimated using the realized quadratic covariation*

$$\widehat{\mathrm{QCov}}_{ijt,t+1} = \sum_{l=1}^{\lfloor \frac{1}{\delta} \rfloor} \Delta X_{it+l\delta} \Delta X_{jt+l\delta} \tag{1.62}$$

Assuming these quantities are observable, their moments are useful for the accurate estimation of parameters of the volatility process. We need to provide first and second moments of the previous volatility-based quantities. The following theorem contains these explicit formulae.

Theorem 1.3.5 *Under assumptions (1.4) - (1.27) and the stationary assumption of* $\mathrm{IV}_{t,t+1}$ *, the following equations hold*

$$\mathbb{E}[\mathrm{IV}_{it,t+1}] = b_i \mathbb{E}\big[\overline{D}_g(V_F)\big] b_i' + \mathbb{E}[V_{Ii}], \quad \forall i = 1, ..., m \tag{1.63}$$

$$\mathbb{E}[\mathrm{QV}_{it,t+1}] - \mathbb{E}[\mathrm{IV}_{it,t+1}] = b_i \mathbb{E}[\overline{D}_g(Z_F)^2] \overline{D}_g(\lambda_F) b_i' + \mathbb{E}\big[Z_{Ii}^2\big]\mathbb{E}[\lambda_{Ii}], \quad \forall i = 1, ..., m \tag{1.64}$$

$$\mathbb{E}[\mathrm{ICov}_{ijt,t+1}] = b_i \mathbb{E}\big[\overline{D}_g(V_F)\big] b_j', \quad \forall i \neq j \tag{1.65}$$

$$\mathbb{E}[\mathrm{QCov}_{ijt,t+1}] - \mathbb{E}[\mathrm{ICov}_{ijt,t+1}] = b_i \mathbb{E}\big[\overline{D}_g(Z_F)^2\big] \overline{D}_g(\lambda_F) b_j', \quad \forall i \neq j \tag{1.66}$$

and

$$\begin{aligned}\mathbb{E}[\mathrm{QV}_{it,t+1}^2] - \mathbb{E}[\mathrm{IV}_{it,t+1}^2] = {} & 2\left\{b_i \mathbb{E}\big[\overline{D}_g(V_F)\big] b_i' + \mathbb{E}[V_{Ii}]\right\}\left\{b_i \mathbb{E}\big[\overline{D}_g(Z_F)^2\big]\overline{D}_g(\lambda_F) b_i' + \mathbb{E}\big[Z_{Ii}^2\big]\mathbb{E}[\lambda_i]\right\} \\ & + \mathbb{E}\left\{\big[b_i \overline{D}_g(Z_F)^2 \overline{D}_g(\lambda_F) b_i'\big]^2\right\} + b_i \overline{D}_g(b_i)^2 \mathbb{E}\big[\overline{D}_g(Z_F)^2\big]^2 \overline{D}_g(\lambda_F)^2 b_i' \\ & + 2\mathbb{E}\big[Z_{Ii}^2\big]\mathbb{E}[\lambda_i] b_i \overline{D}_g(b_i) \mathbb{E}\big[\overline{D}_g(Z_F)^2\big]\overline{D}_g(\lambda_F) b_i' + \mathbb{E}\big[Z_{Ii}^4\big]\mathbb{E}[\lambda_i] \\ & + \mathbb{E}\big[Z_{Ii}^2\big]^2 \mathbb{E}[\lambda_i]^2 + \mathbb{E}\big[Z_{Ii}^2\big]^2 \int_t^{t+1}\int_t^{t+1} R_{Iii}(s-u)duds \end{aligned} \tag{1.67}$$

where $\int_t^{t+1}\int_t^{t+1} R_{Iii}(s-u)duds$ *is the element in row* i *and column* i *of the matrix* $\int_{s=0}^{\Delta}\int_{t=0}^{s} R_I(t-s)dtds$ *as defined in corollary 1.3.1.*

Price jump parameters are neither the part of the integrated volatility first and second moments, nor the integrated covolatility. Thus, in the estimation process, $\mathbb{E}[\mathrm{IV}_{it,t+1}]$ and $\mathbb{E}[\mathrm{ICov}_{it,t+1}]$ will focus on the identification of diffusive component parameters. To be more precise, they will facilitate the estimation of parameters of the volatility (both diffusive and jump parameters of the volatility). On contrary, $\mathbb{E}[\mathrm{QV}_{it,t+1}] - \mathbb{E}[\mathrm{IV}_{it,t+1}]$, $\mathbb{E}[\mathrm{QCov}_{ijt,t+1}] - \mathbb{E}[\mathrm{ICov}_{ijt,t+1}]$ and $\mathbb{E}[\mathrm{QCov}_{ijt,t+1}^2] - \mathbb{E}[\mathrm{ICov}_{ijt,t+1}^2]$ will identify price jump parameters.

In last moment conditions, we compute autocovariance functions of the integrated volatility and the quadratic variation. In order to facilite the identification, our interest will be on $\mathbb{E}\big[\mathrm{QV}_{it,t+1}\mathrm{QV}_{jt+\tau,t+\tau+1}\big]-\mathbb{E}\big[\mathrm{IV}_{it,t+1}\mathrm{IV}_{jt+\tau,t+\tau+1}\big]$. Its expression is given by the next theorem.

Theorem 1.3.6 *Let's call* $\int_t^{t+1}\int_t^{t+\tau+1} R_{Iij}(s-u)duds$ *the element in row* i *and column* j *of the matrix* $\int_t^{t+1}\int_t^{t+\tau+1} R_I(s-u)duds$ *as defined in corollary 1.3.1. Then, differences between autocorrelation functions of integrated volatility and quadratic variation are given by the following expressions, under assumptions (1.4) - (1.27):* $\forall\tau>1$

$$\begin{aligned}
&\mathbb{E}\big[\mathrm{QV}_{it,t+1}\mathrm{QV}_{it+\tau,t+\tau+1}\big]-\mathbb{E}\big[\mathrm{IV}_{it,t+1}\mathrm{IV}_{it+\tau,t+\tau+1}\big]\\
&\qquad=\Big\{b_i\mathbb{E}\big[\overline{D}_g(Z_F)^2\big]\overline{D}_g(\lambda_F)b_i'\Big\}^2+\mathbb{E}\big[Z_{Ii}^2\big]^2\mathbb{E}[\lambda_{Ii}]^2+\mathbb{E}\big[Z_{Ii}^2\big]^2\int_t^{t+1}\int_{t+\tau}^{t+\tau+1}R_{Iii}(u-s)dsdu\\
&\qquad\quad+2b_i\mathbb{E}\big[\overline{D}_g(Z_F)^2\big]\overline{D}_g(\lambda_F)b_i'\mathbb{E}\big[Z_{Ii}^2\big]\mathbb{E}[\lambda_{Ii}]+2\mathbb{E}[\mathrm{IV}_{it,t+1}]\Big\{b_i\mathbb{E}\big[\overline{D}_g(Z_F)^2\big]\overline{D}_g(\lambda_F)b_i'+\mathbb{E}\big[Z_{Ii}^2\big]\mathbb{E}[\lambda_{Ii}]\Big\}
\end{aligned}\tag{1.68}$$

$$\begin{aligned}
&\mathbb{E}\big[\mathrm{QV}_{it,t+1}\mathrm{QV}_{jt+\tau,t+\tau+1}\big]-\mathbb{E}\big[\mathrm{IV}_{it,t+1}\mathrm{IV}_{jt+\tau,t+\tau+1}\big]\\
&\qquad=\mathbb{E}[\mathrm{IV}_{it,t+1}](b_j\mathbb{E}\big[\overline{D}_g(Z_F)^2\big]\overline{D}_g(\lambda_F)b_j'+\mathbb{E}\big[Z_{Ii}^2\big]\mathbb{E}\big[Z_{Ij}^2\big]\int_t^{t+1}\int_{t+\tau}^{t+\tau+1}R_{Iij}(u-s)dsdu\\
&\qquad\quad+\mathbb{E}\big[Z_{Ij}^2\big]\mathbb{E}[\lambda_{Ij}])+\mathbb{E}[\mathrm{IV}_{jt+\tau,t+\tau+1}]\Big\{b_i\mathbb{E}\big[\overline{D}_g(Z_F)^2\big]\overline{D}_g(\lambda_F)b_i'+\mathbb{E}\big[Z_{Ii}^2\big]\mathbb{E}[\lambda_{Ii}]\Big\}\\
&\qquad\quad+\Big\{b_i\mathbb{E}\big[\overline{D}_g(Z_F)^2\big]\overline{D}_g(\lambda_F)b_j'\Big\}^2+b_j\mathbb{E}\big[\overline{D}_g(Z_F)^2\big]\overline{D}_g(\lambda_F)\mathbb{E}\big[Z_{Ii}^2\big]\mathbb{E}[\lambda_{Ii}]b_j'\\
&\qquad\quad+\mathbb{E}\big[Z_{Ij}^2\big]\mathbb{E}[\lambda_{Ij}]b_i\mathbb{E}\big[\overline{D}_g(Z_F)^2\big]\overline{D}_g(\lambda_F)b_i'+\mathbb{E}\big[Z_{Ii}^2\big]\mathbb{E}\big[Z_{Ij}^2\big]\mathbb{E}[\lambda_{Ii}]\mathbb{E}[\lambda_{Ij}]
\end{aligned}\tag{1.69}$$

where $\int_t^{t+1}\int_{t+\tau}^{t+\tau+1} R_{Iii}(s-u)duds$ *is the* ij *element of the matrix* $\int_{s=0}^{\Delta}\int_{t=0}^{s} R_I(t-s)dtds$ *defined in corollary 1.3.1.*

As expected, autocorrelation functions of the integrated volatility $\mathbb{E}[\mathrm{IV}_{it,t+1}\mathrm{IV}_{jt+\tau,t+\tau+1}]$ contain only diffusion parameters (mainly volatility parameters). Contrary to the previous results, diffusion parameters are also present in expression $\mathbb{E}[\mathrm{QV}_{it,t+1}\mathrm{QV}_{jt+\tau,t+\tau+1}]-\mathbb{E}[\mathrm{IV}_{it,t+1}\mathrm{IV}_{jt+\tau,t+\tau+1}]$, through the expected volatility of the idiosyncratic term.

1.4 Monte Carlo study

The aim of this section is to study the finite sample properties of our estimation procedure. More specifically, we want to know firstly how accurate are approximated moments of the order Δ^2 relatively to empirical moments. Secondly, we want to know how moments of realized measures perform in the approximation of moments of integrated quantities. Thirdly, we want to assess the accuracy of the estimation procedure.

1.4.1 Simulation design

We run two simulation experiments. The first is based on a few number of assets ($m = 3$) and the second mimic our empirical study with $m = 12$ stocks. We focus on one factor models ($K = 1$). As described in our framework, the price vector is simulated such that it follows an Itö-semimartingale process with one factor, jumps in price and volatility. More precisely:

• The factor loadings b_i, $\forall i = 1, ..., m$, is generated by a standard normal law:

$$b_i \sim N(0,1) \tag{1.70}$$

• The factor component in the latent return representation is generated by the following equation

$$dF_t = \mu_F dt + \sqrt{V_{Ft}} dB_{Ft} + Z_{Ft} dN_{Ft}$$

with B_{Ft} a brownian motion and V_{Ft} following a $GARCH$ diffusion model:

$$dV_{Ft} = \kappa_F \left(\theta_F - V_{Ft}\right) dt + \eta_F \rho_F \sqrt{V_{Ft}} dB_{Ft} + \eta_F \sqrt{(1-\rho_F^2) V_{Ft}} dW_{Ft} + Z_{Ft}^v dN_{Ft}^v$$

with $dB_F \perp dW_F$, and parameters set as in Maneesoonthorn, Forbes, and Martin (2016): $\mu_F = 0.097$, $\rho_F = -0.5$, $\kappa_F = 0.5$, $\theta_F = 0.0083$, $\eta_F = 0.1\sqrt{2\kappa_F \theta_F}$, $V_{F0} = \theta_F$, $\mu_{Fv} = 45$, $Z_F^v \sim Exp(\mu_{Fv})$, $\lambda_F = 0.032$, $\lambda_F^v = 0.0064$, $dN_{Ft}^v \sim Poiss(\lambda_F^v dt)$, $dN_{Ft} \sim Poiss(\lambda_F dt)$, $Z_{Ft} \sim F_{Z_F}$ as described in equation (1.10) with $1/\gamma_{F1} = 1/\gamma_{F2} = 0.028$, and $p_F = 1$

• The idiosyncratic error term in the factor representation is assumed to satisfy

$$dE_{it} = \mu_{Ii} dt + \sqrt{V_{Iit}} dB_{Iit} + Z_{Iit} dN_{Iit}$$

with

$$dV_{Iit} = \kappa_{Ii} \left(\theta_{Ii} - V_{Iit}\right) dt + \eta_{Ii} \rho_{Ii} \sqrt{V_{Iit}} dB_{Iit} + \eta_{Ii} \sqrt{(1-\rho_{Ii}^2) V_{Iit}} dW_{Iit} + Z_{Iit}^v dN_{Iit}^v$$

$$d\lambda_{Iit} = \alpha_i \left(\lambda_{Ii\infty} - \lambda_{Iit}\right) dt + \textstyle\sum_{j=1}^m \beta_{ij} dN_{Ijt}$$

$$d\lambda_{Iit}^{v} = \alpha_{Ii}^{v}\left(\lambda_{Ii\infty}^{v} - \lambda_{Iit}^{v}\right)dt + \sum_{j=1}^{m}\beta_{ij}^{v}dN_{jt}^{v}$$

We generate the idiosyncratic component as follow:

- The continuous part of the volatility follows a Nelson GARCH diffusion limit model as in Barndorff-Nielsen, Hansen, and Shephard (2008a): $\theta_I = 0.0083$, $\eta_I = 0.1\sqrt{2\kappa_I\theta_I}$, $\mu_I = 0.097$, $\rho_I = -0.6$, $\kappa_I = 0.5$, with $dB_{Ii} \perp dW_{Ii}$;
- As in Aït-Sahalia, Cacho-Diaz, and Leaven (2015), after annualization, the price jump is such that: $\lambda_{I\infty} = 0.00992$; β_I is generated by choosing randomly m values within the set $\{0.378, 0.452, 0.044, 0.039, 0.057, 0.094, 0.079, 0.044\}$; similarly, values of α_I are chosen randomly within the set $\{0.456, 0.463, 0.390, 0.312\}$; $Z_I \sim F_{Z_I}$ as described in equation (1.11) with $1/\gamma_{I1} = 1/\gamma_{I2} = 0.028$, $p_I = 1$;
- The volatility jump satisfies: $\lambda_{I\infty}^{v} = 0.00992$; β_I^{v} is generated by choosing randomly m values within the set $\{0.378, 0.452, 0.044, 0.039, 0.057, 0.094, 0.079, 0.044\}$; similarly, values of α_I^{v} are chosen randomly within the set $\{0.456, 0.463, 0.390, 0.312\}$; $Z_I^{v} \sim Exp(\mu_I^{v})$ with $\mu_I^{v} = 45$.

1.4.2 Simulation results

Moment accuracy

Based on the previous simulation design, we study the accuracy of moment conditions involved in the estimation procedure. Since closed-form expressions of moment's returns are derived up to the order Δ^2, we want to check that this approximation generates negligible errors. Also, moments of realized measures are used to approximate moments of integrated quantities. The current simulation exercise provides evidence of the closeness between these two types of moments.

For each asset, we simulate 10000 paths and compute for each path sample counterparts of each moment. Then, for each moment condition, we compute the mean and the standard deviation over the 10000 replications. These means are then compared with close form formulae of each moment condition. The following table summarizes these comparison results.

For each moment, we compute the theoretical expectation using moment's closed-form expressions and parameter values. We compare this value to the simulated expectation derived from the sample counterparts of each moment. The closeness between these two moments is an evidence of the accuracy of our moment equations. The same exercise is done for integrated measures, but with a small difference: in sample counterparts, integrated measures are replaced by their daily realized estimators. As a result of this simulation-based check, it appears that moments are accurately computed.

Table 1.2. Accuracy of moment conditions

Moments	$\mathbb{E}[r_i]$	$\mathbb{E}[r_i^2]$	$\mathbb{E}[r_i^3]$
Theoretic expectation	0.00182	0.00110	-5.79E-06
Simulated expectation	0.00180	0.00111	-5.67E-06
(Standard deviation)	*(4.94E-05)*	*(7.59E-05)*	*(1.08E-06)*

Moments	$\mathbb{E}[r_i^4]$	$\mathbb{E}[r_i r_j]$	$\mathbb{E}[r_i^2 r_j^2]$
Theoretic expectation	4.55E-06	-0.00016	3.85E-07
Simulated expectation	4.60E-06	-0.00015	4.68E-07
(Standard deviation)	*(9.80E-07)*	*(3.05E-06)*	*(2.87E-07)*

Moments	$\mathbb{E}[r_i r_{jt+2}]$	$\mathbb{E}[r_i^2 r_{jt+2}^2]$	$\mathbb{E}[\mathrm{IV}_{it}]$
Theoretic expectation	1.94E-06	6.60E-08	0.01122
Simulated expectation	1.95E-06	3.88E-08	0.01118
(Standard deviation)	*(5.47E-07)*	*(2.06E-09)*	*(0.00097)*

Moments	$\mathbb{E}[\mathrm{QV}_{it}]$	$\mathbb{E}[\mathrm{ICov}_{ijt}]$	$\mathbb{E}[\mathrm{QCov}_{ijt}]$
Theoretic expectation	0.01124	-0.001420	-0.00168
Simulated expectation	0.01135	-0.001424	-0.00142
(Standard deviation)	*(0.00098)*	*(5.77E-05)*	*(5.77E-05)*

Finite sample properties of the excitation parameters

Since excitation parameters (β and β^v) are our primary interest, we study their finite sample properties. The others parameters are fixed throughout this simulation exercise. We simulate 10000 paths of price processes, and for each path, we estimate the excitation coefficients using our GMM procedure. The following moment conditions are used: $\mathbb{E}[r_i]$, $\mathbb{E}[r_i^2]$, $\mathbb{E}[r_i^3]$, $\mathbb{E}[r_i^4]$, $\mathbb{E}[r_i r_j]$, $\mathbb{E}[r_i^2 r_j^2]$, $\mathbb{E}[\mathrm{IV}_{it}]$, $\mathbb{E}[\mathrm{QV}_{it}]$, and $\mathbb{E}[\mathrm{QV}_{it+2}\mathrm{QV}_{jt}] - \mathbb{E}[\mathrm{IV}_{it+2}\mathrm{IV}_{jt}]$, $i = 1, ..., m$, and $\forall i \neq j$. The table below summarizes our findings for $m = 3$ assets. To save the space, monte carlo results corresponding to $m = 12$ are reported in the appendix (See tables 1.20 to 1.23). We also run a simulation exercise in which we study properties of all parameters in the global model for $m = 3$ and $m = 12$. Those results can be obtain upon request.

From these Monte Carlo exercises, it appears that parameters of our model can be recovered with a fairly good level of precision. If the accuracy of the estimation procedure is not as good as the case of usual stochastic volatility processes, it is because of the latency of some processes as the volatility or the jump intensity. Also, jump events do not happen frequently (See the supplement of Aït-Sahalia, Cacho-Diaz, and Leaven (2015) for more details on this issue).

Table 1.3. Finite sample properties of the excitation coefficients

True parameters					**Average Estimates** *(Standard deviation)*			
β	0.039	0.058	0.039		$\widehat{\beta}$	0.043	0.061	0.044
						(0.012)	*(0.012)*	*(0.014)*
	0.453	0.039	0.079			0.391	0.042	0.068
						(0.130)	*(0.015)*	*(0.015)*
	0.039	0.044	0.039			0.042	0.051	0.044
						(0.011)	*(0.019)*	*(0.023)*
β^v	0.039	0.044	0.094		$\widehat{\beta^v}$	0.043	0.050	0.082
						(0.014)	*(0.009)*	*(0.008)*
	0.079	0.044	0.039			0.068	0.052	0.044
						(0.011)	*(0.015)*	*(0.007)*
	0.039	0.044	0.379			0.029	0.039	0.314
						(0.014)	*(0.014)*	*(0.013)*

1.5 Empirical study

In this section, we outline the estimation of our "doubly hawkes" jump-diffusion model with factors, first within a number of key US banks & insurance companies, and secondly among the nine largest S&P sectors during the period 2000-2014. Also, we are interested in constructing network maps through which the following shocks could propagate: i) negative market perception, liquidity shocks; ii) volatility shocks or panic. We want to assess the system fragility by studying the contagiousness and vulnerability of institutions and sectors.

Our data base comes from the Wharton Research Data Services. Concerning stocks, we rely on intraday data from the Trade and Quote (TAQ) database. We are interested on 12 major financial stocks included in the S&P 500 index, namely: ACE, AIG, AXP, BAC, BK, C, GS, JPM, MET, PNC, USB, and WFC. Our stocks are sufficiently liquid and traded more than 195 times during a given day. We further clean the data following procedures advocated in Barndorff-Nielsen, Hansen, and Shephard (2008a). Sector's intraday data are extracted from SDPR ETF's for the concerned nine largest S&P sectors: Energy (XLE), Materials (XLB), Industrials (XLI), Consumer Discretionary (XLY), Consumer Staples (XLP), Health Care(XLV), Financial(XLF), Information Technology (XLK), and Utilities (XLU). The sampling period spans January 2000 to December 2014.

Figure 1.3. Return dynamics.

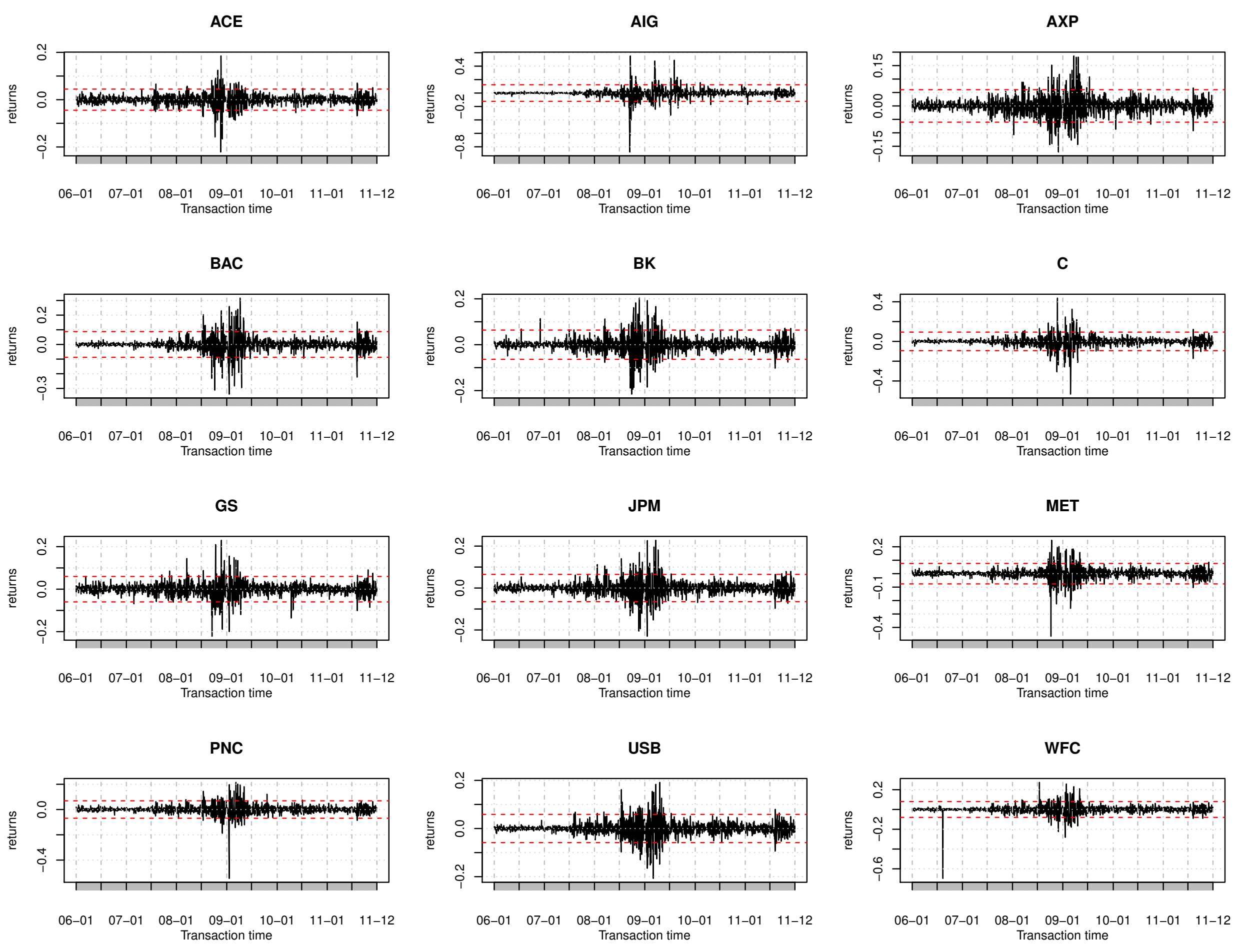

Notes: This figure shows the time series of 12 stock returns traded on NYSE, from january 2006 to december 2011. Jumps are identified when the observed return absolute value is bigger than $2 \times \textit{standard deviation}$. Observations out of the two horizontal red dashed lines correspond to jumps in returns.

Looking at the graphical representation of log-returns (Figure 1.3) and the estimated spot volatility (Figure 1.5) below, we observe a lot of turmoil episodes both in prices and volatilities. Also, self-excitation and cross-sectional clustering are omni-present. To be more convincing about the presence of jumps both in prices and volatility, jump tests need to be carried out.

We run the test of Lee and Mykland (2008) to validate the presence of jumps in log-prices. The intuition of this jump test is the following: the jump detection statistic is the ratio of the last return in a window of length, says, K, to the instantaneous volatility, estimated by bipower variation using returns in the same window. We obtain that, on average, there are around 15 jumps in log-price series per year. Most of jumps on stock returns occur in close succession, both serially and cross-sectionally.

Testing for the presence of jumps in the volatility is more tricky. We rely on the procedure of Todorov and Tauchen (2011) to validate the presence of these jumps. The different steps are as follows: i) We apply the test of Lee and Mykland (2008) to the daily series of the CBOE Volatility Index (VIX). We obtain the list of days with jumps in the VIX; ii) For each of these days, and for each stock estimated spot volatility, we run the jump test of Lee and Mykland (2008) to validate the presence of jumps in the volatility of the considered stock.

Figure 1.4. VIX dynamics.

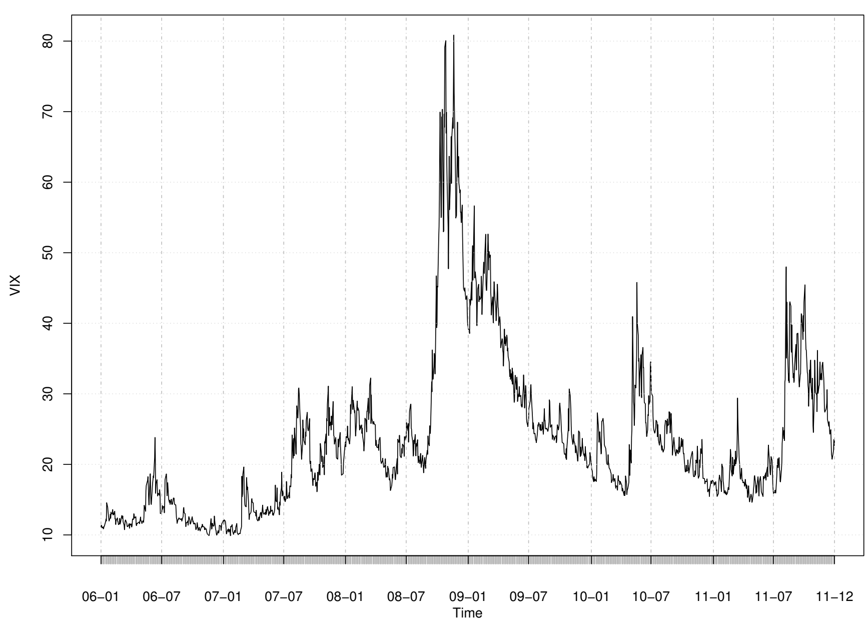

Notes: This figure shows the time series of the CBOE Volatility Index, from january 2006 to december 2011.

This test gives us also the time at which the jump occures. Through this procedure, we obtain that there is on average 10 jumps per years in the volatility of each stock, and these jumps cluster both serially and cross-sectionally.

Figure 1.5. Volatility dynamics.

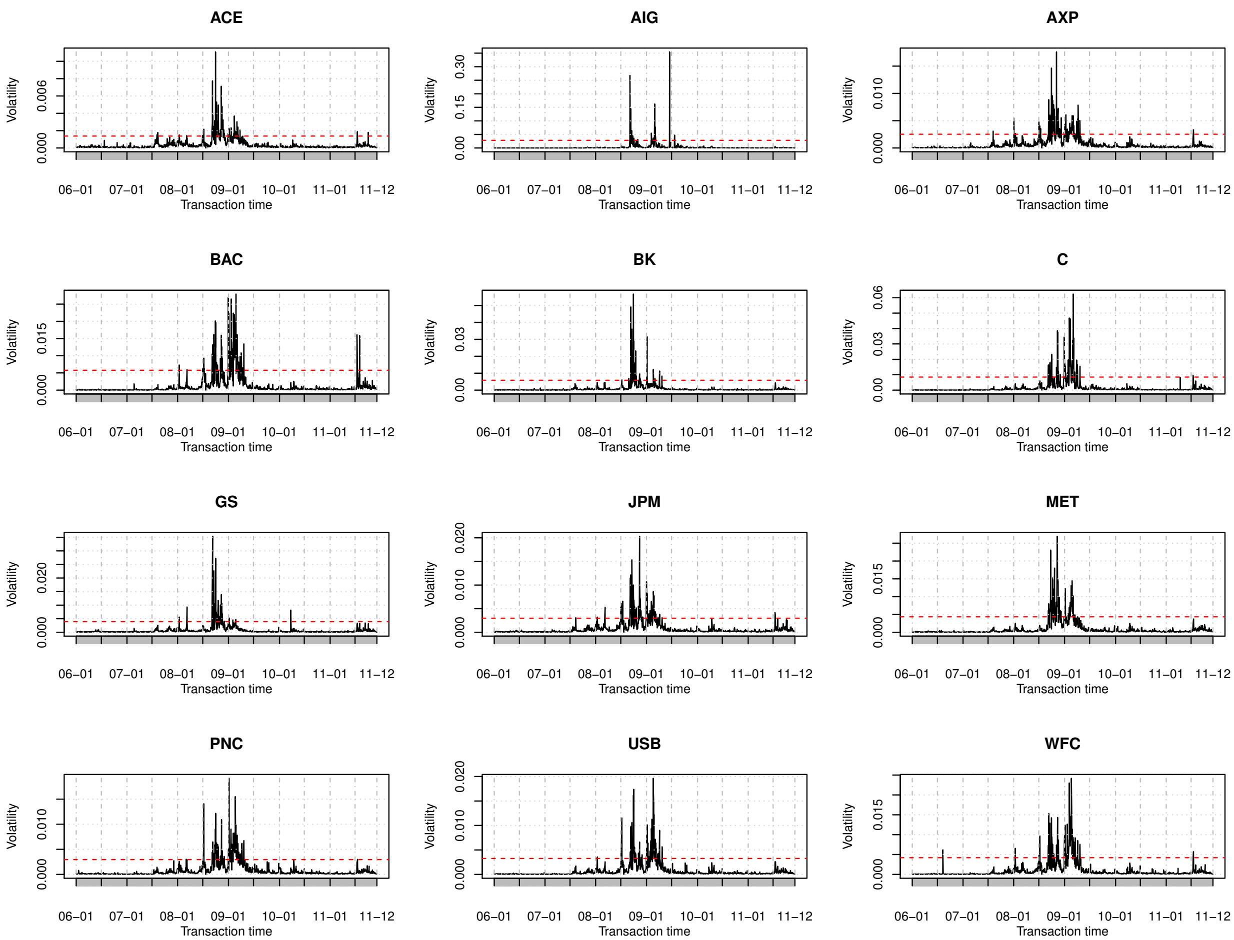

Notes: This figure represents the time series of estimated volatilities of 12 stocks traded on NYSE, from january 2006 to december 2011. Volatility is estimated using the local realized bipower variation estimator as in Lee and Mykland (2008). Jumps are identified when the estimated volatility is bigger than $2 \times \textit{standard deviation}$. Values above the horizontal red dashed line correspond to jumps.

Before focusing on the estimation results of our model, let's recall two main points. Firstly, our model encompenses the approach of Maneesoonthorn, Forbes, and Martin (2016) by allowing $m > 1$ assets, and we allow common factors. By restricting the loading matrix to 0, we obtain their model as a sub-case. Their approach is based on MCMC, while we rely on a GMM estimation strategy. Based on our strategy, tables 1.11 and 1.12 provide estimation results of their model for one sector, namely the sector of materials (XLB). Secondly, our model is more general than the financial contagion model of Aït-Sahalia, Cacho-Diaz, and Leaven (2015). Contrary to their approach: i) we don't restrict the structure of the excitation matrix; ii) we model the volatility as a stochastic process with mutually exciting jumps; iii) we allow additional channels for shock transmission: volatility jumps and common factors; iv) excitation parameters are estimated all at the same time. In order to illustrate the importance of introducing those additional components, we estimate the model of Aït-Sahalia, Cacho-Diaz, and Leaven (2015) for two sectors: the financial sector (XLF) and the industrial sector (XLI). Then, we compare those results with estimation results of our double-hawkes jump diffusion model. Tables 1.13 and 1.14 contain those results. It appears from our model that loadings coefficients, stochastic volatility parameters, volatility excitation parameters are significantly different from 0. Thus, those elements matter and must be introduced into the model.

We now focus on setups with more than 2 assets. In a first part, we estimate the model for 12 financial stocks, namely: ACE, AIG, AXP, BAC, BK, C, GS, JPM, MET, PNC, USB, and WFC. The following table presents estimation results of this first setup. We estimate parameters using the proposed three steps estimation procedure described previously, and the following moments: $\mathbb{E}[r_i]$, $\mathbb{E}[r_i^2]$, $\mathbb{E}[r_i^3]$, $\mathbb{E}[r_i^4]$, $\mathbb{E}[r_i r_j]$, $\mathbb{E}[r_i^2 r_j^2]$, $\mathbb{E}[\mathrm{IV}_t]$, $\mathbb{E}[\mathrm{QV}_t]$, and $\mathbb{E}[\mathrm{QV}_{t+2}\mathrm{QV}_t] - \mathbb{E}[\mathrm{IV}_{t+2}\mathrm{IV}_t]$. The choice of $\tau = 2$ is dictated by autocorrelograms of processes IV_t and QV_t.

Estimation results in tables 1.4-1.7 reveal that the global specification of our model is valid. Since loading coefficients are significantly different from 0, we have a factor structure. Parameters reflecting leverage effects, stochastic volatility, mutually exciting jump both in prices and volatility, are significant. Excitation parameters of the volatility jump are at least at the same level than the ones of price jump. Hence, data validate the presence of a jump component in the volatility, and this volatility jump component must have a hawkes specification. Comparing to the specification in Aït-Sahalia, Cacho-Diaz, and Leaven (2015), they completely ignore the volatility channel for the jump transmission. But data are in favor of the introduction of mutually exciting jumps in price and volatility. The volatility channel is different and complementary to the price channel. It provides information on how the fear/panic, or uncertainty about future profitability is transmitted from one stock to others.

Table 1.4. Parameters estimates: continuous part of the model.

	ACE	AIG	AXP	BAC	BK	C
b	0.141	0.368	0.244	0.354	0.255	0.400
	(0.010)	*(0.029)*	*(0.012)*	*(0.023)*	*(0.014)*	*(0.028)*
ρ	- 0.269	- 0.342	- 0.074	- 0.377	- 0.202	- 0.250
	(0.003)	*(1.715)*	*(0.018)*	*(0.049)*	*(0.019)*	*(0.331)*
θ	0.042	0.278	0.057	0.068	0.052	0.119
	(0.004)	*(0.057)*	*(0.007)*	*(0.012)*	*(0.007)*	*(0.023)*
η	0.572	0.951	0.758	0.664	0.733	0.816
	(0.000)	*(0.484)*	*(0.001)*	*(0.011)*	*(0.003)*	*(0.094)*
κ	3.866	1.716	5.067	3.237	5.140	2.844
	3.7E-05	*(0.500)*	*(0.001)*	*(0.005)*	*(0.001)*	*(0.049)*
μ	- 0.160	- 0.869	- 0.034	- 0.616	- 0.308	- 0.973
	(0.085)	*(0.224)*	*(0.097)*	*(0.111)*	*(0.093)*	*(0.160)*
	GS	JPM	MET	PNC	USB	WFC
b	0.242	0.275	0.279	0.279	0.244	0.317
	(0.013)	*(0.012)*	*(0.016)*	*(0.019)*	*(0.014)*	*(0.019)*
ρ	- 0.006	- 0.219	- 0.151	- 0.373	- 0.332	- 0.310
	(0.014)	*(0.010)*	*(0.028)*	*(0.034)*	*(0.010)*	*(0.028)*
θ	0.059	0.047	0.061	0.059	0.044	0.055
	(0.008)	*(0.007)*	*(0.010)*	*(0.009)*	*(0.006)*	*(0.009)*
η	0.557	0.511	0.603	0.694	0.630	0.507
	(0.000)	*(0.001)*	*(0.003)*	*(0.008)*	*(0.002)*	*(0.004)*
κ	2.636	2.754	2.987	4.087	4.461	2.351
	(0.001)	*(2.8E-04)*	*(0.002)*	*(0.002)*	*(0.000)*	*(0.001)*
μ	- 0.110	- 0.192	- 0.253	- 0.190	- 0.123	- 0.235
	(0.118)	*(0.089)*	*(0.104)*	*(0.095)*	*(0.094)*	*(0.112)*

Notes: The estimation relies on 12 stocks traded on NYSE between january 2006 and december 2011. Parameters are idiosyncratic, meaning they are stock specific. Standard errors are in parenthesis.

Table 1.5. Parameters estimates (Cont'd): the factor component of the continuous part of the model.

	ρ_F	θ_F	η_F	κ_F	μ_F
Estimates	- 0.065	0.900	0.172	2.004	0.348
(s.e)	*(0.466)*	*(0.032)*	*(0.057)*	*(0.053)*	*(0.201)*

Notes: Standard errors are in parenthesis.

Table 1.6. Parameter estimates (cont'd): excitation parameters of price jump intensities (The matrix β).

	ACE	AIG	AXP	BAC	BK	C	GS	JPM	MET	PNC	USB	WFC
ACE	0.28*	0.12*	0.36*	0.21*	0.25*	0.17*	0.08	0.34*	0.59*	0.05	0.80*	0.52*
AIG	0.19*	0.39*	0.29*	0.85*	0.21*	0.22*	0.64*	0.13*	0.65*	0.32*	0.59*	0.95*
AXP	0.47*	1.06*	0.29*	0.39*	0.70*	0.27*	0.30*	0.29*	0.08	0.62*	0.66*	0.68*
BAC	0.64*	0.56*	0.22*	0.16*	0.67*	0.84*	0.61*	0.27*	0.00	0.77*	0.000	0.29*
BK	0.14*	0.17*	0.42*	0.60*	0.29*	0.11*	0.34*	0.87*	0.43*	0.62*	0.00	0.739
C	0.00	0.20*	0.18*	0.57*	0.86*	0.14*	0.18*	0.65*	0.32*	0.43*	0.00	0.03
GS	0.75*	0.16*	0.62*	0.46*	0.21*	0.29*	0.14*	0.62*	0.61*	0.06	0.00	0.46*
JPM	0.08	0.93*	0.79*	0.43*	0.68*	0.68*	0.14*	0.24*	0.27*	0.20*	0.67*	0.37*
MET	0.65*	0.19*	0.32*	0.22*	0.31*	0.47*	0.37*	0.78*	0.65*	0.00	0.74*	0.00
PNC	*0.76**	0.00	0.85*	0.16*	0.00	0.52*	0.58*	0.00	0.87*	0.67*	0.17*	0.76*
USB	0.05	0.07	0.62*	0.92*	0.38*	0.62*	0.00	0.48*	0.12*	0.08	0.89*	0.53*
WFC	0.09	0.37*	0.00	0.66*	0.54*	0.76*	0.17*	0.22*	0.56*	0.42*	0.92*	0.61*

Notes: The estimation relies on 12 stocks traded on NYSE between january 2006 and december 2011. Estimates of β_{ij} significantly higher than zero at the 5 family-wise significance levels are indicated by *.

Table 1.7. Parameter estimates (cont'd): excitation parameters of volatility jump intensities (The matrix β^v).

	ACE	AIG	AXP	BAC	BK	C	GS	JPM	MET	PNC	USB	WFC
ACE	0.53*	0.84*	0.84*	0.21*	0.08*	0.00	0.66*	0.82*	0.00	0.09	0.39*	0.89*
AIG	0.94*	0.77*	0.30*	0.31*	0.69*	0.39*	0.53*	0.53*	0.71*	0.14*	0.89*	0.10*
AXP	0.58*	0.56*	0.48*	0.29*	0.70*	0.31*	0.10*	0.99*	0.29*	0.48*	0.28*	0.83*
BAC	0.34*	0.19*	0.08	0.87*	0.74*	0.78*	0.58*	0.26*	0.87*	0.02	0.58*	0.37*
BK	0.73*	0.14*	0.75*	0.35*	0.81*	0.19*	0.49*	0.52*	0.87*	0.85*	0.33*	0.003
C	0.29*	0.04	0.74*	0.67*	0.00	0.50*	0.88*	0.55*	0.95*	0.75*	0.77*	0.49*
GS	0.71*	0.72*	0.39*	0.13*	0.73*	0.11*	0.09	0.27*	0.71*	0.24*	0.78*	0.19*
JPM	0.66*	0.67*	0.75*	0.83*	0.21*	0.00	0.55*	0.29*	0.35*	0.08	0.76*	0.07
MET	0.17*	0.16*	0.48*	1.01*	0.44*	0.28*	0.45*	0.09	0.87*	0.50*	0.26*	0.47*
PNC	0.42*	0.56*	0.44*	0.74*	0.63*	0.17*	0.56*	0.004	0.85*	0.49*	0.43*	0.28*
USB	0.59*	0.76*	0.41*	0.26*	0.92*	0.12*	0.36*	0.21*	0.013	0.32*	0.61*	0.90*
WFC	0.60*	0.08	0.21*	0.37*	0.64*	0.64*	0.55*	0.90*	0.43*	0.59*	0.27*	0.076

Notes: The estimation relies on 12 stocks traded on NYSE between january 2006 and december 2011. Estimates of β^v_{ij} significantly higher than zero at the 5 family-wise significance levels are indicated by *.

Table 1.8. Parameters estimates (Cont'd). The table provides estimates of others parameters present in the jump part of the model. Standard errors are in parenthesis.

	λ_F	λ_{Fv}	μ_{Fv}	μ_{Iv}	$1/\gamma_{F1}$	$1/\gamma_{F2}$
Estimates	0.144	1.0E-04	1.066	0.544	0.010	0.010
(s.e.)	*(9.5E-02)*	*(1.4E-01)*	*(1.3E-05)*	*(1.2E-02)*	*(2.5E+00)*	(5.4E+00)

	$1/\gamma_1$	$1/\gamma_2$	α_I	α_I^v	$\lambda_{I\infty}$	$\lambda_{I\infty}^v$
Estimates	0.010	0.010	1.993	1.308	0.001	0.826
(s.e.)	*(9.4E-02)*	*(7.9E-02)*	*(1.3E-02)*	*(7.0E-03)*	*(1.6E+00)*	*(7.7E-03)*

Notes: The estimation relies on 12 stocks traded on NYSE between january 2006 and december 2011. Estimates of β_{ij}^v significantly higher than zero at the 5 family-wise significance levels are indicated by *.

We now turn to the use of excitation parameters to construct network maps for shock transmission.

1.5.1 On network construction

There is a rich literature on tracking association between individual firms and proposing different measures for financial fragility. Despite of being widely spread, correlation measures only focus on pairwise associations. They strongly depend on linear Gaussian assumptions, which constitutes a departure from financial market data. As a consequence, they focus only on the dependency in the center and relevant information in the tail area are neglected. The equi-correlation approach of Engle and Kelly (2012) is an example. As a measure of the global interdependence, they propose to average correlations across all pairs. Weakly dependent on Gaussian methods, the CoVaR approach of Adrian and Brunnermeier (2016) and the marginal expected shortfall approach of Acharya, Pedersen, Philippe, and Richardson (2017) are also some popular methods to adress firm interdependency. But according to De Vries (2005), the Gaussian based correlation measures don't adequately capture the dependency structure within firms when the marginal distributions are non-normal. Our approach takes into account dependency structure in the tail.

Our systemic risk features are exclusively based on excitation parameters β_{ij} and β_{ij}^v for $\forall i, j = 1, ..., m$. To develop some intuition for these parameters as a device for studying dependence during periods of financial turmoil, recall that: *A jump in the price of asset j at time t, increases by $\beta_{ij}\Delta$ the likelihood of further jumps in the price of asset i within the* *time interval* $[t; t+\Delta]$. Hence, β_{ij} summarizes the information about the tail dependency between assets i and j. The bigger it is, the stronger will be the tail link between i and j.

We use estimates of price and volatility jump excitation parameters β_{ij} and β_{ij}^v to provide characteristics of the systemic risk within a set of financial firms/sectors. Firstly, we construct two different type of graphs: a graph for the propagation of negative market perception or liquidity schock, and a graph for the propagation of fear/panic or uncertainty about the future profitability. Secondly, excitation parameters are used to define a new measure of the systemic risk during times of crisis. These different elements provide useful information about the tail interdependency structure of considered stocks/sectors. Graphs are constructed using the network methodology.

A network map constitutes of nodes and edges, representing connections between these nodes. We rely on Diebold and Yilmaz (2015a) methodology to construct network associated measures. It requires the specification of three main elements: objects to be connected, variables whose connection is to be examined, a model from which the connection concept will be defined. These objects are respectively called: *vertices, the reference universe and the approximating model*. Throughout this section, the approximating model will remain the same. But depending on the reference universe or connected objects, we will obtain different network maps. We make the following choices:

- *Connected objects or vertices*: financial firms or sectors;
- *The Reference Universe*: returns and volatility;
- *The Approximating Model*: "Doubly hawkes" jump-diffusion model with factors, as defined in section 2.

The next step consists on setting the adjacency matrix and measures of network fragility. The adjacency matrix is a matricial representation which contains all information about the network. For a simple graph, the adjacency matrix is a matrix of ones (if there is a link between two nodes) and zeros (otherwise). But when we want to highlight on strength of links, elements of the adjacency matrix are weigths of the corresponding connections. Since excitation parameters measure strengths of the tail dependency between assets, they will constitute elements of our adjacency matrices. Also, the way one asset i impacts another asset j is not necessary the same than the effect of j on i. Thus, the adjacency matrix need not be symmetric. The output of this network construction is a graph for shock transmission.

Therefore, edges must have a direction, pointing from one stock to another. An edge is drawn from j to i as soon as β_{ij} is significantly different from 0.

- *Network adjacency matrices*: excitation matrices $\beta = (\beta_{ij})_{i,j \leq m}$ and $\beta^v = (\beta^v_{ij})_{i,j \leq m}$.
- *Edge from j to i* iff: β_{ij} is significantly different from 0.

Knowing details of the network structure through adjacency matrices, we can compute directional relatives. They provide information about the system fragility and vulnerability of nodes. We now define such measures:

• *Pairwise directional connectivity*, measures the strength of the connection of the firm i to the firm j:

$$\beta_{i \leftarrow j} = \beta_{ij}$$

• *Net pairwise directional connectivity*, i.e, a balance of the effects between two stocks:

$$\beta_{i \leftarrow j} - \beta_{j \leftarrow i}$$

Depending on its sign, it provides information about which stock is the net provider or the net receiver of a bilateral impact.

• *Total directional connectivity from others to i*:

$$\beta_{i \leftarrow \bullet} = \sum_{j=1, j \neq i}^{m} \beta_{ij}$$

As the Marginal Expected Shortfall (MES), this quantity provides a measure of the sensitivity of the node i to extreme events. It is also interpreted as a market stress test of firm i fragility.

• *Total directional connectivity to others from j*:

$$\beta_{\bullet \leftarrow j} = \sum_{i=1, i \neq j}^{m} \beta_{ij}$$

It measures how a shock to j impacts others financial institutions. It provides a measure of the contribution of j to systemic risk. This value is similar in spirit to the Co-Value at Risk (CoVar). Indeed, CoVar(j) is a measure of the financial sector fragility conditional on institution j being in distress.

• *Net total directional connectivity of* i, a balance of the interaction of the asset i with the market:

$$\bar{\beta}_i = \beta_{\bullet\leftarrow i} - \beta_{i\leftarrow\bullet}$$

• *Connectivity Index*, a measure for system fragility. The bigger it is, the more vulnerable is the system to propagation of shocks:

$$\bar{\beta} = \frac{1}{m}\sum_{i,j=1}^{m} \beta_{ij}$$

In terms of measures for the financial system fragility, several points of distinction arise between our approach and some popular ones. First, even if we use the same tools as Diebold and Yilmaz (2015a), our approximating model is different as their approach is based on variance decomposition. The element (i, j) of their adjacency matrix is the fraction of the $i's$ H-step forecast error variance due to shock to j, which is quite different from our excitation parameters β_{ij}. Their approach is not able to capture the connectivity concept we outline in this paper. As an illustration, we consider the previous simulation design. With simulated data, we apply the connectedness theory of Diebold and Yilmaz (2015a), and we compare the obtained network to the one derived using true excitation coefficients. The figure 1.6 contains the output of this comparison exercise. It appears that the connectedness approah of Diebold and Yilmaz (2015a) can't reproduce our contagion concept. It isolates some nodes, and generates a lot of self-connexion.

Figure 1.6. Network map based on Excitation parameters VS network maps derived from the forecast error variance decomposition of Diebold and Yilmaz

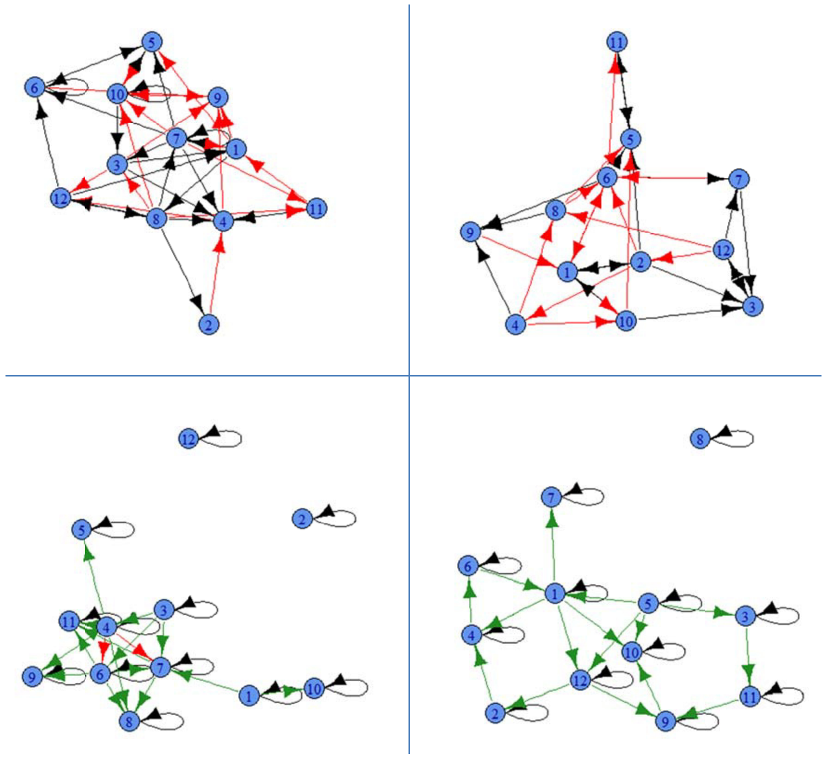

Notes: Based on simulations, the first row contains network maps generated by excitation parameters and the second row, network maps derived from the forecast error variance decomposition of Diebold and Yilmaz (returns in the left and volatility in the right).

Secondly, Dungey and Gajurel (2014) consider a factor model. But they emphasize more on testing for contagion than measuring. They measure contagion as a deviation of the idiosyncratic covariance matrix from the diagonal matrix. Third, comparing to the CoVar of Tobias and Brunnermeier (2016) or the MES of Acharya, Pedersen, Philippon, and Richardson (2010), their approaches are different even if they share same intuitions than total directional impacts "from others" and "to other" respectively, as defined above.

Relying on estimated adjacency matrices $\hat{\beta}$ and $\hat{\beta}^v$, the first part of our empirical exercise consists on studying the connectivity within a financial system of 12 major institutions. More specificaly, we want to assess contagiousness and vulnerability of these financial assets, given the estimated excitation matrices. We compute directionnal indicators useful for the study of system fragility's. Tables 1.9 summarize these findings.

Banks and insurance companies contribute at the same level to shock transmissions.

From the row "From others to i" of the table 1.9, it appears that AIG, AXP and JPM returns are the most sensitive to extreme market events. Togheter with C, their volatilities are the most vulnerable. Distresses of BAC, WFC, ACE and MET have the highest negative impact on the financial system fragility (They present highest values of the variable "To others from j", for prices or volatility). They are the biggest contributors to systemic risk.

Table 1.9. System fragility indicators: 12 financial institutions.

	Negative market perception or liquidity shock transmission					
	ACE	**AIG**	**AXP**	**BAC**	**BK**	**C**
From others to i	3.49	5.04	5.54	4.89	4.45	3.44
To others from j	3.83	3.84	4.68	5.49	4.81	4.93
Net total directional	0.34	-1.19	-0.86	0.61	0.36	1.49
	GS	**JPM**	**MET**	**PNC**	**USB**	**WFC**
From others to i	4.23	5.26	4.03	4.67	3.87	4.72
To others from j	3.42	4.66	4.50	3.58	4.54	5.33
Net total directional	-0.81	-0.60	0.47	-1.09	0.67	0.61
Connectivity Index	**0.41**					

	Volatility shock or fear transmission					
	ACE	**AIG**	**AXP**	**BAC**	**BK**	**C**
From others to i	4.84	5.54	5.44	4.82	5.26	6.14
To others from j	6.03	4.73	5.40	5.17	5.80	3.00
Net total directional	1.19	-0.81	-0.04	0.35	0.54	-3.14
	GS	**JPM**	**MET**	**PNC**	**USB**	**WFC**
From others to i	5.00	4.93	4.32	5.08	4.85	5.28
To others from j	5.72	5.17	6.05	4.07	5.75	4.60
Net total directional	0.72	0.24	1.73	-1.01	0.90	-0.68
Connectivity Index	**0.47**					

Notes: Coefficients in this table are directional relatives computed from adjacency matrices β and β^v, as described in the section 1.5.1.

Between banks and insurance companies, there is not one group which is completely dominated by the other by being always the net receiver. Nevertheless, three financial institutions (two banks and one insurance company) are net receivers both for price and volatility shocks: AIG, AXP and PNC. Those companies are small in term of market capitalization. Concerning the shock instigation, independently on whether we are interested on liquidity shock or fear transmission, ACE, BAC, BK, MET, and USB are net shock providers. They should be main instigators of systemic risk. The City Bank has a particular behavior: it is the biggest shock provider in term of market expectation/liquidity shocks, but also the most important shock receiver in term of volatility shocks.

On average, the connectivity index is bigger for volatility shock/fear transmission than for Market expectation/liquidity shock transmission (respectively 0.47 and 0.41). Thus, the risk of volatility shocks to propagate throughout this financial system is bigger than the one of price shocks. This finding is in line with Maneesoonthorn, Forbes, and Martin (2016) who argued that volatility jump intensity is much more informative than the jump price intensity. Hence, the volatility contribution to the tail dependency between considered stocks is most important than the price contribution.

The main important outputs of these shock transmission analysis are network maps for negative market perception/liquidity shock transmission and network for volatility shock/fear transmission. Based on the considered financial institutions, following graphs display how a shock originating from one specific financial asset could spread through the network.

In order to interpret the network map in figure 1.7, let's consider the bank Wells Fargo (WFC). It is one of the five biggest banks in US. For a risk exposure diversification purpose, the following financial institutions are share holders of WFC: AIG, BK, and PNC. The average numbers of shares held in 2016 were respectively (in millions): 1.5, 42, and 10. Assume that, due to some reasons, WFC becomes unable to meet demands for immediate payment. By the time information about the insolvency of WFC will be released to the market, its price will experience a negative jump. This price drop contains pessimistic market expectation of its future profitability. Traders will fire sale this stocks, generating mark-to-market losses to AIG, BK, and PNC[4]. Combined with connectedness mechanisms and contagion effects, these mark-to-market losses will generate drops of these latter stock prices with a strictly positive probability. The transmission process of this negative market perception will continuous through edges of the network map drawn in figure 1.7. Black edges are the more likely to be realized, followed in a decreasing order by red and green edges.

[4]The underlying assumption is that those banks value their assets at the current market prices.

Figure 1.7. Network map for the propagation of negative market perceptions/liquidity shock.

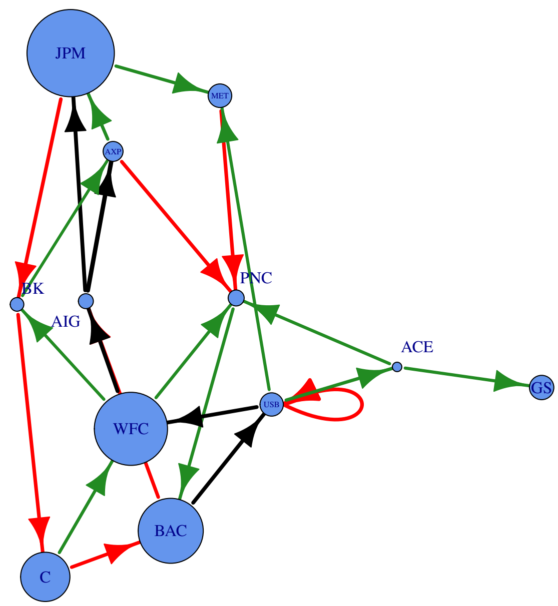

Notes: Each vertex represents a financial stock. We draw the most significant directional connections among pairs of assets. Black links (respectively red and green links) correspond to stongest links (respectively the second strongest and less strong links). The node size indicates stock market capitalization. Edge widths are proportionnal to the link's weights..

Let's now consider a different scenario. Assume that WFC face a liquidity shock, such that there is an unexpected reduction of its funding. It needs to reduce its assets, for example by decreasing its lending. By the figure 1.7, the most affected banks by this measure will be AIG, BK, and PNC. Those financial institutions will also reduce their lendings to others, generating a transmission of this liquidity shock through the network.

The network map in figure 1.7 puts in light not only connections arising from the existence of financial claims, but also links coming from contagion effects.

Interpretation of the network map in figure 1.8 is quite similar to the previous one. The only difference is the nature of signal which is transmitted: here, it is the investor panic which propagates through the network. Let's go back to the example related to the bank WFC. Assume that there are widespread rumors of an eventual bankruptcy of this financial institution. Risk averse investors will liquidate their positions from this bank and customers will ask for immediate payment. As a consequence, its stock price will decline rapidly, increasing tensions and panic of shares holders. Since investors, with limited amount of information, have into their portfolios similar assets, they will proceed to their fire-sales. Corresponding prices will jump down and their variances will increase. Thus, fear about the future profitability of those similar stocks will increase. Hence, through this mechanism, investor fear is likely to propagate from WFC to a set of similar stocks, but with different probabilities of occurrence. The more likely transmission paths of investors stress are in black. In red and green are connexions less likely to happen.

Figure 1.8. Network map for the propagation of volatility shocks/panic transmission.

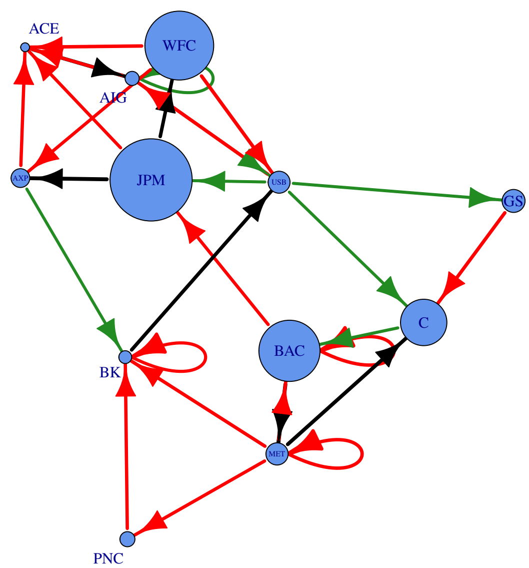

Notes: Each vertex represents a financial stock. We draw the most significant directional connections among pairs of stocks. Black links (respectively red and green links) correspond to stongest links (respectively the second strongest and less strong links). Node size indicates stock market capitalization. Edge widths are proportionnal to link's weights.

The second part of our empirical study concerns the nine largest economic's sectors in the US: Energy (XLE), Materials (XLB), Industrials (XLI), Consumer Discretionary (XLY), Consumer Staples (XLP), Health Care (XLV), Finance (XLF), Information Technology (XLK), and Utilities (XLU). As in the first part, we use the dataset of those sectors to estimate the model, then we focus on construction and properties of resulting networks. We want to know how connected are economic sectors, and how a shock originating from one specific sector can be amplified and transmitted to others economic sectors. Those informations are helpful to contain the collapse of the economic system. They are also useful for the minimization of investment risk through a sector diversification of the portfolio.

Table 1.10 presents some directionnal relatives. They are computed using as adjacency

Table 1.10. System fragility indicators: 9 largest S&P500 economic's sectors.

	Negative market perception or liquidity shock transmission								
	XLB	**XLV**	**XLP**	**XLY**	**XLE**	**XLF**	**XLI**	**XLK**	**XLU**
From others to i	3.90	4.16	3.14	4.36	3.29	3.84	3.45	5.10	4.37
To others from j	3.07	5.22	3.09	4.27	3.80	4.22	4.63	2.90	4.41
Net total directional	-0.83	1.06	-0.05	-0.09	0.51	0.39	1.18	-2.20	0.04
Connectivity Index					**0.44**				

	Volatility shock or fear transmission								
	XLB	**XLV**	**XLP**	**XLY**	**XLE**	**XLF**	**XLI**	**XLK**	**XLU**
From others to i	5.26	3.70	4.43	4.06	4.96	5.16	4.24	4.98	4.21
To others from j	3.94	4.96	5.48	4.63	5.49	5.28	2.59	3.99	4.64
Net total directional	-1.32	1.26	1.05	0.57	0.53	0.12	-1.65	-1.00	0.43
Connectivity Index					**0.51**				

Notes: Coefficients in this table are directional relatives computed from adjacency matrices β and β^v, as described in the section 1.5.1.

matrices $\hat{\beta}$ and $\hat{\beta}^v$, estimated using sectors' data. From this table, we observe that while health care, energy, finance, industry and utilities sectors are net instigators of liquidity shocks, other sectors are net receivers. In term of volatility shocks, materials, industry and technology sectors are net receivers. Also, XLK, XLU and XLY returns on the one hand, materials, finance and technology sectors volatilities on the other hand are the most sensitive to extreme market events. Distresses of XLV, XLP, XLE, and XLF have the highest negative impacts on the economic system fragility.

Depending on the type of shock we care about, the role played by some sectors changes. While the industry sector is instigator of liquidity shocks (With positive net total directionals), it is a net receiver of volatility shocks. Futher, consumer discretionary and consumer staples are net receivers of liquidity shocks but net providers of volatility shocks. Nevertheless, health care, energy and finance are always net providers of shocks, while, materials and information technology are shock receivers independently on the nature of the signal. If the health care sector is resilient to shocks coming from others sectors, it is because people are reluctant to reduce their health expenditure even if their income become tight.

In term of shock transmission, it is well known that "*it is better to give than to receive*". Hence, investors should be more attracted by stocks within health care, energy and financial sectors than others. On contrary, regulators should have a particular look to these sectors' stocks in order to carry out effective and efficient stabilization policies.

Figure 1.9. Sectors: Network map for the propagation of negative market perceptions/liquidity shock transmission.

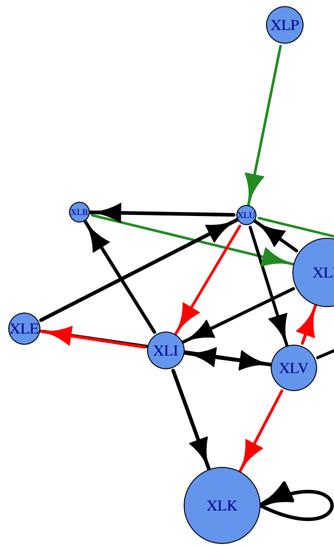

Notes: Each vertex represents a S&P500 sector. Black links (respectively red and green links) correspond to stongest links (respectively the second strongest and less strong links). The node size indicates the sector capitalization. Edge widths are proportionnal to link's weights.

The financial sector plays a central role in modern economies. It provides credit and generates equities for firms: it eases the flow of capital. Network maps of figures 1.9 and 1.10 are evidences of such centrality. From these maps, it comes out that returns and volatility of the financial sector are highly connected to those of others sectors. After a negative market perception of the financial sector, figure 1.9 stipulates that, with a high probability, next affected sectors will be industry and utilities. Once investors reduce their shares in these sectors, contagion will move to technology, materials, energy and health care. Suppose now that the financial sector faces a panic episod. The map to consider is given by figure 1.10. The panic movement is more likely to move firstly to the industry, technology, consumer discretionary and health care sectors. From those latter sectors, the shock will be amplified and transmitted to others.

Figure 1.10. Sectors: Network map for the propagation of volatility shocks/panic transmission. Each vertex represents a S&P500 sector.

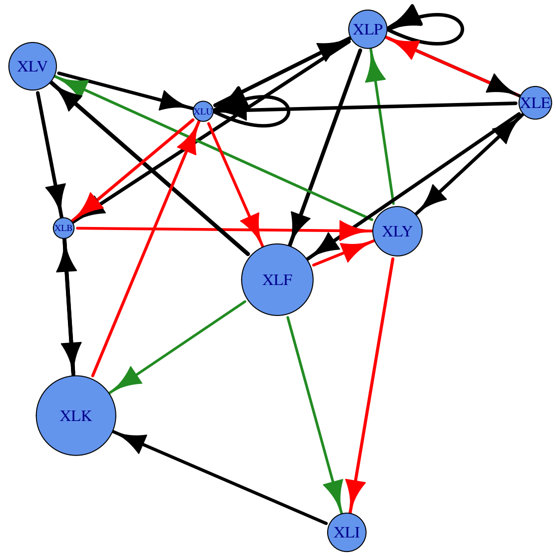

Notes: Black links (respectively red and green links) correspond to stongest links (respectively the second strongest and less strong links). The node size indicates the sector capitalization. Edge widths are proportionnal to link's weights.

1.6 Conclusion

This paper provides a general reduced-form model for the propagation of negative idiosyncratic shocks from any specific economic unit to the entire economic system, namely the systemic risk. The vector of returns is modeled as a multidimensional hawkes jump-diffusion process with a factor component, and mutually exciting jumps both in price and volatility. We account for different sources of systemic failure such as macro risk drivers or common exposures (Through common factors), connectedness and contagion effects (Through mutually exciting jumps both in price and volatility).

We rely on the GMM approach to estimate the model. We take advantage of high frequency data. Using estimates of both jump price excitation parameters $\hat{\beta}$ and volatility excitation parameters $\hat{\beta}^v$, we track associations within a number of US key banks and insurance companies. We also estimate the model for the nine S&P500 largest economic sectors. We construct a network map for the transmission of negative market perceptions or liquidity schocks, and a network map for the transmission of volatility shocks, fear or uncertainty about the future profitability. Futher, we provide information about contagiousness and vulnerability. We find that systemic risk has three related but distinct channels: common factors, price and volatility jumps.

We derive that returns of the technology, utilities and consumer discretionary sectors on the one hand, volatilities of materials, financial and technology sectors on the other hand are more sensitive to extreme market events. Distresses of health care, consumer staples, energy and financial sectors have the highest negative impacts on the economic system fragility. Concerning financial institutions, BAC, WFC, ACE and MET are bigger contributors to systemic risk. Propagation of volatility shocks throughout the system is more likely than price shock transmission.

Our network's maps and fragility measures provide new information to market participants, useful to reduce the adverse selection risk. Since firms know their positions on these network maps, they should adjust their business strategies to account for all this information. Tail dependence structures derived from returns and volatility lead to two different network maps: investors should base their investment strategies on the appropriate network map, depending on the type of risk they want to be edged. We come out with central firms and sectors. Thus, regulators have additional tools for their monitoring, in order to garantee a good trading environment.

Appendix

1.7 Tables

1.7.1 Some empirical results

Table 1.11. Maneesoonthorn, Forbes, and Martin (2016), 1 sector (Materials, XLB), diffusion part

	ρ_I	θ_I	η_I	κ_I	μ_I
Estimates	-0.116	5.4E-05	0.036	12.31	0.039
(t-Stat)	*(2.633)*	*(23.84)*	*(196.9)*	*(1.4E+05)*	*(1.490)*

Table 1.12. Maneesoonthorn, Forbes, and Martin (2016), 1 sector (Materials, XLB), jump part

	β_I	β_I^v	α_I	α_I^v	λ_{Inf}	λ_{Inf}^v	μ_I	γ_1	γ_2
Estimates	0.491	0.0001	1.188	1.433	0.0001	0.01	0.5	0.104	0.072
(t-Stat)	*(2E+06)*	*(2.6E+01)*	*(9E+06)*	*(6E+09)*	*(5E-01)*	*(2E+01)*	*(5E+04)*	*2E+02*	*(3E+01)*

Table 1.13. Aït-Sahalia, Cacho-Diaz, and Leaven (2015), 2 assets

	Financial Sector (XLF)	**Industrial Sector (XLI)**
θ_I	1.1E-04	4.9E-05
	(15.67)	*(15.52)*
μ_I	-0.016	0.076
	(0.337)	*(2.326)*
β_1	0.189	0.414
	(2.366)	*(31.24)*
β_2	0.000	0.139
	(0.002)	*(4.984)*
α_I	0.821	0.821
	(45.36)	*(45.36)*
λ_{Inf}	0.605	0.605
	(7.477)	*(7.477)*
γ_1	0.010	0.010
	(0.209)	*(0.209)*
γ_2	0.015	0.015
	(0.196)	*(0.196)*

Table 1.14. Double-Hawkes jump diffusion model, 2 assets

	Financial Sector (XLF)	Industrial Sector (XLI)		Financial Sector (XLF)	Industrial Sector (XLI)
b	0.083	0.020	β_1	0.089	0.000
	(18.06)	*(0.059)*		*(7.818)*	*(0.008)*
ρ_I	-0.702	-0.499	β_2	0.422	0.000
	(3.0E+02)	*(7.6E+02)*		*(37.04)*	*(0.010)*
θ_I	1.10E-04	1.37E-04	β_1^v	0.000	0.673
	(13.17)	*(0.670)*		*(0.060)*	*(569.7)*
η_I	0.041	0.036	β_2^v	0.000	0.000
	(6.2E+02)	*(3.0E+03)*		*(0.060)*	*(0.085)*
ρ_F	-0.172	-0.172	α_I	1.059	1.059
	(1.5E+02)	*(1.5E+02)*		*(295.7)*	*(295.7)*
θ_F	0.015	0.015	α_I^v	1.640	1.640
	(50.02)	*(50.02)*		*(3.4E+03)*	*(3.4E+03)*
η_F	0.251	0.251	λ_{Inf}	0.004	0.004
	(5.3E+03)	*(5.3E+03)*		*(0.606)*	*(0.606)*
κ_I	7.488	4.783	λ_{Inf}^v	1.00E-04	1.00E-04
	(1.2E+06)	*(3.8E+06)*		*(1.565)*	*(1.565)*
κ_F	2.103	2.103	λ_F	0.843	0.843
	(1.4E+06)	*(1.4E+06)*		*(15.59)*	*(15.59)*
μ_I	0.020	0.085	λ_F^v	0.003	0.003
	(0.417)	*(0.568)*		*(0.503)*	*(0.503)*
μ_F	-0.440	-0.440	μ_F^v	1.130	1.130
	(5.613)	*(5.613)*		*(8.4E+04)*	*(8.4E+04)*
γ_{F1}	0.014	0.014	μ_I^v	1.576	1.576
	(0.013)	*(0.013)*		*(4.1E+08)*	*(4.1E+08)*
γ_{F2}	0.183	0.183	γ_1	0.010	0.010
	0.884	*(0.884)*		*(0.035)*	*(0.035)*
			γ_2	0.144	0.144
				(1.976)	*(1.976)*

Table 1.15. Parameters estimates for sectors: the continuous part of the model.

	XLB	XLV	XLP	XLY	XLE	XLF	XLI	XLK	XLU
b	0.181	0.098	0.084	0.159	0.169	0.207	0.003	0.190	0.090
	8.2E-03	*5.2E-03*	*5.1E-03*	*8.1E-03*	*9.4E-03*	*9.9E-03*	*4.0E-03*	*8.9E-03*	*5.7E-03*
ρ	-0.894	-0.894	-0.894	-0.894	-0.894	-0.894	-0.894	-0.894	-0.894
	5.6E-02	*9.9E-03*	*7.4E-03*	*4.4E-02*	*1.3E-01*	*1.7E-01*	*3.7E-02*	*1.8E-01*	*2.1E-02*
θ	0.014	0.010	0.010	0.011	0.021	0.017	0.017	0.017	0.013
	7.2E-04	*4.4E-04*	*3.7E-04*	*5.0E-04*	*1.1E-03*	*1.2E-03*	*8.3E-04*	*1.5E-03*	*5.4E-04*
η	0.210	0.153	0.161	0.192	0.246	0.236	0.189	0.218	0.184
	1.0E-02	*1.3E-03*	*1.1E-03*	*7.5E-03*	*2.9E-02*	*3.5E-02*	*6.2E-03*	*3.5E-02*	*3.5E-03*
κ	1.590	1.136	1.352	1.652	1.408	1.640	1.078	1.426	1.320
	4.1E-04	*4.0E-05*	*1.7E-05*	*3.4E-04*	*2.0E-03*	*1.2E-03*	*2.0E-04*	*1.7E-03*	*6.1E-05*
μ	-0.033	0.005	0.050	0.006	-0.022	-0.105	0.075	-0.141	0.050
	3.4E-02	*2.5E-02*	*2.3E-02*	*3.1E-02*	*4.4E-02*	*4.5E-02*	*3.3E-02*	*4.6E-02*	*3.0E-02*

Notes: The estimation relies on 12 stocks traded on NYSE between january 2006 and december 2011. Parameters are idiosyncratic, meaning they are stock specific. Standard errors are in parenthesis.

Table 1.16. Parameters estimates for sectors (Cont'd): the factor component of the continuous part of the model.

	Estimates *(s.e.)*
ρ_F	- 0.8936
	(0.1321)
θ_F	0.3592
	(0.0182)
η_F	0.5735
	(0.0670)
κ_F	0.4686
	(0.001)
μ_F	0.4266
	(0.0258)

Notes: Standard errors are in parenthesis.

Table 1.17. Parameter estimates for sectors (cont'd): excitation parameters of price jump intensities (The matrix β).

	XLB	XLV	XLP	XLY	XLE	XLF	XLI	XLK	XLU
XLB	0.099	0.486	0.365	0.419	0.302	0.147	0.899	0.222	0.964
	0.010	*0.012*	*0.007*	*0.008*	*0.014*	*0.014*	*0.008*	*0.005*	*0.011*
XLV	0.133	0.057	0.391	0.533	0.873	0.214	0.914	0.229	0.820
	0.019	*0.006*	*0.008*	*0.011*	*0.018*	*0.028*	*0.020*	*0.008*	*0.016*
XLP	0.608	0.426	0.155	0.581	0.034	0.327	0.253	0.289	0.472
	0.009	*0.012*	*0.008*	*0.007*	*0.011*	*0.013*	*0.017*	*0.004*	*0.008*
XLY	0.249	0.802	0.464	0.595	0.227	0.483	0.601	0.277	0.659
	0.018	*0.011*	*0.009*	*0.005*	*0.016*	*0.027*	*0.015*	*0.007*	*0.017*
XLE	0.079	0.408	0.034	0.275	0.438	0.621	0.774	0.487	0.179
	0.007	*0.018*	*0.011*	*0.013*	*0.013*	*0.013*	*0.017*	*0.009*	*0.021*
XLF	0.687	0.785	0.273	0.929	0.164	0.134	0.165	0.291	0.409
	0.011	*0.027*	*0.019*	*0.021*	*0.023*	*0.014*	*0.030*	*0.016*	*0.035*
XLI	0.078	0.882	0.108	0.077	0.592	0.849	0.043	0.094	0.727
	0.008	*0.016*	*0.007*	*0.009*	*0.012*	*0.018*	*0.027*	*0.005*	*0.013*
XLK	0.558	0.758	0.603	0.470	0.192	0.574	0.982	0.932	0.028
	0.033	*0.013*	*0.016*	*0.014*	*0.023*	*0.042*	*0.020*	*0.008*	*0.029*
XLU	0.581	0.620	0.697	0.388	0.980	0.875	0.000	0.078	0.152
	0.014	*0.012*	*0.006*	*0.009*	*0.009*	*0.017*	*0.014*	*0.005*	*0.012*

Notes: The estimation relies on 12 stocks traded on NYSE between january 2006 and december 2011. Standard errors are in parenthesis.

Table 1.18. Parameter estimates (cont'd): excitation parameters of volatility jump intensities (The matrix β^v).

	XLB	XLV	XLP	XLY	XLE	XLF	XLI	XLK	XLU
XLB	0.547	0.918	0.894	0.448	0.285	0.207	0.177	1.001	0.783
	5.0E-04	*1.0E-03*	*4.4E-04*	*2.9E-05*	*7.4E-04*	*1.1E-03*	*1.2E-03*	*1.1E-03*	*2.5E-04*
XLV	0.364	0.143	0.608	0.690	0.327	1.041	0.118	0.100	0.306
	2.0E-04	*4.3E-04*	*1.8E-04*	*1.4E-05*	*3.0E-04*	*4.4E-04*	*5.0E-04*	*4.6E-04*	*1.0E-04*
XLP	0.079	0.233	0.886	0.674	0.777	0.405	0.239	0.167	0.972
	2.2E-04	*4.6E-04*	*1.9E-04*	*1.8E-05*	*3.3E-04*	*4.8E-04*	*5.4E-04*	*5.0E-04*	*1.1E-04*
XLY	0.702	0.615	0.106	0.366	0.840	0.726	0.205	0.420	0.077
	4.5E-04	*9.3E-04*	*3.9E-04*	*2.5E-05*	*6.6E-04*	*9.7E-04*	*1.1E-03*	*1.0E-03*	*2.3E-04*
XLE	0.278	0.646	0.810	0.808	0.543	0.623	0.248	0.609	0.395
	5.7E-04	*1.2E-03*	*5.0E-04*	*3.5E-05*	*8.5E-04*	*1.2E-03*	*1.4E-03*	*1.3E-03*	*2.9E-04*
XLF	0.467	0.392	0.986	0.414	0.901	0.542	0.219	0.518	0.721
	6.6E-04	*1.4E-03*	*5.8E-04*	*4.5E-05*	*9.8E-04*	*1.4E-03*	*1.6E-03*	*1.5E-03*	*3.4E-04*
XLI	0.550	0.607	0.485	0.790	0.340	0.673	0.543	0.088	0.168
	2.3E-04	*4.7E-04*	*2.0E-04*	*1.5E-05*	*3.4E-04*	*4.9E-04*	*5.5E-04*	*5.1E-04*	*1.1E-04*
XLK	0.952	0.554	0.557	0.205	0.573	0.662	0.809	0.328	0.343
	5.6E-04	*1.2E-03*	*4.9E-04*	*3.8E-05*	*8.3E-04*	*1.2E-03*	*1.4E-03*	*1.3E-03*	*2.8E-04*
XLU	0.000	0.855	0.151	0.232	0.908	0.399	0.035	0.755	0.872
	2.8E-04	*5.8E-04*	*2.4E-04*	*1.6E-05*	*4.1E-04*	*6.0E-04*	*6.8E-04*	*6.2E-04*	*1.4E-04*

Notes: The estimation relies on 12 stocks traded on NYSE between january 2006 and december 2011. Standard errors are in parenthesis.

Table 1.19. Parameters estimates (Cont'd): the factor component of the jump part of the model.

	Estimates ***(t-Stat)***		**Estimates** ***(t-Stat)***
λ_F	6.91E-02	$1/\gamma_1$	1.00E-02
	4.86E-01		*1.99E-01*
λ_{Fv}	1.00E-04	$1/\gamma_2$	3.46E-02
	1.25E-02		*1.34E-01*
μ_{Fv}	1.46E+00	α_I	1.07E+00
	9.80E-07		*3.44E-02*
μ_{Iv}	1.00E+00	α_I^v	9.39E-01
	3.03E-04		*1.11E-03*
$1/\gamma_{F1}$	2.03E-02	$\lambda_{I\infty}$	3.64E-01
	2.52E+00		*2.37E-02*
$1/\gamma_{F2}$	2.22E-01	$\lambda_{I\infty}^v$	1.24E-01
	2.31E-01		*2.48E-03*

Notes: Standard errors are in parenthesis.

1.7.2 Monte Carlo result for $m = 12$

Table 1.20. True excitation matrix β

	A1	A2	A3	A4	A5	A6	A7	A8	A9	A10	A11	A12
A1	0.040	0.040	0.453	0.044	0.040	0.058	0.379	0.094	0.044	0.058	0.379	0.453
A2	0.079	0.044	0.094	0.040	0.058	0.044	0.094	0.453	0.058	0.058	0.040	0.044
A3	0.044	0.044	0.094	0.040	0.044	0.044	0.453	0.379	0.044	0.453	0.040	0.044
A4	0.040	0.379	0.453	0.079	0.079	0.079	0.453	0.453	0.044	0.079	0.453	0.040
A5	0.379	0.058	0.044	0.044	0.094	0.453	0.453	0.040	0.040	0.453	0.079	0.079
A6	0.094	0.040	0.044	0.058	0.094	0.453	0.453	0.044	0.058	0.044	0.044	0.453
A7	0.453	0.044	0.044	0.094	0.044	0.044	0.453	0.453	0.044	0.094	0.094	0.044
A8	0.453	0.044	0.044	0.044	0.040	0.044	0.044	0.044	0.079	0.044	0.044	0.453
A9	0.379	0.044	0.379	0.379	0.094	0.379	0.040	0.079	0.040	0.044	0.044	0.079
A10	0.079	0.044	0.040	0.040	0.379	0.044	0.379	0.379	0.379	0.453	0.044	0.044
A11	0.079	0.040	0.044	0.379	0.044	0.058	0.379	0.379	0.044	0.040	0.079	0.044
A12	0.044	0.044	0.379	0.379	0.058	0.079	0.094	0.453	0.044	0.058	0.079	0.044

Table 1.21. Excitation matrix: Average estimate. Standard deviations are in italic.

	A1	A2	A3	A4	A5	A6	A7	A8	A9	A10	A11	A12
A1	0.036	0.036	0.354	0.037	0.035	0.047	0.302	0.073	0.037	0.043	0.296	0.356
	0.000	*0.001*	*0.028*	*0.001*	*0.000*	*0.004*	*0.022*	*0.009*	*0.002*	*0.005*	*0.028*	*0.030*
A2	0.068	0.037	0.083	0.044	0.055	0.039	0.077	0.361	0.052	0.060	0.039	0.041
	0.007	*0.001*	*0.009*	*0.010*	*0.011*	*0.004*	*0.006*	*0.027*	*0.008*	*0.014*	*0.007*	*0.005*
A3	0.037	0.038	0.073	0.036	0.038	0.038	0.364	0.303	0.038	0.357	0.036	0.038
	0.002	*0.002*	*0.008*	*0.000*	*0.002*	*0.002*	*0.027*	*0.022*	*0.002*	*0.030*	*0.000*	*0.002*
A4	0.039	0.302	0.368	0.068	0.069	0.062	0.365	0.364	0.041	0.073	0.361	0.039
	0.008	*0.023*	*0.026*	*0.016*	*0.009*	*0.007*	*0.028*	*0.025*	*0.009*	*0.011*	*0.029*	*0.006*
A5	0.298	0.047	0.037	0.038	0.068	0.361	0.360	0.036	0.036	0.349	0.062	0.060
	0.023	*0.004*	*0.001*	*0.001*	*0.012*	*0.027*	*0.027*	*0.000*	*0.000*	*0.029*	*0.006*	*0.008*
A6	0.076	0.037	0.039	0.049	0.077	0.364	0.363	0.038	0.049	0.041	0.039	0.360
	0.007	*0.004*	*0.003*	*0.008*	*0.008*	*0.026*	*0.028*	*0.002*	*0.007*	*0.007*	*0.005*	*0.027*
A7	0.355	0.038	0.038	0.073	0.037	0.039	0.359	0.358	0.037	0.067	0.074	0.037
	0.030	*0.002*	*0.002*	*0.009*	*0.001*	*0.002*	*0.028*	*0.027*	*0.001*	*0.011*	*0.010*	*0.002*
A8	0.361	0.038	0.040	0.038	0.037	0.037	0.038	0.038	0.063	0.041	0.038	0.360
	0.028	*0.001*	*0.003*	*0.003*	*0.002*	*0.001*	*0.002*	*0.002*	*0.007*	*0.004*	*0.002*	*0.029*
A9	0.302	0.038	0.298	0.296	0.071	0.303	0.036	0.063	0.035	0.037	0.038	0.061
	0.022	*0.002*	*0.023*	*0.024*	*0.009*	*0.022*	*0.000*	*0.005*	*0.000*	*0.002*	*0.002*	*0.007*
A10	0.060	0.038	0.035	0.035	0.286	0.039	0.302	0.298	0.289	0.339	0.038	0.037
	0.007	*0.002*	*0.000*	*0.000*	*0.035*	*0.002*	*0.024*	*0.024*	*0.035*	*0.041*	*0.002*	*0.001*
A11	0.066	0.036	0.041	0.305	0.041	0.046	0.306	0.302	0.040	0.042	0.063	0.040
	0.006	*0.002*	*0.004*	*0.025*	*0.005*	*0.004*	*0.022*	*0.022*	*0.005*	*0.007*	*0.008*	*0.004*
A12	0.038	0.038	0.298	0.293	0.046	0.063	0.074	0.359	0.038	0.046	0.062	0.038
	0.002	*0.002*	*0.024*	*0.034*	*0.004*	*0.007*	*0.007*	*0.028*	*0.002*	*0.004*	*0.007*	*0.002*

Table 1.22. True excitation matrix β^v

	A1	A2	A3	A4	A5	A6	A7	A8	A9	A10	A11	A12
A1	0.094	0.453	0.040	0.044	0.044	0.379	0.094	0.044	0.379	0.453	0.044	0.044
A2	0.453	0.094	0.040	0.044	0.040	0.044	0.094	0.044	0.044	0.079	0.094	0.379
A3	0.044	0.453	0.044	0.044	0.044	0.058	0.453	0.044	0.079	0.453	0.044	0.453
A4	0.094	0.379	0.094	0.079	0.044	0.079	0.094	0.044	0.044	0.044	0.044	0.044
A5	0.040	0.453	0.044	0.079	0.044	0.453	0.094	0.379	0.040	0.379	0.453	0.058
A6	0.379	0.379	0.044	0.040	0.040	0.094	0.379	0.379	0.044	0.044	0.044	0.044
A7	0.040	0.044	0.044	0.044	0.058	0.453	0.040	0.040	0.058	0.044	0.094	0.453
A8	0.044	0.079	0.094	0.379	0.058	0.079	0.044	0.044	0.044	0.044	0.040	0.379
A9	0.094	0.044	0.044	0.453	0.079	0.453	0.044	0.453	0.044	0.094	0.044	0.044
A10	0.379	0.094	0.044	0.379	0.058	0.044	0.079	0.094	0.058	0.040	0.079	0.044
A11	0.044	0.044	0.058	0.079	0.453	0.379	0.044	0.044	0.044	0.040	0.094	0.094
A12	0.044	0.079	0.453	0.044	0.044	0.044	0.094	0.079	0.040	0.044	0.044	0.044

Table 1.23. Excitation matrix β^v: Average estimate. Standard deviations are in italic.

	A1	A2	A3	A4	A5	A6	A7	A8	A9	A10	A11	A12
A1	0.054	0.346	0.037	0.037	0.053	0.276	0.053	0.033	0.280	0.350	0.050	0.036
	0.024	*0.030*	*0.003*	*0.003*	*0.011*	*0.033*	*0.020*	*0.004*	*0.027*	*0.028*	*0.011*	*0.003*
A2	0.369	0.082	0.042	0.050	0.046	0.048	0.089	0.045	0.047	0.070	0.086	0.310
	0.024	*0.006*	*0.006*	*0.012*	*0.007*	*0.008*	*0.011*	*0.008*	*0.009*	*0.005*	*0.008*	*0.022*
A3	0.048	0.348	0.043	0.037	0.061	0.053	0.322	0.033	0.061	0.348	0.058	0.337
	0.007	*0.031*	*0.004*	*0.003*	*0.020*	*0.005*	*0.040*	*0.003*	*0.013*	*0.029*	*0.019*	*0.034*
A4	0.127	0.337	0.139	0.103	0.104	0.118	0.127	0.059	0.083	0.057	0.085	0.072
	0.035	*0.030*	*0.044*	*0.028*	*0.042*	*0.038*	*0.038*	*0.018*	*0.034*	*0.015*	*0.030*	*0.026*
A5	0.027	0.314	0.029	0.062	0.027	0.276	0.072	0.264	0.029	0.264	0.285	0.046
	0.001	*0.039*	*0.003*	*0.006*	*0.001*	*0.062*	*0.007*	*0.040*	*0.002*	*0.034*	*0.046*	*0.004*
A6	0.302	0.301	0.036	0.037	0.031	0.076	0.305	0.305	0.039	0.036	0.033	0.038
	0.022	*0.022*	*0.005*	*0.007*	*0.005*	*0.008*	*0.021*	*0.022*	*0.006*	*0.004*	*0.005*	*0.004*
A7	0.059	0.052	0.063	0.052	0.087	0.386	0.053	0.040	0.066	0.048	0.108	0.378
	0.014	*0.009*	*0.016*	*0.013*	*0.018*	*0.029*	*0.015*	*0.008*	*0.014*	*0.007*	*0.015*	*0.027*
A8	0.042	0.068	0.084	0.309	0.050	0.072	0.044	0.042	0.043	0.039	0.038	0.310
	0.009	*0.008*	*0.010*	*0.021*	*0.011*	*0.010*	*0.009*	*0.005*	*0.007*	*0.005*	*0.006*	*0.022*
A9	0.055	0.039	0.039	0.321	0.066	0.326	0.038	0.343	0.038	0.060	0.047	0.037
	0.023	*0.003*	*0.003*	*0.037*	*0.022*	*0.037*	*0.003*	*0.030*	*0.003*	*0.015*	*0.010*	*0.003*
A10	0.299	0.075	0.035	0.306	0.046	0.036	0.063	0.077	0.045	0.033	0.065	0.035
	0.022	*0.008*	*0.006*	*0.020*	*0.014*	*0.005*	*0.007*	*0.007*	*0.005*	*0.004*	*0.012*	*0.004*
A11	0.044	0.040	0.050	0.082	0.352	0.313	0.048	0.048	0.048	0.039	0.070	0.084
	0.009	*0.008*	*0.010*	*0.016*	*0.027*	*0.023*	*0.011*	*0.008*	*0.012*	*0.007*	*0.013*	*0.009*
A12	0.070	0.086	0.394	0.061	0.091	0.069	0.105	0.075	0.058	0.053	0.081	0.054
	0.015	*0.010*	*0.028*	*0.017*	*0.020*	*0.018*	*0.019*	*0.013*	*0.017*	*0.008*	*0.018*	*0.013*

1.8 Technical proofs

Proof of Lemma 1.3.1

From the equation 1.8, the variance at time t is given by

$$V_{Fkt} = e^{-\kappa_{Fk}t}V_{Fk0} + \theta_{Fk}(1 - e^{-\kappa_{Fk}t}) + \eta_{Fk}\rho_{Fk}\int_0^t e^{-\kappa_{Fk}(t-u)}\sqrt{V_{Fku}}dB_u + \eta_{Fk}\sqrt{1-\rho_{Fk}^2}\int_0^t e^{-\kappa_{Fk}(t-u)}dW_u + \int_0^t e^{-\kappa_{Fk}(t-u)}Z^v_{Fku}dN_{Fku}$$

By taking the mean and assuming $t \to \infty$, we obtain the unconditional mean $E[V_{Fk}]$. We compute $E[V_{Ii}]$ using the same trick.

V^2_{Fkt} is obtained by applying the Itö Lemma in definition 1.3.2 to the differential equation 1.8, and using the function $f(x) = x^2$:

$$V^2_{Fkt} - V^2_{Fk0} = 2\kappa_{Fk}\int_{t_0}^t(\theta_{Fk}V_{Fks} - V^2_{Fks})ds + {\eta_{Fk}}^2\int_{t_0}^t E[V_{Fks}]ds + \int_{t_0}^t[2V_{Fks}Z^v_{Fks}dN^v_{Fks} + (Z^v_{Fks})^2dN^v_{Fks}]$$

We derive $E[V^2_{Fkt}]$ by taking the expectation of both sides of the equation and setting the left hand side to 0.

Proof of Theorem 1.3.1

The covariance density matrix is defined by

$$\begin{aligned} R_I(\tau)dt^2 &= E[dN_{It+\tau}dN^T_{It}] - E[dN_{It+\tau}]E[dN^T_{It}], \quad \forall\tau > 0 \\ &= E[(N_{It+\tau} - N_{It-dt+\tau}(N_{It} - N_{It-dt})^T] - E[(N_{It+\tau} - N_{It-dt+\tau}E[(N_{It} - N_{It-dt})^T] \end{aligned}$$

Let's assume that $t - dt < t < t + \tau - dt < t + \tau$. From the lemma 5 of Fonseca and Zaatour (2015), it comes out that

$$R_I(\tau)dt^2 = c_2(dt)c_0(\tau - dt)c_2(dt)\left(\bar{\Lambda}_\infty + \beta D\right)$$

where $c_2(dt) = (\beta - \alpha)^{-1}\left[e^{(\beta-\alpha)dt} - I\right]$; $c_0(\tau - dt) = e^{(\beta-\alpha)(\tau-dt)}$; I is the $m \times m$ identity matrix; $\bar{\Lambda}_\infty$ is the solution of the *Lyapounov* matricial equation given by

$$(\beta - \alpha)\bar{\Lambda}_\infty + \bar{\Lambda}_\infty(\beta - \alpha)^T + \beta D\beta = 0$$

With $\beta = (\beta_{Iij})_{1\leqslant i,j\leqslant m}$ the matrix of excitation parameters, $\alpha = \overline{D}_g(\alpha_{I1}, ..., \alpha_{Im})$ and $D = \overline{D}_g(E[\lambda_{I1}], ..., E[\lambda_{Im}])$.

It can be checked that $c_2(dt)c_0(\tau - dt)c_2(dt) = e^{(\beta-\alpha)\tau}dt^2$. Then, we derive that

$$R_I(\tau) = e^{(\beta-\alpha)\tau}\left(\bar{\Lambda}_\infty + \beta D\right)$$

Proof of Corollary 1.3.1

$$\begin{aligned}
\int_0^\Delta \int_0^s R_I(t-s)dtds &= \int_0^\Delta \int_0^s R_I(s-t)^T dtds \\
&= \left[\int_0^\Delta \int_0^s e^{(\beta-\alpha)(s-t)}\left(\bar{\Lambda}_\infty + \beta D\right) dtds\right]^T \\
&= \left[\int_0^\Delta -(\beta-\alpha)^{-1}\left(I - e^{(\beta-\alpha)s}\right) ds \left(\bar{\Lambda}_\infty + \beta D\right) dtds\right]^T \\
&\approx \left[\int_0^\Delta -(\beta-\alpha)^{-1}\left(-(\beta-\alpha)s\right) ds \left(\bar{\Lambda}_\infty + \beta D\right) dtds\right]^T \\
&= \left(\bar{\Lambda}_\infty + \beta D\right)^T \frac{\Delta^2}{2}
\end{aligned}$$

$$\begin{aligned}
\int_0^\Delta \int_\tau^{\Delta+\tau} R_I(s-t)dtds &= \int_0^\Delta \int_\tau^{\Delta+\tau} R_I(t-s)^T dtds \\
&= \left[\int_0^\Delta \int_\tau^{\Delta+\tau} e^{(\beta-\alpha)(t-s)}\left(\bar{\Lambda}_\infty + \beta D\right) dtds\right]^T \\
&= \left[\int_\tau^{\Delta+\tau} e^{(\beta-\alpha)t}dt \cdot \int_0^\Delta e^{-(\beta-\alpha)s}ds \left(\bar{\Lambda}_\infty + \beta D\right)\right]^T \\
&= [(\beta-\alpha)^{-1}\left[e^{(\beta-\alpha)(\Delta+\tau)} - e^{(\beta-\alpha)\tau}\right](\beta-\alpha)^{-1}\left[I - e^{-(\beta-\alpha)\Delta}\right] \\
&\times \left(\bar{\Lambda}_\infty + \beta D\right)]^T \\
&\approx \left[e^{(\beta-\alpha)\tau}\left(\bar{\Lambda}_\infty + \beta D\right)\right]^T \Delta^2
\end{aligned}$$

$$\begin{aligned}
\int_t^{t+1} \int_{t+\tau}^{t+\tau+1} R_I(s-t)dsdu &= \int_t^{t+1} \int_{t+\tau}^{t+\tau+1} e^{(\beta-\alpha)(s-u)}\left(\bar{\Lambda}_\infty + \beta D\right) dsdu \\
&= \int_t^{t+1} e^{-(\beta-\alpha)u}du \cdot \int_{t+\tau}^{t+\tau+1} e^{(\beta-\alpha)s}ds \left(\bar{\Lambda}_\infty + \beta D\right) \\
&= -(\beta-\alpha)^{-1}\left(e^{-(\beta-\alpha)} - I\right)(\beta-\alpha)^{-1}\left(e^{(\beta-\alpha)(\tau+1)} - e^{(\beta-\alpha)\tau}\right) \\
&\times \left(\bar{\Lambda}_\infty + \beta D\right) \\
&= \left(I - e^{-(\beta-\alpha)}\right)(\beta-\alpha)^{-2}\left(e^{(\beta-\alpha)(\tau+1)} - e^{(\beta-\alpha)\tau}\right)\left(\bar{\Lambda}_\infty + \beta D\right)
\end{aligned}$$

Closed form expressions of second moment of V_{Ii}

By resolving the differential equation 1.9, we obtain

$$\begin{aligned}
V_{Iit} = e^{-\kappa_{Iit}}V_{Ii0} + \theta_{Ii}(1-e^{-\kappa_{Ii}}) + \eta_{Ii}\rho_{Ii}\int_0^t e^{-\kappa_{Ii}(t-u)}\sqrt{V_{Iiu}}dB_u + \\
\eta_{Ii}\sqrt{1-\rho_{Ii}^2}\int_0^t e^{-\kappa_{Ii}(t-u)}dW_u + \int_0^t e^{-\kappa_{Ii}(t-u)}Z_{Iiu}^v dN_{Iiu}^v
\end{aligned}$$

Let's consider $s \geq t$, and $V_{Iit}^* = V_{Iit} - \theta$. By the Itö calculus, it comes out that

$$\begin{aligned}
E[V_{Iis}^* V_{Iit}^*] &= e^{-\kappa_{Ii}(s+t)}[E[V_{Ii0}^{*2}] + E[V_{Ii0}]E[Z_{Ii}^v]E[\lambda_{Ii}^v]\tfrac{e^{\kappa_{Ii}t}-1}{\kappa_{Ii}} + \eta_{Ii}^2(E[V_{Ii}^*] + \theta_{Ii})(e^{2\kappa_{Ii}t}-1) \\
&+ E[V_{Ii0}]E[Z_{Ii}^v]E[\lambda_{Ii}^v]\tfrac{e^{\kappa_{Ii}s}-1}{\kappa_{Ii}} + \int_0^s \int_0^t e^{\kappa_{Ii}(u+v)}E[Z_{Iiu}Z_{Iiv}]E\left[\tfrac{dN_{Iiu}^v}{du}\tfrac{dN_{Iiv}^v}{dv}\right]dudv]
\end{aligned}$$

Let's recall that $R_{Iii}(v-u)^v = E\left[\frac{dN_{Iiu}^v}{du}\frac{dN_{Iiv}^v}{dv}\right] - E\left[\frac{dN_{Iiu}^v}{du}\right]\left[\frac{dN_{Iiv}^v}{dv}\right]$. Since R_{Iii}^v is not defined at

0, we consider the complete density matrix $R_{Iii}(v-u)^{v(c)} = R_{Iii}(v-u)^v + \delta_{ii}(v-u)E[\lambda^v_{Ii}]$, with δ_{ii} the Dirac function. We show that

$$\begin{aligned}
&\int_0^s \int_0^t e^{\kappa_{Ii}(u+v)} E[Z_{Iiu}Z_{Iiv}]E\left[\tfrac{dN_{Iiu}}{du}\tfrac{dN_{Iiv}}{dv}\right] dudv \\
&= \int_0^s \int_0^t e^{\kappa_{Ii}(u+v)} E[Z_{Iiu}Z_{Iiv}](R_{Iii}(v-u)^{v(c)} + E[\lambda^v_{Ii}]^2) dudv \\
&= \int_0^s \int_0^t e^{\kappa_{Ii}(u+v)} E[Z_{Iiu}Z_{Iiv}]R_{Iii}(v-u)^v dudv + \int_0^s \int_0^t e^{\kappa_{Ii}(u+v)} E[Z_{Iiu}Z_{Iiv}]\delta_{ii}(v-u)E[\lambda^v_{Ii}]dudv \\
&+ \int_0^s \int_0^t e^{\kappa_{Ii}(u+v)} E[Z_{Iiu}Z_{Iiv}]\delta_{ii}(v-u)E[\lambda^v_{Ii}]^2 dudv \\
&= E[Z_{Ii}]^2 \int_0^s \int_0^t e^{\kappa_{Ii}(u+v)} R_{Iii}(v-u)^v dudv + E[Z^2_{Ii}]E[\lambda^v_{Ii}]\tfrac{(e^{2\kappa_{Ii}t}-1)}{2\kappa_{Ii}} \\
&+ E[Z_{Ii}]^2 E[\lambda^v_{Ii}]^2 \tfrac{(e^{\kappa_{Ii}t}-1)}{\kappa_{Ii}}\tfrac{(e^{\kappa_{Ii}s}-1)}{\kappa_{Ii}}
\end{aligned}$$

Then, $\forall s \geqslant t$:

$$\begin{aligned}
E[V_{Iis}V_{Iit}] &= e^{-\kappa_{Ii}(s+t)}[E[V^2_{Ii0} - \theta_{Ii}E[V_{Ii}] + \theta^2_{Ii} + E[Z_{Ii}]^2 E[\lambda^v_{Ii}]^2 \tfrac{(e^{\kappa_{Ii}t} - e^{\kappa_{Ii}s} - 2)}{\kappa_{Ii}} \\
&+ \eta^2_{Ii}E[V_{Ii}]\tfrac{((e^{2\kappa_{Ii}t}-1)}{2\kappa_{Ii}} + E[Z^2_{Ii}]E[\lambda^v_{Ii}]\tfrac{(e^{2\kappa_{Ii}t}-1)}{2\kappa_{Ii}} + E[Z_{Ii}]^2 E[\lambda^v_{Ii}]^2 \tfrac{(e^{\kappa_{Ii}t}-1)}{\kappa_{Ii}}\tfrac{(e^{\kappa_{Ii}s}-1)}{\kappa_{Ii}} \\
&+ E[Z_{Ii}]^2 \int_0^s \int_0^t e^{\kappa_{Ii}(u+v)} R_{Iii}(v-u)^v dudv] + 2\theta_{Ii}E[V_{Ii}] - \theta^2_{Ii}
\end{aligned}$$

The result is obtained by setting $s = t$ and $t \to \infty$:

$$E[V^2_{Ii}] - E[V_{Ii}]^2 = \frac{\eta^2_{Ii}E[V_{Ii}]}{2\kappa_{Ii}} + \frac{E[(Z^v_{Ii})^2]E[\lambda^v_{Ii}]}{2\kappa_{Ii}} + E[(Z^v_{Ii})^2]\Pi_\infty \tag{1.71}$$

with $\Pi_\infty = \lim_{t\to\infty} \; e^{-2\kappa_{Ii}t}\int_0^t\int_0^t e^{\kappa_{Ii}(u+v)}R^v_{ii}(v-u)dudv$. Using the same tricks, we establish $\forall i \neq j$ that

$$E[(V_{Ii} - \theta_{Ii})(V_{Ij} - \theta_{Ij})] = [\frac{E[\lambda^v_{Ii}]E[\lambda^v_{Ij}]}{\kappa_{Ii}\kappa_{Ij}} + \Phi_\infty]E[Z^v_{Ii}]E[Z^v_{Ij}], \quad \forall i \neq j \tag{1.72}$$

with $\Phi_\infty = \lim_{t\to\infty} \; e^{-(\kappa_{Ii}+\kappa_{Ij})t}\int_0^t\int_0^t e^{(\kappa_{Ii}u+\kappa_{Ij}v)}R^v_{ii}(v-u)dudv$.

Closed form expressions of others covariances of log-returns

$$
\begin{aligned}
&E\left[\left(\Delta X_{i,t}-E[\Delta X_{i,t}]\right)\left(\Delta X_{j,t}-E[\Delta X_{j,t}]\right)^3\right]=\left[b_iE[\overline{D}_g(Z_F)^4]\overline{D}_g(\lambda_F)\overline{D}_g(b_j)^2b_j^{'}\right]\Delta\\
&+\frac{3}{2}\left[b_iE[\overline{D}_g(Z_F)^2]\overline{D}_g(\lambda_F)b_j^{'}+b_iE[\overline{D}_g(V_F)]b_j^{'}\right]\\
&\times\left[E[V_{Ii}]+E[V_{Ij}]+2b_jE[\overline{D}_g(V_F)]b_j{'}+2b_jE[\overline{D}_g(Z_F)^2]\overline{D}_g(\lambda_F)b_j{'}+2E[Z_{Ij}^2]E[\lambda_{Ij}]\right]\Delta^2\\
&-\frac{3}{2}E[Z_{Ij}^2]E[\lambda_{Ij}]b_iE[\overline{D}_g(Z_F)^2]\overline{D}_g(\lambda_F)b_j{'}\Delta^2\\
&+\frac{3}{2}\left[b_j\overline{D}_g(b_j)^2E[\overline{D}_g(Z_F)^3]\lambda_F+E[Z_{Ij}^3]E[\lambda_{Ij}]\right]\left[E[Z_{Ij}]E[\lambda_{Ij}]+b_jE[\overline{D}_g(Z_F)]\lambda_F\right]\\
&+\frac{3}{2}b_iE[\overline{D}_g(Z_F)^3]\overline{D}_g(\lambda_F)\overline{D}_g(b_j)b_j^{'}\left[E[Z_{Ij}]E[\lambda_{Ij}]+b_jE[\overline{D}_g(Z_F)]\lambda_F\right]\Delta^2\\
&+E[Z_{Ii}]E[Z_{Ij}^3]\left[2\int_{s=0}^{\Delta}\int_{t=0}^{s}R_{Iji}(t-s)dtds+\int_{s=0}^{\Delta}\int_{t=0}^{s}R_{Iij}(t-s)dtds\right]
\end{aligned}
\tag{1.73}
$$

$$
\begin{aligned}
&E\left[\left(\Delta X_{i,t}-E[\Delta X_{i,t}]\right)^2\left(\Delta X_{j,t}-E[\Delta X_{j,t}]\right)^2\right]=\left[b_i\overline{D}_g(b_i)E[\overline{D}_g(Z_F)^4]\overline{D}_g(\lambda_F)\overline{D}_g(b_j)b_j^{'}\right]\Delta\\
&+2\left[b_iE[\overline{D}_g(V_F)]b_j^{'}+b_iE[\overline{D}_g(Z_F)^2]\overline{D}_g(\lambda_F)b_j^{'}\right]^2\Delta^2\\
&+3b_i\overline{D}_g(b_i)\left[E[\overline{D}_g(V_F)^2]-\overline{D}_g(E[V_F])^2\right]\overline{D}_g(b_j)b_j^{'}\Delta^2\\
&+\left[b_iE[\overline{D}_g(V_F)]b_i^{'}+b_iE[\overline{D}_g(Z_F)^2]\overline{D}_g(\lambda_F)b_i^{'}\right]\\
&\times\left[b_jE[\overline{D}_g(V_F)]b_j^{'}+b_jE[\overline{D}_g(Z_F)^2]\overline{D}_g(\lambda_F)b_j^{'}\right]\Delta^2\\
&+\left[b_jE[\overline{D}_g(V_F)]b_j^{'}+b_jE[\overline{D}_g(Z_F)^2]\overline{D}_g(\lambda_F)b_j^{'}\right]\left[E[V_{Ii}]+E[Z_{Ii}^2]E[\lambda_{Ii}]\right]\Delta^2\\
&+\left[b_iE[\overline{D}_g(V_F)]b_i^{'}+b_iE[\overline{D}_g(Z_F)^2]\overline{D}_g(\lambda_F)b_i^{'}\right]\left[E[V_{Ij}]+E[Z_{Ij}^2]E[\lambda_{Ij}]\right]\Delta^2\\
&+\left[E[V_{Ii}]+E[Z_{Ii}^2]E[\lambda_{Ii}]\right]\left[E[V_{Ij}]+E[Z_{Ij}^2]E[\lambda_{Ij}]\right]\Delta^2+\left(E[V_{Ii}V_{Ij}]-E[V_{Ii}]E[V_{Ij}]\right)\Delta^2\\
&+\left[b_jE[\overline{D}_g(Z_F)]\lambda_F+E[Z_{Ij}]E[\lambda_{Ij}]\right]b_i\overline{D}_g(b_i)E[\overline{D}_g(Z_F)^3]\overline{D}_g(\lambda_F)b_j^{'}\Delta^2\\
&+\left[b_iE[\overline{D}_g(Z_F)]\lambda_F+E[Z_{Ii}]E[\lambda_{Ii}]\right]b_j\overline{D}_g(b_j)E[\overline{D}_g(Z_F)^3]\overline{D}_g(\lambda_F)b_i^{'}\Delta^2\\
&+E[Z_{Ii}^2]E[Z_{Ij}^2]\left[\int_{s=0}^{\Delta}\int_{t=0}^{s}R_{Iij}(t-s)dtds+\int_{s=0}^{\Delta}\int_{t=0}^{s}R_{Iji}(t-s)dtds\right]
\end{aligned}
\tag{1.74}
$$

Lemma 1.8.1 *Let Δ be the sampling frequency, and τ a strictly positive real number. Under* *assumptions (1.4) - (1.27), the following closed-form formulae hold:*

$$
\begin{aligned}
&\int_0^\Delta \int_\tau^{\Delta+\tau} E[V_{Fks}V_{Fkt}]dtds = E[(V_{Fk0}-\theta_{Fk})^2]\frac{e^{-\kappa_k\Delta}-1}{\kappa_k}\frac{e^{-\kappa_k\tau}-e^{-\kappa_k(\Delta+\tau)}}{\kappa_k} \\
&+\frac{E[(V_{Fk0}-\theta_{Fk})]E[Z^v_{Fk}]\lambda^v_{Fl}}{\kappa_k}\left[\frac{e^{-\kappa_k\tau}-e^{-\kappa_k(\Delta+\tau)}}{\kappa_k}\Delta-\frac{1-e^{-\kappa_k\Delta}}{\kappa_k}\frac{e^{-\kappa_k\tau}-e^{-\kappa_k(\Delta+\tau)}}{\kappa_k}\right] \\
&+\frac{E[(V_{Fk0}-\theta_{Fk})]E[Z^v_{Fk}]\lambda^v_{Fl}}{\kappa_k}\left[\frac{1-e^{-\kappa_k\Delta}}{\kappa_k}\Delta-\frac{1-e^{-\kappa_k\Delta}}{\kappa_k}\frac{e^{-\kappa_k\tau}-e^{-\kappa_k(\Delta+\tau)}}{\kappa_k}\right] \\
&+\left(\frac{\eta^2_{Fk}E[V_{Fk}]}{2\kappa_k}+\frac{E[(Z^v_{Fk})^2]\lambda^v_{Fl}}{2\kappa_k}\right)\left[\frac{e^{\kappa_k\Delta}-1}{\kappa_k}\frac{e^{-\kappa_k\tau}-e^{-\kappa_k(\Delta+\tau)}}{\kappa_k}-\frac{1-e^{-\kappa_k\Delta}}{\kappa_k}\frac{e^{-\kappa_k\tau}-e^{-\kappa_k(\Delta+\tau)}}{\kappa_k}\right] \\
&+\left(\frac{E[Z^v_{Fk}]\lambda^v_{Fk}}{\kappa_k}\right)^2\left[1+\frac{e^{-\kappa_k\Delta}-1}{\kappa_k}\right]\left[\Delta+\frac{e^{-\kappa_k(\Delta+\tau)}-e^{-\kappa_k\tau}}{\kappa_k}\right] \\
&+\left(+2\theta_{Fk}E[(V_{Fk}]-\theta^2_{Fk}\right)\Delta^2
\end{aligned}
\tag{1.75}
$$

Let R^v_{Iij} be the element in row i and column j of the volatility covariance density matrix R^v_I, as defined in Definition 1.3.1. Then, $\forall i \neq j$

$$
\begin{aligned}
&\int_0^\Delta \int_\tau^{\Delta+\tau} E[V_{Iis}V_{Ijt}]dtds = E[(V_{Ii0}-\theta_{Ii})(V_{Ij0}-\theta_{Ij})]\left[\frac{1-e^{-\kappa_j\Delta}}{\kappa_j}\right]\left[\frac{e^{-\kappa_i\tau}-e^{-\kappa_i(\Delta+\tau)}}{\kappa_i}\right] \\
&+\frac{E[(V_{Ii0}-\theta_{Ii})]E[Z^v_{Ij}]E[\lambda^v_{Ij}]}{\kappa_j}\left[\frac{e^{-\kappa_i\tau}-e^{-\kappa_i(\Delta+\tau)}}{\kappa_i}\Delta-\left(\frac{1-e^{-\kappa_j\Delta}}{\kappa_j}\right)\left(\frac{e^{-\kappa_i\tau}-e^{-\kappa_i(\Delta+\tau)}}{\kappa_i}\right)\right] \\
&+\frac{E[(V_{Ij0}-\theta_{Ij})]E[Z^v_{Ii}]E[\lambda^v_{Ii}]}{\kappa_i}\left[\frac{1-e^{-\kappa_j\Delta}}{\kappa_j}\Delta-\left(\frac{1-e^{-\kappa_j\Delta}}{\kappa_j}\right)\left(\frac{e^{-\kappa_i\tau}-e^{-\kappa_i(\Delta+\tau)}}{\kappa_i}\right)\right] \\
&+\left(\frac{E[Z^v_{Ii}]E[Z^v_{Ij}]E[\lambda^v_{Ii}]E[\lambda^v_{Ij}]}{\kappa_i\kappa_j}\right)\left[\Delta+\frac{e^{-\kappa_j\Delta}-1}{\kappa_j}\right]\left[\Delta+\frac{e^{-\kappa_i(\Delta+\tau)}-e^{-\kappa_i\tau}}{\kappa_i}\right] \\
&+E[Z^v_{Ii}]E[Z^v_{Ij}]\int_0^\Delta\int_\tau^{\Delta+\tau}\int_0^s\int_0^u e^{-\kappa_i(s-y)}e^{-\kappa_j(u-x)}R^v_{Iij}(y-x)dxdydsdu \\
&+\left(\theta_{Ij}E[V_{Ii}]+\theta_{Ii}E[(V_{Ij}]-\theta_{Ii}\theta_{Ij}\right)\Delta^2
\end{aligned}
\tag{1.76}
$$

$\int_0^\Delta\int_\tau^{\Delta+\tau}\int_0^s\int_0^t e^{\kappa_i x}e^{\kappa_j y}R^v_{Iij}(y-x)dxdydtds$ is numerically computed, since we know the close form of the function $R^v_{Iij}()$ (cf Theorem 1.3.1)

Proof of lemma 1.8.1

From the equation 1.8 and 1.9, variances at time t are given by

$$V_{Fkt} = e^{-\kappa_{Fk}t}V_{Fk0} + \theta_{Fk}(1 - e^{-\kappa_{Fk}t}) + \eta_{Fk}\rho_{Fk}\int_0^t e^{-\kappa_{Fk}(t-u)}\sqrt{V_{Fku}}dB_u + \eta_{Fk}\sqrt{1-\rho_{Fk}^2}\int_0^t e^{-\kappa_{Fk}(t-u)}dW_u + \int_0^t e^{-\kappa_{Fk}(t-u)}Z_{Fku}^v dN_{Fku}$$

$$V_{Iit} = e^{-\kappa_{Ii}t}V_{Ii0} + \theta_{Ii}(1 - e^{-\kappa_{Ii}t}) + \eta_{Ii}\rho_{Ii}\int_0^t e^{-\kappa_{Ii}(t-u)}\sqrt{V_{Iiu}}dB_u + \eta_{Ii}\sqrt{1-\rho_{Ii}^2}\int_0^t e^{-\kappa_{Ii}(t-u)}dW_u + \int_0^t e^{-\kappa_{Ii}(t-u)}Z_{Iiu}^v dN_{Iiu}$$

Let s and t be two positive numbers, $s \geq t$. We use the Itö calculus to compute $V_{Fks}V_{Fkt}$ and $V_{Iis}V_{Iit}$, and then, we take expectations of both sides to get

$$\begin{aligned} E[V_{Fks}V_{Fkt}] = e^{-(s+t)}[E[(V_{Fk0} - \theta_{Fk})^2] + E[V_{Fk0} - \theta_{Fk}]E[Z_{Fk}^v]\lambda_{Fk}^v\frac{(e^{\kappa_{Fk}t} - 1)}{\kappa_{Fk}} \\ + \eta_{Fk}^2 E[V_{Fk}]\frac{(e^{2\kappa_{Fk}t} - 1)}{2\kappa_{Fk}} + E[V_{Fk0} - \theta_{Fk}]E[Z_{Fk}^v]\lambda_{Fk}^v\frac{(e^{\kappa_{Fk}s} - 1)}{\kappa_{Fk}} \\ + \int_0^s\int_0^t e^{\kappa_{Fk}(u+v)}E[Z_{Fku}^v Z_{Fkv}^v]E[dN_{Fku}^v dN_{Fkv}^v]] + 2\theta_{Fk}E[V_{Fk}] - \theta_{Fk}^2 \end{aligned} \tag{1.77}$$

and

$$\begin{aligned} E\left[V_{Iis}V_{Iit}\right] = e^{-\kappa_{Ii}s-\kappa_{Ij}t}[E[(V_{Ii0} - \theta_{Ii})(V_{Ij0} - \theta_{Ij})] + E[V_{Ii0} - \theta_{Ii}]E[Z_{Ij}^v]E[\lambda_{Ij}^v]\frac{(e^{\kappa_{Ij}t} - 1)}{\kappa_{Ij}} \\ + E[V_{Ij0} - \theta_{Ij}]E[Z_{Ii}^v]E[\lambda_{Ii}^v]\frac{(e^{\kappa_{Ii}s} - 1)}{\kappa_{Ii}} + E[Z_{Ii}^v]E[Z_{Ij}^v]\int_0^s\int_0^t e^{\kappa_{Ii}v}e^{\kappa_{Ij}u}E[dN_{Iiu}^v dN_{Ijv}^v]] \\ + \theta_{Ij}E[V_{Ii}] + \theta_{Ii}E[V_{Ij}] - \theta_{Ii}\theta_{Ij} \end{aligned} \tag{1.78}$$

Since N_{Fk}^v is a point process with constant rate, we get

$$\begin{aligned} E[V_{Fks}V_{Fkt}] = e^{-(s+t)}[E[(V_{Fk0} - \theta_{Fk})^2] + E[V_{Fk0} - \theta_{Fk}]E[Z_{Fk}^v]\lambda_{Fk}^v\frac{(e^{\kappa_{Fk}t} - 1)}{\kappa_{Fk}} \\ + \eta_{Fk}^2 E[V_{Fk}]\frac{(e^{2\kappa_{Fk}t} - 1)}{2\kappa_{Fk}} + E[V_{Fk0} - \theta_{Fk}]E[Z_{Fk}^v]\lambda_{Fk}^v\frac{(e^{\kappa_{Fk}s} - 1)}{\kappa_{Fk}} \\ + E[(Z_{Fk}^v)^2]\lambda_{Fk}^v\frac{(e^{2\kappa_{Fk}t} - 1)}{2\kappa_{Fk}} + (E[Z_{Fk}^v]\lambda_{Fk}^v)^2\left(\frac{(e^{\kappa_{Fk}s} - 1)}{\kappa_{Fk}}\right)\left(\frac{(e^{\kappa_{Fk}t} - 1)}{\kappa_{Fk}}\right)] \\ + 2\theta_{Fk}E[V_{Fk}] - \theta_{Fk}^2 \end{aligned} \tag{1.79}$$

N_{Iiu}^v is a hawkes proces, to compute $E\left[V_{Iis}V_{Iit}\right]$ we need to use the corresponding covariance density matrix defined by

$$R_{Iij}(v-u)^v = E\left[\frac{dN^v_{Iiu}}{du}\frac{dN^v_{Iiv}}{dv}\right] - E\left[\frac{dN^v_{Iiu}}{du}\right]\left[\frac{dN^v_{Ijv}}{dv}\right]$$

It follows that

$$\begin{aligned}E\left[V_{Iis}V_{Iit}\right] &= e^{-\kappa_{Ii}s-\kappa_{Ij}t}[E[(V_{Ii0}-\theta_{Ii})(V_{Ij0}-\theta_{Ij})] + E[V_{Ii0}-\theta_{Ii}]E[Z^v_{Ij}]E[\lambda^v_{Ij}]\frac{(e^{\kappa_{Ij}t}-1)}{\kappa_{Ij}} \\ &+ E[V_{Ij0}-\theta_{Ij}]E[Z^v_{Ii}]E[\lambda^v_{Ii}]\frac{(e^{\kappa_{Ii}s}-1)}{\kappa_{Ii}} + E[Z^v_{Ii}]E[Z^v_{Ij}]\int_0^s\int_0^t e^{\kappa_{Ii}v}e^{\kappa_{Ij}u}R_{Iij}(v-u)^v dudv \\ &+ E[Z^v_{Ii}]E[Z^v_{Ij}]E[\lambda^v_{Ii}]E[\lambda^v_{Ij}]\frac{(e^{\kappa_{Ii}s}-1)}{\kappa_{Ii}}\frac{(e^{\kappa_{Ij}t}-1)}{\kappa_{Ij}}] + \theta_{Ij}E[V_{Ii}] + \theta_{Ii}E[V_{Ij}] - \theta_{Ii}\theta_{Ij}\end{aligned} \tag{1.80}$$

Closed-form expressions of $\int_0^\Delta\int_\tau^{\Delta+\tau} E[V_{Fks}V_{Fkt}]dtds$ and $\int_0^\Delta\int_\tau^{\Delta+\tau} E[V_{Iis}V_{Ijt}]dtds$ are deduced by integrating the previous equations.

Proof of Theorem 1.3.5

$$E[\mathrm{IV}_{it,t+1}] = \sum_{k=1}^K b^2_{ik}E[V_{Fk}] + E[V_{Ii}], \quad \forall i = 1,...,m \tag{1.81}$$

$$E[\mathrm{QV}_{it,t+1}] - E[\mathrm{IV}_{it,t+1}] = \sum_{k=1}^K b^2_{ik}E[Z^2_{Fk}]\lambda_{Fk} + E[Z^2_{Ii}]E[\lambda_{Ii}], \quad \forall i = 1,...,m \tag{1.82}$$

$$E[\mathrm{ICov}_{ijt,t+1}] = \sum_{k=1}^K b_{ik}b_{jk}E[V_{Fk}], \quad \forall i \neq j \tag{1.83}$$

$$E[\mathrm{QCov}_{ijt,t+1}] - E[\mathrm{ICov}_{ijt,t+1}] = \sum_{k=1}^K b_{ik}b_{jk}E[Z^2_{Fk}]\lambda_{Fk}, \quad \forall i \neq j \tag{1.84}$$

$$\begin{aligned}E[\mathrm{QV}^2_{it,t+1}] - E[\mathrm{IV}^2_{it,t+1}] &= 2\left(\sum_{k=1}^K b^2_{ik}E[V_{Fk}] + E[V_{Ii}]\right)\left(\sum_{k=1}^K b^2_{ik}E[Z^2_{Fk}]\lambda_{Fk} + E[Z^2_{Ii}]E[\lambda_i]\right) \\ &+ \sum_{k=1}^K b^4_{ik}\left(\lambda_{Fk}E[Z^4_{Fk}] + \lambda^2_{Fk}E[Z^2_{Fk}]^2\right) \\ &+ \sum_{k=1}^K\sum_{l\neq k}^K b^2_{ik}b^2_{il}E[Z^2_{Fk}]E[Z^2_{Fl}]\lambda_{Fk}\lambda_{Fl} \\ &+ 2E[Z^2_{Ii}]\sum_{k=1}^K b^2_{ik}E[Z^2_{Fk}]E[\lambda_i]\lambda_{Fk} + E[Z^4_{Ii}]E[\lambda_i] + E[Z^2_{Ii}]^2E[\lambda_i]^2 \\ &+ E[Z^2_{Ii}]^2\int_t^{t+1}\int_t^{t+1} R_{Iii}(s-u)duds\end{aligned} \tag{1.85}$$

Proof of Theorem 1.3.2

$E\left[\Delta X_{it}\right]$ is derived from the equation 1.7 by taking the expectation of the two sides. Moment equations of log-returns of order 2, 3, and 4 are derived using the Itö lemma in definition

1.3.2 and assumptions (1.4) - (1.27).

We now present how $E\left[\Delta X_{it}^2\right]$ is derived. Others moments are computed using the same tricks. By the Itö lemma applied to the jump-diffusion process $r_{i\Delta}$ in equation 1.45 and the function $f(x) = x^2$, we get:

$$r_{i\Delta}^2 = \int_0^\Delta (\sum_{k=1}^K b_{ik}\mu_{Fk} + \mu_{Ii}) \times 2r_{is_-}ds + \sum_{k=1}^K 2b_{ik}\int_0^\Delta r_{is_-}\sqrt{V_{Fks_-}}dB_{Fks} +$$
$$2\int_0^\Delta r_{is_-}\sqrt{V_{Iis_-}}dB_{Iis} + \sum_{k=1}^K b_{ik}^2\int_0^\Delta V_{Fks}ds + \int_0^\Delta V_{Iis}ds + \sum_{0\le s\le\Delta}\left(\sum_{k=1}^K b_{ik}Z_{Fks}dN_{Fks}\right)^2 +$$
$$\sum_{0\le s\le\Delta} Z_{Iis}^2 dN_{Iis}^2 + 2\sum_{0\le s\le\Delta} r_{is_-}\sum_{k=1}^K b_{ik}Z_{Fks}dN_{Fks} + 2\sum_{0\le s\le\Delta} r_{is_-}Z_{Iis}dN_{Iis} +$$
$$2\sum_{0\le s\le\Delta}\left(\sum_{k=1}^K b_{ik}Z_{Fks}dN_{Fks}\right)(Z_{Iis}dN_{Iis})$$

We take the expectation of the previous equation. From the Itö calculus, up to the order Δ^2, we obtain:

$$E[r_{i\Delta}^2] =$$
$$2\int_0^\Delta E\left[(\sum_{k=1}^K b_{ik}\mu_{Fk} + \mu_{Ii}) \times r_{is_-}\right]ds + \sum_{k=1}^K b_{ik}^2 E[V_{Fk}]\Delta + E[V_{Ii}]\Delta + \sum_{k=1}^K b_{ik}^2 E[Z_{Fk}^2]\lambda_{Fk}\Delta +$$
$$E[Z_{Ii}^2]E[\lambda_{Ii}]\Delta + 2\sum_{k=1}^K b_{ik}\sum_{0\le s\le\Delta} E\left[r_{is_-}Z_{Fks}dN_{Fks}\right] + 2\sum_{0\le s\le\Delta} E\left[r_{is_-}Z_{Iis}dN_{Iis}\right] + o(\Delta^2)$$

Then, we establish that:

$$2\sum_{k=1}^K b_{ik}\sum_{0\le s\le\Delta} E\left[r_{is_-}Z_{Fks}dN_{Fks}\right] = 2E[r_{i\Delta}]\sum_{k=1}^K b_{ik}E[Z_{Fk}]\lambda_{Fk}\Delta$$

Also:

$$E\left[r_{is_-}Z_{Iis}dN_{Iis}\right] = (\sum_{k=1}^K b_{ik}\mu_{Fk} + \mu_{Ii})\int_0^{s-} E[Z_{Iis}dN_{Iis}]dt +$$
$$\sum_{k=1}^K b_{ik}E[Z_{Fk}]E[Z_{Ii}]\lambda_{Fk}E[\lambda_{Ii}]sds + \int_0^{s-} E[Z_{Iit}Z_{Iis}]E\left[\frac{dN_{Iit}}{dt} \times \frac{dN_{Iis}}{ds}\right]dtds$$

It comes out that:

$$2\sum_{0\le s\le\Delta} E\left[r_{is_-}Z_{Iis}dN_{Iis}\right] = (\sum_{k=1}^K b_{ik}\mu_{Fk} + \mu_{Ii})E[Z_{Ii}]E[\lambda_{Ii}]\Delta^2 +$$
$$\sum_{k=1}^K b_{ik}E[Z_{Fk}]E[Z_{Ii}]\lambda_{Fk}E[\lambda_{Ii}]\Delta^2 + 2\int_0^\Delta\int_0^{s-} E[Z_{Iit}Z_{Iis}]E\left[\frac{dN_{Iit}}{dt} \times \frac{dN_{Iis}}{ds}\right]dtds$$

Using the covariance density matrix as in Definition 1.3.1, we have:

$$\begin{aligned} 2\int_0^\Delta\int_0^{s-} E[Z_{Iit}Z_{Iis}]E\left[\frac{dN_{Iit}}{dt} \times \frac{dN_{Iis}}{ds}\right]dtds &= 2\int_0^\Delta\int_0^{s-} E[Z_{Iit}Z_{Iis}][R_{Iii}(t-s) + E[\lambda_{Ii}]^2]dtds \\ &= 2E[Z_{Ii}]^2\int_0^\Delta\int_0^{s-} R_{Iii}(t-s)dtds + E[Z_{Ii}]^2E[\lambda_{Ii}]^2\Delta^2 \end{aligned}$$

Putting things together, and setting $r_{i\Delta} = \Delta X_{it}$ we get

$$
\begin{aligned}
E\left[\Delta X_{it}^2\right] &= \left[\sum_{k=1}^K b_{ik}^2 E[V_{Fkt}] + E[V_{Iit}] + \sum_{k=1}^K b_{ik}^2 E[Z_{Fk}^2]\lambda_{Fk} + E[Z_{Ii}^2]E[\lambda_{Ii}]\right]\Delta \\
&+ \left(\sum_{k=1}^K b_{ik}\mu_{Fk} + \mu_{Ii}\right)\left[\sum_{k=1}^K b_{ik}\mu_{Fk} + \mu_{Ii} + \sum_{k=1}^K b_{ik}E[Z_{Fk}]\lambda_{Fk} + E[Z_{Ii}]E[\lambda_{Ii}]\right]\Delta^2 \\
&+ \left[\sum_{k=1}^K b_{ik}\sum_{l=1}^K b_{il}\mu_{Fl}E[Z_{Fk}]\lambda_{Fk} + \sum_{k=1}^K b_{ik}\mu_{Ii}E[Z_{Fk}]\lambda_{Fk}\right]\Delta^2 \\
&+ \left[\sum_{k=1}^K b_{ik}\sum_{l\neq k}^K b_{il}E[Z_{Fk}]E[Z_{Fl}]\lambda_{Fk}\lambda_{Fl} + \sum_{k=1}^K b_{ik}^2 E[Z_{Fk}]^2\lambda_{Fk}^2\right]\Delta^2 \\
&+ \left[\sum_{k=1}^K b_{ik}E[Z_{Fk}]E[Z_{Ii}]E[\lambda_{Ii}]\lambda_{Fk} + \sum_{k=1}^K b_{ik}\mu_{Fk}E[Z_{Ii}]E[\lambda_{Ii}] + \mu_{Ii}E[Z_{Ii}]E[\lambda_{Ii}]\right]\Delta^2 \\
&+ \left[\sum_{k=1}^K b_{ik}E[Z_{Fk}]E[Z_{Ii}]\lambda_{Fk}E[\lambda_{Ii}] + E[Z_{Ii}]^2E[\lambda_{Ii}]^2\right]\Delta^2 \\
&+ 2E[Z_{Ii}]\int_0^\Delta\int_0^s R_{Iii}(t-s)dtds
\end{aligned}
$$

Using the same steps, we compute moments of order 3 and 4. Their explicit formulae are the followings:

$$
\begin{aligned}
E\left[\Delta X_{it}^3\right] &= \left[\sum_{k=1}^K b_{ik}^3 E[Z_{Fkt}^3]\lambda_{Fk} + E[Z_{Ii}^3]E[\lambda_{Ii}]\right]\Delta \\
&+ 3\left(\sum_{k=1}^K b_{ik}\mu_{Fk} + \mu_{Ii}\right)\left[\sum_{k=1}^K b_{ik}^2 E[V_{Fkt}] + E[V_{Iit}] + E[Z_{Ii}^2]E[\lambda_{Ii}]\right]\frac{\Delta^2}{2} \\
&+ 3\sum_{k=1}^K b_{ik}^2\left[\sum_{l=1}^K b_{il}\mu_{Fl}E[V_{Fk}] + \sum_{l=1}^K b_{il}E[Z_{Fl}]\lambda_{Fl}E[V_{Fk}] + E[Z_{Ii}]E[\lambda_{Ii}]E[V_{Fk}]\right]\frac{\Delta^2}{2} \\
&+ 3\sum_{k=1}^K b_{ik}^2\left[b_{ik}\eta_{Fk}\rho_{Fk}E[V_{Fkt}]\right]\frac{\Delta^2}{2} \\
&+ \left[3\left(\sum_{k=1}^K b_{ik}\mu_{Fk} + \mu_{Ii}\right) + 3\eta_{Ii}\rho_{Ii}E[V_{Ii}] + 3\sum_{k=1}^K b_{ik}E[Z_{Fk}]\lambda_{Fk}E[V_{Ii}]\right]\frac{\Delta^2}{2} \\
&+ 3E[Z_{Ii}]E[\lambda_{Ii}]E[V_{Iit}]\frac{\Delta^2}{2} \\
&+ 3\sum_{k=1}^K b_{ik}\left[\sum_{l=1}^K b_{il}^2 E[V_{Fl}]E[Z_{Fk}]\lambda_{Fk} + E[V_{Ii}]E[Z_{Fkt}]\lambda_{Fk}\right]\frac{\Delta^2}{2} \\
&+ 3\sum_{k=1}^K b_{ik}\left[\sum_{l=1}^K b_{il}^2 E[Z_{Fl}^2]\lambda_{Fl}E[Z_{Fk}]\lambda_{Fk} + E[Z_{Ii}^2]E[\lambda_{Ii}]E[Z_{Fk}]\lambda_{Fk}\right]\frac{\Delta^2}{2} \\
&+ 3\sum_{k=1}^K b_{ik}^2\left[E[V_{Fk}]E[Z_{Ii}]\lambda_{Ii} + E[V_{Ii}]E[Z_{Ii}]E[\lambda_{Ii}] + E[Z_{Fk}^2]\lambda_{Fk}E[Z_{Ii}]E[\lambda_{Ii}]\right]\frac{\Delta^2}{2} \\
&+ E[Z_{Ii}^2]E[\lambda_{Ii}]E[Z_{Ii}]E[\lambda_{Ii}]\frac{\Delta^2}{2} + 3E[Z_{Ii}^2]E[Z_{Ii}]\int_0^\Delta\int_0^s R_{Iii}(t-s)dtds \\
&+ \left[3\left(\sum_{k=1}^K b_{ik}\mu_{Fk} + \mu_{Ii}\right)\sum_{k=1}^K b_{ik}^2 E[Z_{Fkt}^2]\lambda_{Fk} + \sum_{k=1}^K\sum_{l=1}^K b_{ik}b_{il}^2 E[Z_{Fk}]E[Z_{Fl}^2]\lambda_{Fk}\lambda_{Fl}\right]\frac{\Delta^2}{2} \\
&+ \sum_{l=1}^K b_{il}^2 E[Z_{Fl}^2]\lambda_{Fl}E[Z_{Ii}]E[\lambda_{Ii}]\frac{\Delta^2}{2} \\
&+ \left[3\left(\sum_{k=1}^K b_{ik}\mu_{Fk} + \mu_{Ii}\right)E[Z_{Ii}^2]E[\lambda_{Ii}] + 3\sum_{k=1}^K b_{ik}E[Z_{Fkt}]\lambda_{Fk}E[Z_{Ii}^2]E[\lambda_{Ii}]\right]\frac{\Delta^2}{2} \\
&+ 3E[Z_{Ii}]E[\lambda_{Ii}]^2E[Z_{Ii}^2]\frac{\Delta^2}{2} + 2E[Z_{Ii}]E[Z_{Ii}]\int_0^\Delta\int_0^s R_{Iii}(t-s)dtds
\end{aligned}
$$

$$
\begin{aligned}
E\left[\Delta X_{it}^4\right] &= \left[\sum_{k=1}^K b_{ik}^4 E[Z_{Fkt}^4]\lambda_{Fk} + E[Z_{Ii}^4]E[\lambda_{Ii}]\right]\Delta \\
&+ 4\left(\sum_{k=1}^K b_{ik}\mu_{Fk} + \mu_{Ii}\right)\left[\sum_{k=1}^K b_{ik}^3 E[Z_{Fkt}^3]\lambda_{Fk} + E[Z_{Ii}^3]E[\lambda_{Ii}]\right]\frac{\Delta^2}{2} \\
&+ 6\sum_{k=1}^K b_{ik}^2\left[\sum_{l\neq k}^K b_{il}^2 E[V_{Fk}]E[V_{Fl}] + b_{ik}^2 E[V_{Fk}^2] + E[V_{Fk}]E[V_{Ii}]\right]\frac{\Delta^2}{2} \\
&+ 6\left[E[V_{Fk}]\sum_{l=1}^K b_{il}^2 E[Z_{Fl}^2]\lambda_{Fl} + E[V_{Fk}]E[Z_{Ii}^2]E[\lambda_{Ii}]\right]\frac{\Delta^2}{2} \\
&+ \left[6\sum_{l=1}^K b_{il}^2 E[V_{Fl}]E[V_{Ii}] + 6E[V_{Ii}^2] + 6E[V_{Ii}]\sum_{k=1}^K b_{ik}^2 E[Z_{Fk}^2]\lambda_{Fk}\right]\frac{\Delta^2}{2} \\
&+ 6\left[E[Z_{Ii}^2]E[\lambda_{Ii}]E[V_{Ii}] + \sum_{l=1}^K b_{il}^2 E[V_{Fl}]\sum_{k=1}^K b_{ik}^2 E[Z_{Fkt}^2]\lambda_{Fk}\right]\frac{\Delta^2}{2} \\
&+ 6\left[\sum_{k=1}^K b_{ik}^2 E[Z_{Fkt}^2]\lambda_{Fk}E[V_{Ii}] + \sum_{k=1}^K b_{ik}^4 E[Z_{Fkt}^2]^2\lambda_{Fk}^2\right]\frac{\Delta^2}{2} \\
&+ 6\left[\sum_{k=1}^K b_{ik}^2 E[Z_{Fk}^2]\lambda_{Fk}E[Z_{Ii}^2]E[\lambda_{Ii}]\right]\frac{\Delta^2}{2} \\
&+ 6\left[\sum_{k=1}^K \sum_{l\neq k} b_{ik}^2 b_{il}^2 E[Z_{Fk}^2]E[Z_{Fl}^2]\lambda_{Fk}\lambda_{Fl}\right]\frac{\Delta^2}{2} \\
&+ 6\left[\sum_{l=1}^K b_{il}^2 E[Z_{Ii}^2]E[\lambda_{Ii}]E[V_{Fl}] + E[Z_{Ii}^2]E[\lambda_{Ii}]E[V_{Ii}]\right]\frac{\Delta^2}{2} \\
&+ 6\left[\sum_{k=1}^K b_{ik}^2 E[Z_{Fkt}^2]^2\lambda_{Fk}E[Z_{Ii}^2]E[\lambda_{Ii}]\right]\frac{\Delta^2}{2} \\
&+ E[Z_{Ii}^2]^2\int_0^\Delta\int_0^s R_{Iii}(t-s)dtds + E[Z_{Ii}^2]^2E[\lambda_{Ii}]^2\frac{\Delta^2}{2} \\
&+ 4\left[\sum_{k=1}^K b_{ik}^4 E[Z_{Fk}]E[Z_{Fk}^3]\lambda_{Fk}^2 + \sum_{k=1}^K\sum_{l\neq k} b_{ik}b_{il}^3 E[Z_{Fk}]E[Z_{Fl}^3]\lambda_{Fk}\lambda_{Fl}\right]\frac{\Delta^2}{2} \\
&+ 4\sum_{k=1}^K b_{ik}E[Z_{Fk}]\lambda_{Fk}E[Z_{Ii}^3]E[\lambda_{Ii}]\frac{\Delta^2}{2} \\
&+ 4\left[E[Z_{Ii}]E[\lambda_{Ii}]\sum_{l=1}^K b_{il}^3 E[Z_{Fl}^3]\lambda_{Fl} + E[Z_{Ii}]E[Z_{Ii}^3]E[\lambda_{Ii}]^2\right]\frac{\Delta^2}{2} \\
&+ +4E[Z_{Ii}]E[Z_{Ii}^3]\int_0^\Delta\int_0^s R_{Iii}(t-s)dtds \\
&+ 4\left[\left(\sum_{k=1}^K b_{ik}\mu_{Fk} + \mu_{Ii}\right)\left(\sum_{k=1}^K b_{ik}^3 E[Z_{Fk}^3]\lambda_{Fk}\right)\right]\frac{\Delta^2}{2} \\
&+ 4\left[sum_{k=1}^K b_{ik}^4 E[Z_{Fk}]E[Z_{Fk}^3]\lambda_{Fk}^2 + \sum_{k=1}^K\sum_{l\neq k} b_{ik}b_{il}^3 E[Z_{Fk}]E[Z_{Fl}^3]\lambda_{Fk}\lambda_{Fl}\right]\frac{\Delta^2}{2} \\
&+ 4\left[E[Z_{Ii}]E[\lambda_{Ii}]\sum_{k=1}^K b_{ik}^3 E[Z_{Fk}^3]\lambda_{Fk} + \left(\sum_{k=1}^K b_{ik}\mu_{Fk} + \mu_{Ii}\right)E[Z_{Ii}^3]E[\lambda_{Ii}]\right]\frac{\Delta^2}{2} \\
&+ 4\left[\sum_{k=1}^K b_{ik}E[Z_{Fk}]\lambda_{Fk}E[Z_{Ii}^3]E[\lambda_{Ii}] + E[Z_{Ii}]E[Z_{Ii}^3]E[\lambda_{Ii}]^2\right]\frac{\Delta^2}{2}
\end{aligned}
$$

Proof of Theorem 1.3.3

We want firstly to compute $E\left[\Delta X_{it}\Delta X_{jt}\right]$. Let's call: $\Delta X_{it} = r_{i\Delta}$ and $\Delta X_{jt} = r_{j\Delta}$. We apply the multidimensionnal Itö lemma to the function $f(r_{i\Delta}, r_{j\Delta}) = r_{i\Delta}r_{j\Delta}$ and we obtain

$$
\begin{aligned}
r_{i\Delta}r_{j\Delta} &= \int_0^\Delta r_{js_-}\left[\left(\sum_{k=1}^K b_{ik}\mu_{Fk} + \mu_{Ii}\right)ds + \sum_{k=1}^K\sqrt{V_{Fks}}dB_{Fks} + \sqrt{V_{Iis}}dB_{Iis}\right] \\
&+ \int_0^\Delta r_{is_-}\left[\left(\sum_{k=1}^K b_{jk}\mu_{Fk} + \mu_{Ij}\right)ds + \sum_{k=1}^K\sqrt{V_{Fks}}dB_{Fks} + \sqrt{V_{Ijs}}dB_{Ijs}\right] \\
&+ \left[\left(\sum_{k=1}^K b_{jk}\mu_{Fk} + \mu_{Ij}\right)ds + \sum_{k=1}^K\sqrt{V_{Fks}}dB_{Fks} + \sqrt{V_{Ijs}}dB_{Ijs}\right] \\
&\times \left[\left(\sum_{k=1}^K b_{jk}\mu_{Fk} + \mu_{Ij}\right)ds + \sum_{k=1}^K\sqrt{V_{Fks}}dB_{Fks} + \sqrt{V_{Ijs}}dB_{Ijs}\right] \\
&+ \sum_{0\le s\le\Delta}[\left(r_{is_-} + \sum_{k=1}^K b_{ik}Z_{Fks}dN_{Fks} + Z_{Iis}dN_{Iis}\right) \\
&\times \left(r_{js_-} + \sum_{k=1}^K b_{jk}Z_{Fks}dN_{Fks} + Z_{Ijs}dN_{Ijs}\right) - r_{is_-}r_{js_-}]
\end{aligned}
$$

After taking the expectation of both sides, it follows that

$$
\begin{aligned}
E[r_{i\Delta}r_{j\Delta}] &= \left(\sum_{k=1}^{K} b_{ik}\mu_{Fk}+\mu_{Ii}\right)E[r_j]\Delta+\left(\sum_{k=1}^{K} b_{jk}\mu_{Fk}+\mu_{Ij}\right)E[r_i]\Delta+\sum_{k=1}^{K} b_{ik}b_{jk}E[V_{Fk}]\Delta\\
&+ \sum_{k=1}^{K} b_{jk}\left[\sum_{0\le s\le\Delta} E[Z_{Fks}dN_{Fks}r_{is_-}]\right]+\sum_{0\le s\le\Delta} E[Z_{Ijs}dN_{Ijs}r_{is_-}]\\
&+ \sum_{k=1}^{K} b_{ik}\left[\sum_{0\le s\le\Delta} E[Z_{Fks}dN_{Fks}r_{js_-}]\right]+\sum_{k=1}^{K} b_{ik}b_{jk}E[Z_{Fk}^2]\lambda_{Fk}\Delta\\
&+ \sum_{0\le s\le\Delta} E[Z_{Iis}dN_{Iis}r_{js_-}]
\end{aligned}
$$

It can be easilly shown that

$$
\sum_{0\le s\le\Delta} E[Z_{Fks}dN_{Fks}r_{is_-}]=E[Z_{Fk}]\lambda_{Fk}E[r_i]\Delta
$$

Using the covariance density matrix as in Definition 1.3.1, and the Itö calculus, we derive that

$$
\begin{aligned}
\sum_{0\le s\le\Delta} E[Z_{Ijs}dN_{Ijs}r_{is_-}] &= \left(\sum_{k=1}^{K} b_{ik}\mu_{Fk}+\mu_{Ii}\right)E[Z_{Ij}]E[\lambda_{Ij}]\frac{\Delta^2}{2}\\
&+ \sum_{k=1}^{K} b_{ik}E[Z_{Fk}]E[Z_{I2}]\lambda_{Fk}E[\lambda_{Ij}]\frac{\Delta^2}{2}\\
&+ E[Z_{Ii}]E[Z_{Ij}]E[\lambda_{Ii}]E[\lambda_{Ij}]\frac{\Delta^2}{2}+E[Z_{Ii}]E[Z_{Ij}]\int_0^\Delta\int_0^s R_{Iij}(t-s)dtds
\end{aligned}
$$

To obtain the others terms, i and j are permuted. After replacing $\sum_{0\le s\le\Delta} E[Z_{Ijs}dN_{Ijs}r_{is_-}]$, $\sum_{0\le s\le\Delta} E[Z_{Fks}dN_{Fks}r_{is_-}]$, $E[r_i]$ and $E[r_i]$ by their values, we get

$$
\begin{aligned}
E\left[\Delta X_{it}\Delta X_{jt}\right] &= \left[\sum_{k=1}^{K} b_{ik}b_{jk}E[V_{Fk}]+\sum_{k=1}^{K} b_{ik}b_{jk}E[Z_{Fk}^2]\lambda_{Fk}\right]\Delta\\
&+ \left(\sum_{k=1}^{K} b_{ik}\mu_{Fk}+\mu_{Ii}\right)\left[\sum_{k=1}^{K} b_{jk}\mu_{Fk}+\mu_{Ij}+\sum_{k=1}^{K} b_{jk}E[Z_{Fk}]\lambda_{Fk}\right]\frac{\Delta^2}{2}\\
&+ \left(\sum_{k=1}^{K} b_{ik}\mu_{Fk}+\mu_{Ii}\right)E[Z_{Ij}]E[\lambda_{Ij}\frac{\Delta^2}{2}\\
&+ \left(\sum_{k=1}^{K} b_{jk}\mu_{Fk}+\mu_{Ij}\right)\left[\sum_{k=1}^{K} b_{ik}\mu_{Fk}+\mu_{Ii}+\sum_{k=1}^{K} b_{ik}E[Z_{Fk}]\lambda_{Fk}\right]\frac{\Delta^2}{2}\\
&+ \left(\sum_{k=1}^{K} b_{jk}\mu_{Fk}+\mu_{Ij}\right)E[Z_{Ii}]E[\lambda_{Ii}]\frac{\Delta^2}{2}\\
&+ \sum_{k=1}^{K} b_{jk}\left[\sum_{l=1}^{K} b_{il}\mu_{Fl}E[Z_{Fk}]\lambda_{Fk}+\mu_{Ii}E[Z_{Fk}]\lambda_{Fk}\right]\frac{\Delta^2}{2}\\
&+ \sum_{k=1}^{K} b_{jk}\sum_{l\neq k}^{K} b_{il}E[Z_{Fl}]E[Z_{Fk}]\lambda_{Fl}\lambda_{Fk}\frac{\Delta^2}{2}\\
&+ \sum_{k=1}^{K} b_{jk}\left[b_{ik}E[Z_{Fk}]^2\lambda_{Fk}^2+E[Z_{Ii}]E[Z_{Fk}]E[\lambda_{Ii}]\lambda_{Fk}\right]\frac{\Delta^2}{2}\\
&+ \sum_{k=1}^{K} b_{ik}\left[\sum_{l=1}^{K} b_{jl}\mu_{Fl}E[Z_{Fk}]\lambda_{Fk}+\mu_{Ij}E[Z_{Fk}]\lambda_{Fk}\right]\frac{\Delta^2}{2}\\
&+ \sum_{k=1}^{K} b_{ik}\sum_{l\neq k}^{K} b_{jl}E[Z_{Fl}]E[Z_{Fk}]\lambda_{Fl}\lambda_{Fk}\frac{\Delta^2}{2}\\
&+ \sum_{k=1}^{K} b_{ik}\left[b_{jk}E[Z_{Fk}]^2\lambda_{Fk}^2+E[Z_{Ij}]E[Z_{Fk}]E[\lambda_{Ij}]\lambda_{Fk}\right]\frac{\Delta^2}{2}\\
&+ \left[\left(\sum_{k=1}^{K} b_{ik}\mu_{Fk}+\mu_{Ii}\right)E[Z_{Ij}]E[\lambda_{Ij}]+\sum_{k=1}^{K} b_{ik}E[Z_{Fk}]\lambda_{Fk}E[Z_{Ij}]E[\lambda_{Ij}]\right]\frac{\Delta^2}{2}\\
&+ E[Z_{Ii}]E[Z_{Ij}]E[\lambda_{Ii}]E[\lambda_{Ij}]\frac{\Delta^2}{2}+E[Z_{Ij}]E[Z_{Ii}]\int_0^\Delta\int_0^s R_{Iij}(t-s)dtds\\
&+ \left[\left(\sum_{k=1}^{K} b_{jk}\mu_{Fk}+\mu_{Ij}\right)E[Z_{Ii}]E[\lambda_{Ii}]+\sum_{k=1}^{K} b_{jk}E[Z_{Fk}]\lambda_{Fk}E[Z_{Ii}]E[\lambda_{Ii}]\right]\frac{\Delta^2}{2}\\
&+ E[Z_{Ij}]E[Z_{Ii}]E[\lambda_{Ij}]E[\lambda_{Ii}]\frac{\Delta^2}{2}+E[Z_{Ii}]E[Z_{Ij}]\int_0^\Delta\int_0^s R_{Iji}(t-s)dtds
\end{aligned}
$$

The final expression of $E\left[\Delta X_{it}\Delta X_{jt}\right]-E[\Delta X_{it}]E[\Delta X_{jt}]$ is deduced after using the matricial representation.

$E\left[\Delta X_{it}\Delta X_{jt}^2\right]$, $E\left[\Delta X_{it}\Delta X_{jt}^3\right]$ and $E\left[\Delta X_{it}^2\Delta X_{jt}^2\right]$ are computed using the same approach. We provide below their explicit formulae.

$$
\begin{array}{rcl}
E\left[\Delta X_{it}\Delta X_{jt}^2\right] & = & \sum_{k=1}^K b_{ik}b_{jk}^2 E[Z_{Fk}^3]\lambda_{Fk}\Delta \\
& + & \left(\sum_{k=1}^K b_{ik}\mu_{Fk}+\mu_{Ii}\right)\left[\sum_{k=1}^K b_{jk}^2 E[Z_{Fk}^2]\lambda_{Fk}+E[Z_{Ij}^2]E[\lambda_{Ij}]\right]\frac{\Delta^2}{2} \\
& + & \left(\sum_{k=1}^K b_{ik}\mu_{Fk}+\mu_{Ii}\right)\left[\sum_{k=1}^K b_{jk}^2 E[V_{Fk}^2]+E[V_{Ij}]\right]\frac{\Delta^2}{2} \\
& + & 2\left(\sum_{k=1}^K b_{jk}\mu_{Fk}+\mu_{Ij}\right)\left[\sum_{k=1}^K b_{ik}b_{jk}E[V_{Fk}]+\sum_{k=1}^K b_{ik}b_{jk}E[Z_{Fk}^2]\lambda_{Fk}\right]\frac{\Delta^2}{2} \\
& + & 2\sum_{k=1}^K b_{ik}b_{jk}\left[\sum_{l=1}^K b_{jl}\mu_{Fl}E[V_{Fk}]+\mu_{Ij}E[V_{Fk}]+\sum_{l=1}^K b_{jl}E[Z_{Fl}]\lambda_{Fl}E[V_{Fk}]\right]\frac{\Delta^2}{2} \\
& + & 2\sum_{k=1}^K b_{ik}b_{jk}\left[E[Z_{Ij}]E[\lambda_{Ij}]E[V_{Fk}]+b_{jk}\eta_{Fk}\rho_{Fk}E[V_{Fk}]\right]\frac{\Delta^2}{2} \\
& + & \sum_{k=1}^K b_{jk}^2\left[\sum_{l=1}^K b_{il}\mu_{Fl}E[V_{Fk}]+\mu_{Ii}E[V_{Fk}]+\sum_{l=1}^K b_{il}E[Z_{Fl}]\lambda_{Fl}E[V_{Fk}]\right]\frac{\Delta^2}{2} \\
& + & \sum_{k=1}^K b_{jk}^2\left[E[Z_{Ii}]E[\lambda_{Ii}]E[V_{Fk}]+b_{ik}\eta_{Fk}\rho_{Fk}E[V_{Fk}]\right]\frac{\Delta^2}{2} \\
& + & \left[\left(\sum_{k=1}^K b_{ik}\mu_{Fk}+\mu_{Ii}\right)\sum_{k=1}^K b_{jk}^2 E[Z_{Fk}^2]\lambda_{Fk}\right]\frac{\Delta^2}{2} \\
& + & \left[\sum_{k=1}^K\sum_{l\neq k}^K b_{il}b_{jk}^2 E[Z_{Fk}]E[Z_{Fl}^2]\lambda_{Fk}\lambda_{Fl}+\sum_{k=1}^K b_{ik}b_{jk}^2 E[Z_{Fk}]E[Z_{Fk}^2]\lambda_{Fk}^2\right]\frac{\Delta^2}{2} \\
& + & E[Z_{Ii}]E[\lambda_{Ii}]\sum_{k=1}^K b_{jk}^2 E[Z_{Fk}^2]\lambda_{Fk}\frac{\Delta^2}{2} \\
& + & \left[\left(\sum_{k=1}^K b_{ik}\mu_{Fk}+\mu_{Ii}\right)E[Z_{Ij}^2]E[\lambda_{Ii}]+\sum_{k=1}^K b_{ik}E[Z_{Fk}]\lambda_{Fk}E[Z_{Ij}^2]E[\lambda_{Ii}]\right]\frac{\Delta^2}{2} \\
& + & E[Z_{Ii}]E[Z_{Ij}^2]\int_0^\Delta\int_0^s R_{Iij}(t-s)dtds+E[Z_{Ii}]E[Z_{Ij}^2]E[\lambda_{Ii}]E[\lambda_{Ij}]\frac{\Delta^2}{2} \\
& + & 2\sum_{k=1}^K b_{jk}\left[sum_{l=1}^K b_{il}b_{jl}E[V_{Fl}]\lambda_{Fk}E[Z_{Fk}]+\sum_{l\neq k}^K b_{il}b_{jl}E[Z_{Fl}^2]E[Z_{Fk}]\lambda_{Fl}\lambda_{Fk}\right]\frac{\Delta^2}{2} \\
& + & 2\sum_{k=1}^K b_{ik}b_{jk}^2 E[Z_{Fk}^2]E[Z_{Fk}]\lambda_{Fk}^2\frac{\Delta^2}{2} \\
& + & \left[2\sum_{l=1}^K b_{il}b_{jl}E[V_{Fl}]E[\lambda_{Ij}]E[Z_{Ij}]+2\sum_{l=1}^K b_{il}b_{jl}E[Z_{Fl}^2]E[Z_{Ii}]\lambda_{Fl}E[\lambda_{Ii}]\right]\frac{\Delta^2}{2} \\
& + & \sum_{k=1}^K b_{ik}\left[\sum_{l=1}^K b_{jl}^2 E[V_{Fl}]E[Z_{Fk}]\lambda_{Fk}+E[V_{Ij}]E[Z_{Fk}]\lambda_{Fk}\right]\frac{\Delta^2}{2} \\
& + & \sum_{k=1}^K b_{ik}\left[\sum_{l=1}^K b_{jl}^2 E[Z_{Fl}^2]E[Z_{Fk}]\lambda_{Fk}\lambda_{Fl}+E[Z_{Ij}^2]E[\lambda_{Ij}]E[Z_{Fk}]\lambda_{Fk}\right]\frac{\Delta^2}{2} \\
& + & 2\sum_{k=1}^K b_{ik}b_{jk}E[Z_{Fk}^2]\lambda_{Fk}\left[\left(\sum_{k=1}^K b_{jk}\mu_{Fk}+\mu_{Ij}\right)+E[Z_{Ij}]E[\lambda_{Ij}]\right]\frac{\Delta^2}{2} \\
& + & \left[2\sum_{k=1}^K\sum_{l\neq k}^K b_{jk}b_{il}b_{jl}E[Z_{Fk}]E[Z_{Fl}^2]\lambda_{Fk}\lambda_{Fl}+2\sum_{k=1}^K b_{jk}^2 b_{ik}E[Z_{Fk}]E[Z_{Fk}^2]\lambda_{Fk}^2\right]\frac{\Delta^2}{2} \\
& + & \left[\sum_{k=1}^K b_{jk}^2 E[V_{Fk}]E[Z_{Ii}]E[\lambda_{Ii}]+E[V_{Ij}]E[Z_{Ii}]E[\lambda_{Ii}]\right]\frac{\Delta^2}{2} \\
& + & \left[\sum_{k=1}^K b_{jk}^2 E[Z_{Fk}^2]\lambda_{Fk}E[Z_{Ii}]E[\lambda_{Ii}]+E[Z_{Ij}^2]E[Z_{Ii}]E[\lambda_{Ii}]E[\lambda_{Ij}]\right]\frac{\Delta^2}{2} \\
& + & E[Z_{Ij}^2]E[Z_{Ii}]\int_0^\Delta\int_0^s R_{Iij}(t-s)dtds \\
& + & \left[\left(\sum_{k=1}^K b_{ik}\mu_{Fk}+\mu_{Ii}\right)E[V_{Ij}]+\sum_{k=1}^K b_{ik}E[Z_{Fk}]\lambda_{Fk}E[V_{Ij}]\right]\frac{\Delta^2}{2} \\
& + & E[Z_{Ii}]E[\lambda_{Ii}]E[V_{Ij}]\frac{\Delta^2}{2}
\end{array}
$$

$$
\begin{aligned}
E\left[\Delta X_{it}\Delta X_{jt}^3\right] &= \sum_{k=1}^K b_{ik}b_{jk}^3 E[Z_{Fk}^4]\lambda_{Fk}\Delta \\
&+ \left(\sum_{k=1}^K b_{ik}\mu_{Fk}+\mu_{Ii}\right)\left[\sum_{k=1}^K b_{jk}^3 E[Z_{Fk}^3]\lambda_{Fk}\right]\frac{\Delta^2}{2} \\
&+ \left(\sum_{k=1}^K b_{ik}\mu_{Fk}+\mu_{Ii}\right)E[Z_{Ii}^3]E[\lambda_{Ii}]\frac{\Delta^2}{2} \\
&+ \left[\sum_{k=1}^K b_{ik}b_{jk}^3 E[Z_{Fk}]E[Z_{Fk}^3]\lambda_{Fk}^2+\sum_{k=1}^K\sum_{l\neq k}^K b_{ik}b_{jk}^3 E[Z_{Fk}]E[Z_{Fl}^3]\lambda_{Fk}\lambda_{Fl}\right]\frac{\Delta^2}{2} \\
&+ \left[\sum_{k=1}^K b_{ik}E[Z_{Fk}]\lambda_{Fk}E[Z_{Ij}^3]E[\lambda_{Ij}]+E[Z_{Ii}]E[\lambda_{Ii}]\sum_{k=1}^K b_{jk}^3 E[Z_{Fk}^3]\lambda_{Fk}\right]\frac{\Delta^2}{2} \\
&+ E[Z_{Ii}]E[Z_{Ij}^3]E[\lambda_{Ij}]E[\lambda_{Ii}]\frac{\Delta^2}{2}+E[Z_{Ii}]E[Z_{Ij}^3]\int_0^\Delta\int_0^s R_{Iji}(t-s)dtds \\
&+ 3\left(\sum_{k=1}^K b_{jk}\mu_{Fk}+\mu_{Ij}\right)\left(\sum_{k=1}^K b_{ik}b_{jk}^2 E[Z_{Fk}^3]\lambda_{Fk}\right)\frac{\Delta^2}{2} \\
&+ \left[3\sum_{k=1}^K b_{jk}\sum_{l\neq k}^K b_{il}b_{jl}^2 E[Z_{Fl}^3]E[Z_{Fk}]\lambda_{Fl}\lambda_{Fk}+3\sum_{k=1}^K b_{jk}^3 b_{ik}E[Z_{Fk}^3]E[Z_{Fk}]\lambda_{Fk}^2\right]\frac{\Delta^2}{2} \\
&+ 3\sum_{k=1}^K b_{ik}b_{jk}^2 E[Z_{Fk}^3]E[Z_{Ij}]E[\lambda_{Ij}]\lambda_{Fk}\frac{\Delta^2}{2} \\
&+ 3\sum_{k=1}^K b_{jk}^2\left[\sum_{l\neq k}^K b_{il}b_{jl}E[V_{Fk}]E[V_{Fl}]+b_{ik}b_{jk}E[V_{Fk}^2]\right]\frac{\Delta^2}{2} \\
&+ 3\sum_{k=1}^K b_{jk}^2\sum_{l=1}^K b_{il}b_{jl}E[Z_{Fl}^2]\lambda_{Fl}E[V_{Fk}]\frac{\Delta^2}{2} \\
&+ \left[3\sum_{k=1}^K b_{ik}b_{jk}E[V_{Fk}]E[V_{Ii}]+3\sum_{k=1}^K b_{ik}b_{jk}E[Z_{Fk}^2]\lambda_{Fk}E[V_{Ii}]\right]\frac{\Delta^2}{2} \\
&+ 3\sum_{k=1}^K b_{ik}b_{jk}\left[E[V_{Fk}]E[V_{Ij}]+E[V_{Fk}]\sum_{l=1}^K b_{jl}^2 E[Z_{Fl}^2]\lambda_{Fl}\right]\frac{\Delta^2}{2} \\
&+ 3\sum_{k=1}^K b_{ik}b_{jk}E[V_{Fk}]E[Z_{Ij}^2]E[\lambda_{Ij}]\frac{\Delta^2}{2} \\
&+ 3\sum_{k=1}^K b_{ik}b_{jk}\left[\sum_{l\neq k}^K b_{jl}^2 E[V_{Fk}]E[V_{Fl}]+b_{jk}^2 E[V_{Fk}^2]\right]\frac{\Delta^2}{2} \\
&+ \left[\left(\sum_{k=1}^K b_{jk}^3 E[Z_{Fk}^3]\lambda_{Fk}\right)\left(\sum_{k=1}^K b_{ik}\mu_{Fk}+\mu_{Ii}\right)\right]\frac{\Delta^2}{2} \\
&+ \left(\sum_{k=1}^K b_{ik}E[Z_{Fk}]\lambda_{Fk}\right)\left(\sum_{k=1}^K b_{jk}^3 E[Z_{Fk}^3]\lambda_{Fk}\right)\frac{\Delta^2}{2} \\
&+ E[Z_{Ii}]E[\lambda_{Ii}]\left(\sum_{k=1}^K b_{jk}^3 E[Z_{Fk}^3]\lambda_{Fk}\right)\frac{\Delta^2}{2} \\
&+ \left[\left(\sum_{k=1}^K b_{ik}\mu_{Fk}+\mu_{Ii}\right)+\sum_{k=1}^K b_{ik}E[Z_{Fk}]\lambda_{Fk}E[Z_{Ij}^3]E[\lambda_{Ij}]\right]\frac{\Delta^2}{2} \\
&+ E[Z_{Ii}]E[Z_{Ij}^3]E[\lambda_{Ii}]E[\lambda_{Ij}]\frac{\Delta^2}{2}+E[Z_{Ii}]E[Z_{Ij}^3]\int_0^\Delta\int_0^s R_{Iij}(t-s)dtds \\
&+ \left[3\left(\sum_{k=1}^K b_{ik}b_{jk}E[V_{Fk}]\right)\left(\sum_{k=1}^K b_{jk}^2 E[Z_{Fk}^2]\lambda_{Fk}\right)+3\sum_{k=1}^K b_{ik}b_{jk}^3 E[Z_{Fk}^2]^2\lambda_{Fk}^2\right]\frac{\Delta^2}{2} \\
&+ 3\sum_{k=1}^K\sum_{l\neq k}^K b_{ik}b_{jk}b_{jl}^2 E[Z_{Fk}^2]E[Z_{Fl}^2]\lambda_{Fk}\lambda_{Fl}\frac{\Delta^2}{2} \\
&+ \left[3\sum_{k=1}^K b_{ik}b_{jk}E[V_{Fk}]E[Z_{Ij}^2]E[\lambda_{Ij}]+3\sum_{k=1}^K b_{ik}b_{jk}E[Z_{Fk}^2]\lambda_{Fk}E[Z_{Ij}^2]E[\lambda_{Ij}]\right]\frac{\Delta^2}{2} \\
&+ 3\left(\sum_{k=1}^K b_{ik}b_{jk}E[Z_{Fk}^2]\lambda_{Fk}\right)\left(\sum_{k=1}^K b_{jk}^2 E[V_{Fk}]\right)\frac{\Delta^2}{2} \\
&+ 3\left(\sum_{k=1}^K b_{ik}b_{jk}E[Z_{Fk}^2]\lambda_{Fk}\right)E[V_{Ij}]\frac{\Delta^2}{2} \\
&+ \left[3\sum_{k=1}^K b_{jk}^3 b_{ik}E[Z_{Fk}^2]^2\lambda_{Fk}+\sum_{k=1}^K\sum_{l\neq k}^K b_{jk}^2 b_{il}b_{jl}E[Z_{Fk}^2]E[Z_{Fl}^2]\lambda_{Fk}\lambda_{Fl}\right]\frac{\Delta^2}{2} \\
&+ 3\left(\sum_{k=1}^K b_{ik}b_{jk}^2 E[Z_{Fk}^3]\lambda_{Fk}\right)\left(\sum_{k=1}^K b_{jk}\mu_{Fk}+\mu_{Ij}\right)\frac{\Delta^2}{2} \\
&+ 3\sum_{k=1}^K b_{jk}^3 b_{ik}E[Z_{Fk}^3]E[Z_{Fk}]\lambda_{Fk}^2\frac{\Delta^2}{2} \\
&+ 3\sum_{k=1}^K\sum_{l\neq k}^K b_{jk}b_{il}b_{jl}^2 E[Z_{Fk}]E[Z_{Fl}^3]\lambda_{Fk}\lambda_{Fl}\frac{\Delta^2}{2} \\
&+ 3E[Z_{Ii}]E[\lambda_{Ii}]\sum_{k=1}^K b_{ik}b_{jk}^2 E[Z_{Fk}^3]\lambda_{Fk}\frac{\Delta^2}{2}
\end{aligned}
$$

$$
\begin{aligned}
E\left[\Delta X_{it}^2 \Delta X_{jt}^2\right] &= \textstyle\sum_{k=1}^K b_{ik}^2 b_{jk}^2 E[Z_{Fk}^4]\lambda_{Fk}\Delta \\
&+ 2\left(\textstyle\sum_{k=1}^K b_{ik}\mu_{Fk} + \mu_{Ii}\right)\left(\textstyle\sum_{k=1}^K b_{ik} b_{jk}^2 E[Z_{Fk}^3]\lambda_{Fk}\right)\frac{\Delta^2}{2} \\
&+ 2\textstyle\sum_{k=1}^K b_{ik}\sum_{l\neq k}^K b_{il} b_{jl}^2 E[Z_{Fl}^3]E[Z_{Fk}]\lambda_{Fl}\lambda_{Fk}\frac{\Delta^2}{2} \\
&+ 2\textstyle\sum_{k=1}^K b_{ik}^2 b_{jk}^2 E[Z_{Fk}^3]E[Z_{Fk}]\lambda_{Fk}^2\frac{\Delta^2}{2} \\
&+ 2\textstyle\sum_{k=1}^K b_{ik} b_{jk}^2 E[Z_{Fk}^3]\lambda_{Fk}E[Z_{Ii}]E[\lambda_{Ii}]\frac{\Delta^2}{2} \\
&+ 2\left(\textstyle\sum_{k=1}^K b_{jk}\mu_{Fk} + \mu_{Ij}\right)\textstyle\sum_{k=1}^K b_{jk} b_{ik}^2 E[Z_{Fk}^3]\lambda_{Fk}\frac{\Delta^2}{2} \\
&+ 2\textstyle\sum_{k=1}^K b_{jk}\sum_{l\neq k}^K b_{jl} b_{il}^2 E[Z_{Fl}^3]E[Z_{Fk}]\lambda_{Fl}\lambda_{Fk}\frac{\Delta^2}{2} \\
&+ 2\textstyle\sum_{k=1}^K b_{jk}^2 b_{ik}^2 E[Z_{Fk}^3]E[Z_{Fk}]\lambda_{Fk}^2\frac{\Delta^2}{2} \\
&+ 2\textstyle\sum_{k=1}^K b_{jk} b_{ik}^2 E[Z_{Fk}^3]\lambda_{Fk}E[Z_{Ij}]E[\lambda_{Ij}]\frac{\Delta^2}{2} \\
&+ \textstyle\sum_{k=1}^K b_{ik}^2\left[E[V_{Fk}]E[V_{Ij}] + E[V_{Fk}]\sum_{l=1}^K b_{jl}^2 E[Z_{Fl}^2]\lambda_{Fl} + E[V_{Fk}]E[Z_{Ij}^2]E[\lambda_{Ij}]\right]\frac{\Delta^2}{2} \\
&+ \left[\textstyle\sum_{k=1}^K b_{jk}\sum_{l\neq k}^K b_{ik}^2 b_{jk}^2 E[V_{Fk}]E[V_{Fl}] + \sum_{k=1}^K b_{ik}^2 b_{jk}^2 E[V_{Fk}^2]\right]\frac{\Delta^2}{2} \\
&+ \left[\textstyle\sum_{l=1}^K b_{jl}^2 E[V_{Fl}]E[V_{Ii}] + E[V_{Ii0}V_{Ij0}] + E[V_{Ii}]\sum_{k=1}^K b_{jk}^2 E[Z_{Fk}^2]\lambda_{Fk}\right]\frac{\Delta^2}{2} \\
&+ E[Z_{Ij}^2]E[\lambda_{Ij}]E[V_{Ii}]\frac{\Delta^2}{2} \\
&+ \textstyle\sum_{k=1}^K b_{jk}^2\left[E[V_{Fk}]E[V_{Ii}] + E[V_{Fk}]\sum_{l=1}^K b_{il}^2 E[Z_{Fl}^2]\lambda_{Fl} + E[V_{Fk}]E[Z_{Ii}^2]E[\lambda_{Ii}]\right]\frac{\Delta^2}{2} \\
&+ \left[\textstyle\sum_{k=1}^K b_{ik}\sum_{l\neq k}^K b_{jk}^2 b_{ik}^2 E[V_{Fk}]E[V_{Fl}] + \sum_{k=1}^K b_{jk}^2 b_{ik}^2 E[V_{Fk}^2]\right]\frac{\Delta^2}{2} \\
&+ \left[\textstyle\sum_{l=1}^K b_{il}^2 E[V_{Fl}]E[V_{Ij}] + E[V_{Ij0}V_{Ii0}]\right]\frac{\Delta^2}{2} \\
&+ \left[E[V_{Ij}]\textstyle\sum_{k=1}^K b_{ik}^2 E[Z_{Fk}^2]\lambda_{Fk} + E[Z_{Ii}^2]E[\lambda_{Ii}]E[V_{Ij}]\right]\frac{\Delta^2}{2} \\
&+ 4\textstyle\sum_{k=1}^K b_{ik} b_{jk}\left[\sum_{l\neq k}^K b_{il} b_{jl} E[V_{Fk}]E[V_{Fl}] + b_{ik} b_{jk} E[V_{Fk}^2]\right]\frac{\Delta^2}{2} \\
&+ 4\textstyle\sum_{k=1}^K b_{ik} b_{jk}\sum_{l=1}^K b_{il} b_{jl} E[Z_{Fl}^2]\lambda_{Fl}E[V_{Fk}]\frac{\Delta^2}{2} \\
&+ \left[\textstyle\sum_{k=1}^K b_{ik}^2 E[V_{Fk}]\left(\sum_{l=1}^K b_{jl}^2 E[Z_{Fl}^2]\lambda_{Fl}\right) + E[V_{Ii}]\left(\sum_{l=1}^K b_{jl}^2 E[Z_{Fl}^2]\lambda_{Fl}\right)\right]\frac{\Delta^2}{2} \\
&+ \left[\textstyle\sum_{k=1}^K b_{ik}^2 b_{jk}^2 E[Z_{Fk}^2]^2\lambda_{Fk}^2 + E[Z_{Ii}^2]E[\lambda_{Ii}]\sum_{l=1}^K b_{jl}^2 E[Z_{Fl}^2]\lambda_{Fl}\right]\frac{\Delta^2}{2} \\
&+ \textstyle\sum_{k=1}^K\sum_{l\neq k}^K b_{ik}^2 b_{jl}^2 E[Z_{Fk}^2]E[Z_{Fl}^2]\lambda_{Fk}\lambda_{Fl}\frac{\Delta^2}{2} \\
&+ \left[\textstyle\sum_{k=1}^K b_{ik}^2 E[V_{Fk}]E[Z_{Ij}^2]E[\lambda_{Ij}] + E[V_{Ii}]E[Z_{Ij}^2]E[\lambda_{Ij}]\right]\frac{\Delta^2}{2} \\
&+ \left[\left(\textstyle\sum_{k=1}^K b_{jk}^2 E[Z_{Fk}^2]\lambda_{Fk}\right)E[Z_{Ij}^2]E[\lambda_{Ij}] + E[Z_{Ii}^2]E[Z_{Ij}^2]E[\lambda_{Ii}]E[\lambda_{Ij}]\right]\frac{\Delta^2}{2} \\
&+ E[Z_{Ii}^2]E[Z_{Ij}^2]\textstyle\int_0^\Delta\int_0^s R_{Iij}(t-s)dtds \\
&+ \left[\textstyle\sum_{k=1}^K b_{jk}^2 E[V_{Fk}]\left(\sum_{l=1}^K b_{il}^2 E[Z_{Fl}^2]\lambda_{Fl}\right) + E[V_{Ij}]\left(\sum_{l=1}^K b_{il}^2 E[Z_{Fl}^2]\lambda_{Fl}\right)\right]\frac{\Delta^2}{2} \\
&+ \left[\textstyle\sum_{k=1}^K b_{jk}^2 b_{ik}^2 E[Z_{Fk}^2]^2\lambda_{Fk}^2 + E[Z_{Ij}^2]E[\lambda_{Ij}]\sum_{l=1}^K b_{il}^2 E[Z_{Fl}^2]\lambda_{Fl}\right]\frac{\Delta^2}{2} \\
&+ \textstyle\sum_{k=1}^K\sum_{l\neq k}^K b_{jk}^2 b_{il}^2 E[Z_{Fk}^2]E[Z_{Fl}^2]\lambda_{Fk}\lambda_{Fl}\frac{\Delta^2}{2} \\
&+ \left[2\left(\textstyle\sum_{k=1}^K b_{jk}\mu_{Fk} + \mu_{Ij}\right)\sum_{k=1}^K b_{ik}^2 b_{jk} E[Z_{Fk}^3]\lambda_{Fk}\right]\frac{\Delta^2}{2} \\
&+ 2\textstyle\sum_{k=1}^K b_{jk}^2 b_{ik}^2 E[Z_{Fk}]E[Z_{Fk}^3]\lambda_{Fk}^2\frac{\Delta^2}{2} \\
&+ 2\textstyle\sum_{k=1}^K\sum_{l\neq k}^K b_{jk} b_{il}^2 b_{jl} E[Z_{Fk}]E[Z_{Fl}^3]\lambda_{Fk}\lambda_{Fl}\frac{\Delta^2}{2} \\
&+ 2E[Z_{Ij}]E[\lambda_{Ij}]\textstyle\sum_{k=1}^K b_{ik}^2 b_{jk} E[Z_{Fk}^3]\lambda_{Fk}\frac{\Delta^2}{2} \\
&+ \left[\textstyle\sum_{k=1}^K b_{jk}^2 E[V_{Fk}]E[Z_{Ii}^2]E[\lambda_{Ii}] + E[V_{Ij}]E[Z_{Ii}^2]E[\lambda_{Ii}]\right]\frac{\Delta^2}{2}
\end{aligned}
$$

$$
\begin{aligned}
+ &\quad \left[\left(\sum_{k=1}^{K} b_{ik}^2 E[Z_{Fk}^2]\lambda_{Fk}\right) E[Z_{Ii}^2]E[\lambda_{Ii}] + E[Z_{Ij}^2]E[Z_{Ii}^2]E[\lambda_{Ij}]E[\lambda_{Ii}]\right] \frac{\Delta^2}{2} \\
+ &\quad \left[2\left(\sum_{k=1}^{K} b_{ik}\mu_{Fk} + \mu_{Ii}\right) \sum_{k=1}^{K} b_{jk}^2 b_{ik} E[Z_{Fk}^3]\lambda_{Fk}\right] \frac{\Delta^2}{2} \\
+ &\quad 2\sum_{k=1}^{K} b_{ik}^2 b_{jk}^2 E[Z_{Fk}]E[Z_{Fk}^3]\lambda_{Fk}^2 \frac{\Delta^2}{2} \\
+ &\quad 2\sum_{k=1}^{K}\sum_{l\neq k}^{K} b_{ik} b_{jl}^2 b_{il} E[Z_{Fk}]E[Z_{Fl}^3]\lambda_{Fk}\lambda_{Fl} \frac{\Delta^2}{2} \\
+ &\quad 2E[Z_{Ii}]E[\lambda_{Ii}]\sum_{k=1}^{K} b_{jk}^2 b_{ik} E[Z_{Fk}^3]\lambda_{Fk} \frac{\Delta^2}{2} \\
+ &\quad \left[\sum_{k=1}^{K} b_{jk}^2 E[V_{Fk}]E[Z_{Ii}^2]E[\lambda_{Ii}] + E[V_{Ij}]E[Z_{Ii}^2]E[\lambda_{Ii}]\right] \frac{\Delta^2}{2} \\
+ &\quad \left[\left(\sum_{k=1}^{K} b_{ik}^2 E[Z_{Fk}^2]\lambda_{Fk}\right) E[Z_{Ii}^2]E[\lambda_{Ii}] + E[Z_{Ij}^2]E[Z_{Ii}^2]E[\lambda_{Ij}]E[\lambda_{Ii}]\right] \frac{\Delta^2}{2} \\
+ &\quad E[Z_{Ij}^2]E[Z_{Ii}^2]\int_0^{\Delta}\int_0^{s} R_{Iji}(t-s)\,dtds \\
+ &\quad \left[4\left(\sum_{k=1}^{K} b_{ik}b_{jk}E[V_{Fk}]\right)\left(\sum_{k=1}^{K} b_{ik}b_{jk}E[Z_{Fk}^2]\lambda_{Fk}\right) + \sum_{k=1}^{K} b_{ik}^2 b_{jk}^2 E[Z_{Fk}^2]^2\right] \frac{\Delta^2}{2} \\
+ &\quad \sum_{k=1}^{K}\sum_{l\neq k}^{K} b_{ik}b_{jk}b_{il}b_{jl}E[Z_{Fk}^2]E[Z_{Fl}^2]\lambda_{Fk}\lambda_{Fl} \frac{\Delta^2}{2} \\
+ &\quad \sum_{k=1}^{K} b_{ik}b_{jk}^2 E[Z_{Fk}^3]\lambda_{Fk}E[Z_{Ii}]E[\lambda_{Ii}] \frac{\Delta^2}{2}
\end{aligned}
$$

Chapter 2

High-Dimensional Multivariate Realized Volatility Estimation

With **Tim Bollerslev** and **Nour Meddahi**[1]

Abstract

We provide a new factor-based estimator of the realized covolatility matrix, applicable in situations when the number of assets is large and the high-frequency data are contaminated with microstructure noises. Our estimator relies on the assumption of a factor structure for the noise component, separate from the latent systematic risk factors that characterize the cross-sectional variation in the frictionless returns. The new estimator provides theoretically more efficient and finite-sample more accurate estimates of large-scale integrated covolatility, correlation, and inverse covolatility matrices than other recently developed realized estimation procedures. These theoretical and simulation-based findings are further corroborated by an empirical application related to portfolio allocation and risk minimization involving several hundred individual stocks.

[1]We have benefited from comments by Kevin Sheppard, Jia Li, Andrew Patton, George Tauchen, as well as seminar and conference participants at Toulouse School of Economics, Duke University, the 2016 European Meeting of the Econometric Society, the 2016 Meeting of the International association of Applied Econometrics, and the 2016 Financial Econometrics Conference in Toulouse. The authors acknowledge financial support of the grant ERC POEMH.

2.1 Introduction

We contribute to the literature on the estimation of large-dimensional integrated covolatility matrices from high-frequency intraday data. The covolatility matrix plays a crucial role in many financial applications including risk management, portfolio allocation, hedging and asset pricing, and as such, accurate and well conditioned estimates of the integrated covolatility matrix, its inverse, and the correlation matrix are of great practical import.

Our new covolatility estimator is specifically designed to work in situations when the the number of assets is large and the high-frequency data used in the estimation might be contaminated with microstructure noises. It relies on the assumption of a factor structure for characterizing the microstructure noise component, separate from the factor structure that characterizes the latent genuine returns. The efficiency of the new estimator compares favorably to other recently developed procedures. These theoretical results, derived under the assumption of increasingly finer sampled intraday returns and an increasing number of assets, carry over to more accurate estimates of large-scale integrated covolatility, correlation, and inverse covolatility matrices in empirically realistic situations with hundreds of assets and finitely sampled intrday returns. On applying the new estimator in the construction of minimum variance portfolios with a sample comprised of almost four-hundred individual stocks, it also results in systematically lower ex-post risks than other competing realized covolatility estimation procedures.

To more formally set out the ideas, let $X_t^* = \left(X_{1t}^*, ..., X_{pt}^*\right)'$ denotes the latent p-dimensional frictionless vector log-price process of interest. Importantly, we allow for p to be "large" and possibly in excess of the number of intraday price observations. Consistent with the lack of arbitrage, we will further assume that X_t follows a continuous Itô semimartigale process,

$$dX_t^* \;=\; \mu_t dt \;+\; \sigma_t dB_t, \qquad 0 \leq t \leq 1, \tag{2.1}$$

where the unit time-interval corresponds to a day, $B_t = \left(B_t^{(1)}, ..., B_t^{(p)}\right)'$ is a p-dimensional vector of standard independent Brownian motions, and $\mu_t = \left(\mu_t^{(1)}, ..., \mu_t^{(p)}\right)'$ and $\sigma_t = \left(\sigma_t^{(1)}, ..., \sigma_t^{(p)}\right)'$ denote a p-dimensional predictable locally bounded drift process and a càdlàg $p \times p$ spot covolatility process, respectively. The object of interest is the $p \times p$ integrated covolatility matrix,[2]

$$ICV = \int_0^1 \sigma_s \sigma_s' ds. \tag{2.2}$$

This ex-post measure of the true daily covariation is, of course, latent. By the theory of quadratic variation, it may be consistently estimated by the summation of increasingly finer sampled cross-products of the high-frequency frictionless vector return process,

$$RCV = \sum_{t_i} (X^*_{t_{i+1}} - X^*_{t_i})(X^*_{t_{i+1}} - X^*_{t_i})', \tag{2.3}$$

where $0 \leq t_i \leq 1$ refer to the within day sampling times, $t_i - t_{i-1} \to 0$. In practice, of course, the X_t^* process is not directly observable. Instead, the actually observed price process, is subject to "noise" stemming from a host of market microstructure complications, including bid-ask spreads, non-trading, price discreteness, trades occurring on different markets or networks, rounding errors, among others (see, e.g., Hansen and Lunde (2006) and Diebold and Strasser (2013)),

$$X_t = X_t^* + u_t. \tag{2.4}$$

This in turn renders the estimator for ICV based on RCV with the actually observed X_t price process in place of X_t^* inconsistent.

Several competing estimators that remain consistent in the presence of market microstructure noise have been proposed in the univariate case ($p = 1$), including the subsampling and averaging approach of Zhang, Mykland, and Ait-Sahalia (2005), the realized kernel of Barndorff-Nielsen, Hansen, and Shephard (2008a), and the pre-averaging (henceforth PRV) approach of Jacod, Li, Mykland, Podolskijc, and Vetter (2009a). These estimators are naturally extended to the multivariate case ($p > 1$), provided that the observation times of all the assets are synchronous, and the number of assets is smaller than the number of intraday observations. In practice, of course, prices are generally not recorded at the same time for all assets, which can cause naive estimators of the covolatility matrix that pretend the data are synchronous to be seriously biased.[3]

One solution to the non-synchronicity problem is provided by Hayashi and Yoshida (2005), who propose including all overlapping (in time) intraday returns based on the ac-

[2]Following the literature, we will also interchangeably refer to this as the integrated covariance, integrated volatility, or integrated covariation matrix.

[3]This effect was first noted empirically for sample correlation matrices by Epps (1979), and it is now commonly referred to as the Epps-effect.

tually observed price series in the calculation of RCV. However, the estimator of Hayashi and Yoshida (2005) doesn't deal with the microstructure noise that plagues the use of high-frequency data more generally. The multivariate realized kernel estimator of Barndorff-Nielsen, Hansen, Lunde, and Shephard (2011a) (henceforth $MRker$[4]) simultaneously guarantee consistency, positive semi-definiteness, robustness to microstructure noise, while also accounting for non-synchroneity of observations. The non-synchronicity issue, in particular, is resolved using so-called refresh-time sampling. The modulated realized covariance estimator (henceforth MRC) of Christensen, Kinnebrock, and Podolskij (2010a), based on a multivariate extension of the univariate pre-averaging approach, also works in the presence of market microstructure noise. However, the MRC estimator assumes synchronous data, and it is not guaranteed to be positive semi-definite. Christensen, Kinnebrock, and Podolskij (2010a) introduced the adjusted modulated realized covariance (henceforth MRC^{δ}) and the pre-averaged Hayashi-Yoshida estimator, in order to ensure the positive semi-definiteness, the noise-robustness and to resolve the non-synchronous data problem.

The covolatility estimators discussed above were explicitly designed for situations in which the number of assets is small relative to the number of intraday return observations, or the sample size available for the estimation. Of course, in many practical portfolio allocation, risk measurement and management decisions, the number of assets is often of the same order of magnitude or even larger than the sample size, entailing a curse of dimensionality type problem for any direct estimation of ICV matrix.[5] Two main approaches has emerged in the literature for dealing with this problem: (i) sparsity or decay assumptions pertaining directly to the different entries in the covolatility matrix; and (ii) the use of factor structures.

[4]The realized kernel is defined by:

$$K(Y) = \sum_{h=-n}^{n} k(\frac{h}{H+1})\Gamma_h, \tag{2.5}$$

$$\Gamma_h = \sum_{j=h+1}^{n} y_j y_{j-h}^{'}, \text{ for } h > 0; \qquad \Gamma_h = \Gamma_{-h}^{'}, \text{ for } h < 0,$$

where n is the number of synchronized returns per asset, Γ_h is the h^{th} realized auto-covariance; $y_j = Y_j - Y_{j-1}$ for $j = 1, 2, ..., n$; with $Y_0 = \frac{1}{m}\sum_{j=1}^{m} Y(\tau_{p,j})$; $Y_n = \frac{1}{m}\sum_{j=1}^{m} Y(\tau_{p,p-m+j})$; $Y_j = Y(\tau_{p,j+m})$ for $j = 1, ..., n-1$; $\{\tau_{p,j}\}$ is the series of refresh time ; and k is a non-stochastic weighting function. The rate of convergence of this estimator is $n^{-1/5}$

[5]This mirrors the problem in parametric $GARCH$ and stochastic volatility models, for which the dimensionality of parameter space in unrestricted versions of the models grow at the rate of p^4; see, e.g., Andersen, Bollerslev, Christoffersen, and Diebold (2006).

Estimators that rely on sparsity and decay assumptions include Wang (2010) and Zheng and Li (2011). These estimators typically postulate that the covolatility matrix is comprised of only a small number of non-zero block diagonal matrices, or that the absolute magnitude of the elements in the matrix somehow decay away from the diagonal.[6] The blocking and regularization approach of Hautsch and Podolskij (2013), in which assets with similar observation frequency are grouped together in order to reduce the data loss stemming from the use of refresh-time sampling, also implicitly builds on similar ideas. As does the composite realized kernel estimator (henceforth $\hat{\Sigma}_{comp}$) of Lunde, Shephard, and Sheppard (2016), in which bivariate realized kernel estimators for all pairs of assets is combined and regularized in the construction of an estimation for the full high-dimensional covolatility matrix for all assets.

The use of factor structures that underly the second approach for high-dimensional realized covolatility matrix estimation, is, of course, omnipresent in finance (see, e.g., Ross (1976), Chen, Roll, and Ross (1986), Sharpe (1994), and Ledoit and Wolf (2003)). The use of this approach in the context of high-frequency data realized covolatility estimation was pioneered by Fan, Fan, and Lv (2008). It has the obvious advantages that it guarantees a positive semi-definite and, under weak conditions, invertible estimate of the covolatility matrix. Fan, Fan, and Lv (2008) further examine how the dimensionality of the problem favorably impact the accuracy of the estimator compared to other procedures. Other related factor-based approaches include Tao, Wang, and Chen (2011) and Bannouh, Martens, Oomen, and van Dijk (2012), who rely on mixtures of high-frequency intraday data and daily date for estimating the covolatility matrix implied by a factor structure, Fan, Liao, and Mincheva (2011) through their approximate factor models[7] for the estimation of high-dimensional covariance matrix, Fan, Liao, and Mincheva (2013) introduce the Principal Orthogonal Complement Thresholding Estimator (Henceforth, POET) [8], as well as the principal component analysis for the estimation of high dimensional factor models recently explored by Ait-Sahalia and Xiu (2016) and Dai, Lu, and Xiu (2017) [9].

Building on these ideas, we propose a new high dimensional covolatility matrix estimator

[6] The decay assumption is often somewhat arbitrary, since there is not a natural ordering of the assets.

[7] They assume observable factors and allow the presence of the cross-sectional correlation in a sparse error covariance matrix

[8] They assume a sparse error covariance matrix in an approximate factor model, and allow for the presence of some cross-sectional correlation, after taking out common but unobservable factors.

[9] They rely on the pre-averaging method with refresh time to solve the microstructure problems, while using three different specifications of factor models, and their corresponding estimators, respectively, to battle against the curse of dimensionality

under the assumption that the true dynamics of the returns may be described by a latent factor model. In contrast to the factor-based estimators discussed above, we explicitly allow for the possibility of market microstructure noise in the actually observed price series. Motivated by Hasbrouck and Seppi (2001a), we assume that the cross-sectional dependencies in the market microstructure noise component may be described by its own factor model, resulting in two separately identified factor structures: a latent component of order $O_p(\sqrt{\Delta})$ accounting for the genuine cross-sectional dependencies in the returns, which becomes increasingly less important for discretely sampled observations over diminishing time-intervals of length Δ, and another component of order $O_p(1)$ for describing the noise, which remains invariant to the sampling frequency. Exploiting these differences in the orders of magnitude, and appropriately combining noise-robust $MRker$ and PRV-based estimates of the rotated return factors and their integrated volatilities, along with the corresponding loadings and integrated idiosyncratic volatility components, in turn allows for consistent noise-robust estimation of the full covolatility matrix in large dimensions.

The rest of the paper is organized as follow. Section 2.2 presents the theoretical setup and formally defines the new estimator. Section 2.3 derives the convergence rate of the new and other competing estimators. This section also presents the results from a set of finite-sample simulations involving both synchronous and asynchronous high-frequency prices. Section 2.4 presents the results from an empirical application involving a large cross-section of individual stocks. Section 2.5 concludes. The details of the proofs and other more specific materials are deferred to Appendixes.

2.2 Theoretical setup

2.2.1 The benchmark model

We assume that the continuous Itô semimartingale process X_t in (2.1) follows a factor model of the form,

$$dX_t^* = bdF_t + dE_t, \tag{2.6}$$

where $b = (b_{ik})_{1\leq i\leq p, 1\leq k\leq K}$ denotes the $p \times K$ matrix of factor loadings, $F_t = (F_{1t}, ..., F_{Kt})'$ refers to the latent factor vector, K is supposed to be asymptotically finite and known, and $E_t = (E_{1t}, ..., E_{pt})'$ denotes the vector of idiosyncratic errors. The use of factor models in asset pricing finance is, of course, quite standard and traces back to the seminal work by

Ross (1976) and Gary and Rothschild (1983). The factor F_t is supposed to represent general influences which tend to affect all assets. Following standard assumptions in the literature, we assume that factor loadings b are time invariant and do not depend on t.

We further assume that the F_t and E_t vectors and the individually components therein are uncorrelated and driven by their own standard Brownian motions,

$$dF_{kt} = \sigma_{fkt} dB^F_{kt},$$
$$dE_{it} = \sigma_{\epsilon it} dB^E_{it}.$$

Integrating both sides of the resulting latent factor price process above over a time interval of length Δ, it readily follows that

$$\int_{t-\Delta}^t dX^*_s = b \cdot \int_{t-\Delta}^t \sigma_{fs} dB^F_s + \int_{t-\Delta}^t \sigma_{\epsilon s} dB^E_s.$$

Defining the corresponding returns, factors, and errors over the time-interval Δ,

$$\begin{gathered} r^*_t \equiv r^*_{t,\Delta} \equiv \int_{t-\Delta}^t dX^*_s \\ f_t \equiv f_{t,\Delta} \equiv \int_{t-\Delta}^t \sigma_{fs} dB^F_s \\ \varepsilon_t \equiv \varepsilon_{t,\Delta} \equiv \int_{t-\Delta}^t \sigma_{\epsilon s} dB^E_s \end{gathered}$$

allows for following standard discrete-time factor representation,

$$r^*_t = bf_t + \varepsilon_t \tag{2.7}$$

where $r^*_t = (r^*_{1t}, ..., r^*_{pt})'$, $f_t = (f_{1t}, ..., f_{Kt})'$, and $\varepsilon_t = (\varepsilon_{1t}, ..., \varepsilon_{pt})'$, respectively.

We make the additional assumptions directly pertaining to this representation, where $I_{t-\Delta}$ refers to information set available at time $t - \Delta$.

Assumption 1 $\forall t$, $\forall i, j, k, k' \in \{1, ..., p\}$, $i \neq j$, $k \neq k'$:

- $Cov\left(f_{kt}, \varepsilon_{it} | I_{t-\Delta}\right) = 0$;
- $Cov\left(f_{kt}, f_{k't} | I_{t-\Delta}\right) = 0$;
- $Cov(\varepsilon_{it}, \varepsilon_{jt} | I_{t-\Delta}) = 0$;

- $E\left(\varepsilon_{it}|I_{t-\Delta}\right)=0$.

The latent X^*_{it} prices for each of the p individual assets are not directly observable. Instead, the actually observed prices are contaminated with market microstructure noise,

$$X_{it}=X^*_{it}+u_{it}. \tag{2.8}$$

We assume that this noise component has has its own separate factor representation,

$$u_{it}=c_i g_t+\eta_{it}, \tag{2.9}$$

where the $K'\times 1$ g_t vector accounts for the cross-sectional dependence in the noise, and the $1\times K'$ c_i vector denotes the corresponding factor loadings. We make the following additional assumptions about this structure.

Assumption 2 $\forall t$, $\forall i,k,k'\in\{1,...,p\}$, $k\neq k'$:

- $Cov\left(g_{kt},f_{k't}|I_{t-\Delta}\right)=0$;
- $Cov\left(g_{kt},\varepsilon_{it}|I_{t-\Delta}\right)=0$;
- $Cov\left(\eta_{it},f_{kt}|I_{t-\Delta}\right)=0$, $Cov\left(\eta_{it},g_{kt}|I_{t-\Delta}\right)=0$, $Cov\left(\eta_{it},\varepsilon_{it}|I_{t-\Delta}\right)=0$;
- $Var(\eta_{it})=\sigma^2_{\eta i}$, $\forall i\in\{1,...,p\}$;
- $Var(g_{kt})=\sigma^2_{g_k}$;
- g_{kt}, η_{it} are independent across assets and time.

Two main types of factors models are present in the existing literature: strict factor models and approximated factor models. The main difference between these models is the assumption on the covariance matrix of idiosyncratic components. In a strict factor model, this matrix is assumed to be diagonal while its terms can be weakly correlated in an approximated factor model. For an identification purpose, following assumptions are widely made:

- *Pervasiveness*: factors influence a large number of assets. Loading vectors b are bounded and $\|\frac{1}{p}b'b - D\| \longrightarrow 0$ as $p \longrightarrow \infty$, where D is a $K \times K$ positive definite matrix;
- *Factors*: the fourth moment of factors exists and serial auto-covariance functions of factors converge to definite positive matrices as $n \longrightarrow \infty$;
- Time and cross-section dependence and heteroscedasticity of idiosyncratic terms (for approximated factor models).

Our model is a strict factor model with some normalization assumptions: i) the pervasiveness assumption holds with $D = I_p$; ii) fourth moments of factors exist and the serial auto-covariance function of factors converges to a diagonal matrix without loss of generality, as n goes to infinity; iii) the case of time and cross-section dependence and heteroscedasticity of idiosyncratic terms is left for future research.

As discussed further below, the assumption of a separate factor representation for the microstructure noise makes it possible to disentangle the estimation of the covolatility matrix into two parts: a traditional factor-based approach for the estimation of the latent component of order $O_p(\sqrt{\Delta})$ associated with the traditional factor structure in the returns, and a separate estimation of the factor noise components of order $O_p(1)$.

The use of a factor structure for the microstruture noise is directly motivated by Hasbrouck and Seppi (2001a), who document strong commonalities in various liquidity proxies such as the bid-ask spread. To further corroborate the dominance of common factors in the noise, we run two empirical exercises.

Firstly, we construct the signature plot of the cross-sectional average return, computed from a sample of 384 individual stocks analyzed in the empirical section below. Under a cross-sectional uncorrelation of microstructure noise, the noise component is supposed to vanish by the law of large numbers. As a consequence, the resulting signature plot is supposed to be flat. However, as presented in figure 2.1, we obtain a strictly decreasing curve. This is an evidence that the cross-sectional average return still contain a microstructure term. Thus, microstructure noises must be cross-sectionally correlated and common factors may capture this cross-sectional correlation.

Figure 2.1. Signature plot of the cross-sectional average return

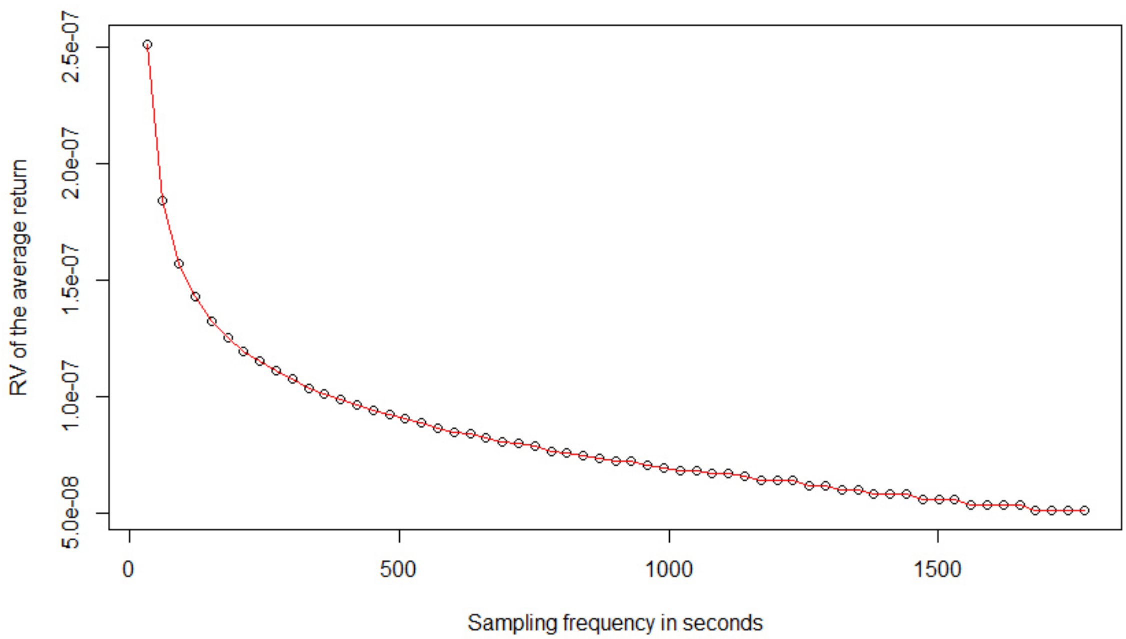

Secondly, we estimated the covariance matrix for the market microstructure noise for the same sample. Decomposing the resulting covariance matrix estimates for each day in the sample, strongly supports the idea that the cross-sectional dependencies may be adequately captured by a few factors. Further details concerning these results are provided in Appendix 2.9.

Figure 2.2 depicts the average shares of the total variability in the observed returns which can be explained by the first six factors. The analysis is done for various frequencies: 5, 15, 30, 60 and 300 seconds. It is well-known that the variance of the market microstructure is better estimated at the highest frequency. Thus, the higher the sampling frequency, the more accurate is the estimation of the shares of the total variability of microstructural noise that can be explained by factors. However, when one increases the frequency, one has less assets. Estimations based on 15, 30 and 60 seconds are robust and corroborate the factor structure of the noise. At the 300 seconds frequency, the observed factor structure concerns latent returns. Clearly, Figure 2.2 supports the factor structure of the noise, especially at the 5-seconds frequency, even if the number of assets is relatively small.[10]

[10] At the 5 seconds frequency, the number of stocks involved drops drastically (only 28 assets remain in the sample in contrast to the others cases where we have more than 282 assets involved). Factor are better understood when the number of stocks is huge. the case 60s, 30s, and 15s are more appropriated in order to understand the factor structure of microstructure noise. Ratios don't need necessarily to be monotonically

Figure 2.2. Ratio of largest eigenvalues relative to the total variation

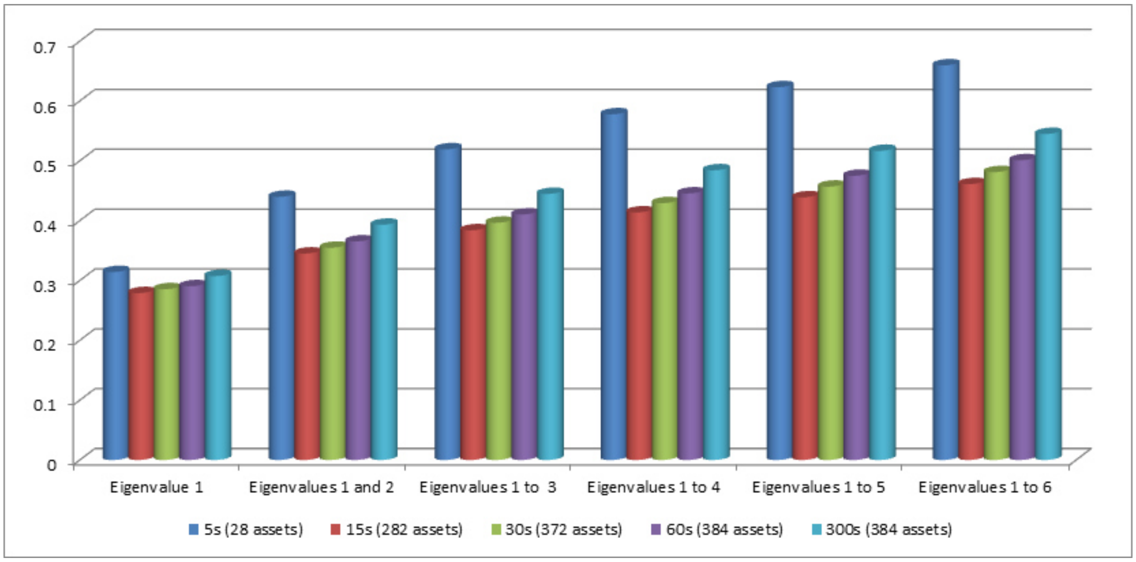

2.2.2 Estimation methodology

The general setup and assumptions outlined in the previous section implies that the integrated covolatility matrix of interest may be succinctly expressed as,

$$\Sigma \;=\; bDiag\left[\int_0^1 \sigma^2_{f1u}du, ..., \int_0^1 \sigma^2_{fKu}du\right]b' + Diag\left[\int_0^1 \sigma^2_{\varepsilon 1u}du, ..., \int_0^1 \sigma^2_{\varepsilon pu}du\right]. \qquad (2.10)$$

We rely on traditional factor analysis together with the pre-averaging approach for conveniently estimating the different components of Σ. As usual, the factors and the factor loadings are only determined up to a rotation.[11] Correspondingly, our estimation strategy is comprised of four separate steps for estimating:

- The rotated factors $\tilde{f}$.
- The integrated volatilities of $\tilde{f}$.
- The rotated loadings $\tilde{b}$.
- The integrated volatility of the idiosyncratic component.

decreasing with the sampling frequency since the object whose factor structure is investigated varies with the sampling frequency (Latent returns for 300s and microstructure noise for others frequencies)

[11] Let H denote a $K \times K$ orthogonal H matrix such that $H'H = I_K$. The Σ matrix defined by the rotated factors $\tilde{f}_t = Hf_t$ and rotated factor loadings $\tilde{b} = bH'$, is then identical to the matrix in (2.10).

We will discuss each of these four steps in turn. We will begin by assuming that all of the high-frequency returns used in the estimation span the same time-interval of length Δ, with $\Delta \to 0$ corresponding to continuous-time case. However, we will also subsequently consider the empirically more realistic case with unevenly spaced non-synchronous discrete-time observations.

Estimation of $\tilde{f}$

Following the Principal Component Analysis (henceforth PCA) of Connor and Korajczyk (1988), $f_{j\Delta}$ is chosen to minimize the scaled sum of squared values of the idiosyncratic component,

$$\begin{cases} \underset{f_{j\Delta},b}{Min} \;\; \frac{1}{p} \sum_{j=1}^{\lfloor 1/\Delta \rfloor} (r^*_{j\Delta} - b f_{j\Delta})'(r^*_{j\Delta} - b f_{j\Delta}) \\ s.t \;\; \frac{1}{p} b'b = I_K \end{cases}$$

It follows readily from the solution to this optimization problem that

$$\hat{f}_{k\Delta} = \tfrac{1}{p} W' r^*_{k\Delta}, \quad \forall k = 1, ..., \lfloor 1/\Delta \rfloor,$$

where W denotes the matrix of ordered eigenvectors of $\sum_{j=1}^{\lfloor 1/\Delta \rfloor} \left[r^*_{j\Delta} r^{*\prime}_{j\Delta} \right]$. Taking $\Delta \to 0$, we obtain the continuous time expression,

$$\hat{f}_t = \frac{1}{p} W' r^*_t, \tag{2.11}$$

in which the columns of W correspond to the ordered eigenvectors of Σ.

The estimator defined by equation (2.11) is not feasible because r^*_t and Σ are latent. In order to obtain a feasible estimator, we need consistent estimates of the ordered eigenvectors W of Σ. Let $\hat{W}$ denote the matrix of K ordered eigenvectors of an estimator $\hat{\Sigma}$ of Σ that is robust to microstructure noise. The simulation results in Appendix 2.11 shows that $MRker$ provides a good candidate.[12] Hence, we propose as feasible estimator:

$$\hat{f}_t = \frac{1}{p} \hat{W}' r_t, \tag{2.12}$$

[12]This approach mirrors the "Linear Shrinkage" estimator of the covariance matrix of Ledoit and Wolf (2003). In order to improve the covariance matrix estimator in large dimensions, a "Linear Shrinkage" estimator is obtained from the spectral decomposition of the sample covariance matrix by keeping the eigenvectors, while transforming the eigenvalues.

where r_t is the $p \times 1$ vector of observed returns, $\hat{W} = \left(\underline{\hat{W}}_1, ..., \underline{\hat{W}}_K\right)$ is a consistent estimator of the $p \times K$ matrix W of ordered eigenvectors of Σ provided by $MRker$.

We need to verify that the resulting $\hat{f}$ consistently estimates a rotation $\tilde{f}$ of f plus a microstruture noise component. To do so, we express $\hat{f}$ as a function of the true factor f, the idiosyncratic component ϵ_t, and the factor representation of the microstructure noise component u_t

$$\hat{f}_t \;=\; \tfrac{1}{p}\hat{W}'bf_t + \tfrac{1}{p}\hat{W}'\epsilon_t + \tfrac{1}{p}\hat{W}'c(g_t - g_{t-\Delta}) + \tfrac{1}{p}\hat{W}'(\eta_t - \eta_{t-\Delta})$$

The consistency result in the estimation of a rotation $\tilde{f}$ of f contaminated by a microstructure noise component is given in the following theorem inspired by the paper of Stock and Watson (2002).

Lemma 2.2.1 *There exists an orthogonal matrix S such that $S\hat{f}$ consistently estimates f up to a microstruture noise component, so that for $\Delta \to 0$ and $p \to \infty$:*

- $\frac{1}{p}S\hat{W}'bf_t \xrightarrow{p} f_t$.
- $\frac{1}{p}S\hat{W}'\epsilon_t \xrightarrow{p} 0$.
- $\frac{1}{p}S\hat{W}'(\eta_t - \eta_{t-\Delta}) \xrightarrow{p} 0$.

Proof: See Appendix 2.6.

Estimation of $\int_0^1 \sigma^2_{\hat{f}ku} du$

Consider the following decomposition of $\hat{f}_t$,

$$\hat{f}_{kt} = \tfrac{1}{p}W_k' r_t^* + \tfrac{1}{p}W_k'(u_t - u_{t-\Delta}) + \tfrac{1}{p}W_k^{\epsilon'} r_t^* + \tfrac{1}{p}W_k^{\epsilon'}(u_t - u_{t-\Delta}),$$

where $W_k^{\epsilon'}$ is the error term in the estimation of W. We assume that $\frac{1}{p}W_k^{\epsilon'} r_t^*$ and $\frac{1}{p}W_k^{\epsilon'}(u_t - u_{t-\Delta})$ are of orders smaller than $max(n,p)^{(-1/2)}$.[13] Since $\frac{1}{p}W_k'\epsilon_t = O_p(n^{-1/2}p^{-1/2})$ and $\frac{1}{p}W_k'(\eta_t - \eta_{t-\Delta}) = O_p(p^{-1/2})$, it follows that

[13] The intuition is that p and n are suffiently large such that error components $\frac{1}{p}W_k^{\epsilon'} r_t^*$ and $\frac{1}{p}W_k^{\epsilon'}(u_t - u_{t-\Delta})$ are dominated by their latent counterparts, $\frac{1}{p}W_k' r_t^*$ and $\frac{1}{p}W_k'(u_t - u_{t-\Delta})$ respectively . Those two latent components are respectively of orders $n^{-1/2}$ and $p^{-1/2}$. The simulation exercise in the appendix 2.11 shows that errors in the estimation of W are very small and decreases with p and n.

$$\hat{f}_{kt} \quad = \quad \tilde{f}_{kt} + \tfrac{1}{p} W_k' c(g_t - g_{t-\Delta}) + O_p(p^{-1/2})$$

For n and p sufficiently large,

$$\hat{f}_{kt} \quad \approx \quad \tilde{f}_{kt} + \tfrac{1}{p} W_k' c(g_t - g_{t-\Delta})$$

Note that $\hat{f}$ is effectively a rotation of the latent factor f contaminated by microstructure noises. Hence, by the literature on the estimation of integrated volatility using data contaminated by microstructure noise, $\int_0^1 \sigma^2_{\tilde{f}ku} du$ can be estimated by,

$$\widehat{\int_0^1 \sigma^2_{\tilde{f}ku} du} = PRV(\hat{f}_k), \tag{2.13}$$

where the PRV estimator is defined in Appendix 2.7.

Estimation of $\tilde{b}_{ik}$

Since the factors are pairwise independent and also independent of the idiosyncratic component, it follows that the integrated covolatility matrix for r_i^* and $\tilde{f}_k$ equals $\tilde{b}_{ik}.IV(\tilde{f}_k)$. Thus, $\tilde{b}_{ik} = ICV(r_i^*, \tilde{f}_k)/IV(\tilde{f}_k)$, so that an estimate for $\tilde{b}_{ik}$ is naturally obtained by,

$$\hat{b}_{ik} = \frac{MRC(r_i, \hat{f}_k)}{PRV(\hat{f}_k)}. \tag{2.14}$$

with the MRC estimator formally defined in Appendix 2.7.

Estimation of $\int_0^1 \sigma^2_{\varepsilon iu} du$

Define $\hat{\epsilon}_{it} = r_{it} - \sum_{k=1}^K \hat{b}_{ik} \cdot \hat{f}_{kt}$. It is easy to show that

$$\hat{\epsilon}_{it} = \epsilon_{it} + (u_t - u_{t-\Delta}) - \sum_{k=1}^K \tilde{b}_{ik} \tilde{f}^\epsilon_{kt} - \sum_{k=1}^K \tilde{b}^\epsilon_{ik} \tilde{f}_{kt} - \sum_{k=1}^K \tilde{b}^\epsilon_{ik} \tilde{f}^\epsilon_{kt} - \tfrac{1}{p} \sum_{k=1}^K \sum_{l=1}^K \tilde{b}_{ik} W_l' c(g_t - g_{t-\Delta}) - \tfrac{1}{p} \sum_{k=1}^K \sum_{l=1}^K \tilde{b}^\epsilon_{ik} W_l' c(g_t - g_{t-\Delta})$$

where $\tilde{f}^\epsilon_{kt}$ and $\tilde{b}^\epsilon_{ik}$ denote the estimation errors in the estimation of $\tilde{f}_{kt} + \frac{1}{p} \sum_{k=1}^K W_k' c(g_t - g_{t-\Delta})$ and $\tilde{b}_{ik}$, respectively. Since $\tilde{f}^\epsilon_{kt} = O_p(p^{-1/2})$ and $\tilde{b}^\epsilon_{ik} = O_p(n^{-1/4})$, let's assume that n and p are both sufficiently large such that $\sum_{k=1}^K \tilde{b}_{ik} \tilde{f}^\epsilon_{kt}$, $\sum_{k=1}^K \tilde{b}^\epsilon_{ik} \tilde{f}_{kt}$, $\sum_{k=1}^K \tilde{b}^\epsilon_{ik} \tilde{f}^\epsilon_{kt}$ and $\frac{1}{p} \sum_{k=1}^K \sum_{l=1}^K \tilde{b}^\epsilon_{ik} W_l' c(g_t - g_{t-\Delta})$ can be neglected. Then,

$$\hat{\epsilon}_{it} \approx \epsilon_{it} + (u_t - u_{t-\Delta}) - \tfrac{1}{p}\textstyle\sum_{k=1}^{K}\sum_{l=1}^{K}\tilde{b}_{ik}W_l'c(g_t - g_{t-\Delta}),$$

it follows that $\hat{\epsilon}_{it}$ equals the idiosyncratic component ϵ_{it} contaminated with microstruture noise. Thus, $\int_0^1 \sigma^2_{\varepsilon iu}du$ may be consistently estimated by,

$$\int_0^1 \widehat{\sigma^2_{\varepsilon iu}du} = PRV(\hat{\epsilon}_i). \tag{2.15}$$

Putting the pieces together

Our covolatility matrix estimator is defined by plugging the different estimators discussed above into the expression for $\widehat{\Sigma}$ in equation (2.10),

$$\begin{aligned}
\widehat{\Sigma} &= \begin{pmatrix} \hat{b}_{11} & \cdots & \hat{b}_{1K} \\ \vdots & & \vdots \\ \hat{b}_{p1} & \cdots & \hat{b}_{p1} \end{pmatrix} \begin{pmatrix} \int_0^1 \widehat{\sigma^2_{f1u}du} & & \\ & \ddots & \\ & & \int_0^1 \widehat{\sigma^2_{fKu}du} \end{pmatrix} \begin{pmatrix} \hat{b}_{11} & \cdots & \hat{b}_{p1} \\ \vdots & & \vdots \\ \hat{b}_{1K} & \cdots & \hat{b}_{pK} \end{pmatrix} \\
&\quad + \begin{pmatrix} \int_0^1 \widehat{\sigma^2_{\varepsilon 1u}du} & & \\ & \ddots & \\ & & \int_0^1 \widehat{\sigma^2_{\varepsilon pu}du} \end{pmatrix} \\
&= \begin{pmatrix} \frac{MRC(r_1,\hat{f}_1)}{PRV(\hat{f}_1)} & \cdots & \frac{MRC(r_1,\hat{f}_K)}{PRV(\hat{f}_K)} \\ \vdots & & \vdots \\ \frac{MRC(r_p,\hat{f}_1)}{PRV(\hat{f}_1)} & \cdots & \frac{MRC(r_p,\hat{f}_K)}{PRV(\hat{f}_K)} \end{pmatrix} \begin{pmatrix} PRV(\hat{f}_1) & & \\ & \ddots & \\ & & PRV(\hat{f}_K) \end{pmatrix} \\
&\quad \begin{pmatrix} \frac{MRC(r_1,\hat{f}_1)}{PRV(\hat{f}_1)} & \cdots & \frac{MRC(r_p,\hat{f}_1)}{PRV(\hat{f}_1)} \\ \vdots & & \vdots \\ \frac{MRC(r_1,\hat{f}_K)}{PRV(\hat{f}_K)} & \cdots & \frac{MRC(r_p,\hat{f}_K)}{PRV(\hat{f}_K)} \end{pmatrix} + \begin{pmatrix} PRV(\hat{\epsilon}_1) & & \\ & \ddots & \\ & & PRV(\hat{\epsilon}_p) \end{pmatrix}.
\end{aligned}$$

Or, more succinctly,

$$\widehat{\Sigma}_{ij} = \sum_{k=1}^{K} \frac{MRC(r_i,\hat{f}_k).MRC(r_j,\hat{f}_k)}{PRV(\hat{f}_k)}; \qquad \widehat{\Sigma}_{ii} = \sum_{k=1}^{K} \frac{MRC(r_i,\hat{f}_k)^2}{PRV(\hat{f}_k)} + PRV(\hat{\epsilon}_i), \tag{2.16}$$

for $i, j = 1, ..., p$[14].

[14] Due to the factor structure of our estimator $\widehat{\Sigma} = \hat{b}\widehat{\Sigma}_f\hat{b}' + \widehat{\Sigma}_\varepsilon$ and since $\widehat{\Sigma}_f$ and $\widehat{\Sigma}_\varepsilon$ are diagonal matrices with positive elements, the positive semi-definiteness is guarantee. It can be easily shown that: $\forall X,\ X'\widehat{\Sigma}X \geq 0$.

Remark: Our estimator is constructed using the pre-averaging estimator PRV and the modulated realized covariance estimator MRC. Since those two estimators have been adapted to account for serially correlated microstructure noises (see, e.g., Jacod, Li, Mykland, Podolskijc, and Vetter (2009a) and Hautsch and Podolskij (2013)), our estimator can easily be adapted into this specific setting. Our setup can also be easily adapted to account for semi-martingale processes with jumps. Tools used in this paper for the estimation strategy ($MRKer$, MRC and PRV) have extensions to the case of semi-martingale processes with jumps. Additionally, as in Pelger (2016), the model can also be split into two sub-models: i) a factor representation for small movement of returns; ii) and a factor representation for big movements using a threshold to identify jumps. Only the first model can be used for the estimation of integrated volatility. Moreover, our model can be extended to the approximate factor model. In that case, factors will be extracted using the procedure in Bai and Ng (2002); loadings and idiosyncratic terms will be estimated using the same procedure as in section 2. Additional parameters to estimate will be covolatility between idiosyncratic terms, and this will be handled using $MRC(\hat{\varepsilon}_i, \hat{\varepsilon}_j)$.

2.3 Comparing different estimators

2.3.1 Convergence rates

Our new estimator defined in (2.16) consistently estimates Σ for $\Delta \to 0$ and $p \to \infty$. It is instructive to more formally assess how the values of $n = 1/\Delta$ and p impact the estimation errors. The following lemma provides the specific convergence rates for the integrated volatilities, the loadings of the rotated factors, and the integrated covolatility matrix of the idiosyncratic errors, where $\|.\|_F$ denotes the Frobenius norm.[15]

Lemma 2.3.1 *Under Assumptions 1-2, for $n \to \infty$ and $p \to \infty$:*

- $\left|\hat{\Sigma}^{\tilde{f}}_{kk} - \Sigma^{\tilde{f}}_{kk}\right| = O_p\left(n^{-1/4}\right)$.
- $\left\|\hat{b}_k - b_k\right\|_F = \left\|\hat{b}_k - b_k\right\|_2 = O_p\left(p^{1/2}n^{-1/4}\right)$.
- $\left\|\hat{\Sigma}^{\epsilon} - \Sigma^{\epsilon}\right\|_F = O_p(p^{1/2}n^{-1/4})$.

[15] The Frobenius norm for the matrix $A = (a_{ij})_{1\leq i,j\leq p}$ is formally defined by $\|A\|_F = \sqrt{\sum_{i=1}^{p}\sum_{j=1}^{p}|a_{ij}|^2}$.

Proof: See Appendix 2.6.

Appropriately combining these convergence rates for the individual components, it is possible to deduce the overall rate of convergence of $\hat{\Sigma}$. In order to compare this rate to other competing large dimensional realized covolatility estimators, the following Theorem provides the convergence rate for $\hat{\Sigma}$ along with the rates for the adjusted modulated realized covariance estimator MRC^{δ} of Christensen, Kinnebrock, and Podolskij (2010a), the multidimensional kernel estimator $MRker$ of Barndorff-Nielsen, Hansen, Lunde, and Shephard (2011a), and the composite realized kernel $\hat{\Sigma}_{comp}$ of Lunde, Shephard, and Sheppard (2016).

Theorem 2.3.1 *Under Asumptions 1-2, for $n \to \infty$ and $p \to \infty$:*

- $\left\|\hat{\Sigma} - \Sigma\right\|_F = O_p(pn^{-1/4})$.
- $\left\|MRC^{\delta} - \Sigma\right\|_F = O_p(pn^{-1/5})$.
- $\left\|MRker - \Sigma\right\|_F = O_p(pn^{-1/5})$.
- $\left\|\hat{\Sigma}_{comp} - \Sigma\right\|_F = O_p(\sqrt{p(p-1)}n^{-1/5})$.

Proof: See Appendix 2.6.

The results in Theorem 2.3.1 suggest that under the Frobenius norm, the dimensionality of the covolatility matrix reduces the speed of convergence for the new $\hat{\Sigma}$ estimator by an order of p. Of course, this is also the case for all of the other estimators. Meanwhile, the speed of convergence of $\hat{\Sigma}$ exceeds that of MRC^{δ}, $MRker$ or $\hat{\Sigma}_{comp}$.

The next theorem derives the convergence rate of $\hat{\Sigma}^{-1}$.

Theorem 2.3.2 *Under Asumptions 1-2, for $n \to \infty$ and $p \to \infty$:*

$$\left\|\hat{\Sigma}^{-1} - \Sigma^{-1}\right\|_F = O_p(p^2 n^{-1/4})$$

Proof: See Appendix 2.6.

The simulation results discussed in the next section confirm that this superior asymptotic performance carries over to empirically realistic finite-sample settings.

2.3.2 Finite-sample simulations: synchronous prices

We simulate artificial high-frequency prices from a K-factor(s) continuous-time stochastic volatility model in which the actually observed prices are contaminated by noise. While K is allowed to vary from 1 to 5, we only report in this section results for the case $K = 2$. Others simulation results are provided in the appendix. We add as competitors, two PCA-based estimators of the covolatility matrix, namely: the *POET* estimator of Fan, Liao, and Mincheva (2013) and the PCA-based estimator of Dai, Lu, and Xiu (2017)(Henceforth, *PCA-PRV*). Specific details concerning the simulation design are provided in Appendix 2.10.

We begin by simulating frictionless price vectors of length $p = 50$, $p = 100$, $p = 300$ and $p = 500$ based on the true covolatility matrix Σ. We then generate noisy prices by adding market microstructure noise to the vectors of frictionless prices. Each path of the noisy price vector is comprised of $n+1$ observations. We start by assuming that all of prices are synchronously recorded, with one observation every five minutes and a trading day of 6.5 hours, resulting in 79 prices per day.[16] We also have simulation results for others sampling frequencies such as: one observation every minute and one observation every 30 seconds (cf. appendix). We consider three different levels of noise in the simulation setup, corresponding to three values of the signal-to-noise ratio parameter ξ^2: 0.001, 0.005, and 0.01. Due to a space constraint, we only report the results for $K = 2$, $\xi^2 = 0.005$ and 79 prices per day. Results of others cases are reported in appendix.

We evaluate the performance of the same four estimators of Σ analyzed in Theorem 2.3.1 by computing the errors relative to the true integrated covolatility matrix (columns labeled *Covariance* in the tables), the integrated correlation matrix (columns labeled *Correlation*), and the inverse of the integrated covariance matrix (columns labeled *Inverse*). We rely on the scaled Frobenius norm for assessing the difference between the estimates and the true matrices.[17]

Tables 2.1 presents the average values based on $1,000$ Monte Carlo replications, with the standard errors across the simulations reported in parentheses. The new $\hat{\Sigma}$ estimator systematically outperforms all of the five alternative estimators $\hat{\Sigma}_{comp}$, $MRker$, MRC^{δ}, $PCA{-}PRV$ and $POET$, in terms of most accurately estimating the true covolatility matrix. This holds

[16] This closely mirrors Lunde, Shephard, and Sheppard (2016), who report around 100 observations on average per day after the synchronization of 473 liquid stocks.

[17] The scaled Frobenius norm is defined by diving the usual Frobenius norm with $\sqrt{p}$. As discussed in Hautsch, Kyj, and Oomen (2012), this scaling allows for a more meaningful comparison across different values of p.

Table 2.1. Covolatility estimators, synchronous prices

Signal-to-Noise ratio $\xi^2 = 0.005$, $K = 2$					
Number of assets: N=50					
	Covariance	Correlation	Inverse	Diag	Off-Diag
$\hat{\Sigma}$	2.492	1.299	4.567	21.09	377.687
	(0.729)	*(0.316)*	*(0.360)*		
MRker	2.645	1.472	5667	23.88	412.6
	(0.714)	*(0.170)*	*(93231)*		
MRC^{δ}	2.607	1.499	1050	22.09	385.3
	(0.605)	*(0.170)*	*(4936)*		
$\hat{\Sigma}_{comp}$	2.625	1.431	4.120	40.92	392.6
	(0.733)	*(0.172)*	*(0.694)*		
$PCA-PRV$	2.587	1.454	7.164	22.09	383.3
	(0.623)	*(0.173)*	*(10.32)*		
$POET$	5.663	2.922	402.6	209.0	1449
	(0.382)	*(0.229)*	*(22.68)*		
Number of assets: N=100					
	Covariance	Correlation	Inverse	Diag	Off-Diag
$\hat{\Sigma}$	3.554	1.792	4.734	41.93	1500
	(1.261)	*(0.394)*	*(27.54)*		
MRker	3.865	2.124	NA	41.63	1701
	(0.927)	*(0.238)*	*NA*		
MRC^{δ}	3.811	2.161	NA	39.152	1589.271
	(0.771)	*(0.229)*	*NA*		
$\hat{\Sigma}_{comp}$	3.809	2.061	5.008	63.44	1639
	(0.942)	*(0.242)*	*(0.833)*		
$PCA-PRV$	3.732	2.067	6.038	39.15	1536
	(0.800)	*(0.236)*	*(10.29)*		
$POET$	7.653	4.371	596.0	364.6	5648
	(0.516)	*(0.334)*	*(130.2)*		
Number of assets: N=300					
	Covariance	Correlation	Inverse	Diag	Off-Diag
$\hat{\Sigma}$	5.642	3.035	9.304	137.048	12669.290
	(2.120)	*(0.724)*	*(0.247)*		
MRker	6.313	3.707	NA	110.6	13623
	(1.546)	*(0.413)*	*NA*		
MRC^{δ}	6.204	3.761	NA	102.1	12685
	(1.250)	*(0.398)*	*NA*		
$\hat{\Sigma}_{comp}$	6.251	3.649	6.821	146.0	13365
	(1.557)	*(0.417)*	*(1.260)*		
$PCA-PRV$	5.991	3.508	5.586	102.123	11884
	(1.300)	*(0.415)*	*(1.877)*		
$POET$	12.17	7.681	NA	981.0	44653
	(0.853)	*(0.559)*	*NA*		
Number of assets: N=500					
	Covariance	Correlation	Inverse	Diag	Off-Diag
$\hat{\Sigma}$	6.940	3.856	14.87	218.2	31870
	(2.678)	*(0.824)*	*(61.76)*		
MRker	7.937	4.765	NA	174.6	36191
	(1.905)	*(0.490)*	*NA*		
MRC^{δ}	7.915	4.871	NA	165.1	33994
	(1.417)	*(0.471)*	*NA*		
$\hat{\Sigma}_{comp}$	7.878	4.716	18.82	221.2	35703
	(1.911)	*(0.494)*	*(1.960)*		
$PCA-PRV$	7.598	4.601	15.68	165.1	31669
	(1.471)	*(0.477)*	*(11.87)*		
$POET$	14.94	10.08	NA	1498	111142
	(0.977)	*(0.717)*	*NA*		

true across all of the different noise levels and the two values of p. As a whole, the estimation errors systematically increase with the dimensionality of the matrix and the magnitude of the market microstructure noise. These results, of course, are consistent with the theoretical predictions from Theorem 2.3.1. Looking at columns five and six, which report the separate (unscaled) norms for estimating the diagonal and the off-diagonal elements in Σ, it does not appear that the more accurate estimates afforded by the new $\hat{\Sigma}$ estimator come solely from one or the other. Interestingly, the $\hat{\Sigma}_{comp}$ estimator of Lunde, Shephard, and Sheppard (2016) appears to perform especially poorly for estimating the diagonal variance elements.

This superior performance of the $\hat{\Sigma}$ estimator carries over to the estimation of the correlation matrix implied by the true covolatility matrix. It also holds true for estimating Σ^{-1} for low noise levels. However, $\hat{\Sigma}_{comp}^{-1}$ performs slightly better than $\hat{\Sigma}^{-1}$ for estimating Σ^{-1} for higher levels of market microstructure noise. Also, whereas $\hat{\Sigma}_{comp}$ and $\hat{\Sigma}$ are both guaranteed to be positive semi-definite, the inverse of both $MRker$ and MRC^{δ} fails to exist when $p > n$, and $MRker^{-1}$ and $\left(MRC^{\delta}\right)^{-1}$ generally also perform very poorly for estimating the inverse when $p = 50$ and close to $n = 78$.

Remark: We checked the good finite sample properties of our estimator under correlated microstructure noise. In this specific case, the higher order dependence is considering by assuming that factors in microstructure noise are the sum of an *iid* process and an *AR(1)* as in Aït-Sahalia, Mykland, and Zhang (2011). Table 2.10 provides such simulation results.

2.3.3 Finite-sample simulations: asynchronous prices

The simulation results discussed above were based on synchronous prices. This section evaluates the performance of the same four estimators in the more realistic situation when the prices for different assets are not necessarily recorded at the same time and therefore first have to be synchronized.[18]

To accommodate this feature within the simulations, we augment the previously discussed two factor setup by dividing the assets into three separate groups of differing observation frequencies. For assets in the first group, an observation is available on average every 30 seconds, in the second group every 90 seconds, and in the final third group every 150 seconds. All of the observation times for each of the individual assets within each of the three groups

[18]This issue is especially acute for the $MRker$ and MRC^{δ} estimators, which require that the synchronization process is applied to full p-dimensional price vector. By comparison, the computation of $\widehat{\Sigma}$ only needs for the prices to be synchronized on a pairwise basis, in turn resulting less of a loss of observations.

Table 2.2. Covolatility estimators, asynchronous prices

	Covariance	Correlation	Inverse	Diag	Off-Diag
Signal-to-Noise ratio $\xi^2 = 0.01$, $K = 2$					
Number of assets: N=50					
	Covariance	Correlation	Inverse	Diag	Off-Diag
$\hat{\Sigma}$	4.914	2.374	3.788	49.88	1182.1
	(0.470)	*(0.173)*	*(7.871)*		
MRker	5.207	2.732	4960.934	44.54	1332
	(0.515)	*(0.205)*	*(13222)*		
MRC^{δ}	5.180	2.689	1594	43.08	1316
	(0.497)	*(0.200)*	*(6580)*		
$\hat{\Sigma}_{comp}$	5.047	2.646	4.430	42.70	1271
	(0.482)	*(0.179)*	*(0.258)*		
$PCA-PRV$	5.155	2.617	7.187	43.08	1292
	(0.498)	*(0.206)*	*(10.49)*		
$POET$	6.233	3.312	385.8	168.5	1841
	(0.512)	*(0.189)*	*(415.6)*		
Number of assets: N=100					
	Covariance	Correlation	Inverse	Diag	Off-Diag
$\hat{\Sigma}$	5.430	3.141	4.041	94.92	2878
	(0.438)	*(0.209)*	*(12.03)*		
MRker	5.768	3.702	NA	71.747	3294.052
	(0.411)	*(0.182)*	*NA*		
MRC^{δ}	5.757	3.655	NA	66.73	3283
	(0.410)	*(0.178)*	*NA*		
$\hat{\Sigma}_{comp}$	5.619	3.565	4.622	60.35	3155
	(0.403)	*(0.153)*	*(0.325)*		
$PCA-PRV$	5.657	3.485	8.110	66.73	3150
	(0.422)	*(0.203)*	*(41.32)*		
$POET$	6.306	4.386	319.9	248.7	3834
	(0.428)	*(0.176)*	*(4848)*		
Number of assets: N=300					
	Covariance	Correlation	Inverse	Diag	Off-Diag
$\hat{\Sigma}$	10.35	5.426	7.315	473.2	32356
	(0.825)	*(0.327)*	*(30.27)*		
MRker	11.15	6.595	NA	295.0	37950
	(0.809)	*(0.307)*	*NA*		
MRC^{δ}	11.11	6.493	NA	281.7	37699
	(0.797)	*(0.353)*	*NA*		
$\hat{\Sigma}_{comp}$	10.97	6.126	8.568	512.4	36548
	(0.912)	*(0.374)*	*(3.578)*		
$PCA-PRV$	10.87	6.094	8.225	281.7	35987
	(0.811)	*(0.346)*	*(8.580)*		
$POET$	12.57	7.468	NA	1000	46936
	(0.892)	*(0.321)*	*NA*		
Number of assets: N=500					
	Covariance	Correlation	Inverse	Diag	Off-Diag
$\hat{\Sigma}$	12.46	6.842	9.780	357.2	78228
	(1.554)	*(0.351)*	*(80.61)*		
MRker	13.61	8.443	NA	416.6	93282
	(0.923)	*(0.335)*	*NA*		
MRC^{δ}	13.58	8.265	NA	396.6	92472
	(0.914)	*(0.381)*	*NA*		
$\hat{\Sigma}_{comp}$	13.45	8.159	10.854	754.2	89258
	(0.932)	*(0.298)*	*(5.365)*		
$PCA-PRV$	13.22	7.742	8.570	396.6	87690
	(0.930)	*(0.372)*	*(10.67)*		
$POET$	15.096	9.419	NA	1461	114468
	(1.039)	*(0.398)*	*NA*		

are drawn from Poisson distributions.

The results from these augmented simulations are reported in Table 2.2. To conserve space we only report the results for the case corresponding to $\xi^2 = 0.01$. As expected, all of the estimators perform worse in an absolute sense compared to the situation with synchronously observed prices in Table 2.1[19]. However, the relative performance of the different estimators is entirely in line with the previously discussed results in Table 2.2, underscoring the superior overall performance of the new $\widehat{\Sigma}$ estimator. The empirical application discussed in the next section also further corroborates this.

2.4 Empirical application

Our empirical application is based on a large cross-section of individual stocks. It closely follows Lunde, Shephard, and Sheppard (2016) in assessing the performance of the different covolatility estimators by comparing the resulting risk minimizing portfolios.

2.4.1 Data

We rely on intraday data from the TAQ database. Our original sample is comprised of all of the stocks included in the S&P 500 during the period spanning January 2007 to December 2011. Following Lunde, Shephard, and Sheppard (2016), we remove stocks that trade less than 195 times during a given day. We further clean the data following the procedures advocated in Barndorff-Nielsen, Hansen, Lunde, and Shephard (2011a). All-in-all, this leaves us with a total of 384 stocks.

2.4.2 Risk minimization

Our comparison of the different covolatility estimators rely on their ability to minimize portfolio risks. Specifically, let $\hat{\Omega}_t$ denote a covolatilty estimate for day t. We will assume that $\hat{\Omega}_t$ follows a random walk, and use it as the forecast for the day $t+1$ covolatility matrix.

[19] The estimation error increases when incorporating the asynchronous sampling times because of the loss of data during the synchronization process. The error size is still acceptable. The consistency of $\hat{\Sigma}$ is the consequence of the consistency of MRC under asynchronous sampling times. Theoretical assumptions about the irregularity and asynchronicity of the sampling times are the same than in Christensen, Kinnebrock, and Podolskij (2010a).

Correspondingly, the portfolio weights $\hat{w}_{t+1}$ that minimize the day $t+1$ risk, subject to a cross exposure constraint, may be found by solving:

$$\begin{cases} Min \quad w_{t+1}^{'}\hat{\Omega}_t w_{t+1} \\ s.t. \quad w_{t+1}^{'}1 = 1 \quad and \quad \sum_{i=1}^{p}|w_{i,t+1}| \leq 1+2s. \end{cases} \tag{2.17}$$

The gross exposure parameter s represents the share of the stocks in the portfolio that can be held short.[20] Setting $s = 0$ restricts the portfolio to long positions only, while higher values of s allow for increasingly larger short positions. We will consider values of s ranging from 0 to 1. The gross exposure constraint also ensures that the optimization problem has a unique solution, even if $\hat{\Omega}_t$ is not positive semi-definite.[21] It also serves to moderate the impact of estimation errors in the covolatility matrices used in place of $\hat{\Omega}_t$ more generally (see, e.g., the discussion Fan, Li, and Yu (2012)).

We evaluate the performance of the different covolatility estimators, by calculating,

$$\hat{w}_{t+1}^{'}RCov_{t+1}\hat{w}_{t+1} \tag{2.18}$$

where $RCov_{t+1}$ denotes the day $t+1$ realized covariance matrix constructed from five-minute returns. This approach closely mirrors that of Lunde, Shephard, and Sheppard (2016). In addition to the results for the four specific covolatility estimators discussed above, we also report the results for a naive equally weighted portfolio $\hat{w}_{t+1} = \frac{1}{p}I_p$, as recently advocated by DeMiguel, Garlappi, and Uppal (2009).

Consistent with the simulation results for the asynchronous price series discussion above, we rely the refresh-time sampling approach of Barndorff-Nielsen, Hansen, Lunde, and Shephard (2011a) to synchronize the data used in the actual implementation of the estimators.[22] The practical implementation of the new $\widehat{\Sigma}$ estimator further requires a choice for the number of systematic risk factors, K. We use the information criteria IC advocated by Bai and Ng

[20] The classical Markowitz portfolio problem corresponds to $s = \infty$.

[21] This is especially useful for the $MRker$ and MRC^{δ} estimators, which are not guaranteed to be positive semi-definite.

[22] Applying the synchronization to all of the stocks results in an average of 104.4 intraday observations.

(2002) for choosing the value of K that minimizes[23],

$$IC = log\left[\frac{1}{p}\sum_{j=1}^{\lfloor 1/\Delta \rfloor}(r^*_{j\Delta} - bf_{j\Delta})'(r^*_{j\Delta} - bf_{j\Delta})\right] + K \times g(p, \lfloor 1/\Delta \rfloor), \tag{2.19}$$

with the penalty function define by $g(p, \lfloor 1/\Delta \rfloor) = \frac{p+\lfloor 1/\Delta \rfloor}{p\lfloor 1/\Delta \rfloor} \times log\left[\frac{p\lfloor 1/\Delta \rfloor}{p+\lfloor 1/\Delta \rfloor}\right]$. In order to reduce the impact of market microstructure noise, IC is applied in the dataset sampled at the 5-minutes frequency. The number of factors chosen by this criteria range between one and four for each of the different days, with an average value of 3.277 over the full sample.

Table 2.3. Minimum variance portfolios

	s=0	s=0.01	s=0.05	s=0.1	s=0.15	s=0.20	s=0.25	s=0.5	s=1
$\hat{\Sigma}$	0.334	0.298	0.287	0.261	0.256	0.252	0.245	0.24	0.241
$\hat{\Sigma}_{comp}$	0.409	0.343	0.31	0.32	0.308	0.303	0.301	0.325	0.326
MRker	0.399	0.351	0.335	0.313	0.305	0.302	0.278	0.263	0.258
MRC^{δ}	0.412	0.368	0.352	0.334	0.331	0.323	0.362	0.343	0.319
EqualWeight	0.636	0.636	0.636	0.636	0.636	0.636	0.636	0.636	0.636
$PCA-PRV$	0.395	0.355	0.339	0.318	0.31	0.302	0.319	0.317	0.327
$POET$	0.401	0.338	0.311	0.287	0.277	0.266	0.289	0.278	0.286

Looking across the different rows of the table 2.3, the portfolios constructed based on the new $\hat{\Sigma}$ estimator systematically result in the lowest ex-post variation. This dominance holds true for all of the different values of the gross exposure constraint s. Meanwhile, the portfolios that rule out short positions reported in the first column ($s = 0$) unambiguously perform the worst. The differences observed across the other values of s are generally small and not always monotonic. All of the realized volatility-based portfolios also convincingly beat the $\frac{1}{p}$ naively diversified portfolios. In contrast to the simulation-based comparisons discussed above, where the $\hat{\Sigma}_{comp}$ systematically outperformed $MRker$ and MRC^{δ} that is not the case here.

[23]Since the number of stocks p and the intraday observations n diverge, we implement the Bai and Ng (2002) estimator of K using intraday observations sampled at 5 minutes frequency. There is an underlining assumption that the number of factors is asymptotically bounded by a fix positive number $kmax$.

2.5 Conclusion

We provide a new realized covolatility estimator that is guaranteed to be positive semi-definite in large dimensions and also works in the presence of market microstructure noise. The estimator relies on two separate factor structures: one of order $O_p(\sqrt{\Delta})$ for describing the cross-sectional variation in the systematic risks, and another of order $O_p(1)$ for describing the noise. The practical implementation of the estimator relies on traditional factor analysis together with already existing procedures for consistently and robustly estimating the different components of the covolatility matrix.

The convergence rate of the new estimator compares favorably to other recently developed procedures, including the adjusted modulated realized covariance estimator MRC^{δ} of Christensen, Kinnebrock, and Podolskij (2010a), the multivariate kernel estimator $MRker$ of Barndorff-Nielsen, Hansen, Lunde, and Shephard (2011a), and the composite realized kernel $\hat{\Sigma}_{comp}$ of Lunde, Shephard, and Sheppard (2016). Simulations confirm that the theoretical results derived under the assumption of synchronous prices observed over increasingly finer time intervals carry over to empirically realistic settings with a finite number of asynchronous intraday observations. Applying the new estimator in the construction of ex-ante minimum variance portfolios from a set comprised of several hundred individual equities also produces the lowest ex-post variation among other competing covolatility estimators.

Appendix

2.6 Technical proofs

Proof of Lemma 2.2.1

The proof proceeds by establishing that $\frac{1}{p}S\hat{W}'bf_t \xrightarrow{p} f_t$ and $\frac{1}{p}S\hat{W}'\epsilon_t \xrightarrow{p} 0$.

A) Proof of: $\frac{1}{p}S\hat{W}'bf_t \xrightarrow{p} f_t$

This proof consists on 12 steps inspired from the paper of Stock and Watson (2002).

Step 1: $\frac{1}{p}\sum_{i=1}^{p}\epsilon_{it}^2 \sim O_p(1)$

We assume that:

- *A1)* $\underset{p\longrightarrow\infty}{lim}\ \underset{t}{Sup}\,\frac{1}{p}\sum_{i=1}^{p}\sum_{j=1}^{p}|E(\epsilon_{it}\epsilon_{jt})| < \infty$;
- *A2)* $\underset{p\longrightarrow\infty}{lim}\ \underset{t,s}{Sup}\,\frac{1}{p}\sum_{i=1}^{p}\sum_{j=1}^{p}|Cov(\epsilon_{is}\epsilon_{it},\epsilon_{js}\epsilon_{jt})| < \infty$

Since

$$\frac{1}{p}\sum_{i=1}^{p}\epsilon_{it}^2 = \frac{1}{p}\sum_{i=1}^{p}E\left[\epsilon_{it}^2\right] + \frac{1}{p}\sum_{i=1}^{p}\left[\epsilon_{it}^2 - E\left(\epsilon_{it}^2\right)\right]$$

we just need to prove that

$$\frac{1}{p}\sum_{i=1}^{p}E\left[\epsilon_{it}^2\right] \sim O(1) \text{ and } \frac{1}{p}\sum_{i=1}^{p}\left[\epsilon_{it}^2 - E\left(\epsilon_{it}^2\right)\right] \sim o_p(1)$$

The following inequalities hold:

$$\frac{1}{p}\sum_{i=1}^{p}E\left[\epsilon_{it}^2\right] \leq \frac{1}{p}\sum_{i=1}^{p}\sum_{j=1}^{p}|E(\epsilon_{it}\epsilon_{jt})| \leq \underset{t}{Sup}\,\frac{1}{p}\sum_{i=1}^{p}\sum_{j=1}^{p}|E(\epsilon_{it}\epsilon_{jt})|$$

Since $\underset{t}{Sup}\,\frac{1}{p}\sum_{i=1}^{p}\sum_{j=1}^{p}|E(\epsilon_{it}\epsilon_{jt})|$ converges, it is bounded. Thus $\frac{1}{p}\sum_{i=1}^{p}E\left[\epsilon_{it}^2\right]$ is bounded, it means $O(1)$. In addition

$$\begin{aligned} E\left[\left(\frac{1}{p}\sum_{i=1}^{p}\left[\epsilon_{it}^2 - E\left(\epsilon_{it}^2\right)\right]\right)^2\right] &= \frac{1}{p^2}\sum_{i=1}^{p}\sum_{j=1}^{p}E\left[(\epsilon_{it}^2 - E(\epsilon_{it}^2))(\epsilon_{jt}^2 - E(\epsilon_{jt}^2))\right] \\ &= \frac{1}{p^2}\sum_{i=1}^{p}\sum_{j=1}^{p}Cov\left(\epsilon_{it}^2,\epsilon_{jt}^2\right) \\ &\leq \frac{1}{p^2}\sum_{i=1}^{p}\sum_{j=1}^{p}\left|Cov\left(\epsilon_{it}^2,\epsilon_{jt}^2\right)\right| \\ &\leq \underset{t,s}{Sup}\,\frac{1}{p^2}\sum_{i=1}^{p}\sum_{j=1}^{p}\left|Cov\left(\epsilon_{it}\epsilon_{is},\epsilon_{jt}\epsilon_{js}\right)\right| \end{aligned}$$

Since $\underset{t,s}{Sup}\,\frac{1}{p}\sum_{i=1}^{p}\sum_{j=1}^{p}\left|Cov\left(\epsilon_{it}\epsilon_{is},\epsilon_{jt}\epsilon_{js}\right)\right|$ is bounded, it follows that

$$\underset{t,s}{Sup}\,\frac{1}{p^2}\sum_{i=1}^{p}\sum_{j=1}^{p}\left|Cov\left(\epsilon_{it}\epsilon_{is},\epsilon_{jt}\epsilon_{js}\right)\right|\longrightarrow 0$$

We deduce that $\frac{1}{p}\sum_{i=1}^{p}\left[\epsilon_{it}^2-E\left(\epsilon_{it}^2\right)\right]$ converges in $2-mean$ to 0. Hence

$$\frac{1}{p}\sum_{i=1}^{p}\left[\epsilon_{it}^2-E\left(\epsilon_{it}^2\right)\right]\xrightarrow{p}0$$

Step 2: Let $\Gamma=\{\gamma\in\Re^p/\gamma'\gamma/p=1\}$. We want to prove that $\underset{\gamma\in\Gamma}{Sup}\,\frac{1}{p^2}\gamma' IV(\epsilon)\gamma\longrightarrow 0$ as $p\longrightarrow\infty$, with $IV(\epsilon)=Diag(IV(\epsilon_1),...,IV(\epsilon_p))$. We make the additional assumption that $\forall\quad i=1,...,p$, the quadratic variation of the idiosyncratic component ϵ_i is bounded by a scalar M. Thus, we can write

$$\begin{array}{rcl}
\frac{1}{p^2}\gamma' IV(\epsilon)\gamma & = & \frac{1}{p^2}\sum_{i=1}^{p}\gamma_i^2.IV(\epsilon_i)\\
& \leq & \left[\frac{1}{p^2}\sum_{i=1}^{p}\gamma_i^4\right]^{1/2}\left[\frac{1}{p^2}\sum_{i=1}^{p}IV(\epsilon_i)^2\right]^{1/2}\\
& \leq & \left[\frac{1}{p^2}\left(\sum_{i=1}^{p}\gamma_i^2\right)^2\right]^{1/2}\left[\frac{1}{p^2}\sum_{i=1}^{p}IV(\epsilon_i)^2\right]^{1/2}\\
& \leq & \left(\frac{1}{p}\gamma'\gamma\right).\left[\frac{1}{p^2}\sum_{i=1}^{p}IV(\epsilon_i)^2\right]^{1/2}\\
& \leq & \left[\frac{1}{p^2}\sum_{i=1}^{p}IV(\epsilon_i)^2\right]^{1/2}\\
& \leq & \left(\frac{M^2}{p}\right)^{1/2}
\end{array}$$

We deduce that $\underset{\gamma\in\Gamma}{Sup}\,\frac{1}{p^2}\gamma' IV(\epsilon)\gamma\longrightarrow 0$ as $p\longrightarrow\infty$.

Step 3: If $\int_0^1 E(q_t^2)dt\sim O(1)$ then $\underset{\gamma\in\Gamma}{Sup}\left|\frac{1}{p}\int_0^1 E(q_t.\gamma'\epsilon_t)dt\right|\longrightarrow 0$ as $p\longrightarrow\infty$

$$\begin{array}{rcl}
\frac{1}{p}\int_0^1 E(q_t.\gamma'\epsilon_t)dt & \leq & \int_0^1\left[E(q_t^2)\right]^{1/2}\left[E\left(\left(\frac{1}{p}\gamma'\epsilon_t\right)^2\right)\right]^{1/2}dt\\
& \leq & \left[\int_0^1 E(q_t^2)dt\right]^{1/2}.\left[\int_0^1 E\left(\left(\frac{1}{p}\gamma'\epsilon_t\right)^2\right)dt\right]^{1/2}\\
& \leq & O(1).\left[\frac{1}{p^2}\int_0^1\gamma' E(\epsilon_t\epsilon_t^{'})\gamma dt\right]^{1/2}\\
& \leq & O(1).\left[\frac{1}{p^2}\gamma' IV(\epsilon)\gamma\right]^{1/2}
\end{array}$$

The first inequality comes from the Cauchy-Schwarz inequality and the second from the Holder inequality. From the last inequality, the result is deduced using the *step 2*.

Step 4: $\underset{\gamma\in\Gamma}{Sup}\left|\frac{1}{p}\int_0^1 E(f_{kt}.\gamma'\epsilon_t)dt\right|\longrightarrow 0$ as $p\longrightarrow 0$, $\forall k=1,...,K$

This result is obtained from the *step 3* by taking $q_t=f_{kt}$. Indeed, $\int_0^1 E(f_{kt}^2)dt=IV(f_k)<\infty$ by assumption.

Step 5: Assume that *A3)* $\frac{b'b}{p} \longrightarrow I_K$ as $p \longrightarrow 0$. Then $\underset{\gamma\in\Gamma}{Sup}\,\frac{1}{p}\gamma' b\int_0^1 E(f_t.\gamma'\epsilon_t)dt \longrightarrow 0$ as $p \longrightarrow 0$

$$\begin{array}{rcl}
\frac{1}{p}\gamma' b\int_0^1 E(f_t.\gamma'\epsilon_t)dt & = & \sum_{k=1}^{K}\gamma'\frac{b_k}{p}.\int_0^1 E(f_{kt}.\frac{\gamma'}{p}\epsilon_t)dt \\
 & = & \sum_{k=1}^{K}\left(\gamma'\frac{b_k}{p}\right).\int_0^1 E\left(f_{kt}.\left(\frac{1}{p}\sum_{i=1}^{p}\gamma_i\epsilon_{it}\right)\right)dt \\
 & \leq & \sum_{k=1}^{K}\left|\gamma'\frac{b_k}{p}\right|.\left|\int_0^1 E\left(f_{kt}.\left(\frac{1}{p}\sum_{i=1}^{p}\gamma_i\epsilon_{it}\right)\right)dt\right| \\
\underset{\gamma\in\Gamma}{Sup}\,\frac{1}{p}\gamma' b\int_0^1 E(f_t.\gamma'\epsilon_t)dt & \leq & \left[\underset{k}{Max}\,\underset{\gamma\in\Gamma}{Sup}\left|\gamma'\frac{b_k}{p}\right|\right].\sum_{k=1}^{K}\underset{\gamma\in\Gamma}{Sup}\left|\int_0^1 E\left(f_{kt}.\left(\frac{1}{p}\sum_{i=1}^{p}\gamma_i\epsilon_{it}\right)\right)dt\right| \\
 & \leq & \left\{\underset{\gamma\in\Gamma}{Sup}\,(\gamma'\gamma/p)^{1/2}\right\}.\left\{\underset{k}{Max}\,(\underline{b}'_k\underline{b}_k/p)^{1/2}\right\} \\
 & & \times\sum_{k=1}^{K}\underset{\gamma\in\Gamma}{Sup}\left|\int_0^1 E\left(f_{kt}.\left(\frac{1}{p}\sum_{i=1}^{p}\gamma_i\epsilon_{it}\right)\right)dt\right|
\end{array}$$

From the definition of Γ and assumption *A3)*, as $p \longrightarrow \infty$,

$$\underset{\gamma\in\Gamma}{Sup}\,(\gamma'\gamma/p)^{1/2} \longrightarrow 1 \text{ and } \underset{k}{Max}\,(\underline{b}'_k\underline{b}_k/p)^{1/2} \longrightarrow 1$$

In addition, from *step 4*, as $p \longrightarrow \infty$,

$$\sum_{k=1}^{K}\underset{\gamma\in\Gamma}{Sup}\left|\int_0^1 E\left(f_{kt}.\left(\frac{1}{p}\sum_{i=1}^{p}\gamma_i\epsilon_{it}\right)\right)dt\right| \longrightarrow 0$$

Then $\underset{\gamma\in\Gamma}{Sup}\,\frac{1}{p}\gamma' b\int_0^1 E(f_t.\gamma'\epsilon_t)dt \longrightarrow 0$ as $p \longrightarrow \infty$.

Step 6: Define $\forall\gamma\in\Gamma$, $R(\gamma) = \frac{1}{p^2}\gamma'\Sigma\gamma$ and $R^*(\gamma) = \frac{1}{p^2}\gamma' b.IV(f).b'\gamma$.
Then $\underset{\gamma\in\Gamma}{Sup}\,|R(\gamma) - R^*(\gamma)| \longrightarrow 0$ as $p \longrightarrow \infty$.

$$\begin{array}{rcl}
|R(\gamma) - R^*(\gamma)| & = & \left|\frac{1}{p^2}\gamma'\Sigma\gamma - \frac{1}{p^2}\gamma' b.IV(f).b'\gamma\right| \\
 & = & \left|\frac{1}{p^2}\gamma'\left[b.IV(f).b' + IV(\epsilon)\right]\gamma - \frac{1}{p^2}\gamma' bIV(f)b'\gamma\right| \\
 & = & \left|\frac{1}{p^2}\gamma' IV(\epsilon)\gamma\right| \\
 & \leq & \underset{\gamma\in\Gamma}{Sup}\,\frac{1}{p^2}\gamma' IV(\epsilon)\gamma
\end{array}$$

Hence, $\underset{\gamma\in\Gamma}{Sup}\,|R(\gamma) - R^*(\gamma)| \leq \underset{\gamma\in\Gamma}{Sup}\,\frac{1}{p^2}\gamma' IV(\epsilon)\gamma$. Since $\underset{\gamma\in\Gamma}{Sup}\,\frac{1}{p^2}\gamma' IV(\epsilon)\gamma \longrightarrow 0$ as $p \longrightarrow \infty$ by the *step 2*, we deduce that $\underset{\gamma\in\Gamma}{Sup}\,|R(\gamma) - R^*(\gamma)| \longrightarrow 0$ as $p \longrightarrow \infty$.

Step 7: $\left|\underset{\gamma\in\Gamma}{Sup}\,R(\gamma) - \underset{\gamma\in\Gamma}{Sup}\,R^*(\gamma)\right| \longrightarrow 0$ as $p \longrightarrow \infty$
From the properties of the *Sup*

$$\left|\underset{\gamma\in\Gamma}{Sup}\, R(\gamma) - \underset{\gamma\in\Gamma}{Sup}\, R^*(\gamma)\right| \leq \underset{\gamma\in\Gamma}{Sup}\, |R(\gamma) - R^*(\gamma)|$$

Since $\underset{\gamma\in\Gamma}{Sup}\, |R(\gamma) - R^*(\gamma)| \longrightarrow 0$ as $p \longrightarrow \infty$ from the *step 7*, the result is obtained.

Step 8: $\underset{\gamma\in\Gamma}{Sup}\, R^*(\gamma) \longrightarrow IV(f)_{11}$ as $p \longrightarrow \infty$, with $IV(f)_{11}$ the element in the first line and first column of $IV(f)$

We consider the following Choleski decomposition of $b'b/p$

$$\tfrac{b'b}{p} = \left(\tfrac{b'b}{p}\right)^{1/2} \left(\tfrac{b'b}{p}\right)^{1/2'}$$

There exist two vectors δ and V such that γ can be represented in the following way

$$\gamma = b\,(b'b/p)^{-1/2}\,\delta + V, \text{ with } V'b = 0 \text{ and } \delta'\delta \leq 1$$

From the previous specification, we derive the following expression of $R^*(\gamma)$

$$\begin{aligned}
R^*(\gamma) &= \tfrac{1}{p^2}\gamma' b IV(f) b'\gamma \\
&= \tfrac{1}{p^2}\left[b\left(\tfrac{b'b}{p}\right)^{-1/2}\delta + V\right]' b.IV(f).b'\left[b\left(\tfrac{b'b}{p}\right)^{-1/2}\delta + V\right] \\
&= \left[\delta'\left(\tfrac{b'b}{p}\right)^{-1/2} b' + V'\right]\tfrac{b}{p}.IV(f).\tfrac{b'}{p}\left[b\left(\tfrac{b'b}{p}\right)^{-1/2}\delta + V\right] \\
&= \left[\delta'\left(\tfrac{b'b}{p}\right)^{1/2} + \tfrac{V'b}{p}\right].IV(f).\left[\left(\tfrac{b'b}{p}\right)^{1/2}\delta + \tfrac{b'V}{p}\right] \\
&= \delta'\left(\tfrac{b'b}{p}\right)^{1/2}.IV(f).\left(\tfrac{b'b}{p}\right)^{1/2}\delta
\end{aligned}$$

Then,

$$\begin{aligned}
\underset{\gamma\in\Gamma}{Sup}\, R^*(\gamma) &= \underset{\delta,\delta'\delta\leq 1}{Sup}\left\{\delta'\left(\tfrac{b'b}{p}\right)^{1/2}.IV(f).\left(\tfrac{b'b}{p}\right)^{1/2}\delta\right\} \\
&= \textit{Largest eigenvalue of } \left(\tfrac{b'b}{p}\right)^{1/2}.IV(f).\left(\tfrac{b'b}{p}\right)^{1/2} \\
&\equiv \hat{\sigma}_{11}
\end{aligned}$$

Since $\frac{b'b}{p} \longrightarrow I_K$ as $p \longrightarrow \infty$, we have

$$\left(\tfrac{b'b}{p}\right)^{1/2} IV(f) \left(\tfrac{b'b}{p}\right)^{1/2} \xrightarrow{p} IV(f)$$

By the continuity of eigenvalues, $\hat{\sigma}_{11} \longrightarrow IV(f)_{11}$ as $p \longrightarrow \infty$. This leads to $\underset{\gamma\in\Gamma}{Sup}\, R^*(\gamma) \longrightarrow IV(f)_{11}$.

Step 9: $\underset{\gamma\in\Gamma}{Sup}\, R(\gamma) \longrightarrow IV(f)_{11}$

Since $\underset{\gamma\in\Gamma}{Sup}\, R^*(\gamma) \longrightarrow IV(f)_{11}$ from the *step 8*, and since $\left|\underset{\gamma\in\Gamma}{Sup}\, R(\gamma) - \underset{\gamma\in\Gamma}{Sup}\, R^*(\gamma)\right| \longrightarrow 0$ as $p \longrightarrow \infty$ from the *step 7*, we conclude that $\underset{\gamma\in\Gamma}{Sup}\, R(\gamma) \longrightarrow IV(f)_{11}$ as $p \longrightarrow \infty$.

Step 10: If $\hat{b}_1 = Arg\, \underset{\gamma\in\Gamma}{Sup}\, R(\gamma)$ then $R^*(\hat{b}_1) \longrightarrow IV(f)_{11}$ as $p \longrightarrow \infty$

If $\hat{b}_1 = Arg\, \underset{\gamma\in\Gamma}{Sup}\, R(\gamma)$, then $R(\hat{b}_1) = \underset{\gamma\in\Gamma}{Sup}\, R(\gamma)$. We derive from the *step 9* that $R(\hat{b}_1) \longrightarrow IV(f)_{11}$ as $p \longrightarrow \infty$. In addition,

$$\left|R(\hat{b}_1) - R^*(\hat{b}_1)\right| \leq \underset{\gamma\in\Gamma}{Sup}\, |R(\gamma) - R^*(\gamma)| \longrightarrow 0 \text{ } as \text{ } p \longrightarrow \infty$$

Hence, $\left|R(\hat{b}_1) - R^*(\hat{b}_1)\right| \longrightarrow 0$ as $p \longrightarrow \infty$. This latter result together with $R(\hat{b}_1) \longrightarrow IV(f)_{11}$ leads to $R^*(\hat{b}_1) \longrightarrow IV(f)_{11}$ as $p \longrightarrow \infty$.

Step 11: Let $\underline{W}_1$ denotes the first column of W (the matrix of ordered eigenvectors of Σ). $\underline{W}_1$ is the eigenvector of Σ associated to its largest eigenvalue. We also define the variable S_1 by: $S_1 = 1$ if $\underline{W'}_1\underline{b}_1 \geq 0$ and $S_1 = -1$ if $\underline{W'}_1\underline{b}_1 \leq 0$, with $\underline{b}_1$ the first column of the loading matrix b. Then $S_1\frac{\underline{W'}_1 b}{p} \xrightarrow{p} l'_1$, with $l_1 = (1, 0, ..., 0)'$.
There exist $\hat{\delta}$ and $\hat{V}$ such that $\underline{W}_1 = b\left(\frac{b'b}{p}\right)^{-1/2}\hat{\delta} + \hat{V}$, with $\hat{V}'b = 0$ and $\hat{\delta}'\hat{\delta} \leq 1$. Let's take $C_{NT} = \left(\frac{b'b}{p}\right)^{1/2}.IV(f).\left(\frac{b'b}{p}\right)^{1/2}$. It follows that $R^*(\underline{W}_1) = \hat{\delta}'.C_{NT}.\hat{\delta}$. Thus

$$\begin{aligned} R^*(\underline{W}_1) - IV(f)_{11} &= \hat{\delta}'\left(C_{NT} - IV(f)\right)\hat{\delta} + \hat{\delta}'.IV(f).\hat{\delta} - IV(f)_{11} \\ &= \hat{\delta}'\left(C_{NT} - IV(f)\right)\hat{\delta} + (\hat{\delta}_1^2 - 1).IV(f)_{11} + \textstyle\sum_{k=2}^{K} \delta_k^2 IV(f)_{kk} \end{aligned}$$

Since $C_{NT} \longrightarrow IV(f)$ as $p \longrightarrow \infty$ and since $\hat{\delta}$ is bounded ($\hat{\delta}'\hat{\delta} \leq 1$), $\hat{\delta}'\left(C_{NT} - IV(f)\right)\hat{\delta}$ is $o_p(1)$. Because $R^*(\underline{W}_1) - IV(f)_{11} \longrightarrow 0$ as $p \longrightarrow \infty$ (this result comes from the *step 10*, by taking $\hat{b}_1 = \underline{W}_1$) and $\hat{\delta}'\left(C_{NT} - IV(f)\right)\hat{\delta} \xrightarrow{p} 0$, we deduce that

$$(\hat{\delta}_1^2 - 1).IV(f)_{11} + \textstyle\sum_{k=2}^{K} \hat{\delta}_k^2.IV(f)_{kk} \xrightarrow{p} 0$$

The previous convergence result is obtained whatever $IV(f)$ is. Because $\forall k = 1, .., K$ $IV(f)_{kk} > 0$, we conclude that $\hat{\delta}_1^2 \longrightarrow 1$ and $\hat{\delta}_k^2 \longrightarrow 0$ $\forall k = 2, .., K$. Hence

$$\begin{aligned}
S_1\frac{{W'}_1\underline{b}_1}{p} &= \left|\frac{{W'}_1\underline{b}_1}{p}\right| \\
&= \left|\left[b\left(\frac{b'b}{p}\right)^{-1/2}\hat{\delta}+\hat{V}\right]'\frac{\underline{b}_1}{p}\right| \\
&= \left|\left[\hat{\delta}'\left(\frac{b'b}{p}\right)^{-1/2}b'+\hat{V}'\right]\frac{\underline{b}_1}{p}\right| \\
&= \left|\hat{\delta}'\left(\frac{b'b}{p}\right)^{-1/2}\left(\frac{b'\underline{b}_1}{p}\right)+\hat{V}'\frac{\underline{b}_1}{p}\right|
\end{aligned}$$

Since $\hat{V}'b=0$, $\frac{b'\underline{b}_1}{p}\longrightarrow(1,0,...,0)'$ and $\frac{b'b}{p}\longrightarrow I_K$ as $p\longrightarrow\infty$,

$$Plim\ \ S_1\frac{{W'}_1\underline{b}_1}{p}=Plim\ \ \hat{\delta}_1$$

Because $\left(\hat{\delta}_1^2,...,\hat{\delta}_K^2\right)\xrightarrow{p}(1,0,...,0)$, it follows that $S_1\frac{\underline{W}_1'\underline{b}_1}{p}\longrightarrow 1$.
We use the same tricks to prove that for $k\in\{2,...,K\}$, $Plim\ \ S_1\frac{\underline{W}_1'\underline{b}_k}{p}=0$.
We conclude that $S_1\frac{\underline{W}_1'b}{p}\longrightarrow(1,0,...,0)\equiv l_1'$

Step 12: We assume that the columns of W are formed by the K ordered eigenvectors of Σ, and is normalized as $\frac{W'W}{p}=I_K$. We define the matrix $S=Diag\left[sign(\underline{W}_1'\underline{b}_1),...,sign(\underline{W}_K'\underline{b}_K)\right]$, where $\underline{A}_k$ is the k^{th} column of the matrix A. Then $S\frac{W'b}{p}\xrightarrow{p}I_K$.
To prove this result, we need to prove that for each column $\underline{W}_k$ of W, $S\frac{\underline{W}_k'b}{p}\longrightarrow(0,...,1,0,...,0)$, with 1 corresponding to the position k. The result for the case of $k=1$ is given by the *step 11*. The results for $k=2,...,K$ are based on steps 8 to 11, and consist on maximizing $R(.)$ and $R^*(.)$ in a sequential way, using orthonormal subspaces of Γ. For example, for the column $\underline{W}_k$ of W, we can write $\underline{W}_k=b\left(\frac{b'b}{p}\right)^{-1/2}\hat{\delta}_k+\hat{V}_k$, with $\hat{V}_k'b=0$ and $\frac{\hat{V}_k'\hat{V}_k}{p}\xrightarrow{p}0$ and $\hat{\delta}_{kl}^2\xrightarrow{p}0$, $\forall\ \ l\neq k$ and $\hat{\delta}_{kk}^2\xrightarrow{p}1$.

Steps 1 to *12* establish that $S\frac{W'b}{p}\xrightarrow{p}I_K$. This leads to $S\frac{W'b}{p}f_t\xrightarrow{p}f_t$. This result corresponds to the case where Σ is known. If Σ is unknown and is consistently estimated by $\hat{\Sigma}$, and if $\hat{W}$ is the matrix of ordered eigenvectors of $\hat{\Sigma}$ ($\hat{W}$ consistently estimates W), we deduce that $S\frac{\hat{W}'b}{p}f_t\xrightarrow{p}f_t$.

B) Proof of: $\frac{1}{p}S\hat{W}'\epsilon_t\xrightarrow{p}0$
S is defined as in the previous subsection. Note that for $k\in\{1,...,K\}$

$$\begin{aligned}
\tfrac{1}{p}S_k\hat{W}_k'\epsilon_t &= \tfrac{1}{p}\textstyle\sum_{i=1}^p S_k\hat{W}_{ik}'\epsilon_{it} \\
&= \tfrac{1}{p}\textstyle\sum_{i=1}^p\left(S_k\hat{W}_{ik}-b_{ik}\right)\epsilon_{it}+\tfrac{1}{p}\sum_{i=1}^p b_{ik}\epsilon_{it}
\end{aligned}$$

We are going to prove that $\frac{1}{p}\sum_{i=1}^p\left(S_k\hat{W}_{ik}-b_{ik}\right)\epsilon_{it}\xrightarrow{p}0$ and $\frac{1}{p}\sum_{i=1}^p b_{ik}\epsilon_{it}\xrightarrow{p}0$. By the Holder inequality

$$\left|\frac{1}{p}\sum_{i=1}^{p}\left(S_k\hat{W}_{ik}-b_{ik}\right)\epsilon_{it}\right| \leq \left[\frac{1}{p}\sum_{i=1}^{p}\left(S_k\hat{W}_{ik}-b_{ik}\right)^2\right]^{1/2}.\left[\frac{1}{p}\sum_{i=1}^{p}\epsilon_{it}^2\right]^{1/2}$$

In addition,

$$\frac{1}{p}\sum_{i=1}^{p}\left(S_k\hat{W}_{ik}-b_{ik}\right)^2 = S_k^2\frac{1}{p}\underline{\hat{W}}_k'\underline{\hat{W}}_k+\frac{1}{p}\sum_{i=1}^{p}b_{ik}^2-2.\frac{1}{p}S_k\underline{\hat{W}}_k'\underline{b}_k$$

The convergence in probability to 0 of $\frac{1}{p}\sum_{i=1}^{p}\left(S_k\hat{W}_{ik}-b_{ik}\right)^2$ is deduced because

$$S_k^2\frac{1}{p}\underline{\hat{W}}_k'\underline{\hat{W}}_k\xrightarrow{p}1,\ \frac{1}{p}\sum_{i=1}^{p}b_{ik}^2\xrightarrow{p}1 \text{ and } \frac{1}{p}S_k\underline{\hat{W}}_k'\underline{b}_k\xrightarrow{p}1.$$

Since $\frac{1}{p}\sum_{i=1}^{p}\epsilon_{it}^2\sim O_p(1)$, it follows that $\frac{1}{p}\sum_{i=1}^{p}\left(S_k\hat{W}_{ik}-b_{ik}\right)\epsilon_{it}\xrightarrow{p}0$.
In other hand,

$$\begin{aligned} E\left[\left(\frac{1}{p}\sum_{i=1}^{p}b_{ik}\epsilon_{it}\right)^2\right] &= \frac{1}{p^2}\sum_{i=1}^{p}\sum_{j=1}^{p}b_{ik}b_{jk}E(\epsilon_{it}\epsilon_{jt}) \\ &\leq \frac{B^2}{p^2}\sum_{i=1}^{p}\sum_{j=1}^{p}E(\epsilon_{it}\epsilon_{jt})\longrightarrow 0 \end{aligned}$$

with B the bound of loadings. The last convergence result is justified by the fact that the loadings and $\frac{1}{p}\sum_{i=1}^{p}\sum_{j=1}^{p}|E(\epsilon_{it}\epsilon_{jt})|$ are bounded. Since the mean-squared convergence implies the convergence in probability, we conclude that $\frac{1}{p}\sum_{i=1}^{p}b_{ik}\epsilon_{it}\xrightarrow{p}0$. Using the same arguments as in the previous subsection, it follows that $\frac{1}{p}S\hat{W}'(u_t-u_{t-\Delta})\xrightarrow{p}0$.

Proof of Lemma 2.3.1

Our estimator of the rotated factor is defined by:

$$\hat{f}_{kt}=\frac{1}{p}W_k'r_t^*+\frac{1}{p}W_k'(u_t-u_{t-\Delta})+\frac{1}{p}W_k^{\epsilon'}r_t^*+\frac{1}{p}W_k^{\epsilon'}(u_t-u_{t-\Delta})$$

Assume that $\frac{1}{p}W_k^{\epsilon'}r_t^*$ and $\frac{1}{p}W_k^{\epsilon'}(u_t-u_{t-\Delta})$ are at most of the order $O_p(p^{-1/2})$. Then, for p and n are sufficiently large, $\frac{1}{p}W_k^{\epsilon'}r_t^*$ and $\frac{1}{p}W_k^{\epsilon'}(u_t-u_{t-\Delta})$ can be neglected. We deduce that

$$\begin{aligned} \hat{f}_{kt} &= \frac{1}{p}W_k'r_t^*+\frac{1}{p}W_k'(u_t-u_{t-\Delta})+\frac{1}{p}W_k^{\epsilon'}r_t^*+\frac{1}{p}W_k^{\epsilon'}(u_t-u_{t-\Delta}) \\ &= \frac{1}{p}W_k'r_t^*+\frac{1}{p}W_k'(u_t-u_{t-\Delta})+O_p(p^{-1/2}) \\ &= \frac{1}{p}W_k'bf_t+\frac{1}{p}W_k'\epsilon_t+\frac{1}{p}W_k'c(g_t-g_{t-\Delta})+\frac{1}{p}W_k'(\eta_t-\eta_{t-\Delta})+O_p(p^{-1/2}) \\ &= \frac{1}{p}W_k'bf_t+\frac{1}{p}W_k'c(g_t-g_{t-\Delta})+O_p(p^{-1/2}) \\ &\approx \tilde{f}_{kt}+\frac{1}{p}W_k'c(g_t-g_{t-\Delta}) \end{aligned}$$

The fourth equality is a consequence of $\frac{1}{p}W_k'\epsilon_t = O_p(n^{-1/2}p^{-1/2})$ and $\frac{1}{p}W_k'(\eta_t - \eta_{t-\Delta}) = O_p(p^{-1/2})$.
Since $\hat{f}_{kt} \approx \tilde{f}_{kt} + \frac{1}{p}W_k'c(g_t - g_{t-\Delta})$, $E\left[\frac{1}{p}W_k'c(g_t - g_{t-\Delta})|W_k', c, g\right] = 0$ and $\frac{1}{p}W_k'c(g_t - g_{t-\Delta}) \perp \frac{1}{p}W_k'c(g_s - g_{s-\Delta})$ $\forall s \neq t$, we deduce from the properties of the pre-averaging estimator of the integrated volatility (Jacod, Li, Mykland, Podolskijc, and Vetter (2009a)) that $PRV(\hat{f}_{kt})$ is an estimator of the integrated volatility of $\tilde{f}_{kt}$ with the rate of convergence of $n^{-1/4}$. We deduce that $\left[\tilde{f}_{kt}\right]^{\epsilon} \equiv PRV(\hat{f}_{kt}) - \left[\tilde{f}_{kt}\right] = O_p(n^{-1/4})$.

Next, let $k \in 1, ..., K$ and $i \in 1, ..., p$. The estimator of the loading of asset i on factor k is defined by $\hat{b}_{ik} = \frac{MRC(r_i, \hat{f}_k)}{PRV(\hat{f}_k)}$. We are going firstly to establish the convergence rate of $\hat{b}_{ik} - b_{ik}$. Let's consider the two following notations:

$$
\begin{aligned}
MRC(r_i, \hat{f}_k) &= \left[r_i^*, \tilde{f}_k\right] + \left[r_i^*, \tilde{f}_k\right]^{\epsilon} \\
PRV(\hat{f}_k) &= \left[\tilde{f}_k\right] + \left[\tilde{f}_k\right]^{\epsilon}
\end{aligned}
$$

where $[X]$ is the covariation of the process X, θ^{ϵ} is the estimation error in the estimation of θ. Using these notations, we obtain

$$
\begin{aligned}
\hat{b}_{ik} &= \frac{\left[r_i^*, \tilde{f}_k\right] + \left[r_i^*, \tilde{f}_k\right]^{\epsilon}}{\left[\tilde{f}_k\right] + \left[\tilde{f}_k\right]^{\epsilon}} \\
&= \left(\frac{\left[r_i^*, \tilde{f}_k\right] + \left[r_i^*, \tilde{f}_k\right]^{\epsilon}}{\left[\tilde{f}_k\right]}\right)\left(1 + \frac{\left[\tilde{f}_k\right]^{\epsilon}}{\left[\tilde{f}_k\right]}\right)^{-1} \\
&= \left(\frac{\left[r_i^*, \tilde{f}_k\right]}{\left[\tilde{f}_k\right]} + \frac{\left[r_i^*, \tilde{f}_k\right]^{\epsilon}}{\left[\tilde{f}_k\right]}\right)\left(1 + \frac{\left[\tilde{f}_k\right]^{\epsilon}}{\left[\tilde{f}_k\right]}\right)^{-1}
\end{aligned}
$$

Since $\left[\tilde{f}_k\right]^{\epsilon}$ is the error in the estimation of $\left[\tilde{f}_k\right]$ using the pre-averaging estimator $PRV(\hat{f}_k)$, we can assume that $\frac{\left[\tilde{f}_k\right]^{\epsilon}}{\left[\tilde{f}_k\right]}$ is closed to 0, such that the following Taylor expansion holds

$$
\left(1 + \frac{\left[\tilde{f}_k\right]^{\epsilon}}{\left[\tilde{f}_k\right]}\right)^{-1} = 1 - \frac{\left[\tilde{f}_k\right]^{\epsilon}}{\left[\tilde{f}_k\right]} + O_p\left(\left(\frac{\left[\tilde{f}_k\right]^{\epsilon}}{\left[\tilde{f}_k\right]}\right)^2\right)
$$

Then

$$
\begin{aligned}
\hat{b}_{ik} &= \left(\frac{\left[r_i^*, \tilde{f}_k\right]}{\left[\tilde{f}_k\right]} + \frac{\left[r_i^*, \tilde{f}_k\right]^{\epsilon}}{\left[\tilde{f}_k\right]}\right)\left(1 - \frac{\left[\tilde{f}_k\right]^{\epsilon}}{\left[\tilde{f}_k\right]} + O\left(\left(\frac{\left[\tilde{f}_k\right]^{\epsilon}}{\left[\tilde{f}_k\right]}\right)^2\right)\right) \\
&= \frac{\left[r_i^*, \tilde{f}_k\right]}{\left[\tilde{f}_k\right]} - \frac{\left[r_i^*, \tilde{f}_k\right]}{\left[\tilde{f}_k\right]} \cdot \frac{\left[\tilde{f}_k\right]^{\epsilon}}{\left[\tilde{f}_k\right]} + \frac{\left[r_i^*, \tilde{f}_k\right]}{\left[\tilde{f}_k\right]} \cdot O\left(\left(\frac{\left[\tilde{f}_k\right]^{\epsilon}}{\left[\tilde{f}_k\right]}\right)^2\right) \\
&\quad + \frac{\left[r_i^*, \tilde{f}_k\right]^{\epsilon}}{\left[\tilde{f}_k\right]} - \frac{\left[r_i^*, \tilde{f}_k\right]^{\epsilon} \cdot \left[\tilde{f}_k\right]^{\epsilon}}{\left[\tilde{f}_k\right]^2} + \frac{\left[r_i^*, \tilde{f}_k\right]^{\epsilon}}{\left[\tilde{f}_k\right]} \cdot O\left(\left(\frac{\left[\tilde{f}_k\right]^{\epsilon}}{\left[\tilde{f}_k\right]}\right)^2\right)
\end{aligned}
$$

It follows that

$$\hat{b}_{ik} - \tilde{b}_{ik} = -\frac{\left[r_i^*, \tilde{f}_k\right]}{\left[\tilde{f}_k\right]} \cdot \frac{\left[\tilde{f}_k\right]^\epsilon}{\left[\tilde{f}_k\right]} + \frac{\left[r_i^*, \tilde{f}_k\right]}{\left[\tilde{f}_k\right]} \cdot O\left(\left(\frac{\left[\tilde{f}_k\right]^\epsilon}{\left[\tilde{f}_k\right]}\right)^2\right) + \frac{\left[r_i^*, \tilde{f}_k\right]^\epsilon}{\left[\tilde{f}_k\right]} - \frac{\left[r_i^*, \tilde{f}_k\right]^\epsilon \cdot \left[\tilde{f}_k\right]^\epsilon}{\left[\tilde{f}_k\right]^2} + \frac{\left[r_i^*, \tilde{f}_k\right]^\epsilon}{\left[\tilde{f}_k\right]} \cdot O\left(\left(\frac{\left[\tilde{f}_k\right]^\epsilon}{\left[\tilde{f}_k\right]}\right)^2\right)$$

Then

$$\begin{array}{rcl} \left|\hat{b}_{ik} - \tilde{b}_{ik}\right| & \leq & \left|\frac{\left[r_i^*, \tilde{f}_k\right]}{\left[\tilde{f}_k\right]^2}\right| \cdot \left|\left[\tilde{f}_k\right]^\epsilon\right| + \left|\frac{\left[r_i^*, \tilde{f}_k\right]}{\left[\tilde{f}_k\right]}\right| \cdot O\left(\left(\frac{\left[\tilde{f}_k\right]^\epsilon}{\left[\tilde{f}_k\right]}\right)^2\right) \\ & & + \frac{1}{\left[\tilde{f}_k\right]} \cdot \left|\left[r_i^*, \tilde{f}_k\right]^\epsilon\right| + \frac{1}{\left[\tilde{f}_k\right]^2} \cdot \left|\left[r_i^*, \tilde{f}_k\right]^\epsilon\right| \cdot \left|\left[\tilde{f}_k\right]^\epsilon\right| + \frac{1}{\left[\tilde{f}_k\right]} \cdot \left|\left[r_i^*, \tilde{f}_k\right]^\epsilon\right| \cdot O\left(\left(\frac{\left[\tilde{f}_k\right]^\epsilon}{\left[\tilde{f}_k\right]}\right)^2\right) \end{array}$$

By properties of the pre-averaging estimator, $\left[\tilde{f}_k\right]^\epsilon = O_p(n^{-1/4})$. In addition, $r_i = r_i^* + (u_t - u_{t-\Delta})$ and $\hat{f}_{kt} \approx \tilde{f}_{kt} + \frac{1}{p} W_k'(u_t - u_{t-\Delta})$. It follows from the pre-averaging estimator of the integrated covariation of Kim Christensen et Al.(2010) that $\left|\left[r_i^*, \tilde{f}_k\right]^\epsilon\right| \equiv \left|MRC(r_i, \hat{f}_k) - \left[r_i^*, \tilde{f}_k\right]\right| = O_p(n^{-1/4})$. Hence

$$\begin{array}{rcl} \left|\hat{b}_{ik} - \tilde{b}_{ik}\right| & \leq & O_p(n^{-1/4}) + O_p(1)O(O_p(1)O_p(n^{-1/4})^2) + O_p(1)O_p(n^{-1/4}) \\ & & +O_p(1)O_p(n^{-1/4})O_p(n^{-1/4}) + O_p(1)O_p(n^{-1/4})O(O_p(1)O_p(n^{-1/4})^2) \\ & \leq & O_p(n^{-1/4}) + O_p(n^{-1/2}) + O_p(n^{-1/4}) + O_p(n^{-1/2}) + O_p(n^{-1/4})O_p(n^{-1/2}) \\ & \leq & O_p(n^{-1/4}) \end{array}$$

Hence $\left|\hat{b}_{ik} - \tilde{b}_{ik}\right| = O_p\left(n^{-1/4}\right)$, $\forall k = 1, ..., K$, $\forall i = 1, ..., p$.
Using the Frobenius norm, we obtain

$$\begin{array}{rcl} \left\|\hat{b}_k - \tilde{b}_k\right\|_F^2 & = & \sum_{i=1}^p \left|\hat{b}_{ik} - \tilde{b}_{ik}\right|^2 \\ & = & \sum_{i=1}^p O_p(n^{-1/2}) \\ & = & O_p(pn^{-1/2}) \end{array}$$

We conclude that $\left\|\hat{b}_k - \tilde{b}_k\right\|_F = \left\|\hat{b}_k - \tilde{b}_k\right\|_2 = O_p(p^{1/2}n^{-1/4})$

We define the estimator of the integrated volatility of the idiosyncratic error terms by,

$$\forall i = 1, ..., p,\ \hat{\Sigma}_{ii}^\epsilon = PRV(\hat{\epsilon}_i),$$

with $\hat{\epsilon}_{it} = r_{it} - \hat{b}_i \hat{f}_t$.
It can be easily established that

$$\hat{\epsilon}_{it} = \epsilon_{it} + (u_t - u_{t-\Delta}) - \sum_{k=1}^{K} \tilde{b}_{ik}\tilde{f}_{kt}^{\epsilon} - \sum_{k=1}^{K} \tilde{b}_{ik}^{\epsilon}\tilde{f}_{kt} - \sum_{k=1}^{K} \tilde{b}_{ik}^{\epsilon}\tilde{f}_{kt}^{\epsilon} - \frac{1}{p}\sum_{k=1}^{K}\sum_{l=1}^{K} \tilde{b}_{ik}W_l'c(g_t - g_{t-\Delta}) - \frac{1}{p}\sum_{k=1}^{K}\sum_{l=1}^{K} \tilde{b}_{ik}^{\epsilon}W_l'c(g_t - g_{t-\Delta})$$

Since $\tilde{f}_{kt}^{\epsilon} = O_p(p^{-1/2})$ and $\tilde{b}_{ik}^{\epsilon} = O_p(n^{-1/4})$, let's assume that n and p are both sufficiently large such that $\sum_{k=1}^{K} \tilde{b}_{ik}\tilde{f}_{kt}^{\epsilon}$, $\sum_{k=1}^{K} \tilde{b}_{ik}^{\epsilon}\tilde{f}_{kt}$, $\sum_{k=1}^{K} \tilde{b}_{ik}^{\epsilon}\tilde{f}_{kt}^{\epsilon}$ and $\frac{1}{p}\sum_{k=1}^{K}\sum_{l=1}^{K} \tilde{b}_{ik}^{\epsilon}W_l'c(g_t - g_{t-\Delta})$ can be neglected. Then,

$$\hat{\epsilon}_{it} \approx \epsilon_{it} + (u_t - u_{t-\Delta}) - \frac{1}{p}\sum_{k=1}^{K}\sum_{l=1}^{K} \tilde{b}_{ik}W_l'c(g_t - g_{t-\Delta}),$$

It follows that

$$PRV(\hat{\epsilon}_i) = [\epsilon_i] + O_p(n^{-1/4})$$

Hence

$$\left|\hat{\Sigma}_{ii}^{\epsilon} - \Sigma_{ii}^{\epsilon}\right| = O_p(n^{-1/4})$$

Under the Frobenius norm

$$\begin{aligned} \left\|\hat{\Sigma}^{\epsilon} - \Sigma^{\epsilon}\right\|_F^2 &= \sum_{i=1}^{p} \left|\hat{\Sigma}_{ii}^{\epsilon} - \Sigma_{ii}^{\epsilon}\right|^2 \\ &= \sum_{i=1}^{p} O_p(n^{-1/2}) \\ &= O_p(pn^{-1/2}) \end{aligned}$$

We conclude that $\left\|\hat{\Sigma}^{\epsilon} - \Sigma^{\epsilon}\right\|_F = O_p(p^{1/2}n^{-1/4})$.

Proof of Theorem 2.3.1

By Lemma 2.3.1, it follows that:

$$
\begin{aligned}
\left\|\hat{\Sigma}-\Sigma\right\| &= \left\|\sum_{k=1}^{K}\left(\hat{b}_k\hat{b}_k'\hat{\Sigma}_{kk}^f - b_kb_k'\Sigma_{kk}^f\right)+\hat{\Sigma}^\epsilon-\Sigma^\epsilon\right\| \\
&\le \left\|\sum_{k=1}^{K}\left(\hat{b}_k\hat{b}_k'\hat{\Sigma}_{kk}^f - b_kb_k'\Sigma_{kk}^f\right)\right\|+\left\|\hat{\Sigma}^\epsilon-\Sigma^\epsilon\right\| \\
&\le \sum_{k=1}^{K}\left[\left\|\left(\hat{b}_k-b_k\right)\left(\hat{b}_k-b_k\right)'\right\|+\left\|\left(\hat{b}_k-b_k\right)b_k'\right\|+\left\|b_k\left(\hat{b}_k-b_k\right)'\right\|\right]\cdot\left|\hat{\Sigma}_{kk}^f-\Sigma_{kk}^f\right| \\
&\quad +\left[\left\|\left(\hat{b}_k-b_k\right)\left(\hat{b}_k-b_k\right)'\right\|+\left\|\left(\hat{b}_k-b_k\right)b_k'\right\|+\left\|b_k\left(\hat{b}_k-b_k\right)'\right\|\right]\cdot\Sigma_{kk}^f+\left\|\hat{\Sigma}^\epsilon-\Sigma^\epsilon\right\| \\
&\le \sum_{k=1}^{K}\left\|\hat{b}_k-b_k\right\|^2\cdot\left|\hat{\Sigma}_{kk}^f-\Sigma_{kk}^f\right|+2\sum_{k=1}^{K}\left\|\hat{b}_k-b_k\right\|\cdot\|b_k'\|\cdot\left|\hat{\Sigma}_{kk}^f-\Sigma_{kk}^f\right| \\
&\quad +\sum_{k=1}^{K}\|b_k\|^2\cdot\left|\hat{\Sigma}_{kk}^f-\Sigma_{kk}^f\right|+\sum_{k=1}^{K}\left\|\hat{b}_k-b_k\right\|^2\Sigma_{kk}^f \\
&\quad +2\sum_{k=1}^{K}\left\|\hat{b}_k-b_k\right\|\cdot\|b_k\|\,\Sigma_{kk}^f+\left\|\hat{\Sigma}^\epsilon-\Sigma^\epsilon\right\| \\
&\le \sum_{k=1}^{K}O_p(pn^{-1/4})O_p(n^{-1/4})+\sum_{k=1}^{K}O_p(p^{1/2}n^{-1/4})O_p(p^{1/2}) \\
&\quad +\sum_{k=1}^{K}O_p(p^{1/2})O_p(p^{1/2}n^{-1/4})O_p(n^{-1/4})+\sum_{k=1}^{K}O_p(p)O_p(n^{-1/4}) \\
&\quad +\sum_{k=1}^{K}O_p(pn^{-1/2})O_p(1)+\sum_{k=1}^{K}O_p(p^{1/2}n^{-1/4})O_p(p^{1/2})O_p(1) \\
&\quad +\sum_{k=1}^{K}O_p(p^{1/2})O_p(p^{1/2}n^{-1/4})O_p(1)+O_p(p^{1/2}n^{-1/4}) \\
&\le O_p(Kpn^{-1/4}).
\end{aligned}
$$

The convergence rates for the pre-averaging estimator of Christensen, Kinnebrock, and Podolskij (2010a) and the kernel estimator of Barndorff-Nielsen, Hansen, Lunde, and Shephard (2011a) may be established by similar arguments, based on the results that $\forall i,j = 1,...,p$, $\left|MRC_{ij}^\delta-\Sigma_{ij}\right| = O_p\left(n^{-1/5}\right)$ and $\forall i,j=1,...,p$, $|MRker_{ij}-\Sigma_{ij}| = O_p\left(n^{-1/5}\right)$.

Proof of Theorem 2.3.2

Due to the factor representation,

$$\hat{\Sigma} = \hat{b}\hat{\Sigma}^f\hat{b}'+\hat{\Sigma}^\varepsilon$$

By the Sherman-Morrison-Woodbury formula:

$$\hat{\Sigma}^{-1} = (\hat{\Sigma}^\varepsilon)^{-1}-(\hat{\Sigma}^\varepsilon)^{-1}\hat{b}\left[(\hat{\Sigma}^f)^{-1}+\hat{b}'(\hat{\Sigma}^\varepsilon)^{-1}\hat{b}\right]^{-1}\hat{b}'(\hat{\Sigma}^\varepsilon)^{-1}$$

and

$$\Sigma^{-1} = (\Sigma^{\varepsilon})^{-1} - (\Sigma^{\varepsilon})^{-1} b \left[(\Sigma^{f})^{-1} + b'(\Sigma^{\varepsilon})^{-1} b \right]^{-1} b'(\Sigma^{\varepsilon})^{-1}$$

Under the Frobenius norm, it follows that:

$$\begin{aligned}
\left\| \hat{\Sigma}^{-1} - \Sigma^{-1} \right\|_F &\leqslant \left\| (\hat{\Sigma}^{\varepsilon})^{-1} - (\Sigma^{\varepsilon})^{-1} \right\|_F + \left\| \left((\hat{\Sigma}^{\varepsilon})^{-1} - (\Sigma^{\varepsilon})^{-1} \right) \hat{b} \left[(\hat{\Sigma}^{f})^{-1} + \hat{b}'(\hat{\Sigma}^{\varepsilon})^{-1} \hat{b} \right]^{-1} \hat{b}'(\hat{\Sigma}^{\varepsilon})^{-1} \right\|_F \\
&+ \left\| (\hat{\Sigma}^{\varepsilon})^{-1} \hat{b} \left[(\hat{\Sigma}^{f})^{-1} + \hat{b}'(\hat{\Sigma}^{\varepsilon})^{-1} \hat{b} \right]^{-1} \hat{b}' \left((\hat{\Sigma}^{\varepsilon})^{-1} - (\Sigma^{\varepsilon})^{-1} \right) \right\|_F \\
&+ \left\| (\Sigma^{\varepsilon})^{-1} (\hat{b} - b) \left[(\hat{\Sigma}^{f})^{-1} + \hat{b}'(\hat{\Sigma}^{\varepsilon})^{-1} \hat{b} \right]^{-1} \hat{b}'(\Sigma^{\varepsilon})^{-1} \right\|_F \\
&+ \left\| (\Sigma^{\varepsilon})^{-1} b \left[(\hat{\Sigma}^{f})^{-1} + \hat{b}'(\hat{\Sigma}^{\varepsilon})^{-1} \hat{b} \right]^{-1} (\hat{b} - b)'(\Sigma^{\varepsilon})^{-1} \right\|_F \\
&+ \left\| (\Sigma^{\varepsilon})^{-1} b \left\{ \left[(\hat{\Sigma}^{f})^{-1} + \hat{b}'(\hat{\Sigma}^{\varepsilon})^{-1} \hat{b} \right]^{-1} - \left[(\Sigma^{f})^{-1} + b'(\Sigma^{\varepsilon})^{-1} b \right]^{-1} \right\} b'(\Sigma^{\varepsilon})^{-1} \right\|_F \\
&\leq \Lambda_1 + \Lambda_2 + \Lambda_3 + \Lambda_4 + \Lambda_5 + \Lambda_6
\end{aligned}$$

In order to compute the convergence rate of $\hat{\Sigma}^{-1}$, we will determine separately the order of Λ_1, Λ_2, Λ_3, Λ_4, Λ_5 and Λ_6.

1) Rate of convergence of $\left\| (\hat{\Sigma}^{\varepsilon})^{-1} - (\Sigma^{\varepsilon})^{-1} \right\|_F$

Using the Frobenius norm expression:

$$\left\| (\hat{\Sigma}^{\varepsilon})^{-1} - (\Sigma^{\varepsilon})^{-1} \right\|_F = \sqrt{\sum_{i=1}^{p} \left(\frac{1}{PRV(\hat{\varepsilon}_i)} - \frac{1}{IV(\varepsilon_i)} \right)^2}$$

By the Taylor expansion around $IV(\varepsilon_i)$, we obtain that:

$$\frac{1}{PRV(\hat{\varepsilon}_i)} = \frac{1}{IV(\varepsilon_i)} + (PRV(\hat{\varepsilon}_i) - IV(\varepsilon_i)) \times \left(-\frac{1}{IV(\varepsilon_i)^2}\right) + O_p((PRV(\hat{\varepsilon}_i) - IV(\varepsilon_i))^2)$$

Since $\frac{1}{IV(\varepsilon_i)^2} = O_p(1)$ and $(PRV(\hat{\varepsilon}_i) - IV(\varepsilon_i)) = O_p(n^{-1/4})$, we get:

$$\begin{aligned}
\frac{1}{PRV(\hat{\varepsilon}_i)} - \frac{1}{IV(\varepsilon_i)} &= O_p(n^{-1/4}) \times O_p(1) + O_p(n^{-1/2}) \\
&= O_p(n^{-1/4})
\end{aligned}$$

Thus,

$$\begin{aligned}
\left\| (\hat{\Sigma}^{\varepsilon})^{-1} - (\Sigma^{\varepsilon})^{-1} \right\|_F &= \sqrt{\sum_{i=1}^{p} O_p(n^{-1/4})^2} \\
&= \sqrt{O_p(pn^{-1/2})} \\
&= O_p(p^{1/2} n^{-1/4})
\end{aligned}$$

2) Convergence rate of $\Lambda_2 = \left\| \left((\hat{\Sigma}^{\varepsilon})^{-1} - (\Sigma^{\varepsilon})^{-1} \right) \hat{b} \left[(\hat{\Sigma}^{f})^{-1} + \hat{b}'(\hat{\Sigma}^{\varepsilon})^{-1}\hat{b} \right]^{-1} \hat{b}'(\hat{\Sigma}^{\varepsilon})^{-1} \right\|_F$

$$
\begin{aligned}
\Lambda_2 &= \left\| \left((\hat{\Sigma}^{\varepsilon})^{-1} - (\Sigma^{\varepsilon})^{-1} \right) \hat{b} \left[(\hat{\Sigma}^{f})^{-1} + \hat{b}'(\hat{\Sigma}^{\varepsilon})^{-1}\hat{b} \right]^{-1} \hat{b}'(\hat{\Sigma}^{\varepsilon})^{-1} \right\|_F \\
&\leq \left\| \left((\hat{\Sigma}^{\varepsilon})^{-1} - (\Sigma^{\varepsilon})^{-1} \right) (\hat{\Sigma}^{\varepsilon})^{1/2} \right\|_F \left\| (\hat{\Sigma}^{\varepsilon})^{-1/2}\hat{b} \left[(\hat{\Sigma}^{f})^{-1} + \hat{b}'(\hat{\Sigma}^{\varepsilon})^{-1}\hat{b} \right]^{-1} \hat{b}'(\hat{\Sigma}^{\varepsilon})^{-1/2} \right\|_F \left\| (\hat{\Sigma}^{\varepsilon})^{-1/2} \right\|_F
\end{aligned}
$$

i) Rate of $\left\| (\hat{\Sigma}^{\varepsilon})^{-1/2} \right\|_F$.
It can easily be shown that $\left\| (\hat{\Sigma}^{\varepsilon})^{-1/2} \right\|_F = \sqrt{\sum_{i=1}^{p} PRV(\hat{\varepsilon}_i)^{-1/2}} = O_p(p^{1/2})$, since $PRV(\hat{\varepsilon}_i)^{-1/2} = O_p(1)$.

ii) Rate of convergence of $\left\| \left((\hat{\Sigma}^{\varepsilon})^{-1} - (\Sigma^{\varepsilon})^{-1} \right) (\hat{\Sigma}^{\varepsilon})^{1/2} \right\|_F$
Since $\hat{\Sigma}^{\varepsilon}$ and Σ^{ε} are diagonal matrices:

$$
\left\| \left((\hat{\Sigma}^{\varepsilon})^{-1} - (\Sigma^{\varepsilon})^{-1} \right) (\hat{\Sigma}^{\varepsilon})^{1/2} \right\|_F = \sqrt{\sum_{i=1}^{p} \left(\frac{IV(\varepsilon_i) - PRV(\hat{\varepsilon}_i)}{PRV(\hat{\varepsilon}_i)^{1/2} IV(\varepsilon_i)} \right)^2}
$$

We know that $IV(\varepsilon_i) - PRV(\hat{\varepsilon}_i) = O_p(n^{-1/4})$, $PRV(\hat{\varepsilon}_i)^{1/2} = O_p(1)$ and $IV(\varepsilon_i) = O_p(1)$. It follows that:

$$
\begin{aligned}
\left\| \left((\hat{\Sigma}^{\varepsilon})^{-1} - (\Sigma^{\varepsilon})^{-1} \right) (\hat{\Sigma}^{\varepsilon})^{1/2} \right\|_F &= \sqrt{\sum_{i=1}^{p} O_p(n^{-1/4})^2} \\
&= O_p(p^{1/2} n^{-1/4})
\end{aligned}
$$

iii) Rate of $\left\| (\hat{\Sigma}^{\varepsilon})^{-1/2}\hat{b} \left[(\hat{\Sigma}^{f})^{-1} + \hat{b}'(\hat{\Sigma}^{\varepsilon})^{-1}\hat{b} \right]^{-1} \hat{b}'(\hat{\Sigma}^{\varepsilon})^{-1/2} \right\|_F$

$(\hat{\Sigma}^{\varepsilon})^{-1/2}\hat{b} \left[(\hat{\Sigma}^{f})^{-1} + \hat{b}'(\hat{\Sigma}^{\varepsilon})^{-1}\hat{b} \right]^{-1} \hat{b}'(\hat{\Sigma}^{\varepsilon})^{-1/2}$ is symetric positive definite, with a rank at most equal to K, and no more than K positive eigenvalues (Since number of positive eigenvalues is smaller than the rank and the latter is smaller than K). Also:

$$
\begin{aligned}
(\hat{\Sigma}^{\varepsilon})^{-1/2}\hat{b} \left[(\hat{\Sigma}^{f})^{-1} + \hat{b}'(\hat{\Sigma}^{\varepsilon})^{-1}\hat{b} \right]^{-1} \hat{b}'(\hat{\Sigma}^{\varepsilon})^{-1/2} &= I_p - (\hat{\Sigma}^{\varepsilon})^{1/2}\hat{\Sigma}^{-1}(\hat{\Sigma}^{\varepsilon})^{1/2} \\
&\leq I_p
\end{aligned}
$$

where $A \leq B$ means that $B - A$ is positive semi-definite. Thus, eigenvalues of $(\hat{\Sigma}^{\varepsilon})^{-1/2}\hat{b} \left[(\hat{\Sigma}^{f})^{-1} + \hat{b}'(\hat{\Sigma}^{\varepsilon})^{-1}\hat{b} \right]^{\cdot}$
are positive and bounded by 1. We derive that:

$$\begin{aligned}\left\|(\hat{\Sigma}^{\varepsilon})^{-1/2}\hat{b}\left[(\hat{\Sigma}^{f})^{-1}+\hat{b}'(\hat{\Sigma}^{\varepsilon})^{-1}\hat{b}\right]^{-1}\hat{b}'(\hat{\Sigma}^{\varepsilon})^{-1/2}\right\|_F &= \sqrt{\sum_{i=1}^{p}\lambda_i}\\ &\leq \sqrt{\sum_{i=1}^{K}O_p(1)}\\ &\leq O_p(\sqrt{K})\end{aligned}$$

From i), ii), and iii) we derive that:

$$\begin{aligned}\Lambda_2 &= O_p(p^{1/2}n^{-1/4})O_p(p^{1/2})O_p(K^{1/2})\\ &= O_p(pn^{-1/4}K^{1/2})\\ &= O_p(pn^{-1/4})\end{aligned}$$

The last equality comes from the fact that k is suppose to be known and fix.

Using the same procedure than for Λ_2, it is easy to verify that $\Lambda_3 = O_p(pn^{-1/4})$.

3) Convergence rate of $\Lambda_4 = \left\|(\Sigma^{\varepsilon})^{-1}(\hat{b}-b)\left[(\hat{\Sigma}^{f})^{-1}+\hat{b}'(\hat{\Sigma}^{\varepsilon})^{-1}\hat{b}\right]^{-1}\hat{b}'(\Sigma^{\varepsilon})^{-1}\right\|_F$
It can be verified that:

$$\Lambda_4 \leq \left\|(\Sigma^{\varepsilon})^{-1}(\hat{b}-b)\right\|_F \times \left\|\left[(\hat{\Sigma}^{f})^{-1}+\hat{b}'(\hat{\Sigma}^{\varepsilon})^{-1}\hat{b}\right]^{-1}\right\|_F \times \left\|\hat{b}'(\Sigma^{\varepsilon})^{-1}\right\|_F$$

* Convergence of $\left\|\left[(\hat{\Sigma}^{f})^{-1}+\hat{b}'(\hat{\Sigma}^{\varepsilon})^{-1}\hat{b}\right]^{-1}\right\|_F$

$$\begin{aligned}(\hat{\Sigma}^{f})^{-1}+\hat{b}'(\hat{\Sigma}^{\varepsilon})^{-1}\hat{b} \geq (\hat{\Sigma}^{f})^{-1} &\implies \left[(\hat{\Sigma}^{f})^{-1}+\hat{b}'(\hat{\Sigma}^{\varepsilon})^{-1}\hat{b}\right]^{-1} \leq \hat{\Sigma}^{f}\\ &\implies \left\|\left[(\hat{\Sigma}^{f})^{-1}+\hat{b}'(\hat{\Sigma}^{\varepsilon})^{-1}\hat{b}\right]^{-1}\right\|_F \leq \left\|\hat{\Sigma}^{f}\right\|_F\end{aligned}$$

But $\left\|\hat{\Sigma}^{f}\right\|_F = \sqrt{\sum_{k=1}^{K}PRV(\hat{f}_k)^2}$ and $\forall k = 1,...,K,\ PRV(\hat{f}_k)^2 = O_p(1)$. Thus, $\left\|\hat{\Sigma}^{f}\right\|_F = O_p(\sqrt{K})$ and $\left\|\left[(\hat{\Sigma}^{f})^{-1}+\hat{b}'(\hat{\Sigma}^{\varepsilon})^{-1}\hat{b}\right]^{-1}\right\|_F = O_p(\sqrt{K})$.

* Convergence of $\left\|(\Sigma^{\varepsilon})^{-1}(\hat{b}-b)\right\|_F$.
Using the explicit formula of the Frobenius norm, it can be established that:

$$\left\|(\Sigma^{\varepsilon})^{-1}(\hat{b}-b)\right\|_F = \sqrt{\sum_{i=1}^{p}\sum_{k=1}^{K}\frac{1}{IV(\varepsilon_i)^2}(\hat{b}_{ik}-b_{ik})^2}$$

From lemma 2.3.1, we know that $(\hat{b}_{ik}-b_{ik}) = O_p(n^{-1/4})$. Also, $\frac{1}{IV(\varepsilon_i)^2} = O_p(1)$. Thus:

$$
\begin{aligned}
\left\|(\Sigma^{\varepsilon})^{-1}(\hat{b}-b)\right\|_F &= \sqrt{\sum_{i=1}^{p}\sum_{k=1}^{K} O_p(1)O_p(n^{-1/2})} \\
&= O_p(p^{1/2}K^{1/2}n^{-1/4})
\end{aligned}
$$

* Convergence of $\left\|\hat{b}'(\Sigma^{\varepsilon})^{-1}\right\|_F$.
Since $(\Sigma^{\varepsilon})^{-1}$ is diagonal, we have:

$$
\left\|\hat{b}'(\Sigma^{\varepsilon})^{-1}\right\|_F = \sqrt{\sum_{i=1}^{p}\sum_{k=1}^{K} \hat{b}_{ik}^2 \frac{1}{IV(\varepsilon_i)^2}}
$$

It can be prove that $\hat{b}_{ik} = O_p(1)$ and $\frac{1}{IV(\varepsilon_i)^2} = O_p(1)$. Then:

$$
\begin{aligned}
\Lambda_4 &= O_p(p^{1/2}K^{1/2}n^{-1/4})O_p(K^{1/2})O_p(p^{1/2}K^{1/2}) \\
&= O_p(pK^{3/2}n^{-1/4})
\end{aligned}
$$

Using the same strategy than previously, we obtain:

$$
\Lambda_5 = O_p(pK^{3/2}n^{-1/4})
$$

4) Rate of convergence of $\Lambda_6 = \left\|(\Sigma^{\varepsilon})^{-1}b\left\{\left[(\hat{\Sigma}^f)^{-1} + \hat{b}'(\hat{\Sigma}^{\varepsilon})^{-1}\hat{b}\right]^{-1} - \left[(\Sigma^f)^{-1} + b'(\Sigma^{\varepsilon})^{-1}b\right]^{-1}\right\}b'(\Sigma^{\varepsilon})^{-1}\right\|_F$

$$
\Lambda_6 \leq \left\|\left[(\hat{\Sigma}^f)^{-1} + \hat{b}'(\hat{\Sigma}^{\varepsilon})^{-1}\hat{b}\right]^{-1} - \left[(\Sigma^f)^{-1} + b'(\Sigma^{\varepsilon})^{-1}b\right]^{-1}\right\|_F \times \|b'(\Sigma^{\varepsilon})^{-2}b\|_F
$$

Let's call $A = (\Sigma^f)^{-1} + b'(\Sigma^{\varepsilon})^{-1}b$, $\hat{A} = (\hat{\Sigma}^f)^{-1} + \hat{b}'(\hat{\Sigma}^{\varepsilon})^{-1}\hat{b}$ and $Q = \hat{A} - A$. Then, it comes out that:

$$
\begin{aligned}
\left\|\hat{A}^{-1} - A^{-1}\right\|_F &\leq \|A^{-1}\|_F \times \frac{\left\|A^{-1}Q\right\|_F}{1-\|A^{-1}Q\|_F} \\
&\leq \frac{\left\|A^{-1}\right\|_F^2 \|Q\|_F}{1-\|A^{-1}\|_F\|Q\|_F}
\end{aligned}
$$

whenever $1 \geq \|A^{-1}\|_F\,\|Q\|_F$.

* Convergence rate of $\|Q\|_F$.

$$\begin{aligned}\|Q\|_F &= \left\|((\hat{\Sigma}^f)^{-1}-(\Sigma^f)^{-1})+(\hat{b}'(\hat{\Sigma}^\varepsilon)^{-1}\hat{b}-b'(\Sigma^\varepsilon)^{-1}b)\right\|_F \\ &\leq \left\|((\hat{\Sigma}^f)^{-1}-(\Sigma^f)^{-1})\right\|_F+\left\|(\hat{b}'(\hat{\Sigma}^\varepsilon)^{-1}\hat{b}-b'(\Sigma^\varepsilon)^{-1}b)\right\|_F\end{aligned}$$

But,

$$\left\|((\hat{\Sigma}^f)^{-1}-(\Sigma^f)^{-1})\right\|_F = \sqrt{\sum_{k=1}^K(\frac{1}{PRV(\hat{f}_k)}-\frac{1}{IV(f_k)})^2}$$

By the taylor expansion, $(\frac{1}{PRV(\hat{f}_k)}-\frac{1}{IV(f_k)}) = O_p(n^{-1/4})$. Then:

$$\begin{aligned}\left\|((\hat{\Sigma}^f)^{-1}-(\Sigma^f)^{-1})\right\|_F &= \sqrt{\sum_{k=1}^K O_p(n^{-1/2})} \\ &= O_p(K^{1/2}n^{-1/4})\end{aligned}$$

In the other hand:

$$\left\|\hat{b}'(\hat{\Sigma}^\varepsilon)^{-1}\hat{b}-b'(\Sigma^\varepsilon)^{-1}b\right\|_F = \sqrt{\sum_{k=1}^K\sum_{l=1}^K(\sum_{i=1}^p(\frac{\hat{b}_{ik}\hat{b}_{il}}{PRV(\hat{\varepsilon}_i)}-\frac{b_{ik}b_{il}}{IV(\varepsilon_i)}))^2}$$

Based on the Taylor expansion and lemma 2.3.1, we get:

$$\frac{\hat{b}_{ik}\hat{b}_{il}}{PRV(\hat{\varepsilon}_i)}-\frac{b_{ik}b_{il}}{IV(\varepsilon_i)} = O_p(n^{-1/4})$$

We obtain that:

$$\begin{aligned}\left\|\hat{b}'(\hat{\Sigma}^\varepsilon)^{-1}\hat{b}-b'(\Sigma^\varepsilon)^{-1}b\right\|_F &= \sqrt{\sum_{k=1}^K\sum_{l=1}^K(\sum_{i=1}^p O_p(n^{-1/4}))^2} \\ &= O_p(pKn^{-1/4})\end{aligned}$$

We derive that:

$$\|Q\|_F = O_p(pKn^{-1/4})+O_p(K^{1/2}n^{-1/4}) = O_p(pKn^{-1/4})$$

* Convergence rate of $\|A^{-1}\|_F$.
Similarly to the part 3), $\|A^{-1}\|_F = O_p(\sqrt{K})$.

Since $\|Q\|_F = O_p(pKn^{-1/4})$ and $\|A^{-1}\|_F = O_p(\sqrt{K})$, and assuming that $K^{3/2}pn^{-1/4} \longrightarrow 0$, we obtain:

$$\left\|\hat{A}^{-1}-A^{-1}\right\|_F = O_p(K^2pn^{-1/4})$$

* Order of $\|b'(\Sigma^{\varepsilon})^{-2}b\|_F$

$$\begin{aligned}\|b'(\Sigma^{\varepsilon})^{-2}b\|_F &= \sqrt{\sum_{k=1}^{K}\sum_{l=1}^{K}(\sum_{i=1}^{p}\frac{b_{ik}b_{il}}{IV(\varepsilon_i)^2})^2} \\ &= \sqrt{O_p(p^2K^2)} \\ &= O_p(pK)\end{aligned}$$

We then derive

$$\Lambda_6 = O_p(K^2pn^{-1/4})O_p(Kp) = O_p(K^3p^2n^{-1/4})$$

We then conclude from the rate of convergence of Λ_1, Λ_2, Λ_3, Λ_4, Λ_5 and Λ_6 that:

$$\left\|\hat{\Sigma}^{-1} - \Sigma^{-1}\right\|_F = O_p(K^3p^2n^{-1/4})$$

2.7 Alternative estimators

- The pre-averaging estimator is defined by:

$$PRV(r) = \frac{\sqrt{\Delta_n}}{\theta\psi_2}\sum_{i=0}^{\lfloor 1/\Delta_n\rfloor - k_n+1}(\overline{Y}_i^n)^2 - \frac{\psi_1\Delta_n}{2\theta^2\psi_2}\sum_{i=1}^{\lfloor 1/\Delta_n\rfloor} r_i^2, \tag{2.20}$$

where n is the number of observed returns; Δ_n is the time interval between two observations; $r_i = Y_{i\Delta_n} - Y_{(i-1)\Delta_n}$ is the i^{th} return computed from the observed price series Y; $\overline{Y}_i^n = \sum_{j=1}^{k_n-1} g(j/n)r_{i+j}$ is the i^{th} pre-averaging return and θ is a setting parameter to choose optimally such that $k_n\sqrt{\Delta_n} = \theta + o(\Delta_n^{1/4})$. Also $\phi_1(s) = \int_s^1 g'(u)g'(u-s)du$, $\phi_2(s) = \int_s^1 g(u)g(u-s)du$, and $\psi_{\mathrm{i}} = \phi_i(0)$. The most important result of the pre-averaging approach is resumed in the asymptotic behavior established in Jacod, Li, Mykland, Podolskijc, and Vetter (2009a).

$$\Delta_n^{-1/4}(PRV(r) - IV) \to N(0;\Gamma), \tag{2.21}$$

with $\Gamma = \int_0^1 \frac{4}{\psi_2^2}\left(\Phi_{22}\theta\sigma_t^4 + 2\Phi_{12}\frac{\sigma_t^2V_\epsilon}{\theta} + \Phi_{11}\frac{V_\epsilon^2}{\theta^3}\right)dt$, V_ϵ is the noise variance, IV the true integrated volatility and $\Phi_{ij} = \int_s^1 \phi_i(s)\phi_j(s)ds$.

- The realized kernel is defined by:

$$K(Y) = \sum_{h=-n}^{n} k(\frac{h}{H+1})\Gamma_h, \tag{2.22}$$

$$\Gamma_h = \sum_{j=h+1}^{n} y_j y_{j-h}^{'}, \text{ for } h > 0; \qquad \Gamma_h = \Gamma_{-h}^{'}, \text{ for } h < 0,$$

where n is the number of synchronized returns per asset, Γ_h is the h^{th} realized autocovariance; $y_j = Y_j - Y_{j-1}$ for $j = 1, 2, ..., n$; with $Y_0 = \frac{1}{m}\sum_{j=1}^{m} Y(\tau_{p,j})$; $Y_n = \frac{1}{m}\sum_{j=1}^{m} Y(\tau_{p,p-m+j})$; $Y_j = Y(\tau_{p,j+m})$ for $j = 1, ..., n-1$; $\{\tau_{p,j}\}$ is the series of refresh time ; and k is a non-stochastic weighting function. The rate of convergence of this estimator is $n^{-1/5}$.

- The modulated realized covariance estimator is defined by:

$$MRC\,[Y]_n = \frac{n}{(n-k_n+2)}\frac{1}{\psi_2 k_n}\sum_{i=0}^{n-k_n+1} \bar{Y}_i^n \left(\bar{Y}_i^n\right)^{'} - \frac{\psi_1^{k_n}}{2n\theta^2\psi_2^{k_n}}\sum_{i=1}^{n}(r_i)(r_i)^{'}, \tag{2.23}$$

where Y is the observed price vector, n is the number of observed returns per asset, $\bar{Y}_i$ the i^{th} averaged return vector, r_i the i^{th} usual return vector defined as in (4), g a weighting function, $\psi_1^{k_n} = k_n \sum_{i=1}^{k_n-1}\left(g(\frac{i}{k_n}) - g(\frac{i-1}{k_n})\right)^2$, $\psi_2^{k_n} = \frac{1}{k_n}\sum_{i=1}^{k_n-1} g^2(\frac{i}{k_n})$, $k_n - 1$ the number of returns in each average, such that $\frac{k_n}{n^{1/2}} = \theta + o(n^{-1/4})$ and θ is a setting parameter. When the assets are not observed at the same time, the non-synchronicity issue is resolved using the refresh time method of Barndorff-Nielsen, Hansen, Lunde, and Shephard (2011a).

- The adjusted modulated realized covariance estimator is defined by:

$$MRC\,[Y]_n^{\delta} = \frac{n}{(n-k_n+2)}\frac{1}{\psi_2 k_n}\sum_{i=0}^{k_n} \bar{Y}_i^n \left(\bar{Y}_i^n\right)^{'}, \tag{2.24}$$

where θ is such that $\frac{k_n}{n^{1/2+\delta}} = \theta + o(n^{-1/4+\delta/2})$. This estimator is consistent, with a sub-optimal rate of convergence of $n^{-1/5}$, and is positive semi-definite.

2.8 Estimation of rotated factors, $\tilde{f}$

Consider the following least squared problem where $f_{j\Delta}$ is chosen to minimize the scaled sum of squared values of the idiosyncratic component:

$$\begin{cases} \underset{f_{j\Delta},b}{Min} \ \ \frac{1}{p}\sum\limits_{j=1}^{\lfloor 1/\Delta \rfloor}(r^*_{j\Delta} - bf_{j\Delta})'(r^*_{j\Delta} - bf_{j\Delta}) \\ s.t \ \ \frac{1}{p}b'b = I_K \end{cases}$$

This is equivalent to:

$$\begin{cases} \underset{f_{j\Delta},b}{Min} \ \ \frac{1}{p}\sum\limits_{j=1}^{\lfloor 1/\Delta \rfloor}(r^*_{j\Delta} - bf_{j\Delta})'(r^*_{j\Delta} - bf_{j\Delta}) \\ s.t \ \ \forall k = 1, ..., K, \frac{1}{p}\underline{b}_k'\underline{b}_k = 1 \\ \forall k = 1, ..., K, \forall l = k+1, ..., K, \underline{b}_k'\underline{b}_l = 0 \end{cases}$$

where $\underline{b}_k$ corresponds to the column k of b. The Lagrangian of this problem is defined by

$$L = \frac{1}{p}\sum\limits_{j=1}^{\lfloor 1/\Delta \rfloor}(r^*_{j\Delta} - bf_{j\Delta})'(r^*_{j\Delta} - bf_{j\Delta}) - \sum_{k=1}^{K}\lambda_k(\underline{b}_k'\underline{b}_k - p) - \sum_{k=1}^{K}\sum_{l=k+1}^{K}\mu_{kl}\underline{b}_k'\underline{b}_l$$

By deriving this Lagrangian with respect to $f_{k\Delta}$, we obtain

$$\begin{aligned} \frac{\partial L}{\partial f_{k\Delta}} &= \frac{\partial}{\partial f_{k\Delta}}\left[\frac{1}{p}\sum\limits_{j=1}^{\lfloor 1/\Delta \rfloor}(r^*_{j\Delta} - bf_{j\Delta})'(r^*_{j\Delta} - bf_{j\Delta})\right] \\ &= \frac{\partial}{\partial f_{k\Delta}}\left[\frac{1}{p}(r^*_{k\Delta} - bf_{k\Delta})'(r^*_{k\Delta} - bf_{k\Delta})\right] \\ &= \frac{\partial}{\partial f_{k\Delta}}\left[\frac{1}{p}(r^{*'}_{k\Delta}r^*_{k\Delta} - r^{*'}_{k\Delta}bf_{k\Delta} - f'_{k\Delta}b'r^*_{k\Delta} + f'_{k\Delta}b'bf_{k\Delta})\right] \\ &= (-b'r^*_{k\Delta} - b'r^*_{k\Delta} + b'bf_{k\Delta} + b'bf_{k\Delta}) \\ &= (-2b'r^*_{k\Delta} + 2b'bf_{k\Delta}) \end{aligned}$$

$$\begin{aligned} \frac{\partial L}{\partial f_{k\Delta}} = 0 &\iff (-2b'r^*_{k\Delta} + 2b'bf_{k\Delta}) = 0 \\ &\iff b'bf_{k\Delta} = b'r^*_{k\Delta} \\ &\iff f_{k\Delta} = (b'b)^{-1}b'r^*_{k\Delta} \\ &\iff f_{k\Delta} = (pI_K)^{-1}b'r^*_{k\Delta} \\ &\iff f_{k\Delta} = \frac{1}{p}b'r^*_{k\Delta} \end{aligned}$$

Hence,

$$f_{k\Delta} = \frac{1}{p}b'r^*_{k\Delta}, \quad \forall k = 1, ..., \lfloor 1/\Delta \rfloor \tag{2.25}$$

We are going now to concentrate the objective function by replacing $f_{j\Delta}$ by its formula given by (17).

$$\begin{aligned}
\frac{1}{p}\sum_{j=1}^{\lfloor 1/\Delta\rfloor}(r^*_{j\Delta}-bf_{j\Delta})'(r^*_{j\Delta}-bf_{j\Delta}) &= \frac{1}{p}\sum_{j=1}^{\lfloor 1/\Delta\rfloor}(r^*_{j\Delta}-b.\tfrac{1}{p}b'r^*_{j\Delta})'(r^*_{j\Delta}-b.\tfrac{1}{p}b'r^*_{j\Delta}) \\
&= \frac{1}{p}\sum_{j=1}^{\lfloor 1/\Delta\rfloor}r^{*'}_{j\Delta}(I_p-\tfrac{1}{p}bb')'(I_p-\tfrac{1}{p}bb')r^*_{j\Delta} \\
&= \frac{1}{p}\sum_{j=1}^{\lfloor 1/\Delta\rfloor}r^{*'}_{j\Delta}r^*_{j\Delta}-\frac{1}{p}\sum_{j=1}^{\lfloor 1/\Delta\rfloor}r^{*'}_{j\Delta}bb'r^*_{j\Delta} \\
&= \frac{1}{p}\sum_{j=1}^{\lfloor 1/\Delta\rfloor}r^{*'}_{j\Delta}r^*_{j\Delta}-\frac{1}{p}\sum_{j=1}^{\lfloor 1/\Delta\rfloor}\sum_{k=1}^{K}r^{*'}_{j\Delta}\underline{b}_k\underline{b}'_kr^*_{j\Delta} \\
&= \frac{1}{p}\sum_{j=1}^{\lfloor 1/\Delta\rfloor}r^{*'}_{j\Delta}r^*_{j\Delta}-\frac{1}{p}\sum_{k=1}^{K}\sum_{j=1}^{\lfloor 1/\Delta\rfloor}r^{*'}_{j\Delta}\underline{b}_k\underline{b}'_kr^*_{j\Delta} \\
&= \frac{1}{p}\sum_{j=1}^{\lfloor 1/\Delta\rfloor}r^{*'}_{j\Delta}r^*_{j\Delta}-\frac{1}{p}\sum_{k=1}^{K}\sum_{j=1}^{\lfloor 1/\Delta\rfloor}\left(r^{*'}_{j\Delta}\underline{b}_k\right)\left(\underline{b}'_kr^*_{j\Delta}\right) \\
&= \frac{1}{p}\sum_{j=1}^{\lfloor 1/\Delta\rfloor}r^{*'}_{j\Delta}r^*_{j\Delta}-\frac{1}{p}\sum_{k=1}^{K}\sum_{j=1}^{\lfloor 1/\Delta\rfloor}\left(\underline{b}'_kr^*_{j\Delta}\right)\left(r'^*_{j\Delta}\underline{b}_k\right) \\
&= \frac{1}{p}\sum_{j=1}^{\lfloor 1/\Delta\rfloor}r^{*'}_{j\Delta}r^*_{j\Delta}-\frac{1}{p}\sum_{k=1}^{K}\underline{b}'_k\left(\sum_{j=1}^{\lfloor 1/\Delta\rfloor}r^*_{j\Delta}r'^*_{j\Delta}\right)\underline{b}_k
\end{aligned}$$

From the last equality, we deduce that the optimal $b=(\underline{b}_1,...,\underline{b}_K)$ is the solution of the following problem

$$\begin{cases}
\underset{\underline{b}_1,\dots,\underline{b}_K}{Max} \quad \frac{1}{p}\sum_{k=1}^{K}\underline{b}'_k\left(\sum_{j=1}^{\lfloor 1/\Delta\rfloor}r^*_{j\Delta}r'^*_{j\Delta}\right)\underline{b}_k \\
s.t \ \ \forall k=1,...,K, \frac{1}{p}\underline{b}'_k\underline{b}_k=1 \\
\forall k=1,...,K, \forall l=k+1,...,K, \underline{b}'_k\underline{b}_l=0
\end{cases}$$

The problem above is equivalent to resolve K optimization problems defining by: $\forall k\in\{1,...,K\}$:

$$\begin{cases}
\underset{\underline{b}_k}{Max} \quad \frac{1}{p}\underline{b}'_k\left(\sum_{j=1}^{\lfloor 1/\Delta\rfloor}r^*_{j\Delta}r'^*_{j\Delta}\right)\underline{b}_k \\
s.t \ \ \frac{1}{p}\underline{b}'_k\underline{b}_k=1 \\
\forall l\neq k, \underline{b}'_k\underline{b}_l=0
\end{cases} \tag{2.26}$$

The Lagrangian of the above problem has the following form

$$L \;=\; \frac{1}{p}\underline{b}'_k\left(\sum_{j=1}^{\lfloor 1/\Delta\rfloor}r^*_{j\Delta}r'^*_{j\Delta}\right)\underline{b}_k-\lambda_k\left(\frac{1}{p}\underline{b}'_k\underline{b}_k-1\right)-\sum_{l\neq k}^{K}\mu_{kl}\underline{b}'_k\underline{b}_l$$

By resolving for $\underline{b}_k$

$$\frac{\partial L}{\partial \underline{b}_k} = \frac{2}{p}\sum_{j=1}^{\lfloor 1/\Delta \rfloor}\left[r^*_{j\Delta}r^{*'}_{j\Delta}\right]\underline{b}_k - \frac{2\lambda_k}{p}\underline{b}_k - \sum_{l\neq k}\mu_{kl}\underline{b}_l$$

$$\frac{\partial L}{\partial b} = 0 \Longleftrightarrow \frac{2}{p}\sum_{j=1}^{\lfloor 1/\Delta \rfloor}\left[r^*_{j\Delta}r^{*'}_{j\Delta}\right]\underline{b}_k - \frac{2\lambda_k}{p}\underline{b}_k - \sum_{l\neq k}\mu_{kl}\underline{b}_l = 0$$

By a left multiplication by $\underline{b}'_m$ ($\forall m \neq k$)

$$\begin{aligned}
& \frac{2}{p}\underline{b}'_m\sum_{j=1}^{\lfloor 1/\Delta \rfloor}\left[r^*_{j\Delta}r^{*'}_{j\Delta}\right]\underline{b}_k - \frac{2\lambda_k}{p}\underline{b}'_m\underline{b}_k - \sum_{l\neq k}\mu_{kl}\underline{b}'_m\underline{b}_l = 0\\
\Leftrightarrow\ & \frac{2}{p}\sum_{j=1}^{\lfloor 1/\Delta \rfloor}\underline{b}'_m\left[r^*_{j\Delta}r^{*'}_{j\Delta}\right]\underline{b}_k - \frac{2\lambda_k}{p}\underline{b}'_m\underline{b}_k - \mu_{km}\underline{b}'_m\underline{b}_m = 0\\
\Leftrightarrow\ & \mu_{km} = 0
\end{aligned}$$

The third equation comes from the uncorrelation assumption of factors and the identification constraint on loadings. Hence, $\forall m \neq k$, $\mu_{km} = 0$. We deduce that

$$\frac{2}{p}\sum_{j=1}^{\lfloor 1/\Delta \rfloor}\left[r^*_{j\Delta}r^{*'}_{j\Delta}\right]\underline{b}_k - \frac{2\lambda_k}{p}\underline{b}_k = 0$$

This is equivalent to

$$\sum_{j=1}^{\lfloor 1/\Delta \rfloor}\left[r^*_{j\Delta}r^{*'}_{j\Delta}\right]\underline{b}_k - \lambda_k\underline{b}_k = 0$$

It follows that $\underline{b}_k$ is an eigenvector associated to the matrix $\sum_{j=1}^{\lfloor 1/\Delta \rfloor}\left[r^*_{j\Delta}r^{*'}_{j\Delta}\right]$.

2.9 Factor structure in the noise

In order to underscore the empirical relevance of factor structures in the market microstructure noise component, we consider a sample of 384 stocks (as further described in Section 2.4) for all trading days from 2006 to 2011. For each trading days, we compute the realized covariance matrix and we divide it by $2n$, where n is the number of intraday transaction times after synchronization. By doing so, we get an estimator of the covolatility of the microstructure noise. The next step consists on a spectral decomposition of the obtained matrix. The following figure plots the ratio of the sum of the largest eigenvalues (the biggest eigenvalue, the first two biggest eigenvalues, the first three biggest eigenvalues, until the first six biggest eigenvalues) to the total sum of eigenvalues: these ratios can been interpreted as the part of the total variability explained by the considered factors (the first factor, the first two factors, until the first six factors).

Figure 2.3. Ratio of largest eigenvalues relative to the total variation

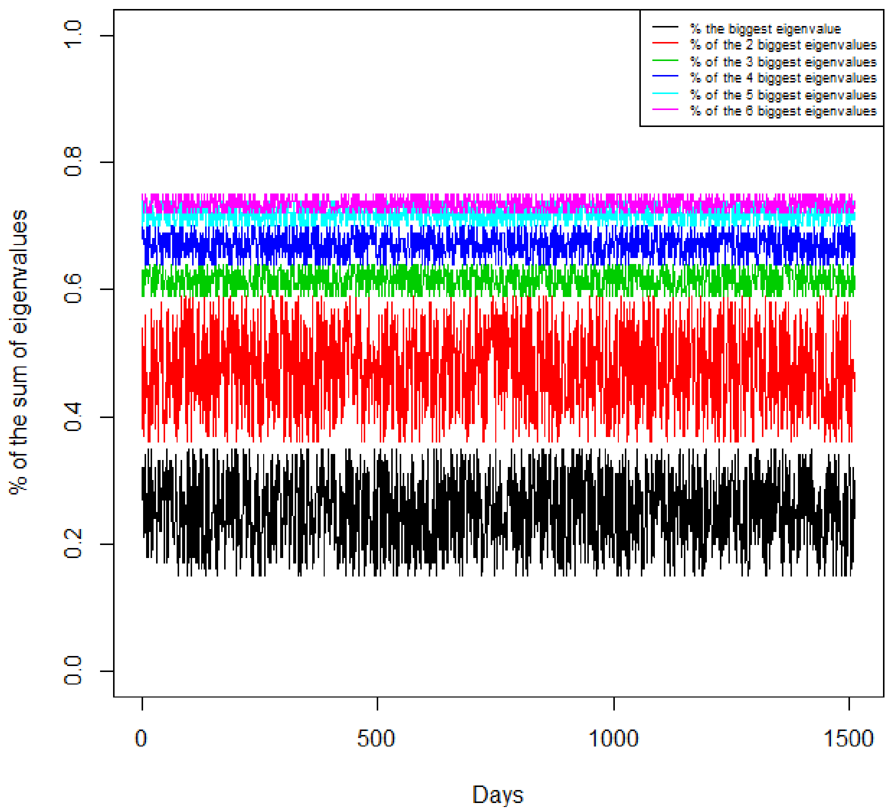

Consistent with the idea of a factor structure in the market microstructure noise component, the figure shows that the four largest eigenvalues of the noise covolatility matrix explain more than 60% of the total variability for each of the six different days.

2.10 Simulation design

Our simulation design replicates a two factor model in which the prices are observed with noise.

- The loading factors b is generated such that elements of the k^{th} column $\underline{b}_k$, for $k = 1, ..., K$, follow a normal law with mean 0 and standard deviation 1: $\underline{b}_{ik} \sim N(0,1)$, $\forall$ $i = 1, ..., p$.
- The two factor components in the frictionless return representation are generated by the following model:[24]
  - Factor 1

$$f_{1t} = \sigma_{f1t} dB_{1t}$$

    with B_{1t} a brownian motion and σ_{f1t} generated by a $GARCH$ diffusion model as in Andersen and Bollerslev (1998),

$$d\sigma^2_{f1t} = \kappa_{f1}\left(\theta_{f1} - \sigma^2_{f1t}\right) dt + \lambda_{f1}\sigma^2_{f1t} dW_{1t}$$

    with $Corr(W_{1t}, B_{1t}) = -0.5$, $\kappa_{f1} = 0.035$, $\theta_{f1} = 0.636$, $\phi_{f1} = 0.296$, $\lambda_{f1} = \sqrt{2\kappa_{f1}\phi_{f1}}$, $\sigma_{f10} = \theta_{f1}$
  - Factor 2

$$f_{2t} = \sigma_{f2t} dB_{2t}$$

    with B_{2t} a brownian motion and σ_{f2t} generated by a $GARCH$ diffusion model as in Andersen and Bollerslev (1998),

$$d\sigma^2_{f2t} = \kappa_{f2}\left(\theta_{f2} - \sigma^2_{f2t}\right) dt + \lambda_{f2}\sigma^2_{f2t} dW_{2t}$$

    with $Corr(W_{2t}, B_{2t}) = -0.5$, $\kappa_{f2} = 0.035$, $\theta_{f2} = 0.3$, $\phi_{f2} = 0.296$, $\lambda_{f2} = \sqrt{2\kappa_{f2}\phi_{f2}}$, $\sigma_{f20} = \theta_{f2}$
- The idiosyncratic error term in the factor representation is assumed to satisfy

$$\varepsilon_{it} = \sigma_{it} dW^{\varepsilon}_{it}$$

[24] Recall that f_{kt} is assumed to be the return of some portfolio

with W_{it}^{ε} a brownian motion such that $W_{it}^{\varepsilon} \perp W_{1t}, W_{2t}$ and $W_{it}^{\varepsilon} \perp B_{1t}, B_{2t}$, with the spot volatility generated by three different representative models:

- For $1 \leq i \leq p/3$, the volatility of the idiosyncratic component is generated by a Nelson GARCH diffusion limit model as in Barndorff-Nielsen and Shephard (2002):

$$d(\sigma_{it}^2) = (0.1 - \sigma_{it}^2)\, dt + 0.2\sigma_{it}^2 dB_{it}^{\varepsilon},$$

  with $Corr(W_{it}^{\varepsilon},\, B_{it}^{\varepsilon}) = -0.3$ and $B_{it}^{\varepsilon} \perp W_{1t}, W_{2t}$ and $B_{it}^{\varepsilon} \perp B_{1t}, B_{2t}$;

- For $p/3 < i \leq 2p/3$, the volatility process is assumed to follow a geometric Ornstein-Uhlenbeck (OU) model as in Barndorff-Nielsen and Shephard (2002):

$$dlog(\sigma_{it}^2) = -0.6\,(0.157 + log(\sigma_{it}^2))\, dt + 0.25 dB_{it}^{\varepsilon},$$

  with $Corr(W_{it}^{\varepsilon},\, B_{it}^{\varepsilon}) = -0.3$ and $B_{it}^{\varepsilon} \perp W_t$ and $B_{it}^{\varepsilon} \perp B_t$;

- For $2p/3 < i \leq p$, the volatility follows a $GARCH$ diffusion model as in Andersen and Bollerslev (1998):

$$d\sigma_{it}^2 = \kappa_{\varepsilon}\,(\theta_{\varepsilon} - \sigma_{it}^2)\, dt + \gamma_{\varepsilon}\sigma_{it} dB_{it}^{\varepsilon},$$

  with $Corr(W_{it}^{\varepsilon},\, B_{it}^{\varepsilon}) = -0.3$ and $B_{it}^{\varepsilon} \perp W_t$ and $B_{it}^{\varepsilon} \perp B_t$; $\kappa_{\varepsilon} = 0.035$, $\theta_{\varepsilon} = 0.636$, $\gamma_{\varepsilon} = 0.296$, $\sigma_{i0} = \theta_{\varepsilon}$

- The slope in the factor representation of the microstructure noise is such that: $c_i \sim N(1,1)$, $\forall i = 1, ..., p$;

- As in Barndorff-Nielsen, Hansen, and Shephard (2008a), the variance of the microstructure noise of the asset i satisfies the equality: $Var(u_i) = \xi^2 \sqrt{\frac{1}{n}\sum_{t=1}^{n} \sigma_{it}^4}$, with ξ^2 the noise-to-signal ratio which takes values in $\{0.001, 0.005, 0.01\}$ and σ_{it} the spot volatility of the true price process of asset i at time t.

- The variance of the idiosyncratic component η_{it} in the factor representation of the microstructure noise is assumed to have a fraction $1/n^{1.1}$ of the total variance $Var(u_i)$. Then, the variance of the factor term in this representation is given by: $\sigma_g^2 = \frac{\left(\overline{Var(u)} - \overline{\sigma_{\eta}^2}\right)}{\bar{C_p^2}}$, with $\bar{C_p^2} = \frac{1}{p}\sum_{i=1}^{p} c_i^2$.

- g_t and η_{it} are such that: $g_t \sim N(0, \sigma_g^2)$ and $\eta_{it} \sim N(0, \frac{1}{n^{1.1}} Var(u_i))$.

2.11 Estimation of W

In order to confirm that the eigenvectors of $MRker$ provide reliable estimates for W, we simulate daily efficient price vectors of dimension $p \in \{50, 100, 300\}$. We consider three different levels of microstructure noise: low, median and high with noise-to-signal ratio equal to 0.001, 0.01 and 0.1, respectively. Prices are generated by the same two factor simulation design describe in Appendix 2.10. We compute the true covolatility matrix $MRker$ for each price path, and derive their spectral decompositions. The following figures illustrate the results for each of the different noise levels.

Figure 2.4. Eigenvectors estimation using the multirealized kernel $MRker$: low noise

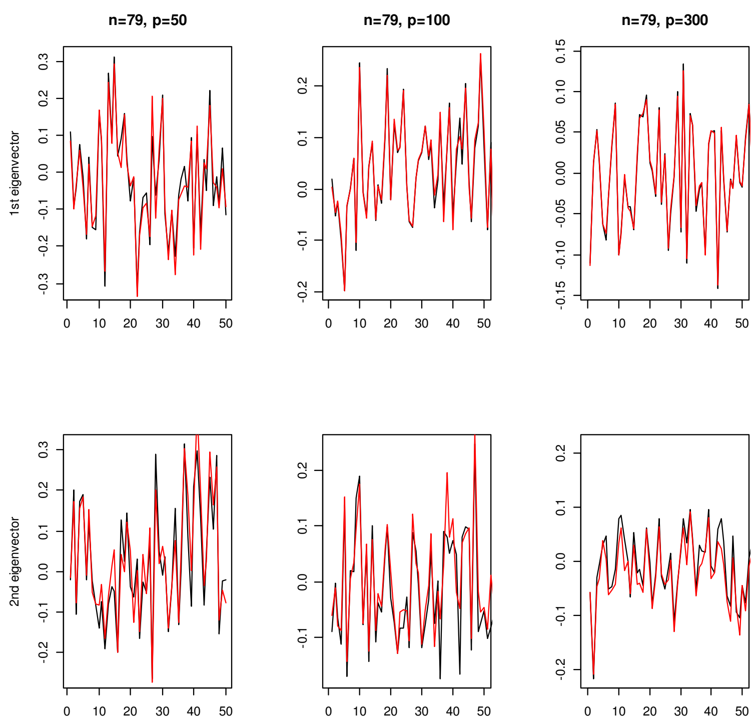

Figure 2.5. Eigenvectors estimation using the multirealized kernel $MRker$: medium noise

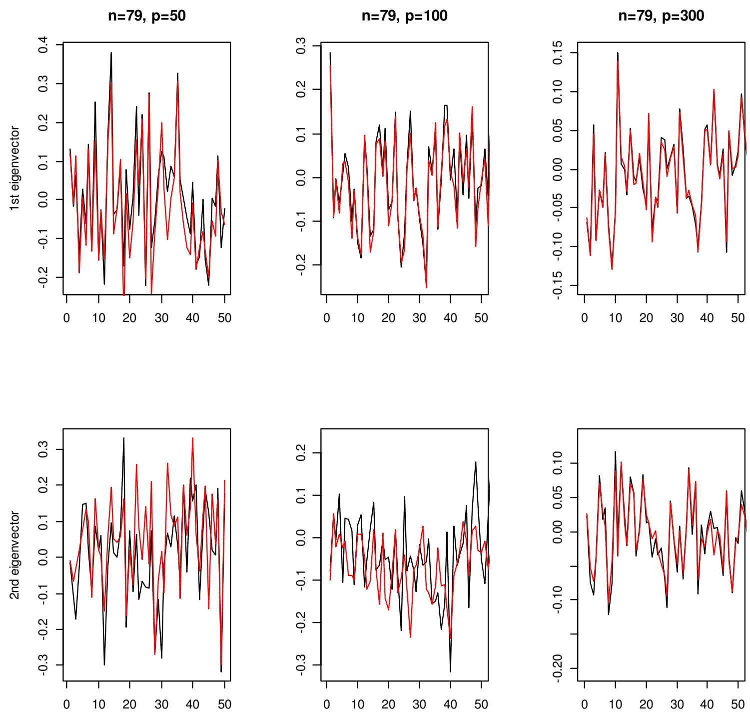

Figure 2.6. Eigenvectors estimation using the multirealized kernel $MRker$: high noise

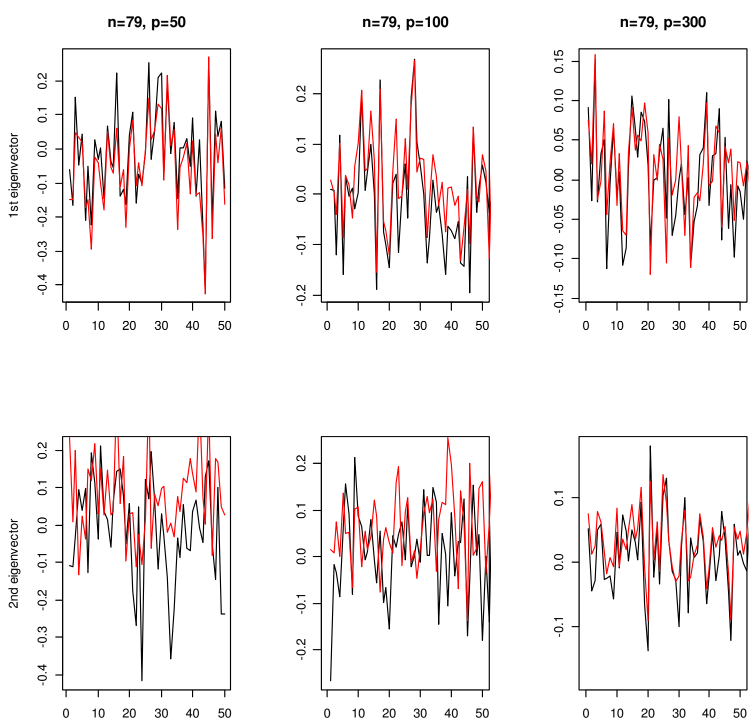

As is evident from the figures, the first two eigenvectors of the latent covolatility matrix are well estimated by the eigenvectors of the $MRker$ matrix. For low noise levels the two are almost indistinguishable, but there is also a close coherence for the high noise case.

Table 2.4. Simulation results: Synchronous prices, Sampling Frequency=5min, $K = 1$, High noise

Signal-to-noise ratio $\xi^2 = 0.01$					
Number of assets: N=50					
	Covariance	Correlation	Inverse	Diag	Off-Diag
$\hat{\Sigma}$	1.818	1.233	7.688	13.69	213.6
	(0.685)	*(0.267)*	*(0.368)*		
MRker	2.345	1.758	7461	16.34	316.6
	(0.641)	*(0.234)*	*(194079)*		
MRC^{δ}	2.336	1.782	6184	15.30	299.5
	(0.523)	*(0.214)*	*(7767)*		
$\hat{\Sigma}_{comp}$	2.311	1.721	5.002	22.84	305.1
	(0.653)	*(0.232)*	*(1.138)*		
$PCA-PRV$	2.307	1.703	9.954	15.303	294.1
	(0.543)	*(0.225)*	*(15.06)*		
$POET$	4.618	4.303	375.3	116.2	979.4
	(0.371)	*(0.212)*	*(22.69)*		
Number of assets: N=100					
	Covariance	Correlation	Inverse	Diag	Off-Diag
$\hat{\Sigma}$	2.584	1.592	10.07	26.28	824.3
	(1.137)	*(0.353)*	*(71.65)*		
MRker	3.047	2.350	NA	29.80	1171
	(0.987)	*(0.280)*	*NA*		
MRC^{δ}	3.059	2.431	NA	30.17	1118
	(0.831)	*(0.271)*	*NA*		
$\hat{\Sigma}_{comp}$	3.011	2.317	11.13	37.81	1145
	(0.994)	*(0.278)*	*(2.251)*		
$PCA-PRV$	2.941	2.254	9.235	30.17	1055
	(0.865)	*(0.277)*	*(19.78)*		
$POET$	5.479	5.915	557.6	173.1	2954
	(0.428)	*(0.291)*	*(89.52)*		
Number of assets: N=300					
	Covariance	Correlation	Inverse	Diag	Off-Diag
$\hat{\Sigma}$	4.437	2.795	26.42	74.68	7086
	(1.698)	*(0.492)*	*(101.3)*		
MRker	5.489	4.277	NA	90.93	11087
	(1.519)	*(0.489)*	*NA*		
MRC^{δ}	5.519	4.419	NA	88.827	10660
	(1.277)	*(0.447)*	*NA*		
$PCA-PRV$	5.207	4.052	7.684	88.82	9713
	(1.349)	*(0.472)*	*(6.266)*		
$POET$	10.31	10.96	NA	593.0	31542
	(0.825)	*(0.469)*	*NA*		
Number of assets: N=500					
	Covariance	Correlation	Inverse	Diag	Off-Diag
$\hat{\Sigma}$	5.980	3.631	31.30	167.3	24530
	(2.251)	*(0.637)*	*(176.5)*		
MRker	7.412	5.535	NA	167.3	33281
	(2.028)	*(0.653)*	*NA*		
MRC^{δ}	7.357	5.665	NA	154.9	31023
	(1.583)	*(0.579)*	*NA*		
$PCA-PRV$	6.942	5.187	34.67	154.9	28150
	(1.672)	*(0.607)*	*90.39*		
$POET$	14.05	14.19	NA	1089	99408
	(1.174)	*(0.607)*	*NA*		

Table 2.5. Simulation results: Synchronous prices, Sampling Frequency=5min, $K = 2$, Low noise

	Covariance	Correlation	Inverse	Diag	Off-Diag
Signal-to-noise ratio $\xi^2 = 0.001$					
Number of assets: N=50					
	Covariance	Correlation	Inverse	Diag	Off-Diag
$\hat{\Sigma}$	1.708	0.901	2.550	35.64	318.2
	(0.490)	*(0.137)*	*(4.176)*		
MRker	1.831	1.103	275.297	10.07	196.0
	(0.452)	*(0.121)*	*(98.92)*		
MRC^{δ}	1.801	1.098	145.7	9.303	184.4
	(0.422)	*(0.125)*	*(1075)*		
$\hat{\Sigma}_{comp}$	1.811	1.043	3.535	21.69	180.2
	(0.472)	*(0.126)*	*(0.356)*		
$PCA-PRV$	1.774	1.057	3.764	9.303	180.871
	(0.435)	*(0.127)*	*(2.493)*		
$POET$	4.954	1.281	486.5	166.2	1111.0
	(0.304)	*(0.274)*	*(45.21)*		
Number of assets: N=100					
	Covariance	Correlation	Inverse	Diag	Off-Diag
$\hat{\Sigma}$	2.423	1.252	2.870	60.65	1234
	(0.724)	*(0.175)*	*(4.69)*		
MRker	2.624	1.541	NA	19.49	808.9
	(0.679)	*(0.162)*	*NA*		
MRC^{δ}	2.559	1.521	NA	18.26	758.8
	(0.633)	*(0.168)*	*NA*		
$\hat{\Sigma}_{comp}$	2.559	1.455	3.779	41.26	753.1
	(0.699)	*(0.166)*	*(0.261)*		
$PCA-PRV$	2.486	1.439	9.421	18.26	726.7
	(0.650)	*(0.170)*	*(3.363)*		
$POET$	7.219	1.756	438.651	322.787	5009.923
	(0.494)	*(0.511)*	*(387.5)*		
Number of assets: N=300					
	Covariance	Correlation	Inverse	Diag	Off-Diag
$\hat{\Sigma}$	3.971	2.150	3.178	49.69	5565
	(1.024)	*(0.275)*	*(4.619)*		
MRker	4.362	2.711	NA	50.23	6544
	(0.955)	*(0.262)*	*NA*		
MRC^{δ}	4.258	2.674	NA	47.13	6202
	(0.907)	*(0.307)*	*NA*		
$\hat{\Sigma}_{comp}$	4.226	2.555	4.218	96.26	6146
	(0.981)	*(0.270)*	*(0.231)*		
$PCA-PRV$	4.039	2.453	7.425	47.13	5685
	0.939	0.307	1.504		
$POET$	11.65	2.561	NA	890.2	40660
	(0.828)	*(0.936)*	*NA*		
Number of assets: N=500					
	Covariance	Correlation	Inverse	Diag	Off-Diag
$\hat{\Sigma}$	5.438	2.797	3.256	99.40	18190
	(1.499)	*(0.378)*	*(14.04)*		
MRker	5.931	3.519	NA	99.90	21047
	(1.403)	*(0.349)*	*NA*		
MRC^{δ}	5.840	3.483	NA	94.04	19861
	(1.333)	*(0.368)*	*NA*		
$\hat{\Sigma}_{comp}$	5.785	3.352	4.550	180.4	20084
	(1.431)	*(0.362)*	*(0.347)*		
$PCA-PRV$	5.564	3.182	3.457	94.03	18261
	1.381	0.372	0.288	0.277	
$POET$	16.25	3.636	NA	1681	130959
	(1.155)	*(1.292)*	*NA*		

Table 2.6. Simulation results: Synchronous prices, Sampling Frequency=5min, $K = 2$, High noise

	Covariance	Correlation	Inverse	Diag	Off-Diag
Signal-to-noise ratio $\xi^2 = 0.01$					
Number of assets: N=50					
	Covariance	Correlation	Inverse	Diag	Off-Diag
$\hat{\Sigma}$	2.675	1.467	8.278	2301	22898
	(0.766)	*(0.326)*	*(35.81)*		
MRker	2.820	1.775	6861	23.41	443.3
	(0.693)	*(0.193)*	*(223603)*		
MRC^{δ}	2.799	1.799	4677	22.46	428.6
	(0.609)	*(0.180)*	*(6525)*		
$\hat{\Sigma}_{comp}$	2.774	1.735	3.778	34.11	424.4
	(0.708)	*(0.195)*	*(0.438)*		
$PCA-PRV$	2.771	1.745	8.385	22.46	422.6
	(0.632)	*(0.189)*	*(20.78)*		
$POET$	4.635	3.747	390.7	148.8	954.8
	(0.315)	*(0.233)*	*(21.55)*		
Number of assets: N=100					
	Covariance	Correlation	Inverse	Diag	Off-Diag
$\hat{\Sigma}$	3.844	2.032	13.35	41.93	1535
	(1.050)	*(0.480)*	*(50.55)*		
MRker	4.070	2.480	NA	41.08	1931
	(0.851)	*(0.283)*	*NA*		
MRC^{δ}	4.111	2.517	NA	42.33	1910
	(0.791)	*(0.262)*	*NA*		
$\hat{\Sigma}_{comp}$	4.023	2.434	4.867	55.67	1875
	(0.860)	*(0.286)*	*(0.762)*		
$PCA-PRV$	4.002	2.385	8.253	42.33	1834
	(0.827)	*(0.270)*	*(16.03)*		
$POET$	6.700	5.598	550.7	282.0	4604
	(0.397)	*(0.330)*	*(60.31)*		
Number of assets: N=300					
	Covariance	Correlation	Inverse	Diag	Off-Diag
$\hat{\Sigma}$	6.803	3.582	26.42	135.3	14831
	1.971	*0.780*	*0.275*		
MRker	7.312	4.290	NA	144.1	18516
	(1.760)	*(0.482)*	*NA*		
MRC^{δ}	7.262	4.338	NA	144.4	18118
	(1.552)	*(0.453)*	*NA*		
$PCA-PRV$	6.996	4.091	7.259	144.4	17084
	(1.612)	*(0.474)*	*(3.043)*		
$POET$	12.08	9.595	NA	913.7	43662
	(0.749)	*(0.569)*	*NA*		
Number of assets: N=500					
	Covariance	Correlation	Inverse	Diag	Off-Diag
$\hat{\Sigma}$	9.042	4.566	29.59	262.2	48451
	(2.645)	*(1.100)*	*(100.5)*		
MRker	9.622	5.467	NA	262.1	53310
	(2.367)	*(0.640)*	*NA*		
MRC^{δ}	9.485	5.561	NA	261.3	52004
	(2.118)	*(0.608)*	*NA*		
$PCA-PRV$	9.148	5.221	31.94	261.3	48969
	(2.192)	*(0.618)*	*0.435*		
$POET$	16.47	12.56	NA	1746	134674
	(1.183)	*(0.803)*	*NA*		

Table 2.7. Simulation results: Synchronous prices, Sampling Frequency=5min, $K = 3$, High noise

Signal-to-noise ratio $\xi^2 = 0.01$					
Number of assets: N=50					
	Covariance	Correlation	Inverse	Diag	Off-Diag
$\hat{\Sigma}$	3.129	1.677	6.646	26.46	534.9
	(0.715)	*(0.307)*	*(24.48)*		
MRker	3.368	1.689	6502.835	29.43	608.8
	(0.690)	*(0.193)*	*(60478)*		
MRC^{δ}	3.391	1.703	4911	29.95	602.1
	(0.635)	*(0.196)*	*(6063)*		
$\hat{\Sigma}_{comp}$	3.340	1.660	3.775	43.04	585.9
	(0.700)	*(0.196)*	*(0.318)*		
$PCA-PRV$	3.425	1.689	7.011	29.952	615.430
	(0.682)	*(0.226)*	*(5.320)*		
$POET$	5.149	3.565	357.4	185.9	1148
	(0.292)	*(0.249)*	*(18.62)*		
Number of assets: N=100					
	Covariance	Correlation	Inverse	Diag	Off-Diag
$\hat{\Sigma}$	4.675	2.451	12.11	56.65	2465
	(1.089)	*(0.519)*	*(166.9)*		
MRker	4.876	2.440	NA	60.54	2590
	(0.928)	*(0.259)*	*NA*		
MRC^{δ}	4.946	2.457	NA	61.15	2579
	(0.892)	*(0.253)*	*NA*		
$\hat{\Sigma}_{comp}$	4.826	2.396	5.356	84.10	2515
	(0.939)	*(0.264)*	*(0.864)*		
$PCA-PRV$	4.934	2.447	6.388	61.146	2596.268
	(0.969)	*(0.330)*	*(5.928)*		
$POET$	7.808	5.295	555.9	428.7	5884
	(0.453)	*(0.335)*	*(51.19)*		
Number of assets: N=300					
	Covariance	Correlation	Inverse	Diag	Off-Diag
$\hat{\Sigma}$	7.606	4.227	16.96	180.8	22110
	(1.805)	*(0.614)*	*(40.63)*		
MRker	8.071	4.213	NA	176.7	22003
	(1.721)	*(0.407)*	*NA*		
MRC^{δ}	8.144	4.266	NA	180.8	21963
	(1.540)	*(0.396)*	*NA*		
$PCA-PRV$	8.143	4.288	23.62	180.8	22110
	(1.712)	*(0.591)*	*(4.845)*		
$POET$	12.14	9.009	NA	1095	43556
	(0.739)	*(0.574)*	*NA*		
Number of assets: N=500					
	Covariance	Correlation	Inverse	Diag	Off-Diag
$\hat{\Sigma}$	9.619	5.273	36.160	257.9	51680
	(2.216)	*(0.991)*	*(176.9)*		
MRker	10.32	5.458	NA	276.9	59517
	(2.137)	*(0.540)*	*NA*		
MRC^{δ}	10.37	5.523	NA	285.9	59899
	(2.106)	*(0.544)*	*NA*		
$PCA-PRV$	10.25	5.462	38.42	285.9	59699
	(2.318)	*(0.777)*	*179.7*		
$POET$	15.45	11.96	NA	1766	118785
	(0.998)	*(0.763)*	*NA*		

Table 2.8. Simulation results: Synchronous prices, Sampling Frequency=5min, $K = 4$, High noise

	Covariance	Correlation	Inverse	Diag	Off-Diag
Signal-to-noise ratio $\xi^2 = 0.01$					
Number of assets: N=50					
$\hat{\Sigma}$	4.037	1.708	4.581	43.629	970.002
	1.234	*0.201*	*5.785*		
MRker	4.011	1.692	6199.281	43.629	953.945
	1.222	*0.197*	*29868.210*		
MRC^{δ}	3.993	1.705	4640.197	41.786	889.712
	0.962	*0.185*	*7034.374*		
$PCA - PRV$	4.068	1.739	6.011	41.786	919.580
	1.001	0.209	9.516		
$POET$	6.705	3.573	346.307	249.893	2014.248
	0.457	*0.243*	*16.055*		
Number of assets: N=100					
$\hat{\Sigma}$	5.446	2.364	6.178	82.130	3306.777
	1.240	*0.260*	*9.254*		
MRker	5.384	2.355	NA	82.130	3265.596
	1.224	*0.249*	*NA*		
MRC^{δ}	5.383	2.377	NA	84.718	3228.142
	1.133	*0.251*	*NA*		
$PCA - PRV$	5.506	2.420	4.883	84.718	3344.141
	1.204	0.286	7.228		
$POET$	8.226	4.896	518.627	492.257	6320.638
	0.502	*0.350*	*26.906*		
Number of assets: N=300					
$\hat{\Sigma}$	9.290	4.188	10.746	221.483	29644.100
	2.085	*0.445*	*24.31*		
MRker	9.302	4.186	NA	221.483	29681.950
	2.064	*0.421*	*NA*		
MRC^{δ}	9.389	4.252	NA	224.378	29448.470
	1.898	*0.408*	*NA*		
$PCA - PRV$	9.543	4.353	13.37	224.3	30318
	2.016	*0.528*	*4.719*		
$POET$	14.411	9.106	NA	1446.328	61600.530
	0.952	*0.612*	*NA*		
Number of assets: N=500					
$\hat{\Sigma}$	10.746	5.381	16.14	10.165	64240.270
	2.037	*0.510*	*47.51*		
MRker	10.792	5.445	NA	310.165	64937.160
	2.007	*0.475*	*NA*		
MRC^{δ}	10.906	5.526	NA	317.049	65213.200
	1.848	*0.493*	*NA*		
$PCA - PRV$	11.027	5.592	16.26	317.049	66440.870
	1.996	0.635	4.531		
$POET$	15.511	11.465	NA	1988.647	120393.340
	0.936	*0.755*	*NA*		

Table 2.9. Simulation results: Synchronous prices, Sampling Frequency=5min, $K = 5$, High noise

Signal-to-noise ratio $\xi^2 = 0.01$					
Number of assets: N=50					
	Covariance	Correlation	Inverse	Diag	Off-Diag
$\hat{\Sigma}$	3.988	1.701	4.640	39.695	866.751
	0.912	*0.197*	*6.337*		
MRker	3.947	1.688	6090.921	39.695	851.667
	0.902	*0.194*	*58262.954*		
MRC^δ	3.921	1.715	4437.210	40.095	839.118
	0.852	*0.191*	*6254.129*		
$PCA-PRV$	4.031	1.756	4.826	40.095	882.369
	0.899	0.217	4.178		
$POET$	6.161	3.553	331.220	239.196	1682.909
	0.401	*0.265*	*15.638*		
Number of assets: N=100					
	Covariance	Correlation	Inverse	Diag	Off-Diag
$\hat{\Sigma}$	4.734	2.377	6.181	58.74	2448
	0.934	*0.249*	*7.226*		
MRker	4.761	2.414	NA	58.746	2470.152
	0.917	*0.240*	*NA*		
MRC^δ	4.823	2.438	NA	59.484	2470.405
	0.839	*0.235*	*NA*		
$PCA-PRV$	4.823	2.436	4.757	59.484	2505.438
	0.893	0.282	7.067		
$POET$	6.726	4.762	488.530	384.193	4160.014
	0.369	*0.303*	*22.880*		
Number of assets: N=300					
	Covariance	Correlation	Inverse	Diag	Off-Diag
$\hat{\Sigma}$	8.913	4.108	10.71	209.4	26550
	1.748	*0.405*	*14.42*		
MRker	9.009	4.184	NA	209.404	27052.980
	1.726	*0.393*	*NA*		
MRC^δ	9.041	4.222	NA	214.609	27031.750
	1.645	*0.399*	*NA*		
$PCA-PRV$	9.170	4.302	13.35	214.6	27684
	1.787	*0.527*	*3.410*		
$POET$	12.888	8.735	NA	1331.835	48912.060
	0.788	*0.617*	*NA*		
Number of assets: N=500					
	Covariance	Correlation	Inverse	Diag	Off-Diag
$\hat{\Sigma}$	11.417	5.363	14.46	348.2	72834.800
	2.388	*0.546*	*20.89*		
MRker	11.549	5.466	NA	348.2	74332
	2.361	*0.532*	*NA*		
MRC^δ	11.537	5.534	NA	353.803	73584.290
	2.196	*0.535*	*NA*		
$PCA-PRV$	11.787	5.669	16.390	353.803	75752.390
	2.355	0.656	3.220		
$POET$	16.329	11.163	NA	2149.455	132573.010
	1.073	*0.792*	*NA*		

Table 2.14. Asynchronous prices, Sampling Frequency=5min, $K = 4$

	Covariance	Correlation	Inverse	Diag	Off-Diag
Signal-to-noise ratio $\xi^2 = 0.01$					
Number of assets: N=50					
$\hat{\Sigma}$	5.967	2.504	3.611	70.989	1715.118
	0.481	*0.145*	*0.170*		
MRker	6.127	2.714	4358.820	80.787	1804.064
	0.475	*0.160*	*60242.320*		
MRC^{δ}	6.107	2.672	1412.715	79.490	1784.155
	0.470	*0.149*	*4273.349*		
$PCA - PRV$	6.053	2.610	4.512	79.490	1757.607
	0.479	0.161	6.031		
$POET$	6.757	3.217	239.251	248.195	2072.353
	0.470	*0.133*	*38.075*		
Number of assets: N=100					
$\hat{\Sigma}$	5.837	3.035	3.604	90.274	3308.031
	0.333	*0.127*	*0.188*		
MRker	6.102	3.475	NA	109.339	3611.086
	0.335	*0.139*	*NA*		
MRC^{δ}	6.101	3.433	NA	106.142	3617.816
	0.335	*0.162*	*NA*		
$PCA - PRV$	6.021	3.257	4.810	106.142	3517.404
	0.349	0.168	10.782		
$POET$	6.554	3.957	284.599	355.956	3985.780
	0.349	*0.154*	*286.727*		
Number of assets: N=300					
$\hat{\Sigma}$	11.868	5.387	4.534	281.265	43113
	0.754	*0.162*	*0.244*		
MRker	12.566	6.207	NA	363.867	47669.990
	0.762	*0.198*	*NA*		
MRC^{δ}	12.527	6.120	NA	351.565	47551.680
	0.767	*0.286*	*NA*		
$PCA - PRV$	12.317	5.725	3.603	351.565	45909.100
	0.781	0.264	11.014		
$POET$	14.058	6.626	NA	1332.691	59404.770
	0.859	*0.266*	*NA*		
Number of assets: N=500					
$\hat{\Sigma}$	14.676	6.979	5.911	450.438	108472.500
	1.127	*0.255*	*0.256*		
MRker	15.569	8.141	NA	571.719	120045.100
	1.080	*0.281*	*NA*		
MRC^{δ}	15.521	7.906	NA	535.546	119769.300
	1.063	*0.332*	*NA*		
$PCA - PRV$	15.243	7.475	3.433	535.546	116003.200
	1.078	0.303	2.749		
$POET$	16.912	8.643	NA	2050.302	143111.900
	1.263	*0.354*	*NA*		

Table 2.10. Simulation results: Synchronous prices, Sampling Frequency=5min, $K = 1$, Medium noise, correlated noise

Signal-to-noise ration: $\xi^2 = 0.005$					
Number of assets: N=50					
	Covariance	Correlation	Inverse	Diag	Off-Diag
$\hat{\Sigma}$	1.829	0.960	2.502	18.170	219.713
	(0.814)	*(0.180)*	*(11.02)*		
MRker	2.117	1.442	5737	16.639	276.5
	(0.723)	*(0.145)*	*(217998)*		
MRC^{δ}	1.887	1.395	187.2	10.62	197.6
	(0.472)	*(0.148)*	*(2651)*		
$\hat{\Sigma_{comp}}$	2.109	1.397	5.306	27.71	266.2
	(0.739)	*(0.144)*	*(1.056)*		
$PCA-PRV$	1.876	1.358	4.251	10.62	197.3
	(0.478)	*(0.151)*	*(4.094)*		
$POET$	5.428	1.544	470.4	167.4	1329
	(0.424)	*(0.226)*	*(39.32)*		
Number of assets: N=100					
	Covariance	Correlation	Inverse	Diag	Off-Diag
$\hat{\Sigma}$	1.859	1.329	2.511	16.79	473.6
	(0.724)	*(0.200)*	*(7.467)*		
MRker	2.334	1.992	NA	16.06	672.1
	(0.666)	*(0.213)*	*NA*		
MRC^{δ}	2.104	1.963	NA	11.51	491.9
	(0.449)	*(0.225)*	*NA*		
$\hat{\Sigma_{comp}}$	2.290	1.940	6.351	21.93	646.2
	(0.677)	*(0.211)*	*(1.238)*		
$PCA-PRV$	2.030	1.849	8.606	11.51	461.0
	(0.467)	*(0.237)*	*(3.533)*		
$POET$	5.200	1.516	284.9	164.6	2585
	(0.442)	*(0.404)*	*(1754)*		
Number of assets: N=300					
	Covariance	Correlation	Inverse	Diag	Off-Diag
$\hat{\Sigma}$	3.732	2.217	2.747	68.185	5636.770
	(1.453)	*(0.269)*	*(3.142)*		
MRker	4.526	3.431	NA	71.36	7991
	(1.343)	*(0.254)*	*NA*		
MRC^{δ}	4.104	3.356	NA	49.09	5727
	(1.013)	*(0.323)*	*NA*		
$\hat{\Sigma_{comp}}$	4.499	3.386	18.46	89.21	7895
	(1.349)	*(0.252)*	*(2.533)*		
$PCA-PRV$	3.882	3.092	6.972	49.09	5210
	(1.043)	*(0.308)*	*(1.877)*		
$POET$	10.70	2.344	NA	681.4	34203
	(0.882)	*(0.929)*	*NA*		
Number of assets: N=500					
	Covariance	Correlation	Inverse	Diag	Off-Diag
$\hat{\Sigma}$	4.839	2.971	2.846	113.168	15501.250
	1.806	*0.404*	*1.981*		
MRker	5.873	4.493	NA	113.085	21355.820
	1.386	*0.453*	*NA*		
MRC^{δ}	5.338	4.422	NA	78.921	15866
	(0.970)	*(0.475)*	*NA*		
$\hat{\Sigma_{comp}}$	5.848	4.460	NA	129.1	21199
	(1.391)	*(0.453)*	NA		
$PCA-PRV$	5.017	3.951	3.112	78.92	14204
	(1.008)	*(0.502)*	1.997		
$POET$	14.19	3.046	NA	1187	99332
	(1.114)	*(0.737)*	*NA*		

Table 2.11. Simulation results: Asynchronous prices, Sampling Frequency=5min, $K = 2$, Medium noise, correlated noise

	Covariance	Correlation	Inverse	Diag	Off-Diag
Panel A: Low noise ($\xi^2 = 0.005$)					
Number of assets: N=50					
$\hat{\Sigma}$	3.727	2.153	3.282	31.63	668.0
	0.289	*0.151*	*0.241*		
MRker	3.938	2.491	4573	33.14	747.4
	0.303	*0.137*	*33330*		
MRC^{δ}	3.868	2.413	208.6	29.29	722.6
	0.290	*0.120*	*1312*		
$\hat{\Sigma_{comp}}$	3.864	2.424	3.813	32.498	717.8
	0.296	0.128	0.173		
$PCA-PRV$	3.815	2.335	5.361	29.291	702.347
	0.294	0.131	4.119		
$POET$	4.666	2.643	433.1	135.4	971.1
	0.322	*0.117*	*68.99*		
Number of assets: N=100					
	Covariance	Correlation	Inverse	Diag	Off-Diag
$\hat{\Sigma}$	6.139	3.172	3.229	77.94	3756
	0.506	*0.199*	*0.372*		
MRker	6.496	3.586	NA	81.45	4140
	0.568	*0.200*	*NA*		
MRC^{δ}	6.371	3.500	NA	68.61	3989
	0.529	*0.186*	*NA*		
$\hat{\Sigma_{comp}}$	6.312	3.499	4.836	72.44	3943
	0.515	0.165	0.305		
$PCA-PRV$	6.329	3.372	7.729	68.61	3900
	0.536	0.203	2.684		
$POET$	7.758	3.819	394.7	333.7	5759
	0.574	*0.170*	*440.5*		
Number of assets: N=300					
	Covariance	Correlation	Inverse	Diag	Off-Diag
$\hat{\Sigma}$	9.720	5.254	3.133	211.0	28502
	0.682	*0.227*	*0.277*		
MRker	10.45	6.258	NA	236.1	32742
	0.711	*0.252*	*NA*		
MRC^{δ}	10.18	5.991	NA	198.8	31405
	0.705	*0.269*	*NA*		
$\hat{\Sigma_{comp}}$	10.15	5.940	5.865	182.4	30789
	0.688	0.223	0.237		
$PCA-PRV$	10.02	5.694	4.903	198.8	30416
	0.713	0.272	10.50		
$POET$	12.03	6.544	NA	867.0	42874
	0.787	*0.280*	*NA*		
Number of assets: N=500					
	Covariance	Correlation	Inverse	Diag	Off-Diag
$\hat{\Sigma}$	13.64	6.692	3.212	449.6	93345
	0.991	*0.302*	*0.270*		
MRker	14.63	7.977	NA	502.3	106688
	1.064	*0.314*	*NA*		
MRC^{δ}	14.32	7.620	NA	430.0	102831
	1.034	*0.318*	*NA*		
$\hat{\Sigma_{comp}}$	14.20	7.580	6.038	370.2	100502
	0.997	0.271	0.182		
$PCA-PRV$	14.12	7.209	5.888	430.0	99859
	1.042	0.325	10.86		
$POET$	17.02	8.159	NA	1737	141842
	1.200	*0.331*	*NA*		

Table 2.12. Asynchronous prices, Sampling Frequency=5min, $K = 1$

	Covariance	Correlation	Inverse	Diag	Off-Diag
Signal-to-noise ratio $\xi^2 = 0.01$					
Number of assets: N=50					
$\hat{\Sigma}$	3.403	2.164	3.002	21.873	566.696
	(0.331)	*(0.194)*	*(0.214)*		
MRker	3.690	2.547	5985	25.37	655.6
	(0.329)	*(0.192)*	*(636880)*		
MRC^{δ}	3.651	2.506	2251	25.57	646.3
	(0.322)	*(0.186)*	*(3624)*		
$\hat{\Sigma}_{comp}$	3.613	2.469	4.462	24.50	631.5
	(0.309)	*(0.157)*	*(0.328)*		
$PCA-PRV$	3.581	2.396	9.760	25.58	625.5
	(0.327)	*(0.196)*	*(7.680)*		
$POET$	4.252	3.326	337.89	92.54	838.4
	(0.313)	*(0.113)*	*(64.63)*		
Number of assets: N=100					
	Covariance	Correlation	Inverse	Diag	Off-Diag
$\hat{\Sigma}$	6.795	3.514	3.188	74.988	4657.375
	(0.630)	*(0.235)*	*(0.224)*		
MRker	7.248	4.074	NA	95.66	5227
	(0.646)	*(0.252)*	*NA*		
MRC^{δ}	7.258	4.046	NA	96.119	5182
	(0.635)	*(0.242)*	*NA*		
$\hat{\Sigma}_{comp}$	7.062	3.946	6.483	88.01	4967
	(0.591)	*(0.219)*	*(0.584)*		
$PCA-PRV$	7.163	3.857	10.86	96.119	5049
	(0.642)	*(0.253)*	*(13.31)*		
$POET$	8.789	5.008	484.8	332.281	7491
	(0.651)	*(0.191)*	*(406.6)*		
Number of assets: N=300					
	Covariance	Correlation	Inverse	Diag	Off-Diag
$\hat{\Sigma}$	9.109	5.483	8.822	144.7	25457
	(0.799)	*(0.326)*	*(0.190)*		
MRker	9.907	6.759	NA	186.9	29961
	(0.848)	*(0.374)*	*NA*		
MRC^{δ}	9.833	6.633	NA	176.4	29540
	(0.819)	*(0.364)*	*NA*		
$PCA-PRV$	9.601	6.223	9.318	176.39	28192
	(0.833)	*(0.376)*	*(9.233)*		
$POET$	11.21	8.259	NA	656.8	37695
	(0.916)	*(0.285)*	*NA*		
Number of assets: N=500					
	Covariance	Correlation	Inverse	Diag	Off-Diag
$\hat{\Sigma}$	11.86	7.079	11.77	269.0	70047
	(1.000)	*(0.409)*	*(0.171)*		
MRker	12.80	8.706	NA	334.3	82166
	(1.000)	*(0.440)*	*NA*		
MRC^{δ}	12.76	8.538	NA	324.2	81195.840
	(0.982)	*(0.447)*	*NA*		
$PCA-PRV$	12.46	7.969	13.06	324.2	77288
	(0.999)	*(0.447)*	*0.211*		
$POET$	14.35	10.57	NA	1114	103646
	(1.099)	*(0.353)*	*NA*		

Table 2.13. Asynchronous prices, Sampling Frequency=5min, $K = 3$

Signal-to-noise ratio $\xi^2 = 0.01$					
Number of assets: N=50					
	Covariance	Correlation	Inverse	Diag	Off-Diag
$\hat{\Sigma}$	4.249	2.073	3.514	28.32	878.6
	(0.283)	*(0.102)*	*(0.200)*		
MRker	4.525	2.373	5271	37.98	1002
	(0.341)	*(0.107)*	*(15556)*		
MRC^{δ}	4.491	2.312	1399	36.96	979.9
	(0.297)	*(0.113)*	*(1501)*		
$\hat{\Sigma}_{comp}$	4.356	2.248	4.849	38.74	916.9
	(0.268)	*(0.099)*	*(0.392)*		
$PCA-PRV$	4.438	2.202	5.052	36.96	961.09
	(0.310)	*(0.118)*	*(6.009)*		
$POET$	5.661	2.620	352.9	203.1	1427
	(0.300)	*(0.108)*	*(161.9)*		
Number of assets: N=100					
	Covariance	Correlation	Inverse	Diag	Off-Diag
$\hat{\Sigma}$	6.905	3.243	3.774	97.39	4711
	(0.466)	*(0.147)*	*(0.235)*		
MRker	7.230	3.616	NA	121.5	5189
	(0.476)	*(0.168)*	*NA*		
MRC^{δ}	7.174	3.516	NA	119.9	5112
	(0.458)	*(0.166)*	*NA*		
$\hat{\Sigma}_{comp}$	7.021	3.460	4.434	106.9	4881
	(0.459)	*(0.137)*	*(0.213)*		
$PCA-PRV$	7.051	3.362	6.471	119.9	4972
	(0.472)	*(0.173)*	*(12.52)*		
$POET$	8.247	4.050	316.685	440.608	6449.541
	(0.472)	*(0.146)*	*(231.2)*		
Number of assets: N=300					
	Covariance	Correlation	Inverse	Diag	Off-Diag
$\hat{\Sigma}$	10.57	5.420	5.993	259.8	33528
	(0.700)	*(0.221)*	*(12.70)*		
MRker	11.12	6.259	NA	323.4	37194
	(0.671)	*(0.212)*	*NA*		
MRC^{δ}	11.09	6.157	NA	307.7	37069
	(0.671)	*(0.253)*	*NA*		
$PCA-PRV$	10.88	5.785	4.412	307.6	35613
	(0.691)	*(0.261)*	*(13.37)*		
$POET$	12.14	6.969	NA	1099	44168
	(0.777)	*(0.233)*	*NA*		
Number of assets: N=500					
	Covariance	Correlation	Inverse	Diag	Off-Diag
$\hat{\Sigma}$	14.28	7.148	8.795	490.2	102280
	(0.986)	*(0.317)*	*(22.23)*		
MRker	15.04	8.259	NA	604.2	112820
	(0.942)	*(0.308)*	*NA*		
MRC^{δ}	14.98	8.097	NA	574.8	112529
	(0.943)	*(0.378)*	*NA*		
$PCA-PRV$	14.75	7.635	3.763	574.8	108431
	(0.970)	*(0.367)*	*(3.801)*		
$POET$	16.38	9.032	NA	1900	132647
	(1.072)	*(0.345)*	*NA*		

Table 2.25. Asynchronous prices, Sampling Frequency=1min, $K = 2$

Signal-to-noise ratio $\xi^2 = 0.01$					
Number of assets: N=50					
	Covariance	Correlation	Inverse	Diag	Off-Diag
$\hat{\Sigma}$	3.549	2.206	3.005	23.46	602.2
	0.273	*0.132*	*0.220*		
MRker	3.728	2.409	503.944	25.073	687.014
	0.272	*0.144*	*77.900*		
MRC^{δ}	3.673	2.389	155.423	25.177	673.813
	0.268	*0.137*	*307.990*		
$\hat{\Sigma_{comp}}$	3.632	2.353	3.867	24.183	653.677
	0.260	0.124	0.282		
$PCA-PRV$	3.625	2.294	5.746	25.177	653.366
	0.270	0.138	4.007		
$POET$	4.517	3.258	516.774	118.411	919.489
	0.286	*0.081*	*107.522*		
Number of assets: N=100					
	Covariance	Correlation	Inverse	Diag	Off-Diag
$\hat{\Sigma}$	6.048	3.306	3.593	99.06	3593
	0.680	*0.217*	*0.278*		
MRker	6.407	3.635	19661.696	67.218	4051.629
	0.531	*0.182*	*55683.470*		
MRC^{δ}	6.349	3.614	15532.681	63.905	4037.431
	0.537	*0.194*	*9748.741*		
$\hat{\Sigma_{comp}}$	6.266	3.543	4.584	62.598	3889.042
	0.494	0.143	0.209		
$PCA-PRV$	6.234	3.457	6.900	63.905	3895.525
	0.547	0.199	6.913		
$POET$	7.525	5.000	425.956	305.532	5382.059
	0.563	*0.137*	*249.791*		
Number of assets: N=300					
	Covariance	Correlation	Inverse	Diag	Off-Diag
$\hat{\Sigma}$	9.857	5.236	4.402	229.5	27765
	0.679	*0.243*	*0.225*		
MRker	10.272	5.801	NA	222.099	31940.730
	0.686	*0.217*	*NA*		
MRC^{δ}	10.206	5.724	NA	217.697	31744.340
	0.675	*0.213*	*NA*		
$PCA-PRV$	10.015	5.476	6.885	217.697	30625.980
	0.680	0.228	7.868		
$POET$	12.381	8.713	NA	941.205	44672.550
	0.816	*0.151*	*NA*		
Number of assets: N=500					
	Covariance	Correlation	Inverse	Diag	Off-Diag
$\hat{\Sigma}$	10.662	6.405	9.894	536.4	93371
	0.659	*0.319*	*0.151*		
MRker	11.269	7.489	NA	235.425	63823.950
	0.646	*0.336*	*NA*		
MRC^{δ}	11.242	7.505	NA	240.186	63362.090
	0.676	*0.335*	*NA*		
$PCA-PRV$	11.041	7.083	4.349	240.186	60979.120
	0.682	0.348	1.679		
$POET$	13.171	11.329	NA	997.334	88386.030
	1.012	*0.215*	*NA*		

Table 2.15. Asynchronous prices, Sampling Frequency=5min, $K = 5$

	Covariance	Correlation	Inverse	Diag	Off-Diag
Signal-to-noise ratio $\xi^2 = 0.01$					
Number of assets: N=50					
$\hat{\Sigma}$	4.818	2.128	3.742	79.790	1091.115
	0.388	*0.106*	*0.560*		
MRker	5.040	2.391	3983.302	63.686	1217.798
	0.380	*0.114*	*24531.540*		
MRC^{δ}	5.028	2.326	987.014	60.937	1201.145
	0.370	*0.120*	*2306.474*		
$PCA-PRV$	4.984	2.263	3.987	60.937	1187.083
	0.379	0.117	5.863		
$POET$	5.952	2.606	239.436	224.348	1558.666
	0.398	*0.103*	*59.179*		
Number of assets: N=100					
	Covariance	Correlation	Inverse	Diag	Off-Diag
$\hat{\Sigma}$	6.487	3.025	3.988	89.896	4180.667
	0.424	*0.112*	*0.157*		
MRker	6.800	3.438	NA	111.017	4512.112
	0.436	*0.139*	*NA*		
MRC^{δ}	6.788	3.374	NA	104.005	4494.498
	0.432	*0.158*	*NA*		
$PCA-PRV$	6.658	3.197	3.561	104.005	4354.841
	0.443	0.158	17.389		
$POET$	7.577	3.788	253.404	423.524	5414.165
	0.483	*0.142*	*64.306*		
Number of assets: N=300					
	Covariance	Correlation	Inverse	Diag	Off-Diag
$\hat{\Sigma}$	12.049	5.330	4.394	353.669	44164.960
	0.834	*0.182*	*0.224*		
MRker	12.596	6.158	NA	430.394	47721.310
	0.842	*0.219*	*NA*		
MRC^{δ}	12.576	6.063	NA	410.577	47682.990
	0.832	*0.288*	*NA*		
$PCA-PRV$	12.335	5.675	3.578	410.577	46026.020
	0.848	0.279	2.377		
$POET$	13.626	6.726	NA	1389.440	55991.250
	0.916	*0.261*	*NA*		
Number of assets: N=500					
	Covariance	Correlation	Inverse	Diag	Off-Diag
$\hat{\Sigma}$	14.403	6.818	5.719	505.900	104444.500
	0.924	*0.228*	*0.221*		
MRker	15.152	7.973	NA	634.692	114955.700
	0.908	*0.272*	*NA*		
MRC^{δ}	15.182	7.786	NA	615.791	115351.900
	0.898	*0.373*	*NA*		
$PCA-PRV$	14.946	7.326	3.395	615.791	110955.500
	0.923	0.331	1.278		
$POET$	16.513	8.576	NA	2064.410	133301.600
	1.002	*0.325*	*NA*		

Table 2.16. Synchronous prices, Sampling Frequency=1min, $K = 1$

Signal-to-noise ratio $\xi^2 = 0.01$					
Number of assets: N=50					
	Covariance	Correlation	Inverse	Diag	Off-Diag
$\hat{\Sigma}$	1.402	0.863	2.358	6.754	105.1
	0.531	*0.160*	*19.45*		
MRker	1.791	1.378	165.716	10.235	184.883
	0.456	*0.163*	*28.963*		
MRC^{δ}	1.711	1.332	244.412	9.264	169.660
	0.435	*0.145*	*332.178*		
$\hat{\Sigma_{comp}}$	1.788	1.370	4.872	14.972	180.890
	0.465	0.161	0.771		
$PCA-PRV$	1.694	1.291	5.718	9.264	169.208
	0.455	0.160	5.483		
$POET$	4.577	5.716	1581.676	124.820	1036.842
	0.349	*0.075*	*46.520*		
Number of assets: N=100					
	Covariance	Correlation	Inverse	Diag	Off-Diag
$\hat{\Sigma}$	1.859	1.329	2.510	16.792	473.631
	0.724	*0.200*	*7.467*		
MRker	2.334	1.992	NA	16.066	672.109
	0.666	*0.213*	*NA*		
MRC^{δ}	2.104	1.963	NA	11.511	491.949
	0.449	*0.225*	*NA*		
$\hat{\Sigma_{comp}}$	2.290	1.940	6.351	21.931	646.273
	0.677	0.211	1.238		
$PCA-PRV$	2.030	1.849	8.606	11.511	461.006
	0.467	0.237	3.533		
$POET$	5.200	1.516	284.952	164.678	2585.705
	0.442	*0.404*	*1754.719*		
Number of assets: N=300					
	Covariance	Correlation	Inverse	Diag	Off-Diag
$\hat{\Sigma}$	2.644	2.045	3.299	29.77	2969
	1.020	*0.356*	*0.180*		
MRker	4.074	3.370	NA	47.911	5845.232
	0.911	*0.358*	*NA*		
MRC^{δ}	3.982	3.308	NA	45.686	5528.287
	0.850	*0.310*	*NA*		
$\hat{\Sigma_{comp}}$	3.714	2.978	5.423	45.686	4956.766
	0.908	0.349	12.660		
$PCA-PRV$	3.714	2.978	5.422	45.68	4956
	0.908	*0.349*	*12.66*		
$POET$	10.32	14.12	NA	594.2	31913
	0.502	*0.124*	*96.510*		
Number of assets: N=500					
	Covariance	Correlation	Inverse	Diag	Off-Diag
$\hat{\Sigma}$	4.839	2.971	3.952	58.04	8880
	1.806	*0.404*	*1.981*		
MRker	5.873	4.493	NA	113.085	21355.820
	1.386	*0.453*	*NA*		
MRC^{δ}	5.338	4.422	NA	78.921	15866.410
	0.970	*0.475*	*NA*		
$PCA-PRV$	5.017	3.951	4.607	78.921	14204.250
	1.008	*0.502*	*7.675*		
$POET$	14.190	3.046	NA	1187.214	99332.680
	1.114	*0.737*	*NA*		

Table 2.17. Synchronous prices, Sampling Frequency=1min, $K = 2$

	Covariance	Correlation	Inverse	Diag	Off-Diag
Signal-to-noise ratio $\xi^2 = 0.01$					
Number of assets: N=50					
	Covariance	Correlation	Inverse	Diag	Off-Diag
$\hat{\Sigma}$	1.760	1.005	2.727	6.530	175.188
	0.468	*0.224*	*0.244*		
MRker	1.955	1.262	156.597	9.981	209.233
	0.393	*0.150*	*25.783*		
MRC^{δ}	1.925	1.241	232.436	9.524	198.566
	0.389	*0.143*	*291.456*		
$\hat{\Sigma_{comp}}$	1.938	1.254	3.640	14.271	202.336
	0.398	0.150	0.267		
$PCA-PRV$	1.909	1.194	5.220	9.524	197.967
	0.410	0.150	5.842		
$POET$	4.086	5.423	1588.886	104.949	739.163
	0.255	*0.090*	*46.261*		
Number of assets: N=100					
	Covariance	Correlation	Inverse	Diag	Off-Diag
$\hat{\Sigma}$	2.753	1.466	2.969	25.24	834.605
	0.684	*0.333*	*0.217*		
MRker	3.112	1.902	2385.393	25.76	1038.536
	0.559	*0.210*	*132.426*		
MRC^{δ}	3.022	1.837	3122.936	24.460	988.567
	0.578	*0.199*	*2346.389*		
$\hat{\Sigma_{comp}}$	3.092	1.888	5.199	36.085	1016.635
	0.564	0.210	0.690		
$PCA-PRV$	2.947	1.747	6.960	24.460	949.173
	0.607	0.216	9.510		
$POET$	6.987	7.794	2015.151	312.294	4575.535
	0.483	*0.114*	*158.396*		
Number of assets: N=300					
	Covariance	Correlation	Inverse	Diag	Off-Diag
$\hat{\Sigma}$	4.675	2.523	4.201	54.67	6092
	1.252	*0.540*	*0.180*		
MRker	5.439	3.283	NA	78.240	9564
	1.075	*0.344*	*NA*		
MRC^{δ}	5.228	3.181	NA	71.64	8947.801
	1.012	*0.312*	*NA*		
$PCA-PRV$	5.020	2.971	5.229	71.646	8327.332
	1.063	0.331	13.663		
$POET$	11.992	13.242	NA	883.875	42785.279
	0.907	*0.225*	*NA*		
Number of assets: N=500					
	Covariance	Correlation	Inverse	Diag	Off-Diag
$\hat{\Sigma}$	5.303	3.222	9.074	101.6	16153
	1.624	*0.707*	*0.177*		
MRker	6.949	4.355	NA	132.269	26740.610
	1.354	*0.451*	*NA*		
MRC^{δ}	6.723	4.210	NA	124.675	25079.080
	1.253	*0.412*	*NA*		
$PCA-PRV$	6.431	3.923	4.217	124.675	23217.030
	1.318	0.438	6.081		
$POET$	15.137	17.317	NA	1486.634	114542.250
	1.008	*0.256*	*NA*		

Table 2.18. Synchronous prices, Sampling Frequency=1min, $K = 3$

	Covariance	Correlation	Inverse	Diag	Off-Diag
Signal-to-noise ratio $\xi^2 = 0.01$					
Number of assets: N=50					
$\hat{\Sigma}$	2.325	1.153	3.343	11.383	280.158
	0.507	*0.266*	*6.195*		
MRker	2.857	1.373	2.886	19.650	428.635
	0.603	*0.245*	*0.278*		
MRC^{δ}	2.755	1.322	151.251	19.650	407.589
	0.545	*0.147*	*24.199*		
$\hat{\Sigma_{comp}}$	2.692	1.282	216.203	18.903	389.874
	0.558	0.139	236.966		
$PCA-PRV$	2.750	1.316	3.946	29.564	395.440
	0.551	0.147	0.278		
$POET$	2.678	1.255	5.959	18.903	395.000
	0.613	*0.190*	*3.554*		
Number of assets: N=100					
	Covariance	Correlation	Inverse	Diag	Off-Diag
$\hat{\Sigma}$	3.171	1.551	3.486	43.719	1223.984
	1.131	*0.375*	*14.679*		
MRker	3.450	1.896	2321.267	29.547	1235.390
	0.511	*0.170*	*118.565*		
MRC^{δ}	3.368	1.858	2898.652	28.235	1175.572
	0.505	*0.163*	*1748.858*		
$\hat{\Sigma_{comp}}$	3.426	1.878	3.994	42.292	1204.254
	0.516	0.171	0.327		
$PCA-PRV$	3.240	1.730	5.286	28.235	1112.246
	0.596	0.275	9.479		
$POET$	6.691	7.494	1821.782	340.262	4179.766
	0.373	*0.118*	*52.693*		
Number of assets: N=300					
	Covariance	Correlation	Inverse	Diag	Off-Diag
$\hat{\Sigma}$	5.226	2.717	5.487	65.84	9154.182
	1.285	*0.681*	*38.23*		
MRker	6.399	3.233	NA	111.6	13901
	1.309	*0.340*	*NA*		
MRC^{δ}	6.250	3.166	NA	106.950	13243.474
	1.326	*0.326*	*NA*		
$PCA-PRV$	5.935	2.844	2.836	106.950	12659.655
	1.599	0.596	3.777		
$POET$	13.836	13.470	NA	1265.373	56591.524
	0.907	*0.222*	*NA*		
Number of assets: N=500					
	Covariance	Correlation	Inverse	Diag	Off-Diag
$\hat{\Sigma}$	6.331	3.579	5.916	93.24	23354.110
	1.747	*1.082*	*32.41*		
MRker	7.838	4.227	NA	160.0	33619
	1.327	*0.413*	*NA*		
MRC^{δ}	7.611	4.144	NA	156.001	32576.480
	1.313	*0.394*	*NA*		
$PCA-PRV$	7.464	3.923	2.750	156.001	30983
	1.596	0.734	4.002		
$POET$	16.425	17.320	NA	1909	134012
	1.025	*0.248*	*NA*		

Table 2.19. Synchronous prices, Sampling Frequency=30s, $K = 1$

Signal-to-noise ratio $\xi^2 = 0.01$					
Number of assets: N=50					
	Covariance	Correlation	Inverse	Diag	Off-Diag
$\hat{\Sigma}$	1.257	0.705	2.444	8.089	98.758
	0.470	*0.137*	*0.206*		
MRker	1.634	1.159	46.192	8.089	152.281
	0.403	*0.141*	*6.995*		
MRC^{δ}	1.545	1.104	98.080	7.294	136.677
	0.397	*0.135*	*153.366*		
$\hat{\Sigma_{comp}}$	1.627	1.157	4.422	10.693	149.279
	0.406	0.139	0.620		
$PCA-PRV$	1.537	1.064	3.641	7.294	137.600
	0.416	0.146	1.692		
$POET$	5.191	6.412	3048.553	130.001	1211.080
	0.385	*0.060*	*72.130*		
Number of assets: N=100					
	Covariance	Correlation	Inverse	Diag	Off-Diag
$\hat{\Sigma}$	1.634	1.145	2.750	14.806	403.545
	0.849	*0.197*	*0.233*		
MRker	2.155	1.851	950.298	14.806	588.130
	0.748	*0.222*	*55.125*		
MRC^{δ}	2.043	1.711	1711.735	12.584	503.330
	0.598	*0.221*	*1312.939*		
$\hat{\Sigma_{comp}}$	2.148	1.845	5.445	19.866	580.497
	0.752	0.221	0.489		
$PCA-PRV$	1.962	1.627	7.177	12.584	478.687
	0.626	0.249	13.969		
$POET$	6.106	8.712	3233.019	205.572	3563.967
	0.544	*0.076*	*73.224*		
Number of assets: N=300					
	Covariance	Correlation	Inverse	Diag	Off-Diag
$\hat{\Sigma}$	2.628	1.812	2.788	19.52	1924
	0.995	*0.276*	*0.168*		
MRker	3.616	3.156	NA	36.972	4588.095
	0.828	*0.296*	*NA*		
MRC^{δ}	3.375	2.935	NA	33.655	4182.825
	0.795	*0.280*	*NA*		
$PCA-PRV$	3.152	2.624	5.058	33.655	3728.817
	0.855	0.339	7.243		
$POET$	10.416	15.437	NA	580.325	32046.972
	0.839	*0.124*	*NA*		
Number of assets: N=500					
	Covariance	Correlation	Inverse	Diag	Off-Diag
$\hat{\Sigma}$	3.591	2.340	4.546	41.34	6371
	1.746	*0.383*	*0.173*		
MRker	4.877	4.090	NA	81.342	15390.607
	1.543	*0.407*	*NA*		
MRC^{δ}	4.626	3.910	NA	72.887	13929.861
	1.357	*0.407*	*NA*		
$PCA-PRV$	4.315	3.495	4.869	72.887	12558.205
	1.440	0.500	7.682		
$POET$	13.803	19.942	NA	1082.538	96063.676
	1.210	*0.184*	*NA*		

Table 2.20. Synchronous prices, Sampling Frequency=30s, $K = 2$

Signal-to-noise ratio $\xi^2 = 0.01$					
Number of assets: N=50					
	Covariance	Correlation	Inverse	Diag	Off-Diag
$\hat{\Sigma}$	2.171	0.973	2.966	16.179	268.490
	0.740	*0.283*	*0.229*		
MRker	2.364	1.251	43.537	16.179	312.247
	0.619	*0.142*	*6.594*		
MRC^{δ}	2.262	1.176	74.271	14.121	280.751
	0.577	*0.157*	*132.576*		
$\hat{\Sigma_{comp}}$	2.358	1.253	4.198	23.741	304.601
	0.622	0.141	0.391		
$PCA-PRV$	2.267	1.162	3.402	14.121	280.906
	0.591	0.166	1.518		
$POET$	7.450	5.712	2898.912	256.036	2561.767
	0.494	*0.056*	*76.897*		
Number of assets: N=100					
	Covariance	Correlation	Inverse	Diag	Off-Diag
$\hat{\Sigma}$	2.491	1.241	2.869	25.302	710.078
	0.742	*0.263*	*0.161*		
MRker	2.896	1.680	925.328	25.302	925.507
	0.614	*0.180*	*61.115*		
MRC^{δ}	2.773	1.619	1597.341	22.486	840.257
	0.592	*0.170*	*1216.858*		
$\hat{\Sigma_{comp}}$	2.880	1.671	5.425	37.724	908.015
	0.618	0.179	0.623		
$PCA-PRV$	2.713	1.531	6.409	22.486	814.074
	0.615	0.179	13.217		
$POET$	7.586	8.034	3658.237	333.557	5535.384
	0.496	*0.080*	*112.518*		
Number of assets: N=300					
	Covariance	Correlation	Inverse	Diag	Off-Diag
$\hat{\Sigma}$	4.075	2.119	7.001	32.16	3434
	0.958	*0.438*	*0.188*		
MRker	4.938	2.959	NA	60.024	7635.184
	0.831	*0.358*	*NA*		
MRC^{δ}	4.677	2.759	NA	56.197	7124.655
	0.895	*0.345*	*NA*		
$\hat{\Sigma_{comp}}$	4.500	2.563	4.474	56.197	6655.273
	0.942	0.373	5.251		
$PCA-PRV$	4.500	2.563	4.474	56.197	6655.273
	0.942	0.373	5.251		
$POET$	12.534	14.958	NA	951.486	46646.743
	0.867	*0.116*	*NA*		
Number of assets: N=500					
	Covariance	Correlation	Inverse	Diag	Off-Diag
$\hat{\Sigma}$	4.782	2.762	7.943	51.20	9510
	1.455	*0.535*	*0.151*		
MRker	6.029	3.872	NA	99.420	20401.754
	1.262	*0.389*	*NA*		
MRC^{δ}	5.692	3.639	NA	88.506	18433.154
	1.210	*0.358*	*NA*		
$\hat{\Sigma_{comp}}$	5.422	3.377	4.392	88.506	16999.631
	1.272	0.399	4.471		
$PCA-PRV$	15.365	18.915	NA	1489.080	116477.704
	1.073	0.176	NA		
$POET$	4.782	2.762	2.955	99.420	14684.452
	1.455	*0.535*	*0.151*		

Table 2.21. Synchronous prices, Sampling Frequency=30s, $K = 3$

Signal-to-noise ratio $\xi^2 = 0.01$					
Number of assets: N=50					
	Covariance	Correlation	Inverse	Diag	Off-Diag
$\hat{\Sigma}$	2.164	1.022	3.223	8.869	296.250
	0.836	*0.433*	*7.891*		
MRker	2.519	1.172	43.050	16.573	332.866
	0.440	*0.141*	*5.744*		
MRC^{δ}	2.376	1.110	96.129	14.426	305.749
	0.476	*0.135*	*112.426*		
$\hat{\Sigma_{comp}}$	2.503	1.170	3.795	24.704	323.691
	0.443	0.141	0.219		
$PCA-PRV$	2.375	1.068	5.358	14.426	309.646
	0.529	0.184	3.321		
$POET$	7.017	5.786	3066.955	255.029	2192.846
	0.462	*0.054*	*70.115*		
Number of assets: N=100					
	Covariance	Correlation	Inverse	Diag	Off-Diag
$\hat{\Sigma}$	2.400	1.342	3.498	107.012	1536.609
	2.873	*0.413*	*10.007*		
MRker	2.799	1.735	906.677	19.946	821.309
	0.382	*0.164*	*54.562*		
MRC^{δ}	2.715	1.651	1655.213	18.277	759.159
	0.374	*0.141*	*947.838*		
$\hat{\Sigma_{comp}}$	2.791	1.727	3.826	28.966	804.964
	0.385	0.164	0.174		
$PCA-PRV$	2.598	1.448	5.846	18.277	705.603
	0.477	0.259	16.130		
$POET$	6.450	8.176	3594.918	313.622	3932.506
	0.406	*0.066*	*74.295*		
Number of assets: N=300					
	Covariance	Correlation	Inverse	Diag	Off-Diag
$\hat{\Sigma}$	4.365	2.125	6.148	251.0	12526
	1.239	*0.714*	*32.836*		
MRker	5.718	2.901	NA	89.650	11043.414
	1.161	*0.317*	*NA*		
MRC^{δ}	5.520	2.814	NA	83.153	10187.868
	1.089	*0.283*	*NA*		
$PCA-PRV$	5.331	2.583	2.644	83.153	9598.054
	1.273	0.491	3.845		
$POET$	13.648	14.984	NA	1266.672	54978.458
	0.876	*0.129*	*NA*		
Number of assets: N=500					
	Covariance	Correlation	Inverse	Diag	Off-Diag
$\hat{\Sigma}$	5.432	2.788	6.388	82.774	18954.170
	1.628	*0.972*	*41.651*		
MRker	7.410	3.728	NA	153.286	30023.820
	1.438	*0.375*	*NA*		
MRC^{δ}	7.051	3.618	NA	141.235	27753.260
	1.360	*0.306*	*NA*		
$PCA-PRV$	6.675	3.163	2.667	141.235	25969.560
	1.679	0.651	1.656		
$POET$	18.022	18.810	NA	2262.741	161758.260
	1.135	*0.155*	*NA*		

Table 2.22. Asynchronous prices, Sampling Frequency=5min, $K = 1$

	Covariance	Correlation	Inverse	Diag	Off-Diag
Signal-to-noise ratio $\xi^2 = 0.01$					
Number of assets: N=50					
$\hat{\Sigma}$	3.403	2.164	2.825	23.18	553.9
	0.331	*0.194*	*0.214*		
MRker	3.690	2.547	5985.302	25.368	655.568
	0.329	*0.192*	*636880.400*		
MRC^{δ}	3.651	2.506	2251.927	25.577	646.338
	0.322	*0.186*	*3624.942*		
$\hat{\Sigma_{comp}}$	3.613	2.469	4.462	24.503	631.539
	0.309	0.157	0.328		
$PCA-PRV$	3.581	2.396	9.760	25.577	625.472
	0.327	0.196	7.680		
$POET$	4.252	3.326	337.887	92.544	838.372
	0.313	*0.113*	*64.628*		
Number of assets: N=100					
	Covariance	Correlation	Inverse	Diag	Off-Diag
$\hat{\Sigma}$	6.795	3.514	3.486	76.71	4598
	0.630	*0.235*	*0.224*		
MRker	7.248	4.074	NA	95.665	5227.592
	0.646	*0.252*	*NA*		
MRC^{δ}	7.258	4.046	NA	96.119	5182.841
	0.635	*0.242*	*NA*		
$\hat{\Sigma_{comp}}$	7.062	3.946	6.483	88.009	4967.783
	0.591	0.219	0.584		
$PCA-PRV$	7.163	3.857	10.864	96.119	5049.237
	0.642	0.253	13.312		
$POET$	8.789	5.008	484.784	332.281	7491.832
	0.651	*0.191*	*406.584*		
Number of assets: N=300					
	Covariance	Correlation	Inverse	Diag	Off-Diag
$\hat{\Sigma}$	9.109	5.483	8.822	168.9	25079
	0.799	*0.326*	*0.190*		
MRker	9.907	6.759	NA	186.992	29961.660
	0.848	*0.374*	*NA*		
MRC^{δ}	9.833	6.633	NA	176.398	29540.090
	0.819	*0.364*	*NA*		
$PCA-PRV$	9.601	6.223	9.318	176.398	28192.250
	0.833	0.376	9.233		
$POET$	11.208	8.259	NA	656.778	37695.620
	0.916	*0.285*	*NA*		
Number of assets: N=500					
	Covariance	Correlation	Inverse	Diag	Off-Diag
$\hat{\Sigma}$	11.859	7.079	11.77	309.3	69106
	1.000	*0.409*	*0.171*		
MRker	12.800	8.706	NA	334.281	82166.590
	1.000	*0.440*	*NA*		
MRC^{δ}	12.761	8.538	NA	324.175	81195.840
	0.982	*0.447*	*NA*		
$PCA-PRV$	12.463	7.969	13.98	324.175	77288.470
	0.999	0.447	1.222		
$POET$	14.347	10.570	NA	1114.855	103646.530
	1.099	*0.353*	*NA*		

Table 2.23. Asynchronous prices, Sampling Frequency=5min, $K = 3$

	Covariance	Correlation	Inverse	Diag	Off-Diag
Signal-to-noise ratio $\xi^2 = 0.01$					
Number of assets: N=50					
$\hat{\Sigma}$	4.249	2.073	3.778	40.14	861.4
	0.283	*0.102*	*0.200*		
MRker	4.525	2.373	5271.528	37.987	1002.069
	0.341	*0.107*	*15556.160*		
MRC^{δ}	4.491	2.312	1399.579	36.957	979.880
	0.297	*0.113*	*1501.990*		
$\hat{\Sigma_{comp}}$	4.356	2.248	4.849	38.745	916.864
	0.268	0.099	0.392		
$PCA-PRV$	4.438	2.202	5.052	36.957	961.087
	0.310	0.118	6.009		
$POET$	5.661	2.620	352.895	203.071	1427.955
	0.300	*0.108*	*161.978*		
Number of assets: N=100					
	Covariance	Correlation	Inverse	Diag	Off-Diag
$\hat{\Sigma}$	6.905	3.243	3.809	121.0	4579
	0.466	*0.147*	*0.235*		
MRker	7.230	3.616	NA	121.499	5189
	0.476	*0.168*	*NA*		
MRC^{δ}	7.174	3.516	NA	119.957	5112.960
	0.458	*0.166*	*NA*		
$\hat{\Sigma_{comp}}$	7.021	3.460	4.434	106.874	4881.537
	0.459	0.137	0.213		
$PCA-PRV$	7.051	3.362	6.471	119.957	4971.999
	0.472	0.173	12.516		
$POET$	8.247	4.050	316.685	440.608	6449.541
	0.472	*0.146*	*231.219*		
Number of assets: N=300					
	Covariance	Correlation	Inverse	Diag	Off-Diag
$\hat{\Sigma}$	10.570	5.420	5.993	259.856	33528.890
	0.700	*0.221*	*0.188*		
MRker	11.124	6.259	NA	323.358	37194.140
	0.671	*0.212*	*NA*		
MRC^{δ}	11.090	6.157	NA	307.651	37068.830
	0.671	*0.253*	*NA*		
$PCA-PRV$	10.880	5.785	4.412	307.651	35613.900
	0.691	0.261	13.370		
$POET$	12.141	6.969	NA	1099.284	44168.980
	0.777	*0.233*	*NA*		
Number of assets: N=500					
	Covariance	Correlation	Inverse	Diag	Off-Diag
$\hat{\Sigma}$	14.280	7.148	8.795	490.1	102280.440
	0.986	*0.317*	*0.202*		
MRker	15.04	8.259	NA	604.2	112820
	0.942	*0.308*	*NA*		
MRC^{δ}	14.98	8.097	NA	574.767	112529
	0.943	*0.378*	*NA*		
$PCA-PRV$	14.745	7.635	3.763	574.767	108431.870
	0.970	0.367	3.801		
$POET$	16.377	9.032	NA	1900.928	132647.910
	1.072	*0.345*	*NA*		

Table 2.24. Asynchronous prices, Sampling Frequency=1min, $K = 1$

Signal-to-noise ratio $\xi^2 = 0.01$					
Number of assets: N=50					
	Covariance	Correlation	Inverse	Diag	Off-Diag
$\hat{\Sigma}$	3.400	2.210	2.631	18.67	551.8
	0.307	*0.161*	*0.245*		
MRker	3.629	2.513	539.282	18.767	624.401
	0.297	*0.157*	*106.177*		
MRC^{δ}	3.603	2.508	175.563	19.432	619.029
	0.288	*0.134*	*803.654*		
$\hat{\Sigma_{comp}}$	3.578	2.504	4.292	18.313	611.140
	0.290	0.139	0.362		
$PCA-PRV$	3.559	2.427	6.862	19.432	603.598
	0.293	0.143	3.475		
$POET$	4.296	3.445	589.969	81.038	840.164
	0.311	*0.093*	*1066.088*		
Number of assets: N=100					
	Covariance	Correlation	Inverse	Diag	Off-Diag
$\hat{\Sigma}$	5.303	3.160	3.062	63.27	2765
	0.479	*0.190*	*0.165*		
MRker	5.642	3.649	20217.000	63.717	3150.591
	0.467	*0.197*	*49581.740*		
MRC^{δ}	5.617	3.611	12411.800	64.260	3102.177
	0.470	*0.178*	*16082.420*		
$\hat{\Sigma_{comp}}$	5.562	3.571	6.363	58.644	3064.322
	0.469	0.169	0.500		
$PCA-PRV$	5.508	3.441	7.701	64.260	2992.306
	0.473	0.197	5.535		
$POET$	6.397	4.953	537.642	217.987	3935.613
	0.513	*0.127*	*898.606*		
Number of assets: N=300					
	Covariance	Correlation	Inverse	Diag	Off-Diag
$\hat{\Sigma}$	8.377	4.750	2.645	142.070	20980.660
	0.736	*0.220*	*95.205*		
MRker	8.853	5.809	NA	136.782	23536
	0.756	*0.254*	*NA*		
MRC^{δ}	8.840	5.805	NA	136.369	23450.960
	0.762	*0.259*	*NA*		
$PCA-PRV$	8.663	5.475	7.615	136.369	22597.510
	0.769	0.285	3.549		
$POET$	10.536	8.735	NA	623.118	32491.480
	0.881	*0.190*	*NA*		
Number of assets: N=500					
	Covariance	Correlation	Inverse	Diag	Off-Diag
$\hat{\Sigma}$	9.793	6.094	2.645	209.055	49152.810
	0.908	*0.326*	*91.637*		
MRker	10.369	7.438	NA	202.553	54724.110
	0.890	*0.343*	*NA*		
MRC^{δ}	10.327	7.424	NA	202.525	54432.540
	0.882	*0.349*	*NA*		
$PCA-PRV$	10.108	6.987	4.758	202.525	52007.530
	0.893	0.364	1.981		
$POET$	12.126	11.315	NA	883.689	74464.050
	1.070	*0.270*	*NA*		

Table 2.26. Asynchronous prices, Sampling Frequency=1min, $K = 3$

	Covariance	Correlation	Inverse	Diag	Off-Diag
Signal-to-noise ratio $\xi^2 = 0.01$					
Number of assets: N=50					
	Covariance	Correlation	Inverse	Diag	Off-Diag
$\hat{\Sigma}$	3.981	2.062	3.735	100.7	734.7
	0.407	*0.102*	*4.623*		
MRker	4.184	2.331	496.018	49.484	823.986
	0.248	*0.121*	*77.102*		
MRC^{δ}	4.172	2.349	372.509	48.811	818.385
	0.249	*0.125*	*815.212*		
$\hat{\Sigma}_{comp}$	4.078	2.325	3.831	49.843	805.012
	0.241	0.098	0.142		
$PCA-PRV$	4.099	2.265	5.675	48.811	794.262
	0.248	0.129	9.045		
$POET$	4.888	3.268	563.730	175.609	1033.610
	0.235	*0.067*	*118.888*		
Number of assets: N=100					
	Covariance	Correlation	Inverse	Diag	Off-Diag
$\hat{\Sigma}$	6.548	3.154	3.815	75.201	4284.501
	0.464	*0.117*	*0.226*		
MRker	6.714	3.412	18784.944	89.631	4501.805
	0.462	*0.125*	*80538.060*		
MRC^{δ}	6.716	3.390	13021.839	86.991	4478.863
	0.443	*0.118*	*8021.708*		
$\hat{\Sigma}_{comp}$	6.579	3.335	4.561	86.572	4319.042
	0.450	0.117	0.190		
$PCA-PRV$	6.628	3.262	5.276	86.991	4365.976
	0.448	0.132	4.739		
$POET$	8.140	4.354	527.333	391.642	6221.560
	0.538	*0.115*	*278.336*		
Number of assets: N=300					
	Covariance	Correlation	Inverse	Diag	Off-Diag
$\hat{\Sigma}$	11.147	5.139	5.752	643.2	36593
	0.692	*0.212*	*11.889*		
MRker	11.605	5.578	NA	312.277	39826.280
	0.765	*0.162*	*NA*		
MRC^{δ}	11.565	5.612	NA	307.382	39665.880
	0.742	*0.152*	*NA*		
$PCA-PRV$	11.425	5.388	4.231	307.382	38777.880
	0.764	0.191	2.953		
$POET$	13.468	8.284	NA	1238.280	52670.410
	0.870	*0.144*	*NA*		
Number of assets: N=500					
	Covariance	Correlation	Inverse	Diag	Off-Diag
$\hat{\Sigma}$	14.204	6.675	10.97	6328.828	95181.790
	1.305	*0.253*	*7.780*		
MRker	14.630	7.216	NA	493.031	104202.670
	0.949	*0.209*	*NA*		
MRC^{δ}	14.603	7.186	NA	482.631	103763.310
	0.941	*0.207*	*NA*		
$PCA-PRV$	14.445	6.930	3.293	482.631	101621.480
	0.958	0.266	1.722		
$POET$	16.999	10.408	NA	1994.152	141900.110
	1.242	*0.182*	*NA*		

Table 2.27. Asynchronous prices, Sampling Frequency=30s, $K = 1$

Signal-to-noise ratio $\xi^2 = 0.01$					
Number of assets: N=50					
	Covariance	Correlation	Inverse	Diag	Off-Diag
$\hat{\Sigma}$	3.416	2.123	2.544	301.482	564.982
	0.778	*0.272*	*6.392*		
MRker	3.556	2.333	34.042	291.106	608.913
	0.744	*0.199*	*4.393*		
MRC^{δ}	3.508	2.296	22.871	286.283	592.445
	0.736	*0.198*	*128.553*		
$\hat{\Sigma_{comp}}$	3.543	2.276	3.961	287.665	602.628
	0.735	0.190	0.361		
$PCA-PRV$	3.437	2.214	2.904	281.514	567.742
	0.735	0.206	1.797		
$POET$	4.249	3.724	1856.430	409.202	801.424
	0.909	*0.240*	*4382.951*		
Number of assets: N=100					
	Covariance	Correlation	Inverse	Diag	Off-Diag
$\hat{\Sigma}$	4.930	2.975	2.597	783.994	2389.652
	0.766	*0.280*	*0.366*		
MRker	5.108	3.265	560.116	825.412	2565.475
	0.775	*0.230*	*49.841*		
MRC^{δ}	5.099	3.214	278.166	814.974	2556.652
	0.767	*0.238*	*913.005*		
$\hat{\Sigma_{comp}}$	5.067	3.241	5.402	805.910	2523.896
	0.764	0.246	0.566		
$PCA-PRV$	5.031	3.103	5.241	807.153	2487.890
	0.769	0.247	5.223		
$POET$	5.846	5.225	1478.072	1123.056	3230.180
	0.908	*0.251*	*1888.548*		
Number of assets: N=300					
	Covariance	Correlation	Inverse	Diag	Off-Diag
$\hat{\Sigma}$	9.383	5.230	3.144	3663.692	9.383
	0.638	*0.308*	*0.268*		
MRker	9.766	5.590	NA	3900.626	9.766
	0.641	*0.214*	*NA*		
MRC^{δ}	9.718	5.571	NA	3734.895	9.718
	0.617	*0.215*	*NA*		
$\hat{\Sigma_{comp}}$	9.561	5.302	3.696	3733.223	9.561
	0.626	0.250	4.673		
$PCA-PRV$	11.919	8.823	NA	6303.668	11.919
	0.912	0.178	NA		
$POET$	9.383	5.230	3.144	3663.692	9.383
	0.638	*0.308*	*0.268*		
Number of assets: N=500					
	Covariance	Correlation	Inverse	Diag	Off-Diag
$\hat{\Sigma}$	10.857	6.491	2.484	17971.290	58778.540
	1.502	*0.447*	*0.245*		
MRker	11.248	7.375	NA	18910.360	63072.630
	1.525	*0.464*	*NA*		
MRC^{δ}	11.177	7.227	NA	18787.650	62263.920
	1.524	*0.480*	*NA*		
$PCA-PRV$	13.862	11.628	NA	22622.460	95058.110
	1.595	0.366	NA		
$POET$	13.862	11.628	NA	22622.460	95058.110
	1.595	*0.366*	*NA*		

Table 2.28. Asynchronous prices, Sampling Frequency=30s, $K = 2$

Signal-to-noise ratio $\xi^2 = 0.01$					
Number of assets: N=50					
	Covariance	Correlation	Inverse	Diag	Off-Diag
$\hat{\Sigma}$	3.963	2.192	3.777	362.408	757.145
	0.891	*0.231*	*0.372*		
MRker	4.019	2.212	30.594	350.346	787.372
	0.845	*0.188*	*4.758*		
MRC^{δ}	4.024	2.202	25.252	344.362	782.485
	0.835	*0.190*	*91.475*		
$\hat{\Sigma_{comp}}$	4.040	2.214	3.820	344.619	789.605
	0.841	0.190	0.244		
$PCA-PRV$	3.941	2.135	2.993	341.046	749.571
	0.840	0.204	2.117		
$POET$	5.188	3.598	2877.240	451.253	1207.574
	0.928	*0.198*	*9022.950*		
Number of assets: N=100					
	Covariance	Correlation	Inverse	Diag	Off-Diag
$\hat{\Sigma}$	5.589	2.982	3.200	861.161	2950.496
	0.773	*0.139*	*1.895*		
MRker	5.578	3.172	511.025	942.135	3029.835
	0.818	*0.114*	*42.989*		
MRC^{δ}	5.535	3.145	399.599	928.988	2983.166
	0.813	*0.137*	*813.036*		
$\hat{\Sigma_{comp}}$	5.587	3.160	4.390	909.688	3035.229
	0.803	0.107	0.298		
$PCA-PRV$	5.459	3.036	5.301	916.343	2900.096
	0.815	0.146	3.055		
$POET$	7.129	5.114	1850.969	1513.986	4788.059
	1.085	*0.187*	*865.150*		
Number of assets: N=300					
	Covariance	Correlation	Inverse	Diag	Off-Diag
$\hat{\Sigma}$	8.314	5.030	2.578	4226.601	20621.130
	0.863	*0.311*	*0.147*		
MRker	8.603	5.574	NA	4296.534	22071.120
	0.848	*0.281*	*NA*		
MRC^{δ}	8.567	5.574	NA	4502.501	21885.110
	0.884	*0.267*	*NA*		
$PCA-PRV$	8.435	5.360	4.809	4451.909	21209.980
	0.888	0.258	7.005		
$POET$	10.703	9.221	NA	6999.849	33750.330
	1.116	*0.331*	*NA*		
Number of assets: N=500					
	Covariance	Correlation	Inverse	Diag	Off-Diag
$\hat{\Sigma}$	12.932	6.504	6.315	10110.880	83015.940
	0.807	*0.318*	*6.211*		
MRker	13.448	7.288	NA	11537.000	90120.640
	0.876	*0.269*	*NA*		
MRC^{δ}	13.364	7.283	NA	11580.780	89006.180
	0.882	*0.273*	*NA*		
$PCA-PRV$	13.183	6.951	6.399	11651.560	86601.570
	0.901	0.322	13.782		
$POET$	16.009	11.434	NA	16529.590	126567.720
	1.053	*0.219*	*NA*		

Table 2.29. Asynchronous prices, Sampling Frequency=30s, $K = 3$

Signal-to-noise ratio $\xi^2 = 0.01$					
Number of assets: N=50					
	Covariance	Correlation	Inverse	Diag	Off-Diag
$\hat{\Sigma}$	4.110	2.133	3.841	355.748	789.484
	0.853	*0.180*	*0.794*		
MRker	3.966	2.136	29.634	353.994	755.836
	0.835	*0.131*	*5.445*		
MRC^{δ}	3.939	2.116	26.456	351.163	744.296
	0.834	*0.131*	*62.149*		
$\hat{\Sigma_{comp}}$	3.961	2.113	3.761	358.219	749.254
	0.845	0.137	0.281		
$PCA-PRV$	3.876	2.061	2.984	344.453	720.156
	0.834	0.140	1.019		
$POET$	4.968	3.423	2484.268	511.659	1079.354
	1.012	*0.196*	*1904.887*		
Number of assets: N=100					
	Covariance	Correlation	Inverse	Diag	Off-Diag
$\hat{\Sigma}$	5.786	2.919	3.635	1158.320	3207.442
	0.964	*0.169*	*2.618*		
MRker	5.886	3.044	484.073	1153.881	3388.831
	0.931	*0.126*	*45.818*		
MRC^{δ}	5.853	3.043	537.427	1145.724	3350.789
	0.929	*0.129*	*421.498*		
$\hat{\Sigma_{comp}}$	5.840	3.052	4.038	1168.896	3328.554
	0.942	0.127	0.256		
$PCA-PRV$	5.802	2.917	5.621	1109.138	3291.742
	0.913	0.129	13.170		
$POET$	7.312	4.932	2417.052	1857.105	4962.468
	1.207	*0.196*	*1524.093*		
Number of assets: N=300					
	Covariance	Correlation	Inverse	Diag	Off-Diag
$\hat{\Sigma}$	10.552	4.919	4.598	5683.269	33186.640
	0.937	*0.278*	*27.900*		
MRker	11.037	5.409	NA	6875.356	36299.550
	1.024	*0.241*	*NA*		
MRC^{δ}	11.046	5.402	NA	6708.402	36367.210
	1.005	*0.236*	*NA*		
$\hat{\Sigma_{comp}}$	10.872	5.105	4.235	7017.927	35219.680
	1.057	0.338	1.683		
$PCA-PRV$	13.092	8.597	NA	8635.407	50239.490
	1.097	0.140	NA		
$POET$	10.552	4.919	4.598	5683.269	33186.640
	0.937	*0.278*	*27.900*		
Number of assets: N=500					
	Covariance	Correlation	Inverse	Diag	Off-Diag
$\hat{\Sigma}$	14.628	6.995	3.582	14529.670	96784.340
	1.574	*0.354*	*0.288*		
MRker	14.317	7.083	NA	15796.730	102042.330
	1.098	*0.275*	*NA*		
MRC^{δ}	14.264	7.005	NA	15441.900	101274.640
	1.077	*0.273*	*NA*		
$PCA-PRV$	17.581	11.078	NA	18464.700	152408.560
	1.113	0.161	NA		
$POET$	17.581	11.078	NA	18464.700	152408.560
	1.113	*0.161*	*NA*		

Chapter 3

Understanding Microstructure Noise in a High Dimensional Framework

Abstract

We provide a new methodology to estimate microstructure noise characteristics and frictionless prices under a high dimensional setup. We rely on factor assumptions both in latent returns and microstructure noise. The methodology is able to estimate rotations of common factors, loading coefficients and volatilities in microstructure noise for a huge number of stocks. Using stocks included in the S&P500 during the period spanning January 2007 to December 2011, we estimate microstructure noise common factors and compare them to some market-wide liquidity measures computed from real financial variables. We obtain that: the first factor is correlated to the average spread and the average number of shares outstanding; the second and third factors are related to the spread; the fourth and fifth factors are significantly linked to the closing log price. In addition, volatilities of those microstructure noise factors are widely explained by the average spread, the average volume, the average number of trades and the average trade size.

3.1 Introduction

Using high frequency data, volatility estimation has been a major theme in the recent financial econometrics literature. It is commonly assumed that latent log-price processes follow semi-martingale processes. But observed prices are polluted by noise called market microstructure noise (Henceforth, MSN). This noise represents a deviation from fundamental price value, induced by characteristics of the market under consideration, such as: the bid-ask bounce, the discreteness of price change, rounding errors, transaction costs, and the asymmetry of information of traders. Available estimation methodologies consist on reducing the impact of noise prevalent at high frequency, while accurately estimating volatility of the latent log-price. A non-exhaustive list of such estimation strategies is: the subsampling and averaging approach of Aït-Sahalia, Mykland, and Zhang (2005), which provides the averaging and two scales estimators; the realized kernels of Barndorff-Nielsen, Hansen, Lunde, and Shephard (2008b); and the pre-averaging approach of Podolskij and Vetter (2009). In empirical studies, the impact of noise is reduced by sampling less often (every 15 or 30 minutes).

In general, understanding microstructure noise is not the main purpose when estimating volatility. Authors just want to get rid of it. In the empirical literature on microstructure noise, existing procedures are most often limited to estimate only the noise volatility. Nevertheless, useful information can be extracted from this noise component for a better understanding of its behavior. Only few studies have taken this direction. Aït-Sahalia and Yu (2009) study the nature of the information contained in high frequency statistical measurements of microstructure noise volatility and relate them to observable financial characteristics of the underlying assets and, in particular, to different financial measures of their liquidity. Li, Xie, and Zheng (2016) consider a setting where market microstructure noise is a parametric function of trading information, possibly with a remaining noise component, and show that higher efficiency can be obtained by modeling and removing the noise component caused by trading and then applying existing estimators to the estimated log-prices. Jacod, Li, and Zheng (2017) study the non-parametric estimation of autocovariances and autocorrelations of microstructure noise based on high frequency data. Chaker (2017) explicitly models microstructure noise and removes it from observed prices to obtain an estimate of the frictionless price.

The objective of this paper is to contribute to the growing literature which consists on studying the information contain of microstructure noise. Considering a huge number of stocks, our aim is firstly to estimate microstructure noise components through a factorial decomposition. Secondly, we want to extract the information contain of the factor component of this noise by relating it to some liquidity measures. Thirdly, we are interested on approximating frictionless prices. Our paper is more related to the ones by Aït-Sahalia and Yu (2009), Li, Xie, and Zheng (2016) and Chaker (2017), but with important differences. Firstly, our methodology relies on factor assumptions both in latent returns and microstructure noise. Thus, variables that explain microstructure noise are unobservable latent common factors. They will be estimated through the process. Contrary to the existing literature, when specifying noise equations, our approach will not suffer for the misspecification or missing explanatory variables issues. Secondly, our approach is high dimensional in term of number of stocks: microstructure noise characteristics and frictionless prices are estimated jointly for huge number of stocks. As it is common in this literature, we compare the extracted common factors of microstructure noises to some liquidity measures. Here, liquidity measures are not stock specific, but are averages or principal components of individual stock liquidity measures.

The rest of the paper is organized as follow: in section 2, we present the benchmark model. Section 3 describes the estimation strategy of microstructure noise characteristics and frictionless prices. An empirical study is carry out in section 4 and section 5 concludes.

3.2 The benchmark model

As in the paper by Bollerslev, Meddahi, and Nyawa (2018), we assume that the dynamics of the log-price process X_t is given by a continuous process with a factor representation of the form,

$$dX_t^* = bdF_t + dE_t, \tag{3.1}$$

where $b = (b_{ik})_{1\leq i\leq p, 1\leq k\leq K}$ denotes the $p \times K$ matrix of factor loadings, $F_t = (F_{1t}, ..., F_{Kt})'$ refers to the latent factor vector, and $E_t = (E_{1t}, ..., E_{pt})'$ denotes the vector of idiosyncratic errors. In order to obtain the continuous Itö semimartingale representation of the log-price process X_t, we further assume that,

$$dF_{kt} = \sigma_{fkt} dB_{kt}^F,$$
$$dE_{it} = \sigma_{\epsilon it} dB_{it}^I.$$

Integrating both sides of the resulting latent factor price process above over a time interval of length Δ, it readily follows that

$$\int_{t-\Delta}^{t} dX_s^* = b \cdot \int_{t-\Delta}^{t} \sigma_{fs} dB_s^F + \int_{t-\Delta}^{t} \sigma_{\epsilon s} dB_s^I.$$

Defining the corresponding returns, factors, and errors over the time-interval Δ,

$$\begin{aligned} r_t^* \equiv r_{t,\Delta}^* \equiv \int_{t-\Delta}^{t} dX_s^* \\ f_t \equiv f_{t,\Delta} \equiv \int_{t-\Delta}^{t} \sigma_{ft} dB_s^F \\ \epsilon_t \equiv \epsilon_{t,\Delta} \equiv \int_{t-\Delta}^{t} \sigma_{\epsilon s} dB_s^I \end{aligned}$$

allows for following standard discrete-time factor representation,

$$r_t^* = b f_t + \varepsilon_t \tag{3.2}$$

where $r_t^* = (r_{1t}^*, ..., r_{pt}^*)'$, $f_t = (f_{1t}, ..., f_{Kt})'$, and $\varepsilon_t = (\varepsilon_{1t}, ..., \varepsilon_{pt})'$, respectively.

Factors and idiosyncratic components satisfied the same orthogonality assumptions than Assumption 1 in Bollerslev, Meddahi, and Nyawa (2018).

The latent prices X_{it}^* for each of the p individual assets are not directly observable. Instead, the actually observed prices are additively contaminated with market microstructure noise, such as

$$X_{it} = X_{it}^* + u_{it} \tag{3.3}$$

As in Hasbrouck and Seppi (2001b), we assume that this noise component has its own separate factor representation,

$$u_{it} = c_i g_t + \eta_{it} \tag{3.4}$$

where the $K' \times 1$ vector g_t accounts for the cross-sectional dependence in the noise, and the $1 \times K'$ vector c_i denotes the corresponding factor loadings. Assumption 2 in Bollerslev, Meddahi, and Nyawa (2018) is also assumed to hold.

3.3 Estimation

The aim of this section is to estimate the factor component of the microstructure noise (loadings and factors), and its volatility. The estimation strategy will take advantage of some results established in Bollerslev, Meddahi, and Nyawa (2018).

3.3.1 Estimation of factors and loadings of the microstructure noise

From the estimation strategy developped in Bollerslev, Meddahi, and Nyawa (2018), we are able to consistently estimate: the loading matrix b by $\hat{b}$; and a noisy version of a rotation of the true factor f in the latent return equation by $\hat{f}$:

$$\hat{b}_{ik} = \frac{MRC(\hat{f}_{kt}, r_{it})}{PRV(\hat{f}_{kt})} \tag{3.5}$$

$$\hat{f}_{kt} = \frac{1}{p}\underline{\hat{W}}_k' r_t \tag{3.6}$$

where MRC and PRV represent respectively the modulated realized covariance estimator of Christensen, Kinnebrock, and Podolskij (2010b) and the pre-averaging estimator of Jacod, Li, Mykland, Podolskijc, and Vetter (2009b); $\underline{\hat{W}}_k$ is a consistent estimator of the eigenvector associated to the k^{th} biggest eigenvalue of the integrated covolatility matrix, $\underline{W}_k$.

From the model specification, the expression of the noisy return for a stock i is given by:

$$\begin{aligned} r_{it} &= b_i f_t + \varepsilon_{it} + c_i(g_t - g_{t-\Delta}) + (\eta_{it} - \eta_{it-\Delta}) && (3.7)\\ &= b_i\left[\hat{f}_t - \frac{1}{p}\underline{W}'c(g_t - g_{t-\Delta})\right] + c_i(g_t - g_{t-\Delta}) + \varepsilon_{it} + (\eta_{it} - \eta_{it-\Delta}) && (3.8) \end{aligned}$$

We derive that

$$r_{it} - b_i\hat{f}_t \approx \left(c_i - \frac{1}{p}b_i\underline{W}'c\right)(g_t - g_{t-\Delta}) + \varepsilon_{it} + (\eta_{it} - \eta_{it-\Delta}) \tag{3.9}$$

For Δ sufficiently small and p sufficiently large, we assume that b_i is well estimated by $\hat{b}_i$. We obtain

$$r_{it} - \hat{b}_i\hat{f}_t = \left(c_i - \frac{1}{p}b_i\underline{W}'c\right)(g_t - g_{t-\Delta}) + \varepsilon_{it} + (\eta_{it} - \eta_{it-\Delta}) \tag{3.10}$$

In a matricial representation, we can write

$$r_t - \hat{b}\hat{f}_t = \left(c - \frac{1}{p}b\underline{W}'c\right)(g_t - g_{t-\Delta}) + \varepsilon_{it} + (\eta_t - \eta_{t-\Delta}) \tag{3.11}$$

The previous equation is a factor decomposition of the observed series $r_t - \hat{b}\hat{f}_t$. In this factor representation, $\left(c - \frac{1}{p}b\underline{W}'c\right)$ is the matrix of loadings, $(g_t - g_{t-\Delta})$ are factors and $\varepsilon_t + (\eta_t - \eta_{t-\Delta})$ the idiosyncratic component. The principal component analysis can be used to extract common factors. In that sense, $(g_t - g_{t-\Delta})$ will be estimated in the following way:

$$\widehat{(g_{kt} - g_{kt-\Delta})} = \underline{\Omega}_k' \left(r_t - \hat{b}\hat{f}_t\right), \forall k = 1, ..., K' \tag{3.12}$$

where $\Omega = (\underline{\Omega}_1, ..., \underline{\Omega}_{K'})$ is the matrix of ordered eigenvectors of the covariance matrix of $r_t - \hat{b}\hat{f}_t$ and $\underline{\Omega_k}$ is the k^{th} column of Ω.

For two processes X and Y, we call $[X, Y]$ and $[X]$ respectively the quadratic covariation of X and Y, and the quadratic variation of X. In order to compute the loading matrix c, we firstly compute $[r_t - \hat{b}\hat{f}_t, g_{kt} - g_{kt-\Delta}]$.

$$\begin{aligned}
\left[r_{it} - \hat{b}_i\hat{f}_t, g_{kt} - g_{kt-\Delta}\right] &= \left[\left(c_i - \frac{1}{p}b_i\underline{W}'c\right)(g_t - g_{t-\Delta}) + \varepsilon_{it} + (\eta_{it} - \eta_{it-\Delta}), g_{kt} - g_{kt-\Delta}\right] \\
&= \left[\sum_{l=1}^{K'}\left(c_{il} - \frac{1}{p}\sum_{s=1}^{K} b_{is}\underline{W}_s'\underline{c}_l\right)(g_{lt} - g_{lt-\Delta}) + \varepsilon_{it} + (\eta_{it} - \eta_{it-\Delta}); g_{kt} - g_{kt-\Delta}\right] \\
&= \left[\sum_{l=1}^{K'}\left(c_{il} - \frac{1}{p}\sum_{s=1}^{K} b_{is}\underline{W}_s'\underline{c}_l\right)(g_{lt} - g_{lt-\Delta}); g_{kt} - g_{kt-\Delta}\right] \\
&= \left(c_{ik} - \frac{1}{p}\sum_{s=1}^{K} b_{is}\underline{W}_s'\underline{c}_k\right)[g_{kt} - g_{kt-\Delta}] \\
&= \left(c_{ik} - \frac{1}{p}b_i\underline{W}'\underline{c}_k\right)[g_{kt} - g_{kt-\Delta}]
\end{aligned}$$

We derive from the last equality that

$$\left(c_{ik} - b_i\left(\frac{1}{p}\underline{W}'\underline{c}_k\right)\right) = \frac{\left[r_{it} - \hat{b}_i\hat{f}_t, g_{kt} - g_{kt-\Delta}\right]}{[g_{kt} - g_{kt-\Delta}]} \tag{3.13}$$

The next step consists on computing $\frac{1}{p}\underline{W}'\underline{c}_k$.

$$
\begin{aligned}
c_{ik} - b_i\left(\frac{1}{p}\underline{W}'\underline{c}_k\right) &= \frac{\left[r_{it} - \hat{b}_i\hat{f}_t, g_{kt} - g_{kt-\Delta}\right]}{\left[g_{kt} - g_{kt-\Delta}\right]} \\
\frac{1}{p}\sum_{i=1}^{p} w_{il}c_{ik} - \frac{1}{p}\sum_{i=1}^{p} w_{il}b_i\left(\frac{1}{p}\underline{W}'\underline{c}_k\right) &= \frac{1}{p}\sum_{i=1}^{p} w_{il}\frac{\left[r_{it} - \hat{b}_i\hat{f}_t, g_{kt} - g_{kt-\Delta}\right]}{\left[g_{kt} - g_{kt-\Delta}\right]} \\
\frac{1}{p}\underline{W}_l'\underline{c}_k - \frac{1}{p}\underline{W}_l b\left(\frac{1}{p}\underline{W}'\underline{c}_k\right) &= \frac{1}{p}\sum_{i=1}^{p} w_{il}\frac{\left[r_{it} - \hat{b}_i\hat{f}_t, g_{kt} - g_{kt-\Delta}\right]}{\left[g_{kt} - g_{kt-\Delta}\right]}, \forall l = 1, ..., K'
\end{aligned}
$$

In a matricial representation, we get

$$
\begin{aligned}
\begin{pmatrix} \frac{1}{p}\underline{W}_1'\underline{c}_k - \frac{1}{p}\underline{W}_1 b\left(\frac{1}{p}\underline{W}'\underline{c}_k\right) \\ \vdots \\ \frac{1}{p}\underline{W}_K'\underline{c}_k - \frac{1}{p}\underline{W}_K b\left(\frac{1}{p}\underline{W}'\underline{c}_k\right) \end{pmatrix} &= \begin{pmatrix} \frac{1}{p}\sum_{i=1}^{p} w_{i1}\frac{\left[r_{it}-\hat{b}_i\hat{f}_t, g_{kt}-g_{kt-\Delta}\right]}{\left[g_{kt}-g_{kt-\Delta}\right]} \\ \vdots \\ \frac{1}{p}\sum_{i=1}^{p} w_{iK}\frac{\left[r_{it}-\hat{b}_i\hat{f}_t, g_{kt}-g_{kt-\Delta}\right]}{\left[g_{kt}-g_{kt-\Delta}\right]} \end{pmatrix} \\
\frac{1}{p}\begin{bmatrix} \underline{W}_1' \\ \vdots \\ \underline{W}_K' \end{bmatrix}\left(\underline{c}_k - b\left(\frac{1}{p}\underline{W}'\underline{c}_k\right)\right) &= \begin{pmatrix} \frac{1}{p}\sum_{i=1}^{p} w_{i1}\frac{\left[r_{it}-\hat{b}_i\hat{f}_t, g_{kt}-g_{kt-\Delta}\right]}{\left[g_{kt}-g_{kt-\Delta}\right]} \\ \vdots \\ \frac{1}{p}\sum_{i=1}^{p} w_{iK}\frac{\left[r_{it}-\hat{b}_i\hat{f}_t, g_{kt}-g_{kt-\Delta}\right]}{\left[g_{kt}-g_{kt-\Delta}\right]} \end{pmatrix} \\
\frac{1}{p}W'\underline{c}_k - \left(\frac{1}{p}W'b\right)\left(\frac{1}{p}W'\underline{c}_k\right) &= \begin{pmatrix} \frac{1}{p}\sum_{i=1}^{p} w_{i1}\frac{\left[r_{it}-\hat{b}_i\hat{f}_t, g_{kt}-g_{kt-\Delta}\right]}{\left[g_{kt}-g_{kt-\Delta}\right]} \\ \vdots \\ \frac{1}{p}\sum_{i=1}^{p} w_{iK}\frac{\left[r_{it}-\hat{b}_i\hat{f}_t, g_{kt}-g_{kt-\Delta}\right]}{\left[g_{kt}-g_{kt-\Delta}\right]} \end{pmatrix}
\end{aligned}
$$

We obtain

$$
\frac{1}{p}W'\underline{c}_k = \left[I_K - \left(\frac{1}{p}W'b\right)\right]^{-1} \begin{pmatrix} \frac{1}{p}\sum_{i=1}^{p} w_{i1}\frac{\left[r_{it}-\hat{b}_i\hat{f}_t, g_{kt}-g_{kt-\Delta}\right]}{\left[g_{kt}-g_{kt-\Delta}\right]} \\ \vdots \\ \frac{1}{p}\sum_{i=1}^{p} w_{iK}\frac{\left[r_{it}-\hat{b}_i\hat{f}_t, g_{kt}-g_{kt-\Delta}\right]}{\left[g_{kt}-g_{kt-\Delta}\right]} \end{pmatrix} \tag{3.14}
$$

From 3.13 and 3.14 we derive an estimator of c_{ik}, $\forall i = 1, ..., p$ and $\forall k = 1, ..., K'$

$$\hat{c}_{ik} = \hat{b}_i \left[I_K - \left(\frac{1}{p} \hat{W}' \hat{b} \right) \right]^{-1} \begin{pmatrix} \frac{1}{p} \sum_{i=1}^{p} w_{i1} \frac{\left[r_{it} - \hat{b}_i \hat{f}_t, \widehat{g_{kt} - g_{kt-\Delta}} \right]}{\left[\widehat{g_{kt} - g_{kt-\Delta}} \right]} \\ \vdots \\ \frac{1}{p} \sum_{i=1}^{p} w_{iK} \frac{\left[r_{it} - \hat{b}_i \hat{f}_t, \widehat{g_{kt} - g_{kt-\Delta}} \right]}{\left[\widehat{g_{kt} - g_{kt-\Delta}} \right]} \end{pmatrix} + \frac{\left[r_{it} - \hat{b}_i \hat{f}_t, \widehat{g_{kt} - g_{kt-\Delta}} \right]}{\left[\widehat{g_{kt} - g_{kt-\Delta}} \right]} \quad (3.15)$$

3.3.2 Estimation of the volatility of the microstructure noise

In this section, we want to estimate Σ_g and Σ_η which correspond respectively to covolatility matrices of factors and idiosyncratic components. They are diagonal matrices. The starting point of this estimation is the following expression for common factors of microstructure noise

$$(\widehat{g_{kt} - g_{kt-\Delta}}) = \Omega_k' \left(r_t - \hat{b} \hat{f}_t \right), \forall k = 1, ..., K'$$

From the previous expression, it comes out that

$$\hat{\sigma}_{g_k}^2 = \frac{1}{2} \underline{\Omega}_k' \hat{\Sigma}_{r - \hat{b}\hat{f}} \underline{\Omega}_k, \forall k = 1, ..., K' \quad (3.16)$$

where $\underline{\Omega}_k$ is the eigenvector associated to the k^{th} largest eigenvalue of $\hat{\Sigma}_{r-\hat{b}\hat{f}}$, an estimator of the covariance matrix of $r - \hat{b}\hat{f}$.

We consider the realized variance function RV_{all}, defined for a process X_t as follow

$$RV_{all}(X) = \Sigma_{t_i} (X_{t_{i+1}} - X_{t_i})^2 \quad (3.17)$$

Applied to a latent process contaminated by microstructure noise, it is well established in the literature that this estimator consistently estimate the volatility of microstructure noise. $r_{it} - \hat{b}_i \hat{f}_t$ can be written as the sum of ε_{it} and a microstructure noise component:

$$r_{it} - \hat{b}_i \hat{f}_t = \varepsilon_{it} + \left(c_i - \frac{1}{p} b_i \underline{W}' c \right) (g_t - g_{t-\Delta}) + (\eta_t - \eta_{t-\Delta}) \quad (3.18)$$

By applying RV_{all} to $r_{it} - \hat{b}_i \hat{f}_t$, we get a consistent estimator of the volatility of $\left(c_i - \frac{1}{p} b_i \underline{W}' c \right) (g_t - g_{t-\Delta}) + (\eta_{it} - \eta_{it-\Delta})$. Since volatility of factors in the noise equation are assumed to be constant, we have the following equation

$$RV_{all}(r_{it} - \hat{b}_i\hat{f}_t) = \left(c_i - \frac{1}{p}b_i\underline{W}'c\right)(2\hat{\Sigma}_g)\left(c_i - \frac{1}{p}b_i\underline{W}'c\right)' + 2\hat{\Sigma}_{\eta_{ii}} \tag{3.19}$$

Thus, an estimator of Σ_η is given by

$$\hat{\Sigma}_{\eta_{ii}} = \frac{1}{2}RV_{all}(r_{it} - \hat{b}_i\hat{f}_t) - \left(\hat{c}_i - \frac{1}{p}\hat{b}_i\underline{\hat{W}}'\hat{c}\right)\hat{\Sigma}_g\left(\hat{c}_i - \frac{1}{p}b_i\underline{\hat{W}}'\hat{c}\right)' \tag{3.20}$$

Based on (3.15), (3.16) and (3.20), the variance of microstructure noise of each stock can easily be recorvered: $\forall i = 1, ..., p$

$$\hat{\sigma}^2_{u_i} = \hat{c}_i\hat{\Sigma}_g\hat{c}_i' + \hat{\Sigma}_{\eta_{ii}} \tag{3.21}$$

3.3.3 Estimation of the frictionless return

In the high frequency financial econometrics literature, frictionless prices, i.e true prices, are usually assumed to be latent. Recorded prices are noisy and additively contaminated with microstructure noise (bid-ask bounces, discreteness of price changes, differences in trade sizes or informational content of price changes, gradual response of prices to a block trade, strategic component of the order flow, inventory control effects, etc. See, e.g, Aït-Sahalia and Yu (2009)). The presence of such noise has a negative impact in the estimation of objects of interest such as the integrated volatility, the spot volatility, leverage effects, integrated betas, etc. Thus, accuracy can be improved if the latent return is estimated prior to the use (See, e.g, Chaker (2017)).

The aim of this section is to take advantage of estimates of the common component of the microstructure noise, in order to estimate frictionless returns.

From assumptions of the model, it is easily established that

$$r_{it} = r^*_{it} + c_i(g_t - g_{t-\Delta}) + (\eta_{it} - \eta_{it-\Delta}) \tag{3.22}$$

Writting things differently, we get

$$r^*_{it} = r_{it} - c_i(g_t - g_{t-\Delta}) - (\eta_{it} - \eta_{it-\Delta}) \tag{3.23}$$

Since we know how to estimate c_i and $(g_t - g_{t-\Delta})$, we propose the following quantity to estimate the latent return

$$\widehat{r_{it}^*} = r_{it} - \hat{c}_i(\widehat{g_t - g_{t-\Delta}}), \forall i = 1, ..., p \tag{3.24}$$

where r_i is the observed return of the asset i, $\hat{c}_i$ and $(\widehat{g_t - g_{t-\Delta}})$ are given respectively by equations 3.15 and 3.12.

Based on an artificial set of data, we can assess the accuracy gain generates by our new procedure when estimating the integrated volatility or the integrated covolatility of processes. Depending on the noise level present on our estimate of the latent returns, our estimator can be either $RV(\hat{r}_i^*)$ or $PRV(\hat{r}_i^*)$. These estimators can be compared to the Kernel estimator $Ker(r_i)$, the pre-averaging estimator $PRV(r_i)$ and the realized variance $RV(r_i)$.

We can replicate a two factors model in which prices are observed with noise. Parameters can be set as in Bollerslev, Meddahi, and Nyawa (2018)

- The loading factors b can be generated such that elements of the k^{th} column $\underline{b}_k$, for $k = 1, 2$, follow a normal law with mean 0 and standard deviation 1: $b_{ik} \sim N(0, 1)$, $\forall$ $i = 1, ..., p$.
- The two factor components in the frictionless return representation can be generated by the following model: $\forall k = 1, 2$

  $$f_{kt} = \sigma_{fkt} dB_{kt}$$

  with B_{kt} a brownian motion and σ_{fkt} generated by a $GARCH$ diffusion model,

  $$d\sigma_{fkt}^2 = \kappa_{fk}\left(\theta_{fk} - \sigma_{fkt}^2\right)dt + \lambda_{fk}\sigma_{fkt}^2 dW_{kt}$$

- The idiosyncratic error term in the factor representation can be assumed to satisfy

  $$\varepsilon_{it} = \sigma_{it} dW_{it}^{\varepsilon}$$

  with W_{it}^{ε} a brownian motion such that $W_{it}^{\varepsilon} \perp W_{1t}, W_{2t}$ and $W_{it}^{\varepsilon} \perp B_{1t}, B_{2t}$, with the spot volatility generated by three different representative models:

  - For $1 \leq i \leq p/3$, the volatility of the idiosyncratic component can be generated by a Nelson GARCH diffusion limit model as in Barndorff-Nielsen and Shephard (2002):

$$d(\sigma^2_{it}) = (\theta_\infty - \sigma^2_{it})\, dt + \eta\sigma^2_{it} dB^{\varepsilon}_{it},$$

- For $p/3 < i \leq 2p/3$, the volatility process can be assumed to follow a geometric Ornstein-Uhlenbeck (OU) model as in Barndorff-Nielsen and Shephard (2002):

$$dlog(\sigma^2_{it}) = \kappa\, (\sigma + log(\sigma^2_{it}))\, dt + \nu dB^{\varepsilon}_{it},$$

- For $2p/3 < i \leq p$, the volatility can follow a $GARCH$ diffusion model:

$$d\sigma^2_{it} = \kappa_\varepsilon\, (\theta_\varepsilon - \sigma^2_{it})\, dt + \gamma_\varepsilon \sigma_{it} dB^{\varepsilon}_{it},$$

- The slope in the factor representation of the microstructure noise can be such that: $c_i \sim N(1,1)$, $\forall i = 1, ..., p$;
- As in Barndorff-Nielsen, Hansen, and Shephard (2008a), microstructure noise variance of the asset i can satisfy the equality: $Var(u_i) = \xi^2 \sqrt{\frac{1}{n}\sum_{t=1}^{n} \sigma^4_{it}}$, with ξ^2 the noise-to-signal ratio and σ_{it} the spot volatility of the true price process of asset i at time t.

3.4 Empirical Study

The aim of this section is to study the information contain of microstructure noise. This will be achieved by comparing microstructure noise extracted factors to some observable financial characteristics such as liquidity measures. Information on links between microstructure noise common factors and liquidity measures has important implications for asset management, statistical arbitrage or proprietary trading (see, e.g., Aït-Sahalia and Yu (2009)).

Our study relies on stocks included in the S&P500 during the period spanning January 2007 to December 2011. Those data come from the TAQ Database of WRDS. Price data are available at a high frequency intraday level. We clean the data following the procedures in Barndorff-Nielsen, Hansen, Lunde, and Shephard (2011b). This leaves us with a total of 384 stocks.

Based on our high dimensional set of price intraday data, and following the methodology described in Bollerslev, Meddahi, and Nyawa (2018), we compute estimates of factors and loadings of the latent return equation, namely $\hat{f}_t$ and $\hat{b}$. The next step consists on applying the estimation strategy developped in section 3 in order to extract the factor component of microstructure noises. These steps are carried out for each trading day within the sample.

For a given day, the main output is an intra day time series of microstructure noise factors $(\widehat{g_t - g_{t-\Delta}})$. The latter variable will be compared to some popular liquidity measures.

Data of liquidity measures come from the WRDS database and concern:

- **Spread**: the difference between the closing ask and bid prices;
- **Trade size**: the average number of shares per trade;
- **Number of trades**: the number of trades made on the Stock Market for a given security;
- **Daily share volume**: the total number of shares of a stock sold on a given day, expressed in units of one share;
- **Total shares outstanding**: the number of publicly held shares, recorded in thousands.

Liquidity measures are observed for each stock during the period spanned, at a daily frequency. For a comparison purpose, firstly, the frequency of extracted factors of the microstructure noise $(\widehat{g_t - g_{t-\Delta}})$ must be daily. This is not yet the case since estimated factors of noise are in an intraday frequency. To overcome this issue, we use as daily value of $(\widehat{g_t - g_{t-\Delta}})$, its closing value. Alternative aggregation technics are possible, such as the sum or the mean of intraday observations. Secondly, for each liquidity measure, the correponding available panel data must be transformed to obtain one index with whom the daily measure of $(\widehat{g_t - g_{t-\Delta}})$ will be compared. We consider the cross-sectional average of each liquidity measure as a market-wide liquidity measure. The underlying assumption behind this transformation of the data is that liquidity across many different stocks could co-move (See, e.g., Aït-Sahalia and Yu (2009) for futher explanation). Another option for getting market-wide liquidity measures is through the PCA based on panel data of each liquidity measure. This technic will provide factors which drive each liquidity measure and these factors will be compared to microstructure noise factors. The two approaches are going to be considered in this paper.

The following graphics represent the dynamics of five first extracted factors of microstructure noises. We only care about the first five factors, since, using the same dataset, Bollerslev, Meddahi, and Nyawa (2018) established that those factors can explain around 63% of the total variability of microstruture noise. Since those extracted factors can be noisy, we consider their serial monthly average in order to reduce the impact of estimation errors.

Figure 3.1. Dynamics of some microstructure noise common factors: monthly frequency.

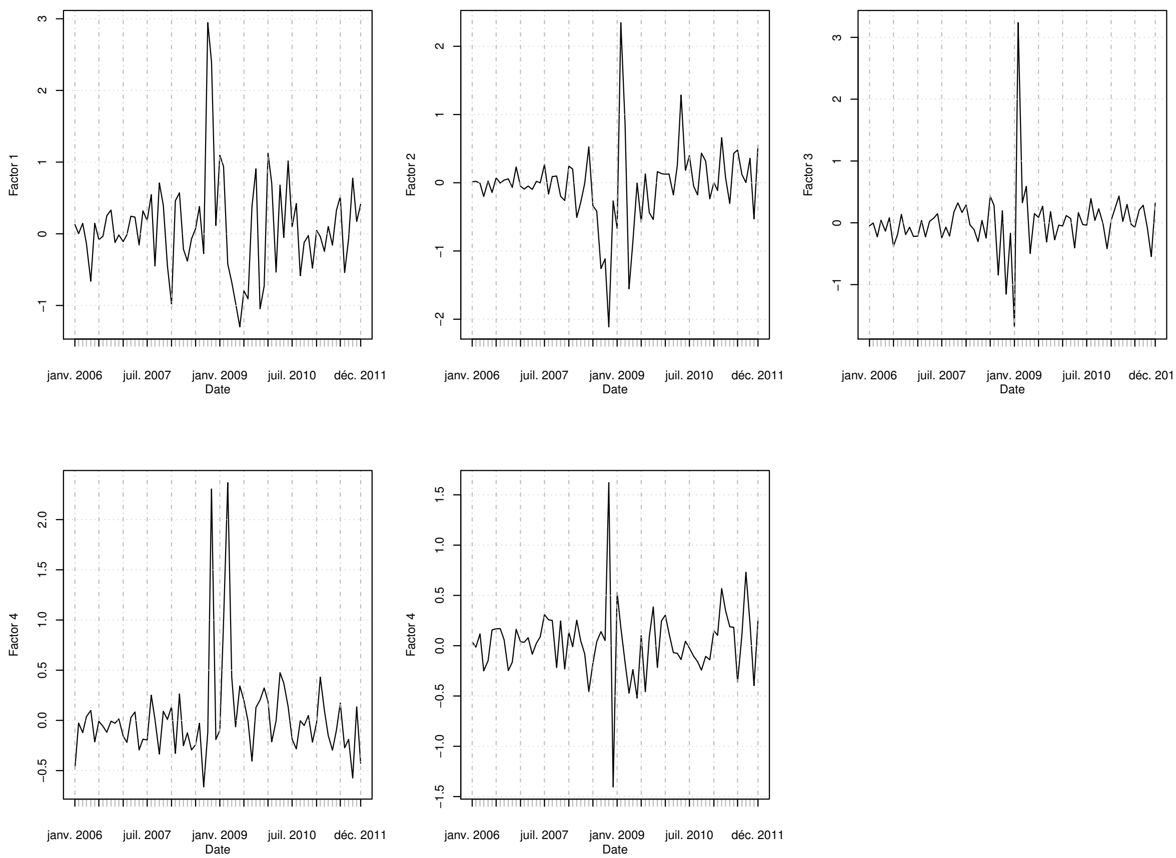

As in Aït-Sahalia and Yu (2009), the information contain of microstruture noise can also be assessed using its volatility time series. Another empirical exercise will consist on comparing the daily quadratic variation of extracted microstructure noise factors to liquidity measures. We represent in the following graphics the dynamics of daily quadratic variations for the five first factors of microstructure noises.

Figure 3.2. Dynamics of some microstructure noise common factors.

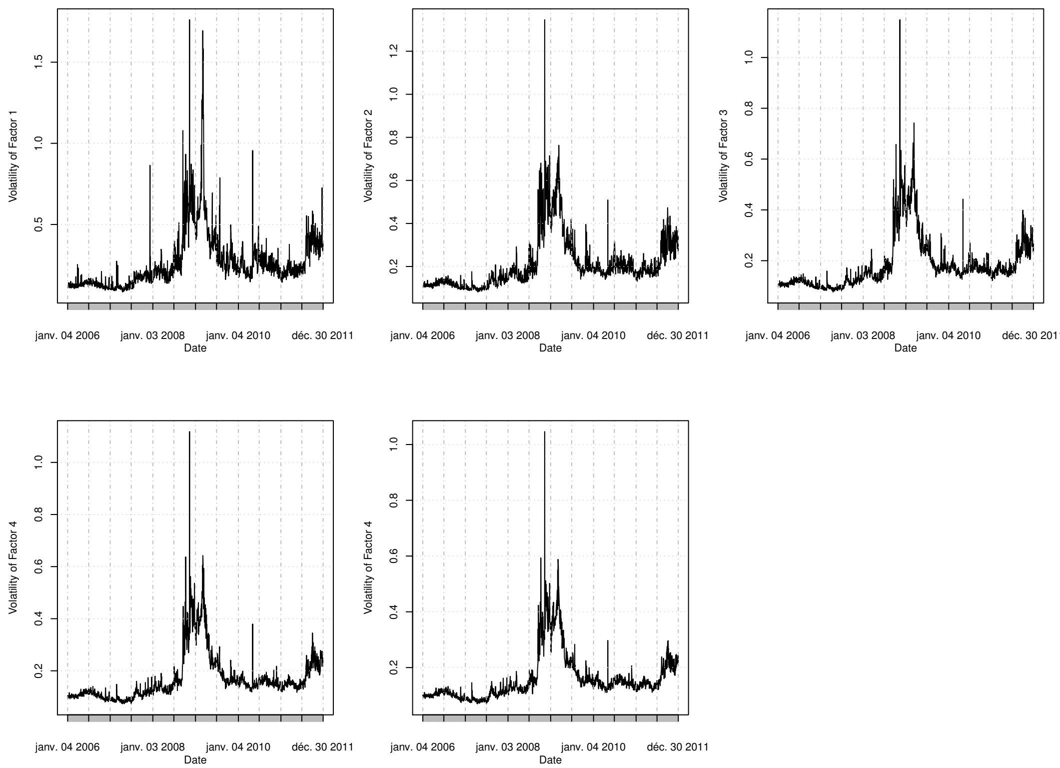

3.4.1 Information Content of microstructure noise factors

We want to measure the extent to which our extracted factors of microstructure noises correlate with liquidity measures. To achieve this goal, we will run a set of regressions of the following form:

$$g_{kt} = c_k + \alpha_k x_t + \varepsilon_{kt} \tag{3.25}$$

where g_{kt} is the k^{th} extracted factor of microstructure noises (or its daily quadratic variation), and x_t is a vector of market-wide liquidity measures available in the literature (*spread*, *trade size*, *number of trades*, *daily share volume*, *total share outstanding*). Market-wide liquidity measures are computed from the panel of each liquidity measure by taking the cross sectional average or by running a principal component analysis from which the first factor will be considered. The sampling frequency is daily for regressions involving quadratic variations of microstructure noise, and monthly for regressions with extracted factor of microstructure noises.

The following tables present results of theses different regressions, starting from regressions based on extracted factor of microstructure noises.

Table 3.1. Regression of the MSN first factor on liquidity measures

	Estimate	Std.Error	Error	t. value	Pr(>|t|)
Spread	0.474	0.227	2.084	0.041	*
log(Price)	-1.097	0.706	-1.555	0.125	
log(Share.outsd)	6.521	2.401	2.716	0.008	**
log(Volume)	-9.329	7.224	-1.291	0.201	
log(Nb.trades)	9.303	7.157	1.300	0.198	
trade.size	0.041	0.042	0.981	0.330	

Signif. codes: 0 '***' 0.001 '**' 0.01 '*' 0.05 '.' 0.1 ' ' 1

Residual standard error: 0.627 on 65 degrees of freedom.

R^2: 0.235, $Adj.R^2$: 0.164. F-stat: 3.327 on 6 and 65 DF, p-value: 0.006413

Table 3.2. Regression of the MSN second factor on liquidity measures

	Estimate	Std.Error	Error	t. value	Pr(>|t|)
Spread	0.337	0.177	1.898	0.042	*
log(Price)	-0.712	0.628	-1.133	0.261	
log(Share.outsd)	0.850	1.763	0.482	0.632	
log(Volume)	-1.590	4.884	-0.326	0.746	
log(Nb.trades)	1.530	4.759	0.322	0.749	
trade.size	0.007	0.027	0.266	0.791	

Signif. codes: 0 '***' 0.001 '**' 0.01 '*' 0.05 '.' 0.1 ' ' 1

Residual standard error: 0.562 on 66 degrees of freedom.

R^2: 0.115, $Adj.R^2$: 0.034. F-stat: 1.422 on 6 and 66 DF, p-value: 0.2196

Table 3.3. Regression of the MSN third factor on liquidity measures

	Estimate	Std.Error	Error	t. value	Pr(>|t|)
α	-0.254	0.137	-1.851	0.069	.
$\Delta Spread$	7.691	3.839	2.003	0.049	*
$\Delta log(Price)$	2.030	1.397	1.453	0.151	
$\Delta log(Share.outsd)$	2.799	5.227	0.535	0.594	
$\Delta log(Nb.trades)$	-0.136	0.385	-0.353	0.725	
$\Delta trade.size$	0.338	0.816	0.414	0.680	

Signif. codes: 0 '***' 0.001 '**' 0.01 '*' 0.05 '.' 0.1 ' ' 1

Residual standard error: 0.520 on 66 degrees of freedom.

R^2: 0.182, $Adj.R^2$: 0.112. F-stat: 1.422 on 5 and 65 DF, p-value: 0.335

Table 3.4. Regression of the MSN fourth factor on liquidity measures

	Estimate	Std.Error	Error	t. value	Pr(>|t|)
$Spread$	0.179	0.151	1.185	0.240	
$log(Price)$	-1.383	0.467	-2.961	0.004	**
$log(Share.outsd)$	0.357	1.590	0.225	0.823	
$log(Volume)$	1.711	4.784	0.358	0.722	
$log(Nb.trades)$	-1.822	4.739	-0.384	0.702	
$trade.size$	-0.008	0.028	-0.280	0.780	

Signif. codes: 0 '***' 0.001 '**' 0.01 '*' 0.05 '.' 0.1 ' ' 1

Residual standard error: 0.520 on 66 degrees of freedom.

R^2: 0.289, $Adj.R^2$: 0.223. F-stat: 1.422 on 5 and 65 DF, p-value: 0.001

Table 3.5. Regression of the MSN fifth factor on liquidity measures

	Estimate	Std.Error	Error	t. value	Pr(>|t|)
α	-0.061	0.092	-0.665	0.508	
$\Delta Spread$	1.163	2.586	0.450	0.654	
$\Delta log(Price)$	2.089	0.941	2.221	0.030	*
$\Delta log(Share.outsd)$	-0.164	3.521	-0.047	0.963	
$\Delta log(Nb.trades)$	-0.025	0.259	-0.097	0.923	
$\Delta trade.size$	-0.370	0.549	-0.674	0.503	

Signif. codes: 0 '***' 0.001 '**' 0.01 '*' 0.05 '.' 0.1 ' ' 1

Residual standard error: 0.520 on 66 degrees of freedom.

R^2: 0.289, $Adj.R^2$: 0.223. F-stat: 1.422 on 5 and 65 DF, p-value: 0.001

From these previous regression results, it comes out that microstrucutre noise common factors are mostly related to the average spread, the average price level and the average share outstanding. More precisely, average spread and average share outstanding are the more significant explanatory variables of the first factor. The second and the third factors are highly related to the average spread while the fourth and the fifth factors are strongly correlated to the average price level.

We now look at results of regressions based on daily quadratic variation of extracted microstructure noise factors and liquidity measures. Tables below display those results. We obtain that volatility of microstructure noise factors are highly correlated with the considered liquidity measures, namely: the average spread, the average price level, the average number of publicly held shares, the average number of trades, the average number of shares sold and the average number of shares per trade.

Table 3.6. Regression of the volatility of the MSN first factor on liquidity measures.

	Estimate	Std.Error	Error	t. value	Pr(>|t|)
α	-2.478	0.995	-2.490	0.013	*
$Spread$	0.029	0.007	4.273	0.000	***
$log(Price)$	-0.658	0.020	-32.102	0.000	***
$log(Share.outsd)$	0.105	0.071	1.477	0.140	
$log(Volume)$	0.621	0.147	4.235	0.000	***
$log(Nb.trades)$	-0.490	0.145	-3.384	0.001	***
$trade.size$	-0.004	0.001	-4.889	0.000	***

Signif. codes: 0 '***' 0.001 '**' 0.01 '*' 0.05 '.' 0.1 ' ' 1

Residual standard error: 0.105 on 1502 degrees of freedom.

R^2: 0.662, $Adj.R^2$: 0.661. F-stat: 490.1 on 6 and 1502 DF, p-value: < 2.2e-16

Table 3.7. Regression of the volatility of the MSN second factor on liquidity measures.

	Estimate	Std.Error	Error	t. value	Pr(>|t|)
α	-1.345	0.637	-2.112	0.035	*
$Spread$	0.021	0.004	4.850	0.000	***
$log(Price)$	-0.495	0.013	-37.795	0.000	***
$log(Share.outsd)$	0.097	0.045	2.144	0.032	*
$log(Volume)$	0.366	0.094	3.896	0.000	***
$log(Nb.trades)$	-0.298	0.093	-3.217	0.001	**
$trade.size$	-0.003	0.001	-4.728	0.000	***

Signif. codes: 0 '***' 0.001 '**' 0.01 '*' 0.05 '.' 0.1 ' ' 1

Residual standard error: 0.067 on 1502 degrees of freedom.

R^2: 0.699, $Adj.R^2$: 0.697. F-stat: 580.8 on 6 and 1502 DF, p-value: < 2.2e-16

Table 3.8. Regression of the volatility of the MSN third factor on liquidity measures.

	Estimate	Std.Error	Error	t. value	Pr(>|t|)
α	-0.747	0.523	-1.428	0.154	
$Spread$	0.020	0.004	5.491	0.000	***
$log(Price)$	-0.441	0.011	-40.979	0.000	***
$log(Share.outsd)$	0.064	0.037	1.714	0.087	.
$log(Volume)$	0.322	0.077	4.181	0.000	***
$log(Nb.trades)$	-0.275	0.076	-3.610	0.000	***
$trade.size$	-0.002	0.000	-5.011	0.000	***

Signif. codes: 0 '***' 0.001 '**' 0.01 '*' 0.05 '.' 0.1 ' ' 1

Residual standard error: 0.055 on 1502 degrees of freedom.

R^2: 0.718, $Adj.R^2$: 0.717. F-stat: 638.9 on 6 and 1502 DF, p-value: < 2.2e-16

Table 3.9. Regression of the volatility of the MSN fourth factor on liquidity measures.

	Estimate	Std.Error	Error	t. value	Pr(>|t|)
α	-0.524	0.462	-1.135	0.257	
$Spread$	0.022	0.003	7.000	0.000	***
$log(Price)$	-0.409	0.010	-43.044	0.000	***
$log(Share.outsd)$	0.073	0.033	2.200	0.028	*
$log(Volume)$	0.239	0.068	3.504	0.000	***
$log(Nb.trades)$	-0.202	0.067	-3.007	0.003	**
$trade.size$	-0.002	0.000	-4.396	0.000	***
Signif. codes: 0 '***' 0.001 '**' 0.01 '*' 0.05 '.' 0.1 ' ' 1					
Residual standard error: 0.048 on 1502 degrees of freedom.					
R^2: 0.729, $Adj.R^2$: 0.728. F-stat: 675.4 on 6 and 1502 DF, p-value: < 2.2e-16					

Table 3.10. Regression of the volatility of the MSN fifth factor on liquidity measures.

	Estimate	Std.Error	Error	t. value	Pr(>|t|)
α	-0.254	0.416	-0.609	0.543	
$Spread$	0.021	0.003	7.303	0.000	***
$log(Price)$	-0.382	0.009	-44.627	0.000	***
$log(Share.outsd)$	0.065	0.030	2.177	0.030	*
$log(Volume)$	0.184	0.061	3.006	0.003	**
$log(Nb.trades)$	-0.153	0.061	-2.531	0.011	*
$trade.size$	-0.001	0.000	-3.971	0.000	***
Signif. codes: 0 '***' 0.001 '**' 0.01 '*' 0.05 '.' 0.1 ' ' 1					
Residual standard error: 0.044 on 1502 degrees of freedom.					
R^2: 0.740, $Adj.R^2$: 0.738. F-stat: 711.5 on 6 and 1502 DF, p-value: < 2.2e-16					

3.5 Conclusion

We provide a new methodology to estimate microstructure noise characteristics and frictionless prices under a high dimensional setup. We rely on factor assumptions both in latent returns and microstructure noise. Inspired from the principal component analysis, the methodology is able to estimate rotations of common factors, corresponding loading coefficients and volatilities from the microstructure noise factorial representation, for a huge number of stocks.

We show how we can take advantage of estimates of the common factor component of microstructure noises, firstly in order to estimate frictionless returns, and secondly to improve the accuracy when estimating the integrated volatility or the integrated covolatility of processes.

Using stocks included in the S&P500 during the period spanning January 2007 to December 2011, we estimate factors in the microstructure noise factorial representation and compare them to some market-wide liquidity measures computed from real financial variables. We obtain that: the first factor is correlated to the average spread and the average number of shares outstanding; the second and third factors are related to the spread; the fourth and fifth factors are significantly linked to the closing average log price level. In addition, volatilities of those microstructure noise factors are widely explained by the average spread, the average volume, the average number of trades and the average trade size.

Bibliography

Acharya, V., Pedersen, L., Philippe, T., Richardson, M., 2017. Measuring systemic risk. The Review of Financial Studies 30, 2–47.

Acharya, V., Pedersen, L., Philippon, T., Richardson, M., 2010. Measuring systemic risk. Working Paper, Federal Reserve Bank of Cleveland 1002.

Adrian, T., Brunnermeier, M., 2016. Covar. American Economic Review 106(7), 1705–1741.

Aït-Sahalia, Y., Cacho-Diaz, J., Leaven, R., 2015. Modeling financial contagion using mutually exciting jump processes. Journal of Financial Economics 117, 585–606.

Aït-Sahalia, Y., Jacod, J., 2014. High-frequency financial econometrics. Princeton University Press.

Aït-Sahalia, Y., Mykland, P. A., Zhang, L., 2005. How often to sample a continuous-time process in the presence of market microstructure noise. The Review of Financial Studies 18.

Aït-Sahalia, Y., Mykland, P. A., Zhang, L., 2011. Ultra high frequency volatility estimation with dependent microstructure noise. Journal of Econometrics 160, 160–175.

Ait-Sahalia, Y., Xiu, D., 2016. Using principal component analysis to estimate a high dimensional factor model with high-frequency data. Journal of Econometrics, forthcoming.

Aït-Sahalia, Y., Yu, J., 2009. High frequency market microstructure noise estimates and liquidity measures. The Annals of Applied Statistics 3, 422–457.

Andersen, T., Bollerslev, T., 1998. Answering the skeptics: Yes standard volatility models do provide accurate forecasts. International Economic Review 39, 885–905.

Andersen, T., Bollerslev, T., Christoffersen, P., Diebold, F., 2006. Volatility and correlation forecasting. Handbook of Economic Forecasting (eds. G. Elliott, C.W.J. Granger and A. Timmermann).

Andersen, T. G., Diebold, F. X., Labys, P., 2001. The distribution of realized exchange rate volatility. Journal of the American Statistical Association 96, 42–55.

Bai, J., Ng, S., 2002. Determining the number of factors in approximate factor models. Econometrica 70, 191–221.

Bannouh, K., Martens, M., Oomen, R., van Dijk, D., 2012. Realized mixed frequency factor models for vast dimensional covariance estimation. Working paper, Erasmus University.

Barndorff-Nielsen, O., Hansen, P.R.and Lunde, A., Shephard, N., 2008a. Designing realised kernels to measure the ex-post variation of equity prices in the presence of noise. Econometrica 76, 1481–1536.

Barndorff-Nielsen, O., Hansen, P., Lunde, A., Shephard, N., 2008b. Designing realised kernels to measure the ex-post variation of equity prices in the presence of noise. Econometrica 76, 1481–1536.

Barndorff-Nielsen, O., Hansen, P., Lunde, A., Shephard, N., 2011a. Multivariate realised kernels: Consistent positive semi-definite estimators of the covariation of equity prices with noise and non-synchronous trading. Journal of Econometrics 162, 149–169.

Barndorff-Nielsen, O., Shephard, N., 2002. Econometric analysis of realised volatility and its use in estimating stochastic volatility models. Journal of the Royal Statistical Society, Series B 64, 253–280.

Barndorff-Nielsen, O. E., Hansen, P., Lunde, A., Shephard, N., 2011b. Multivariate realised kernels: Consistent positive semi-definite estimators of the covariation of equity prices with noise and non-synchronous trading. Journal of Econometrics 162(2), 149.

Barndorff-Nielsen, O. E., Shephard, N., 2003. Realised power variation and stochastic volatility. Bernoulli 9, 243–265.

Bollerslev, T., Meddahi, N., Nyawa, S., 2018. High-dimensional multivariate realized volatility estimation. Working Paper.

Chaker, S., 2017. On high frequency estimation of the frictionless price: The use of observed liquidity variables. Journal of Econometrics 201, 127–143.

Chen, N.-F., Roll, R., Ross, S. A., 1986. Economic forces and the stock market. Journal of Business 59, 383–403.

Christensen, K., Kinnebrock, S., Podolskij, M., 2010a. Preaveraging estimators of the ex-post covariance matrix in noisy diffusion models with nonsynchronous data. Journal of Econometrics 159, 116–133.

Christensen, K., Kinnebrock, S., Podolskij, M., 2010b. Preaveraging estimators of the ex-post covariance matrix in noisy diffusion models with nonsynchronous data. Journal of Econometrics 159 159, 116–133.

Clark, P. K., 1973. A subordinated stochastic process model with finite variance for speculative prices. Econometrica 41, 135–155.

Clements, A. E., Todorova, N., 2016. Information flow, trading activity and commodity futures volatility. The Journal of Features Markets 36, 88–104.

Connor, G., Korajczyk, R., 1988. Risk and return in an equilibrium apt: Application of a new test methodology. Journal of Financial Economics 21, 255–289.

Crosby, J., 2012. Introduction to jump and levy processes. Course in Mathematical Finance at the Mathematical Institute, Oxford University.

Dai, C., Lu, K., Xiu, D., 2017. Knowing factors or factor loadings, or neither? evaluating estimators of large covariance matrices with noisy and asynchronous data. Working Paper.

De Vries, C., 2005. The simple economics of bank fragility. Journal of Banking and Finance 29, 803–825.

DeMiguel, V., Garlappi, L., Uppal, R., 2009. Optimal versus naive diversification: How inefficient is the 1/N portfolio strategy? Review of Financial Studies 22, 1916–1953.

Diebold, F., Strasser, G., 2013. On the correlation structure of microstructure noise: A financial economic approach. Review of Economic Studies 80, 1304–1337.

Diebold, F., Yilmaz, K., 2015a. Financial and macroeconomic connectedness: A network approach to measurement and monitoring. Oxford University Press.

Diebold, F. X., Yilmaz, K., 2015b. Financial and macroeconomic connectedness: A network approach to measurement and monitoring. Oxford University Press.

Dungey, M., Gajurel, D., 2014. Equity market contagion during the global financial crisis: Evidence from the world's eight largest economies. Economic Systems 38, 161–177.

Engle, R., Kelly, B., 2012. Dynamic equicorrelation. Journal of Business and Economic Statistics 30, 212–228.

Epps, T., 1979. Comovements in stock prices in the very short run. Journal of the American Statistical Association 74, 291–298.

Eraker, B., 2004. Do stock prices and volatility jump? Journal of Finance 59, 1367–1404.

Fan, J., Fan, Y., Lv, J., 2008. High dimensional covariance matrix estimation using a factor model. Journal of Econometrics 147, 186–197.

Fan, J., Li, Y., Yu, K., 2012. Vast volatility matrix estimation using high-frequency data for portfolio selection. Journal of the American Statistical Association 107:497, 412–428.

Fan, J., Liao, Y., Mincheva, M., 2011. High-dimensional covariance matrix estimation in approximate factor models. Annals of Statistics 39, 3320–3356.

Fan, J., Liao, Y., Mincheva, M., 2013. Large covariance estimation by thresholding principal orthogonal complements. Royal Statistical Society 75, 1–44.

Feller, W., 1951. Two singular diffusion problems. Annals of Mathematics 54, 173–182.

Fernandez-Rodriguez, F., Sosvilla-Rivero, S., 2016. Volatility transmission between stock and exchange-rate markets: A connectedness analysis. Bath Economics Research Papers 54/16.

Fonseca, J. d., Zaatour, R., 2015. Clustering and mean reversion in a hawkes microstructure model. The journal of futures markets 35, 813–838.

Gary, C., Rothschild, M., 1983. Arbitrage, factor structure, and mean-variance analysis on large asset markets. Econometrica 51, 1281–1304.

Hansen, P., Lunde, A., 2006. Realized variance and market microstruture noise. Journal of Business and Economic Statistics 24, 127–161.

Hasbrouck, J., Seppi, D., 2001a. Common factors in prices, order flows, and liquidity. Journal of Financial Economics 59, 383–411.

Hasbrouck, J., Seppi, D., 2001b. Common factors in prices, order flows, and liquidity. Journal of Financial Economics 59, 383–411.

Hautsch, N., Kyj, L., Oomen, R., 2012. A blocking and regularization approach to high dimensional realized covariance estimation. Journal of Applied Econometrics 27, 625–645.

Hautsch, N., Podolskij, M., 2013. Pre-averaging based estimation of quadratic variation in the presence of noise and jumps: Theory, implementation, and empirical evidence. Journal of Business and Economic Statistics 31, 165–183.

Hawkes, A. G., 1971a. Spectra of some self-exciting and mutually exciting point processes. Biometrika 58, 83–90.

Hawkes, A. G., 1971b. Spectra of some self-exciting and mutually exciting point processes. Journal of the Royal Statistical Society Series B 33, 438–443.

Hawkes, A. G., David, O., 1974. A cluster representation of a self-exciting process. Journal of Applied Probability 11, 493–503.

Hayashi, T., Yoshida, N., 2005. On covariance estimation of non-synchronously observed diffusion processes. Bernoulli 11, 359–379.

Hellwig, M., 2009. Systemic risk in the financial sector: an analysis of the subprime-mortgage financial crisis. De Economist 157, 129–207.

Heston, S. L., 1993. A closed-form solution for options with stochastic volatility with applications to bond and currency options. The Review of Financial Studies 6(2), 327–343.

Jacod, J., 1994. Limit of random measures associated with the increments of a brownian semimartingale. Tech. Rep., Universite de Paris VI.

Jacod, J., Li, Y., Mykland, P. A., Podolskijc, M., Vetter, M., 2009a. Microstructure noise in the continuous case: The pre-averaging approach. Stochastic Processes and their Applications 119, 2249–2276.

Jacod, J., Li, Y., Mykland, P. A., Podolskijc, M., Vetter, M., 2009b. Preaveraging estimators of the expost covariance matrix in noisy diffusion models with nonsynchronous data. Stochastic Processes and their Applications 119, 2249–2276.

Jacod, J., Li, Y., Zheng, X., 2017. Statistical properties of microstructure noise. Econometrica 84, 1133–1174.

Jacod, J., Protter, P., 1998. Asymptotic error distributions for the euler method for stochastic differential equations. Annals of Probability 26, 267–307.

Jenkins, A. M., 2011. Financial regulation, systemic risk, and the audit of financial contagion. Committee On Capital Markets Regulation.

Joulin, A., Lefevre, A., Grunberg, D., Bouchaud, J.-P., 2008. Stock price jumps: news and volume play a minor role. Technical report.

Kou, G., S., 2002. A jump-diffusion model for option pricing. Management Science 48, 1086–1101.

Ledoit, O., Wolf, 2003. Improved estimation of the covariance matrix of stock returns with an application to portfolio selection. Journal of Empirical Finance 23, 603–621.

Lee, S. S., Mykland, P. A., 2008. Jumps in financial markets: A new nonparametric test and jump dynamics. The Review of Financial Studies 21, 2535–2563.

Li, Y., Xie, S., Zheng, X., 2016. Efficient estimation of integrated volatility incorporating trading information. Journal of Econometrics 195, 33–50.

Lunde, A., Shephard, N., Sheppard, K., 2016. Econometric analysis of vast covariance matrices using composite realized kernels and their application to portfolio choice. Journal of Business and Economic Statistics 34, 504–518.

Maneesoonthorn, W., Forbes, C., Martin, G., 2016. Inference on self-exciting jumps in prices and volatility using high frequency measures. Journal of Applied Econometrics 29(3), 356–371.

Pelger, M., 2016. Large-dimensional factor modeling based on high-frequency observations. Working Paper.

Podolskij, Vetter, M., 2009. Estimation of volatility functionals in the simultaneous presence of microstructure noise and jumps. Bernoulli 15, 634–658.

Polson, N., Scott, J., 2012. Explosive volatility: A model of financial contagion. Manuscript, University of Chicago.

Rauch, J., Litan, R., 1998. American finance for the 21st century. The Brookings Institution.

Ross, S. A., 1976. The arbitrage theory of capital asset pricing. Journal of Economic Theory 13, 341–360.

Scott, H. S., 2010. How to improve five important areas of financial regulation. Harvard Journal of Law and Public Policy 671, 672–79.

Sharpe, W. F., 1994. The Sharpe ratio. Journal of Portfolio Management 23, 49–58.

Stock, J. H., Watson, M. W., 2002. Forecasting using principal components from a large number of predictors. Journal of the American Statistical Association 97, 1167–1179.

Tao, M., Wang, Y., Chen, X., 2011. Fast convergence rates in estimating large volatility matrices using high-frequency financial data. Journal of the American Statistical Association 106.

Tobias, A., Brunnermeier, M. K., 2016. Covar. American Economic Review 106, 1705–1741.

Todorov, V., Tauchen, G., 2011. Volatility jumps. Journal of Business and Economic Statistics 29(3), 356–371.

Wang, Y.and Zou, J., 2010. Estimating covariation: Epps effect, microstructure noise. Journal of Econometrics 160, 33–47.

Zhang, L., Mykland, P., Ait-Sahalia, Y., 2005. A tale of two time scales: Determining integrated volatility with noisy high-frequency data. Journal of the American Statistical Association 100.

Zheng, X., Li, Y., 2011. On the estimation of integrated covariance matrices of high dimensional diffusion processes. Annals of Statistics 39, 3121–3151.